



University
of Glasgow

Kaiserli, Eirini (2008) *Subcellular localisation and functional analysis of UVR8, a UV-B specific signalling component in Arabidopsis*.
PhD thesis.

<http://theses.gla.ac.uk/57/>

Copyright and moral rights for this thesis are retained by the author

A copy can be downloaded for personal non-commercial research or study, without prior permission or charge

This thesis cannot be reproduced or quoted extensively from without first obtaining permission in writing from the Author

The content must not be changed in any way or sold commercially in any format or medium without the formal permission of the Author

When referring to this work, full bibliographic details including the author, title, awarding institution and date of the thesis must be given

Subcellular localisation and functional analysis of UVR8, a UV-B specific signalling component in *Arabidopsis*

A thesis submitted to the University of Glasgow for the degree of
Doctor of Philosophy

Eirini Kaiserli

November, 2007

Plant Molecular Science Group,
Division of Biochemistry and Molecular Biology,
Faculty of Biomedical and Life Sciences,
University of Glasgow

© Eirini Kaiserli, 2007

To my parents, Kostas and Popi Kaiserli

ACKNOWLEDGEMENTS

I am very grateful to my supervisor Professor Gareth I. Jenkins for the advice, support and encouragement throughout my *Ph.D.* and the University of Glasgow for the award of an IBLS studentship. Many thanks to all the members of the Brian lab, past and present, for providing a pleasant scientific environment to work and socialise with. I would like to thank Dr. Cat Cloix, in particular, not only for teaching me complex molecular techniques, but also and most importantly for being a friend at the research and personal level. Also, many thanks to Drs. Bobby Brown, Stuart Sullivan and Cat Thomson for providing me with many protocols, advice and great company and my bench-mate, Matthew Alan Jones, for his singing entertainment.

I am very grateful to Professor Mike Blatt and Dr. Ufo Sutter for their expertise training in confocal microscopy. Many thanks to Prof. D. Kliebenstein (U.C. Davis, U.S.A.) for providing the *uvr8-1 (Ler)* mutant, Dr. Roman Ulm for the *cop1-4 (Ws)* mutant and Dr. R. Sablowski (John Innes Centre, Norwich, U.K.) for the 35S_{pro}GFP (*Ler*) seeds. I would also like to acknowledge my assessors at the University of Glasgow, Professor Bill Cushley, Dr. Joel Milner and Dr. Pawel Herzyk for all their suggestions and encouragement during my *Ph.D.* I am very grateful to the Gatsby Charitable Foundation for funding my attendance to scientific conferences and for giving me the opportunity to be a member of the Gatsby family. Many thanks to the Gatsby Advisers, Dr. John Gray, Dr. Jane Langdale, Dr. Enrico Coen and Dr. Liam Dolan for their constant support and invaluable advice during the Gatsby Training weekends in Cambridge. Also, I am extremely grateful to Professor Winslow Briggs, who introduced me into the fascinating world of photobiological research by allowing me to work in his lab during my undergraduate work placement. Many thanks to Dr. Trevor Swartz for inspiring conversations on photoreceptors, and Dr. Meng Chen for his extremely useful

suggestions on my research project during the Gordon Conference in Il Ciocco. A very special thank you to Dr. John M. Christie for being my second, unofficial supervisor and a source of inspiration for my research. And finally, and most importantly, I would like to thank my family for their constant love, support and encouragement and for providing the ideal environment for writing up most of this thesis on the island of Kos.

PREFACE

The experimental work of this study has resulted in two publications. The majority of Chapters 3 and 4 are published in Kaiserli and Jenkins (2007) UV-B promotes rapid nuclear translocation of the Arabidopsis UV-B specific signalling component UVR8 and activates its function in the nucleus. *Plant Cell*, **19**, 2662-2673. Eirini Kaiserli is also a co-author of Brown B. A., Cloix C., Jiang G. H., Kaiserli E., Herzyk P., Kliebenstein D. J., and Jenkins G.I. (2005) A UV-B-specific signaling component orchestrates plant UV protection. *Proc. Natl. Acad. Sci. USA*. **102**, 18225-18230.

CONTENTS

Section	Page
Title	i
Dedication	ii
Acknowledgements	iii
Preface	v
Contents	vi
Figures	xii
Abbreviations	xvi
Summary	1
References	219

CHAPTER 1: PHOTORECEPTION AND SIGNAL TRANSDUCTION IN ARABIDOPSIS

1.1	Introduction	4
1.2	Light perception and signalling in Arabidopsis	5
1.3	UV-B mediated responses	10
1.4	Regulation of gene expression by UV-B in Arabidopsis	15
1.5	UV-B signal transduction in plants	16
1.6	UV-B signalling in mammalian systems	21
1.7	Mutants altered in UV-B signalling – a genetic approach	23
1.8	Isolation and characterisation of UVR8	26
1.9	Conclusions	29
1.10	Aims of this study	30

CHAPTER 2: MATERIALS AND METHODS

2.1	Materials	40
2.2	General Laboratory Preparation Procedures	42
2.3	Plant Material	43
2.4	Plant Treatments	44
2.5	Amplification of Plasmid DNA	47
2.6	DNA and RNA methods	48
2.7	Semi-quantitative Reverse-Transcriptase Polymerase Chain Reaction	52
2.8	Generation of stable transgenic Arabidopsis lines	54

2.9	Protein Methods	59
2.10	Immunoprecipitation of GFP-tagged proteins from plant extracts	63
2.11	Chromatin Immunoprecipitation Assay	64
2.12	Confocal Microscopy	66
2.13.	Yeast-Two-Hybrid Methods	66

CHAPTER 3: PROTEIN ANALYSIS AND SUBCELLULAR LOCALISATION OF UVR8

3.1	Introduction	70
3.2	Characterisation of UVR8-specific antibodies	70
3.3	UVR8 is abundant and ubiquitously expressed in Arabidopsis	71
3.4	The abundance of UVR8 is unaffected by light	72
3.5	GFP-UVR8 stably expressed in Arabidopsis is functional	73
3.6	GFP-UVR8 is localised in the cytoplasm and the nucleus of plant cells	75
3.7	GFP-UVR8 subcellular localisation is observed in a range of cell types and throughout development	76
3.8	UV-B induces nuclear enrichment of GFP-UVR8 and native UVR8	77
3.9	The nuclear accumulation of GFP-UVR8 is specific to UV-B, rapid and sensitive to low fluence rates of UV-B	80
3.10	The induction of UVR8-regulated genes in response to UV-B is consistent with the nuclear enrichment of UVR8	82

3.11	Discussion	83
------	------------	----

CHAPTER 4: ANALYSIS OF UV-B INDUCED NUCLEAR ACCUMULATION AND ACTIVITY OF CYTOSOLIC AND NUCLEAR UVR8

4.1	Introduction	116
4.2	UVR8 is functional in the presence of a nuclear export signal	116
4.3	Cytosolic NES-GFP-UVR8 is imported into the nucleus in response to UV-B	117
4.4	Kinetics and fluence rate dependence of NES-GFP-UVR8 nuclear import	119
4.5	Pharmacological studies on the nuclear import of NES-GFP-UVR8	120
4.6	A transient expression system for rapid analysis UVR8 nuclear import	122
4.7	Constitutively nuclear localised NLS-GFP-UVR8 is functional	123
4.8	Nuclear accumulation of NLS-GFP-UVR8 is unaffected by UV-B	124
4.9	Discussion	125

CHAPTER 5: STRUCTURE –FUNCTION ANALYSES OF UVR8

5.1	Introduction	151
5.2	Deletion analysis of UVR8 based on sequence alignment with RCC1	151
5.3	The N-terminus of UVR8 is important for function	152

5.4	GFP- Δ NUVR8 is defective in the UV-B dependent nuclear enrichment response but retains its chromatin association	153
5.5	GFP- Δ CUVR8 is not functional in Arabidopsis	154
5.6	The C-terminus of UVR8 is not required for the UV-B specific nuclear enrichment	155
5.7	GFP- Δ NLSUVR8 is active in Arabidopsis	157
5.8	Deletion of the putative NLS does not impair UVR8 nuclear localisation or UV-B induced nuclear import	158
5.9	UVR8 antibodies are highly specific	159
5.10	Discussion	160

CHAPTER 6: YEAST-TWO-HYBRID STUDIES FOR THE IDENTIFICATION OF PROTEINS INTERACTING WITH UVR8

6.1	Introduction	182
6.2	UVR8 used as a bait protein in the yeast-two-hybrid system	182
6.3	Screening of an Arabidopsis cDNA library for identification of UVR8 interacting partner(s)	184
6.4	UVR8 used as the bait in a directed yeast-two-hybrid approach	185
6.5	Purification of GFP-UVR8 <i>in planta</i>	188
6.6	Discussion	189

CHAPTER 7: FINAL DISCUSSION

7.1	Introduction	202
-----	--------------	-----

7.2	UV-B stimulates rapid nuclear accumulation of UVR8	203
7.3	What is the mechanism underlying the UV-B induced nuclear accumulation of UVR8?	205
7.4	The N-terminus of UVR8 is required for nuclear accumulation in response to UV-B	209
7.5	UVR8 is responsive to UV-B in the cytosol and in the nucleus	210
7.6	The C-terminus of UVR8 is essential for function	212
7.7	Attempts to identify UVR8-interacting proteins	213
7.8	Conclusions	214
7.9	Future work	215

FIGURES

Figure	Title	Page
CHAPTER 1		
1.1	Photoreceptor families in Arabidopsis	33
1.2	A schematic of the phenylpropanoid biosynthesis pathway	35
1.3	Model of the cross-talk between light signalling pathways controlling <i>CHS</i> expression in mature Arabidopsis leaf tissue	36
1.4	A fraction of genes regulated by UVR8 in response to UV-B	37
1.5	Primary and secondary sequence alignment of human RCC1 and Arabidopsis UVR8	38
1.6	Superimposition of RCC1 and UVR8 structure	39
CHAPTER 2		
2.1	Spectra of light qualities used in this study	46
CHAPTER 3		
3.1	Characterisation of UVR8-specific antibodies	92
3.2	UVR8 protein is abundant in most plant tissues	93
3.3	UVR8 protein levels are unaffected by different light qualities	94
3.4	Generation of transgenic Arabidopsis plants expressing GFP-UVR8 from the native <i>UVR8</i> promoter	96
3.5	GFP-UVR8 is functional in transgenic <i>uvr8-1</i> plants	98
3.6	GFP-UVR8 is associated with the promoter region of <i>HY5</i>	100
3.7	GFP-UVR8 is subcellularly localised in the nucleus and cytosol of epidermal cells	101

3.8	UVR8 co-purifies with the total and soluble protein fractions from wild-type plants	102
3.9	GFP-UVR8 is subcellularly localised in the nucleus and cytosol of cells in different plant tissues	103
3.10	UVR8 _{pro} GFP-UVR8 is expressed at very early developmental stages	105
3.11	UV-B induces nuclear enrichment of GFP-UVR8	107
3.12	Quantification of the UV-B-induced nuclear enrichment of GFP-UVR8	108
3.13	UV-B induces nuclear enrichment of UVR8 protein in wild-type plants	109
3.14	Nuclear enrichment of GFP-UVR8 is UV-B specific, rapid and very sensitive to UV-B	110
3.15	UV-B stimulates a rapid increase in UVR8 regulated gene Expression	112
3.16	UV-B stimulates UVR8 regulated gene expression at very low fluence rates of UV-B	114
 CHAPTER 4		
4.1	Generation of transgenic Arabidopsis plants expressing NES-GFP-UVR8	133
4.2	NES-GFP-UVR8 is functional in <i>uvr8-1</i> transgenic plants	134
4.3	UV-B overcomes the nuclear export signal (NES) and induces nuclear import of NES-GFP-UVR8	136
4.4	NES-GFP-UVR8 protein levels are unaffected by UV-B exposure	138
4.5	UV-B stimulates a rapid nuclear enrichment of NES-GFP-UVR8	139

4.6	UV-B stimulates nuclear enrichment of NES-GFP-UVR8 at very low fluence rates	141
4.7	UV-B induced nuclear enrichment of NES-GFP-UVR8 is unaffected by inhibitors of phosphorylation, de-phosphorylation or protein synthesis	143
4.8	UV-B induces nuclear enrichment of transiently expressed NES-GFP-UVR8 in <i>Nicotiana benthamiana</i>	145
4.9	Generation of transgenic Arabidopsis plants expressing NLS-GFP-UVR8	146
4.10	NLS-GFP-UVR8 is functional in <i>uvr8-1</i> transgenic plants	147
4.11	NLS-GFP-UVR8 is constitutively localised in the nucleus in all light conditions	149
4.12	NLS-GFP-UVR8 protein levels are unaffected by UV-B exposure.	150

CHAPTER 5

5.1	Deleted peptide sequences of UVR8 positioned on a structure alignment of RCC1 and UVR8	165
5.2	Generation of transgenic Arabidopsis plants expressing GFP- Δ NUVR8	166
5.3	GFP- Δ NUVR8 is not functional in transgenic <i>uvr8-1</i> plants	167
5.4	GFP- Δ NUVR8 shows impaired nuclear accumulation in response to UV-B	169
5.5	GFP- Δ NUVR8 is associated with the promoter region of <i>HY5</i>	170
5.6	Generation of transgenic Arabidopsis plants expressing GFP- Δ CUVR8	171
5.7	GFP- Δ CUVR8 is not functional in <i>uvr8-1</i> transgenic plants	172
5.8	UV-B induces nuclear accumulation of GFP- Δ CUVR8	174

5.9	GFP-ΔCUVR8 is associated with the promoter region of <i>HY5</i>	174
5.10	Generation of transgenic Arabidopsis plants expressing GFP-ΔNLSUVR8	176
5.11	GFP-ΔNLSUVR8 is functional in <i>uvr8-1</i> transgenic plants	177
5.12	UV-B induces nuclear accumulation of GFP-ΔNLSUVR8	179
5.13	GFP-ΔNLSUVR8 is associated with the promoter region of <i>HY5</i>	180
5.14	Specificity of UVR8 specific antibodies	181

CHAPTER 6

6.1	Expression of UVR8 in yeast	195
6.2	Autoactivation test of UVR8 in yeast	196
6.3	Titration test of 3-Amino-1,2,4-Triazole concentration as a His ^r reporter marker	197
6.4	UVR8 does not interact with either DET1 or HY5 in yeast	198
6.5	UVR8 does not interact with COP1 in yeast and is not degraded via COP1 in Arabidopsis	199
6.6	UVR8 does not interact with either BRI1 kinase or CRY2 in yeast	200
6.7	GFP-UVR8 can be immunoprecipitated and detected on a silver-stained protein gel	201

CHAPTER 7

7.1	Schematic of UVR8 activation in response to UV-B	218
-----	--	-----

ABBREVIATIONS

AD	activation domain
ADO	Adagio
AMV	Avian Myeloblastosis Virus
3AT	3-Amino-1, 2, 4-Triazole
BD	DNA binding domain
BLAST	Basic Local Alignment Search Tool
BR	Brassinosteroid
BZR1	Brassinazole resistant 1
BSA	Bovine Serum Albumin
bZIP	b-helix zipper
ChIP	Chromatin Immunoprecipitation
CHS	Chalcone synthase
<i>chum</i>	Chalcone synthase underexpressing mutant
Col	Columbia
COP	Constitutive photomorphogenic
CPD	Constitutive photomorphogenesis and dwarfism
CPDs	Cyclobutane pyrimidine dimers
CRY	Cryptochrome
CSN	COP9 signalosome
Δ	deletion
DAPI	4',6-Diamidino-2-phenylindole

DASH	Drosophila Arabidopsis Synechocystis Human
DDB1	Damaged DNA binding protein 1
DEPC	Diethyl pyrocarbonate
DET	De-etiolated
DFR	Dihydroflavonol 4-reductase
DMSO	Dimethyl sulfoxide
ds	double stranded
DTT	1,4-Dithiothreitol
EDTA	Ethylenediaminetetraacetic acid
ELIP	Early light-induced protein
EMS	Ethyl methane sulfonate
ERK	Extracellular signal-regulated kinase
EtBr	Ethidium bromide
EtOH	Ethanol
FAD	Flavin adenine dinucleotide
fah	Ferrulic acid hydroxylase
FHY	Far-red elongated hypocotyl
FHL	Far-red elongated hypocotyl-like
FKF	Flavin-binding kelch domain f box protein
FMN	Flavin mononucleotide
FR	Far-red light
GAL	Galactosidase

GEF	Guanine nucleotide exchange factor
GFP	Green fluorescent protein
H	Histone
HXK1	Hexokinase receptor 1
HFR	High fluence response
HRP	Horseradish peroxidase
HY	Long hypocotyl
H ₂ O ₂	Hydrogen peroxide
HFR	High fluence response
HW	High white light
HY	Long hypocotyl
ICX	Increased chalcone synthase expression
LB	Luria broth medium
<i>L. er</i>	Landsberg <i>erecta</i>
LFR	Low fluence response
LMB	Leptomycin B
LKP	LOV KELCH protein
LOV	Light oxygen voltage
LRU	Light responsive unit
Luc	Luciferase
LW	Low white light
MALDI-TOF MS	Matrix-assisted laser desorption time-of-flight mass spectrometry

MAPK	Mitogen-activated protein kinase
MES	2-(N-morpholino)ethanesulfonic acid
MOPS	3-(N-Morpholino)propanesulfonic acid
NASC	Nottingham <i>Arabidopsis</i> Stock Centre
NCBI	National Center for Biotechnology Information
NER	Nucleotide excision repair
NES	Nuclear export signal
NF	Nuclear factor
NLS	Nuclear localisation signal
NO	Nitric oxide
NPH	Non-phototropic hypocotyl
OD	Optical density
P _{FR}	Far-red light absorbing form of phytochrome
P _R	Red light absorbing form of phytochrome
PAL	Phenylalanine ammonia-lyase
PAR	Photosynthetically active radiation
PAS	Per / Arnt / Sim
PCR	Polymerase chain reaction
pH	$-\log_{10}$ (hydrogen ion concentration)
PHOT	Phototropin
PHR1	<i>Arabidopsis</i> type II CPD photolyase
PHY	Phytochrome

PIF	Phytochrome interacting factor
PKI	Protein kinase A inhibitor
PKS	Phytochrome kinase substrate
PMSF	Phenylmethanesulphonylfluoride
PR	Pathogenesis-related
Pro	Promoter
PYROA	Pyridoxine biosynthesis protein A
qRT-PCR	Quantitative reverse transcriptase polymerase chain reaction
RBCS	Ribulose-1,5-bisphosphate carboxylase small subunit
RCC1	Regulator of chromatin condensation
ROS	Reactive oxygen species
RT	Reverse transcriptase
RTK	Receptor tyrosine kinase
35S	Cauliflower mosaic virus 35S promoter
SA	Salicylic acid
SDS PAGE	Sodium dodecyl sulfate polyacrylamide gel electrophoresis
SE	Standard error of the mean
SOD	Superoxide dismutase
ss	single stranded
SV	Simian virus
TE	Tris-EDTA
tt	transparent testa

TAE	Tris-acetate EDTA
TBS-T	Tris buffered saline triton-X
TBS-TT	Tris buffered saline triton-X Tween
T-DNA	Transfer DNA
TEMED	N,N,N',N'-tetramethylethane-1,2-diamine
TF	Transcription factor
UGPase	UDP-glucose pyrophosphorylase
<i>uli3</i>	UV-B light insensitive mutant
UV	Ultraviolet
uvi	UV-B insensitive mutant
UVR	UV resistance locus
VLFR	Very low fluence response
v/v	Volume / volume
WT	Wild type
w/v	Weight / volume
x- α -gal	5-Bromo-4-chloro-3-indolyl alpha-D-galactopyranoside
YPD	Yeast Extract/Peptone/Dextrose medium
ZTL	Zeitlupe

SUMMARY

UV-B is an integral component of the daylight spectrum that regulates plant gene expression and development, but very little is known about how plants perceive UV-B. Although UV-B-induced damage and repair have been extensively investigated, the mechanisms by which UV-B is perceived as a signal, which mediates physiological and protective responses is not yet clearly understood neither in mammals, nor in higher plants. Low fluence rates of UV-B induce the expression of genes involved in UV-protective responses such as flavonoid biosynthesis and promote plant survival in UV-B.

The aim of this study is to contribute to the elucidation of the signal transduction events that lead to the acclimation of plants in response to non-damaging levels of UV-B ($< 3.5 \mu\text{mol m}^{-2} \text{s}^{-1}$). In particular, the characterisation of UVR8 (UV-RESISTANCE LOCUS 8), a UV-B specific signalling component, is carried out at the protein level. The function of UVR8 involves the orchestration of the expression of a range of genes mediating vital UV-protective responses, including those encoding light-regulated transcription factors HY5 and HYH, enzymes involved in the phenylpropanoid pathway, antioxidant and stress proteins (Brown *et al.*, 2005). UVR8 shows 30% sequence identity to the human regulator of chromatin condensation (RCC1) but differs both in activity and function. The phenotype of *uvr8* mutant plants is characterised by an increased susceptibility to UV-B and the lack of the UV-B-specific induction of genes involved in UV-protection, such as *CHS* (encoding the flavonoid biosynthetic enzyme chalcone synthase) and the transcription factor *HY5*. The UVR8-mediated regulation of transcription in response to UV-B seems to occur via the association of UVR8 with chromatin via histones in the promoter region of *HY5* (Brown *et al.*, 2005) and other genes involved in light signalling.

In this study, further investigation of the mechanism by which UVR8 acts as a UV-B specific signalling component is performed by employing a number of approaches including: spatial, temporal protein analysis, subcellular localisation studies, structure-function analyses, and the yeast-two-hybrid assay for the

identification of UVR8 interacting proteins.

To study spatial, temporal and wavelength specific UVR8 protein abundance anti-UVR8 peptide antibodies were generated. Western blot analyses showed that UVR8 is ubiquitously expressed in all plant tissues from the very early stages of development and at every light treatment tested (dark, white light, UV-B).

The subcellular localisation of UVR8 analysed by confocal fluorescence microscopy revealed that a fusion of UVR8 with green fluorescent protein (GFP) is localised in the cytoplasm and the nucleus of various plant tissues (leaf, hypocotyl, root, flower) and under various light fluence rates and qualities (white, red, UV-A, UV-B).

Interestingly, a treatment of low fluence rates of UV-B led to an increase of GFP-UVR8 protein accumulation in the nucleus, which was confirmed by western blot analysis based on protein fractionation studies in wild-type plants. The wavelength specificity, the kinetics and the fluence-rate sensitivity of GFP-UVR8 nuclear accumulation suggest that this response is UV-B specific, rapid (10 min UV-B) and very sensitive to very low fluence rates of UV-B ($0.1 \mu\text{mol m}^{-2} \text{s}^{-1}$). Protein synthesis does not seem to be involved in this process, as there is no change in the protein levels before and after a UV-B irradiation.

To assess the importance of the presence of UVR8 in the nucleus and the cytoplasm of the plant cell, *uvr8-1* transgenic plants were produced expressing either constitutively nuclear localised GFP-UVR8 fused to a nuclear localisation signal (NLS), or cytosolically retained GFP-UVR8 fused to a nuclear export signal (NES). Nuclear exclusion of NES-GFP-UVR8 fusion protein was sustained under most light conditions apart from UV-B, which induced nuclear import of the protein. This indicates that the mechanism involved in the nuclear accumulation of UVR8 can overcome an export signal either by masking it or by simply superseding it. Furthermore, the NES-GFP-UVR8 construct was functional after UV-B treatment, since it rescued the mutant *uvr8* phenotype. None of the inhibitor treatments tested (staurosporine, cycloheximide, cantharidin) was successful in blocking the UV-B induced nuclear import of NES-GFP-UVR8, although they impaired the UVR8

regulated induction of *CHS* expression. Thus, no evidence is presented for a specific protein modification, which could control this response.

Constitutive nuclear localisation of NLS-GFP-UVR8 had no effect on the function of the protein according to complementation analyses. Furthermore, no change in localisation, fluorescence intensity or protein abundance was observed in response to white light or after a UV-B irradiation. These results indicate that the constitutive nuclear localisation of UVR8 is not sufficient for constitutive activation of UVR8 regulated gene expression and that a UV-B stimulus is still necessary to trigger these responses. Unfortunately, based on the current data it cannot be concluded whether the UV-B signal perception occurs in the nucleus or in the cytosol of the plant cell.

To investigate the structure-function relationship within the UVR8 protein, deletion analyses followed by complementation studies in transgenic plants were performed. More specifically, deletion of the first 23 amino acids at the N-terminus of UVR8 impaired its nuclear accumulation in response to UV-B. Deletion of a 27 amino acid region near the C-terminus had no effect on the UV-B dependent re-localisation of the protein, but abolished UVR8 regulated gene expression. In addition, a highly basic sequence at the extreme C-terminal of UVR8, resembling a putative monopartite nuclear localisation signal, was deleted. Subcellular localisation and complementation analyses suggest that this sequence does not serve as a nuclear localisation signal, it is not involved in the UV-B induced nuclear accumulation and its absence does not affect UVR8 protein function. Chromatin immunoprecipitation assays show that none of the regions deleted is required for chromatin association and none of the deletions affects subcellular localisation in white light.

In order to identify interacting partners for UVR8, the yeast-two hybrid system was used. Unfortunately no interacting proteins have been identified, neither from a screen, nor by directed-interaction studies. A different approach could be employed in the future involving size exclusion chromatography of protein extracts from plants in order to establish whether UVR8 functions as part of a complex *in vivo*.

CHAPTER 1

LIGHT PERCEPTION AND SIGNALLING IN ARABIDOPSIS

1.1 Introduction

Solar radiation is a vital source of energy for all terrestrial organisms. The quality of light that reaches the surface of the earth ranges from non-visible ultraviolet (280 nm) to visible (350-700 nm) regions of the electromagnetic spectrum. According to quantum mechanics, the shorter the wavelength, the higher the energy it contains and the more detrimental its effects on biological macromolecules. Fortunately, the earth is surrounded by a stratospheric ozone layer, which completely filters out UV-C and absorbs a great proportion of the UV-B irradiation. As a result, the UV-B light content is minimised to approximately 2% of the total amount of solar radiation (Caldwell *et al.*, 2003). However, minor fluctuations in the depth of the ozone layer either due to anthropogenic, atmospheric pollutants or natural factors (latitude, altitude, season), allow higher amounts of UV-B to penetrate, and may potentially cause severe damage to biological systems. Exposure to high levels of UV-B is associated with melanomas, eye damage and immunosuppression in mammals, whereas inhibition of phototaxis and impaired growth have been observed in ciliates and plants, respectively. On the other hand, low levels of UV-B, not only have non-damaging effects, but most importantly trigger adaptive responses such as protection against damage, which are necessary for survival under stress conditions (Jansen *et al.*, 1998; Jenkins and Brown, 2007).

Although UV-B-induced damage and repair have been extensively investigated, the mechanisms by which UV-B is perceived as a signal, which mediates protective responses is not yet clearly understood either in mammals, or in higher plants. The aim of this project is to contribute to the elucidation of the signal transduction events that lead to the acclimation of plants in response to non-damaging levels of UV-B ($< 4\mu\text{mol m}^{-2} \text{ s}^{-1}$). In particular, the focal point of this research is a gene product; UV-resistance

locus 8 (UVR8) that seems to be a key signalling component with a significant role in the regulation of expression of a number of specific photo-protective genes. The biological approaches that have been employed in order to identify the receptor-transducers-effectors involved in UV-B signalling in plants will be discussed, with the aim to explain the importance of the protein under investigation in this context.

1.2 Light perception and signalling in Arabidopsis

Most living organisms have acquired a photosensory system to optimise their survival. Photosensory mechanisms have been developed throughout evolution to mediate responses ranging from the phototactic behaviour of microorganisms to the visual capability of animals. As one would expect, out of all organisms, it is plants that have evolved the most sophisticated photoreceptor systems, due to their direct dependence on light for survival. There are three families of photoreceptors in plants, each specialised in the perception of specific light qualities depending on the type of their associated chromophore(s) (Figure 1.1).

1.2.1 Phytochromes

The phytochrome family consists of five members (phyA, phyB, phyC, phyD, phyE) and was the first class of plant photoreceptors to be identified. Phytochromes absorb principally within the red and far-red region of the electromagnetic spectrum and mediate a plethora of light-regulated developmental responses in plants (Franklin *et al.*, 2005). Phytochrome protein structure is characterised by an N-terminal photosensory domain that non-covalently associates with the tetrapyrrole chromophore, phytochromobilin, and a histidine-like kinase at the C-terminus (Jiao *et al.*, 2007). Depending on the red/far-red light content, phytochromes exist in two

isoforms, Pr or Pfr. Pr primarily absorbs red light, which results in photoconversion to its biologically active, Pfr, form (Franklin *et al.*, 2005).

Upon illumination, both phyA and phyB in the form of activated homo-dimers translocate from the cytoplasm into the nucleus, where they form “speckles” (Yamaguchi *et al.*, 1999, Gil *et al.*, 2000, Hisada *et al.*, 2000). The biological role of phytochrome nuclear speckle formation is not clear yet, but it is speculated that nuclear bodies are sites for either storage or assembly of splicesomal components, whose activity is regulated by phosphorylation (Docquier *et al.*, 2004). From phytochrome photoactivation to the induction of biological responses, a number of signal transduction events are involved. Homo and hetero-dimerisation among phytochromes, phosphorylation/dephosphorylation and protein-protein interactions play a major role in the induction of a wide array of light-regulated responses (Spalding and Folta, 2005).

Yeast-two-hybrid analyses have identified a number of interacting partners including transcription factors, such as PIF3 (phytochrome interacting factor 3), a basic-helix-loop-helix factor that binds a light response element of many light regulated genes (Martinez-Garcia *et al.*, 2000). Although PIF3 was originally considered as a positive regulator of phytochrome-induced signalling, recent evidence shows that light mediates phytochrome-dependent PIF3 degradation, suggesting that PIF3 is a negative regulator of phy-induced signalling (Monte *et al.*, 2007).

Furthermore, the C-terminal histidine-like kinase domain of phytochrome interacts with various phosphorylation substrates such as: PKS1 (phytochrome kinase substrate 1) (Fankhauser *et al.*, 1999), the UV-A/blue light photoreceptors cryptochromes 1 and 2 (Ahmad *et al.*, 1998) and the clock proteins ZTL/ADO1 (zeitlupe/adagio1) (Jarillo *et al.*, 2001), resulting in photoreceptor regulation and integration of other light signal transduction pathways.

1.2.2 Cryptochromes

The cryptochromes (cry1 and cry2) absorb primarily UV-A and blue light through their two chromophores, an FAD and a pterin molecule, located at the N-terminal part of each protein (Batschauer *et al.*, 2007). Cryptochromes undergo blue light-dependent phosphorylation, which is regulated by their C-terminal DAS domain (Shalitin *et al.*, 2002). Membrane depolarisation events have been shown to be involved in cryptochrome-mediated signal transduction (Spalding *et al.*, 2002). A protein phosphatase, PP7, seems to play an indirect role in blue light responses mediated by cry1 with the former de-phosphorylating a yet unknown key signalling component (Moller *et al.*, 2003).

The subcellular localisation of cryptochromes varies. Cry1 is mainly nuclear in the dark and translocates in the cytoplasm in response to light, whereas cry2 is constitutively nuclear (Wang *et al.*, 2001; Jiao *et al.*, 2007). There, they interact with the ubiquitin ligase COP1 (Yang *et al.*, 2001) and rescue HY5 from degradation. HY5 is a bZIP transcription factor, which positively regulates phytochrome and cryptochrome-induced photomorphogenesis (Koorneff *et al.*, 1980; Ulm and Nagy, 2005). Furthermore, cryptochromes have been shown to interact with phytochromes and the ZTL clock protein, demonstrating an integration of different light signals for the oscillation of the circadian clock (Shalitin and Lin, 2003).

Although cryptochromes show sequence similarity to bacterial DNA photolyases, their function involves the regulation of photomorphogenic responses including inhibition of hypocotyl elongation, cotyledon expansion, flowering and circadian rhythms (Spalding & Folta, 2005). Cryptochromes are also found in bacteria and mammals but are mainly associated with the regulation of circadian rhythms (Lin and Shalitin, 2003).

However, the newly identified member of the cryptochrome family cry3 or cry-DASH, actually has DNA photolyase activity and specialises in recognising cyclobutane pyrimidine dimers in ssDNA (Selpy and Sancar, 2006). Subcellular localisation studies have shown that Cry3 is targeted to the chloroplasts, thus possibly

protecting and regulating the chloroplastic genome. (Kleine *et al.*, 2003; Jiao *et al.*, 2007).

1.2.3 Phototropins

Although phototropism is one of the first photo-responses monitored in plants, the photoreceptors that elicit this response, the phototropins, are the most recently discovered plant photoreceptor family in Arabidopsis (Briggs, 2006). There are two members in the phototropin family in Arabidopsis, phot1 and phot2, both absorbing within the UV-A and blue light region of the electromagnetic spectrum.

Phot1 and phot2 are Ser/Thr protein kinases, which undergo a blue light-dependent autophosphorylation (Christie *et al.*, 1998). Phototropins were named after their main function in phototropism, the directional orientation of plant hypocotyls towards blue light (Huala *et al.*, 1997). In addition, phot1 and phot2 mediate stomatal opening, chloroplast movement, inhibition of hypocotyl elongation, leaf expansion and, possibly, solar tracking (Christie and Briggs, 2002).

One of the most interesting aspects of phototropin action is the photocycling of their chromophores. Each phototropin contains two chromophore binding domains LOV1 and LOV2 (light, oxygen or voltage sensing), which form a covalent association with FMN (flavin mononucleotide) in response to blue light (Christie *et al.*, 2002). Nuclear magnetic resonance studies have shown a light-dependent conformational change possibly induced by the formation of the covalent bond between the protein and the chromophore. This structural change is believed to mediate intramolecular signal transduction from the sensor to the kinase domain (Harper *et al.*, 2003).

Phot1 and phot2 are both associated with the plasma membrane of various plant cell types and organs (Sakamoto and Briggs, 2002; Kong *et al.*, 2006). However, blue light illumination induces internalisation of phototropins, which is necessary either for receptor desensitisation or for signal transduction purposes (Sakamoto and Briggs, 2002; Kong *et al.*, 2006).

To date, no kinase substrate has been identified for either phot1 or phot2. However, a number of phototropin-interacting proteins have been isolated. NPH3 was identified based on its non-phototropic hypocotyl phenotype and quite possibly serves as a molecular scaffold for the assembly of phototropin-associated signalling components (Liscum and Stow-Evans, 2000). Further investigation is required to unravel the intermolecular signal transduction pathways of phototropins.

Although the phototropins are the only higher plant proteins containing two LOV domains (LOV1 and LOV2), there are various proteins in plants, fungi and bacteria containing a single phototropin-like LOV domain (Christie, 2007). For example, a novel family of plant photoreceptors, consisting of ZTL, LKP2 and FKF1, each contain a LOV domain and are involved in the regulation of circadian rhythms (Christie, 2007). Furthermore, 29 more LOV-containing proteins have been reported in various bacterial species. Whether they all behave as photoreceptors or have evolved other sensory roles remains to be discovered (Christie, 2007).

1.2.4 UV-B photoreceptor?

The existence of a UV-B photoreceptor has been very controversial for many years. A number of factors contribute to the difficulty in the identification of this elusive photoreceptor. First, many biological molecules, such as the tryptophan residues in proteins, nucleic acids, phospholipids and any aromatic compound, can absorb UV-B non-specifically. Furthermore, many UV-B responses are also regulated by other photoreceptors through complex networks of interacting signal transduction pathways (Frohnmeier & Staiger, 2003). There are diverse theories contradicting the existence of a UV-B specific photoreceptor, which were renounced by experimental evidence. For example, phytochromes and cryptochromes were thought to act as UV-B sensors because they partially but not optimally absorb in the UV-B region of the spectrum. A number of physiological responses, such as the inhibition of hypocotyl growth, are regulated by all three families of plant photoreceptors (Spalding & Folta,

2005). Mutants of these photoreceptors, however retain a UV-B specific induction of inhibition of hypocotyl growth (Kim *et al.*, 1998; Suesslin & Froh Meyer, 2003). In addition, as will be discussed later, a UV-B specific induction of *CHALCONE SYNTHASE (CHS)* gene expression is still evident in phytochrome and cryptochrome mutants (Wade *et al.*, 2001).

A different hypothesis suggests that DNA damage could act as the signal for UV-B signal transduction (Britt, 1999). If this is true, a general stress response would be triggered involving DNA repair, cell cycle arrest and ROS detoxification. The existence of physiological non-stress related UV-B responses (inhibition of hypocotyl growth, photoprotective pigment accumulation) and the lack of correlation between DNA damage and induction of these responses argue against the above hypothesis (Kim *et al.*, 1998, Frohnmeyer, *et al.*, 1999). In addition, the UV-B specific response action spectrum has a maximum between 290 to 310 nm, whereas the DNA absorption spectrum is between 250-280 nm (Herrlich *et al.*, 1997).

Recent data suggest that brassinosteroids (BR) are involved in the signalling pathway during UV-B stress (Savenstrand *et al.*, 2004). Brassinosteroids regulate photomorphogenesis, developmental and stress tolerance responses. Mutants in BR perception or synthesis show impaired but not blocked UV-B induction of some UV-B regulated genes: *CHS*, *CHI*, *PRI*, *PYROA*. (Savenstrand *et al.*, 2004). Further studies are necessary in order to clarify the role of BR in UV-B signal transduction.

1.3 UV-B mediated responses

The impact of solar UV-B on plants varies depending on the fluence rates that reach the surface of the earth. Field studies have shown that the higher the altitude and the latitude, the more pronounced the effect of the ozone layer depletion is on plants (Caldwell *et al.*, 2007). Although subsoil environments allow minimal UV-B penetration, the morphology of the roots and the chemical composition of the soil are greatly affected by UV-B (Caldwell *et al.*, 2007).

In general, the responses induced by higher than ambient levels of UV-B have inhibitory effects on plant growth and development mainly due to macromolecular damage. When the rate of damage exceeds the rate of repair, more pronounced effects, such as leaf necrosis and senescence can be observed. On the contrary, lower fluence rates of UV-B are necessary for plant acclimation by mediating several photo-protective responses, such as UV-absorbing pigment accumulation and the activation of antioxidant and DNA repair enzymes. An indirect effect of the UV-B induced acclimation in plants is the phenomenon of cross-tolerance, which enhances the resistance of plants to additional biotic and abiotic stress factors following UV-B exposure (Stratmann, 2003; Ulm and Nagy, 2005; Caldwell *et al.*, 2007).

1.3.1 UV-B as a damaging agent

The molecular nature of UV-B induced damage predominantly occurs at the level of macromolecular inactivation by cross-linking, oxidation or mutagenesis. Due to their absorption spectra, nucleic acids, lipids and proteins are prone to UV-B damage. UV-B photons have high energy levels. As a result, their reaction with DNA triggers the formation of cyclobutane-pyrimidine dimers (CPDs) and pyrimidine (6,4)-pyrimidinone products (Britt *et al.*, 1993). Such chemical alterations of the DNA can act as mutagenic agents, which impair the access of DNA/RNA polymerases and inhibit replication and expression of vital genes. In order to cope with these damages, most organisms have developed DNA repair mechanisms, which involve photoreactivation, excision repair and homologous recombination. DNA photolyases are the enzymes responsible for specific recognition and light-activated repair of CPDs and 6-4 photoproducts by catalysing the breakage of the cyclobutane ring (Waterworth *et al.*, 2002). Endonucleolytic cleavage and homologous recombination are general repair mechanisms for removing mutations and DNA lesions. Ries *et al.*, (2002) have shown that UV-B radiation increases the frequency of chromosomal rearrangement by homologous recombination. Although excision repair and homologous recombination

are considered as the “dark” repair machinery, photosynthetically active radiation (PAR) can potentiate UV-B induced homologous recombination (Ries *et al.*, 2000).

At the protein level, UV-B has adverse effects on the photosynthetic (D1 and D2 proteins of photosystem II) and translation machinery (Vass *et al.*, 1996; Casati and Walbot, 2004). Ribosomal protein – rRNA cross-linking and ribosomal protein oxidation are the mechanisms by which UV-B inhibits protein synthesis (Casati and Walbot, 2004). This phenomenon would explain why many components of the translational machinery in maize are affected by UV-B based on transcriptome analysis (Casati and Walbot, 2004).

High levels of UV-B are damaging. As a consequence, general cellular stress responses are induced. At the whole-plant level, extensive exposure to UV-B results in reduced plant biomass and crop yield, mainly due to growth inhibition as well as tissue destruction (Casati & Walbot, 2004; Caldwell *et al.*, 2007). There is evidence that growth inhibition can be caused by an interference in the levels of the phytohormone auxin. Auxin is a positive regulator of plant growth and development. Destruction of auxin by UV-B-induced photooxidation creates hormonal imbalance, which may change plant morphology (Huang *et al.*, 1997). Decomposition of auxin at the site of UV-B irradiation was suggested to be the reason for the residual positive phototropic response of the double mutant *phot1phot2* (Eisinger *et al.*, 2003).

Some of the morphological repercussions of UV-B on plant tissue are the characteristic leaf curling and chlorophyll redistribution (Day and Vogelmann, 1995), which minimise exposure and consequently damage by UV-B (Jansen, *et al.*, 1998). An equivalent phenomenon is the chloroplast movement away from high intensities of blue light, and is mediated by *phot2* (Kagawa *et al.*, 2001). Increases in flavonoid accumulation and epidermal layer thickening serve as a photoprotective screen, which specifically blocks the penetration of UV-B into photosynthetically active tissues.

1.3.2 UV-B induced developmental and acclimation responses

Despite its harmful effects on biological tissues, low levels of UV-B mediate various physiological responses. One of the first stages in plant development involves photomorphogenesis, the generation of photosynthetic apparatus and alterations in plant morphology and gene expression in order to maximise light utilisation for energy production. The inhibition of hypocotyl elongation, cotyledon expansion, stomatal opening and the induction of positive phototropic curvature are regulated by the known plant photoreceptors in addition to a distinct UV-B specific pathway (Kim *et al.*, 1998, Eisinger *et al.*, 2003; Suesslin and Frohnmeyer, 2003; Shinkle *et al.*, 2004). The UV-B specific pathway that regulates developmental processes appears to operate independently of the DNA damage pathway according to action spectra comparisons (Kucera *et al.*, 2003). UV-B specific acclimation responses are primarily induced by changes in gene expression, which lead to an increase in the activity of photo-protective enzymes, accumulation of UV-absorbing secondary metabolites and stimulation of DNA damage repair.

1.3.2.1 Photoprotective compounds

The colonisation of plant predecessors on land exposed them for the first time to the harmful effects of UV-B radiation. As an evolutionary adaptation, plants developed physiological protective mechanisms such as the biosynthesis of UV-B absorbing pigments. Aromatic compounds are very efficient in absorbing ultraviolet radiation due to the unsaturated propene side chains and the hydroxyl rings they contain. Phenylpropanoids are secondary metabolites found in most plant species. There are many enzymes involved in the phenylpropanoid pathway (Figure 1.2) leading to various classes of by-products. L-phenylalanine ammonia lyase (PAL) catalyses the first step of phenylpropanoid biosynthesis. Some of the phenolic compounds produced by this metabolic pathway include hydroxycinnamic acids and

flavonoids. Hydroxycinnamic acids are polyphenols that are oxidised in response to pathogen attack and mechanical wounding and trigger the inactivation of invading proteins (hydrolytic enzymes of pathogens) (Taiz and Zeiger, 1998).

Flavonoids constitute the largest class of phenolic compounds. Chalcone synthase (CHS) is the enzyme that catalyses the condensation of two by-products from distinct biosynthetic pathways, the shikimate and the malonic acid pathway. Flavonoids are divided into four sub-groups: flavonols, isoflavones, flavones and anthocyanins. Anthocyanins are pigmented flavonoids that mainly accumulate in flowers and fruit that act as attractants mediating pollination and symbiotic relationships. Isoflavonoids act as phytoalexins, a type of antimicrobial agent. And, finally, flavones and flavonols are responsible for absorbing ultra-violet radiation as a protective mechanism against macromolecular damage. Flavones and flavonols are primarily located in flowers, and epidermal layers of leaves and stems and are stored in the vacuoles of the cells. Their specificity in absorbing only the harmful UV-B wavelengths and allowing the photosynthetically active radiation (PAR) to penetrate into the cells is a remarkable example of adaptive evolution of plants to solar radiation (Taiz and Zeiger, 1998). Exposure to UV-B increases the levels of flavonoid production, via the induction of CHS and other necessary biosynthetic enzymes (Jenkins and Brown, 2007).

The accumulation of secondary metabolites belongs to the acclimation class of UV-B mediated responses. In addition to UV-screening, flavonoids have a free radical scavenging activity (Landry *et al.*, 1995), which protects plant cells from the damaging effects of reactive oxygen species (ROS). It has been shown that mutants in flavonoid synthesis and accumulation are hypersensitive to UV-B radiation and oxidative damage (Landry *et al.*, 1995).

The induction of *CHS* expression, a key biosynthetic enzyme of the flavonoid pathway, is regulated by UV-B independently and in concert with UV-A/blue and red light (Wade *et al.*, 2001). Flavonoids and other phenolic compounds function as photoprotective pigments due to their ability to absorb the harmful component of solar radiation in addition to their anti-oxidative activity. The increase in the production of

such compounds allows plants that inhabit high latitudes/altitudes to endure extensive exposure to UV-B (Jordan, 1996).

Another acclimating response to UV-B is the induction of antioxidant enzymes, such as glutathione reductase, ascorbate peroxidase and superoxide dismutase (Rao *et al.*, 1996). Reactive oxygen species (ROS) are produced in response to biotic and abiotic stress stimuli (pathogens, wounding, UV-B). Their highly reactive status can damage lipids, nucleic acids and chlorophyll molecules (Shalitin *et al.*, 1986) and consequently impair growth and normal plant development. Scavenging of hydrogen peroxide (a form of ROS) has been shown to trigger the polymerisation of precursor compounds enhancing lignification – another UV-B screen layer (Shalitin *et al.*, 1986).

1.4 Regulation of gene expression by UV-B in Arabidopsis

Depending on the fluence levels of UV-B irradiation and the interaction with other light qualities and environmental factors, different classes of genes are regulated by UV-B. Low levels of UV-B stimulate the expression of genes involved in the phenylpropanoid biosynthetic pathway (*PAL*, *CHS*, *CHI*), ROS scavenging (superoxide dismutase, glutathione reductase, ascorbate peroxidase), plant photomorphogenesis (*HY5*, *HYH* and *MYB* transcription factors), photoprotection (*PHR1*) and genes encoding uncharacterised proteins such as *PYROA* (Brosche *et al.*, 2002, Ulm *et al.*, 2004; Brown *et al.*, 2005). Such changes in gene expression promote an acclimation response to protect plants prior to damage.

Higher levels of UV-B are required for the induction of the expression of DNA-repair genes (*RAD*) and stress-related genes (*PR1*) and the down-regulation of genes involved in photosynthesis (*RBCS*, *PSII D1*, *LHCB6*) and the control of the cell cycle, which leads to a reduced photosynthetic activity and growth arrest until damage is repaired (Casati and Walbot, 2004). Microarray analysis performed in maize demonstrates that several genes promoting chromatin remodelling are regulated by UV-B (Casati *et al.*, 2006). Chromatin remodelling regulates the accessibility of

transcription factors, other signalling components and photolyases to DNA. As a result, transcription and DNA repair are affected by the status and the conformation of chromatin (Casati *et al.*, 2006). The UV-B induced chromatin modification is a relatively unexplored area that may reveal important information on the mechanisms of UV-B-induced gene expression and UV-protection.

1.5 UV-B signal transduction in plants

Unlike the plethora of information obtained for the red and UV-A/blue light photoreceptor systems, the molecular identity of a putative UV-B photoreceptor is still unknown. As a means of identifying the receptor and the signalling components of the UV-B specific pathway(s), a series of approaches has been employed during the last few decades. The focus of such studies was mainly the characterisation of the pathway induced by lower than ambient levels of UV-B, which leads to UV-B specific developmental and acclimation response. A series of pharmacological, biochemical and genetic studies have provided valuable information on the signalling intermediates and key signal transducer components involved in UV-B signalling.

1.5.1 CHS-a system for studying UV-B induced gene expression

Chalcone synthase is a key metabolic enzyme, which is regulated by environmental stimuli, including light. The regulation of gene expression occurs at the level of transcription and varies temporally (developmental stage) and spatially (tissue) (Frohnmeyer *et al.*, 1992). In dark-grown plants *CHS* expression is regulated by phytochromes, the red/far-red photoreceptors (Frohnmeyer *et al.*, 1992). In addition, UV-B and UV-A/blue light induce an increase of *CHS* expression in etiolated seedlings and mature leaves in *Arabidopsis*, which is mediated by an unknown UV-B photoreceptor and the UV-A/blue light photoreceptors, predominantly cry1 (Jackson

and Jenkins, 1995). The interaction between UV-B and UV-A/blue signal transduction pathways for the induction of *CHS* expression has been shown to be synergistic, as the increase of the response was higher than additive (Fuglevand *et al.*, 1996). A separate pathway seems to induce a UV-B specific increase of *CHS* transcript levels mediated by an unknown photoreceptor, as *cry1* and *cry2* mutants retain *CHS* induction in response to UV-B (Fuglevand *et al.*, 1996, Wade *et al.*, 2001). A red light pre-irradiation seems to increase the *cry1*-mediated *CHS* expression via a functionally redundant action of phyA and phyB (Wade *et al.*, 2001). This event is also known as potentiation. A distinct mechanism of co-action of UV-A/blue and red light mediated predominantly by *cry1* and phyB respectively adds to the complexity of the model. On the other hand, phyB has been shown to act as a negative regulator of the UV-B inductive pathway (Wade *et al.*, 2001) (Figure 1.3). Investigation of the control of *CHS* gene expression has proven to be a good system to identify the components of UV-B signal transduction, since it is not induced by the known photoreceptors. Various methods, such as pharmacological, biochemical assays as well as molecular biological and genetic analyses have been employed in order to understand UV-B signalling. Most studies used *Arabidopsis thaliana* as a model plant, however other plant species such as parsley, tobacco, wheat, and oat have contributed significantly to our knowledge of UV-B regulated gene expression.

Pharmacological studies were based on an *Arabidopsis* photomixotrophic cell culture system, which had identical regulation of *CHS* expression as those observed in mature plant tissue (Christie and Jenkins, 1996). The effects of various inhibitors and agonists on the induction of *CHS* transcription in response to UV-A/blue and UV-B light were examined as a means to identify the signalling components involved. Experiments using nifedipine (a calcium channel blocker) and lanthanum (competitor of external Ca^{+2}) suggest that intracellular Ca^{+2} acts as a second messenger for UV-A/blue and UV-B mediated *CHS* induction. However, the fact that artificially increased levels of Ca^{+2} have no effect on *CHS* expression would imply that Ca^{+2} is essential but not sufficient as a signal transducer for this response (Christie and Jenkins, 1996). Alternatively, specifically localised Ca^{+2} sparks instead of total elevation of Ca^{+2} levels

may be required (Jenkins, 1997). Equivalent studies in parsley cell cultures have also shown that UV-B pulses lead to an increase in cytosolic $[Ca^{+2}]$ and activation of *CHS* expression (Frohnmeyer *et al.*, 1997; 1998; 1999). Although Ca^{+2} seems to be a common component of the distinct UV-A/blue and UV-B pathways, calmodulin is only involved in the signal transduction mediated by UV-B specifically (Christie and Jenkins, 1996). This was tested by using a calmodulin antagonist, which blocked the induction of *CHS* expression in response to UV-B. Incubations with additional pharmacological compounds, such as the Ser/Thr kinase inhibitors (staurosporine and K52a) and Ser/Thr phosphatase inhibitors (okadaic acid, cantharidin), blocked both UV-A/blue and UV-B induced *CHS* expression in Arabidopsis (Christie and Jenkins, 1996). In addition, UV-B irradiation can mediate changes in the phosphorylation status of cytoplasmic proteins in parsley (Harter *et al.*, 1994). These findings indicate that kinases and phosphatases are components of the UV-A/blue and UV-B signal transduction pathways. More recent results have suggested that nitric oxide has a role in *CHS* regulation by UV-B, although the way it functions is yet unclear (Mackerness *et al.*, 2001).

UV-B is responsible for the generation of reactive oxygen species (ROS), which can act as second messengers for UV-B stress responses (such as induction of pathogenesis related protein 1, PR1) but not for the induction of *CHS* expression (Kalbin *et al.*, 1997; Green and Fluhr, 1995; Brosche and Strid, 2003).

In order to understand the regulation of *CHS* gene expression at the level of transcription in response to UV-B, it was necessary to identify promoter elements and transcription factors necessary for this response. Most light regulated genes possess light responsive units (LRU) in their promoter regions. Parsley *CHS* promoter has two LRU, each containing consensus sequences for association of bZIP and MYB transcription factors in response to UV-B (Schultze-Lefert *et al.*, 1989; Weisshaar *et al.*, 1991). Arabidopsis *CHS* promoter contains a very similar LRU to the ones in parsley *CHS*. Fusions of the Arabidopsis *CHS* promoter to the molecular marker GUS were tested in cell cultures. The *CHS* promoter alone is sufficient to confer UV-A/blue and UV-B mediated induction of GUS expression in a similar manner as endogenous

CHS is normally induced (Hartmann *et al.*, 1998). Further studies on the transcription factors themselves will give more information on the regulation of gene expression in response to UV-B.

1.5.2 Transcription factors and other components regulating UV-B signalling in plants

As mentioned earlier, the induction of *CHS* expression leading to flavonoid biosynthesis is one of the best-characterised UV-B responses in plants (Brown and Jenkins, 2007). One of the major transcription factors regulating photomorphogenesis and light signalling in response to red/far-red, UV-A/blue and UV-B irradiation is HY5 (Osterlund *et al.*, 2000; Ulm *et al.*, 2004). HY5 is a basic leucine zipper transcription factor that is itself regulated at the level of transcription by UV-B (Ulm *et al.*, 2004; Brown *et al.*, 2005). At the post-translational level, HY5 protein stability is regulated by light, as the E3 ubiquitin ligase COP1 targets HY5 for degradation in the absence of a light stimulus (Osterlund *et al.*, 2000). HY5 associates with specific promoter light responsive elements *in vitro* and *in planta* and regulates the transcription of several light-induced genes (Chattopadhyay *et al.*, 1998; Lee *et al.*, 2007). Regulation of approximately 20% of all light-induced genes is attributed to the action of HY5 (Jiao *et al.*, 2007).

A very similar transcription factor to HY5 at the sequence level, HYH, is also regulated by UV-B, although the UV-B-specific regulation of gene expression by HYH is not well established yet (Ulm *et al.*, 2004; Brown *et al.*, 2005).

The E3 ubiquitin ligase COP1 is a light signalling component widely considered as a negative regulator of photomorphogenesis (Osterlund *et al.*, 2000). However, it has recently been shown to act as a positive regulator of light development specifically in response to UV-B irradiation (Oravec *et al.*, 2006). Mutant *cop1-4* plants show impaired induction of *HY5* and *CHS* gene expression in response to UV-B and fail to survive in the presence of higher than ambient levels of UV-B (Oravec *et*

al., 2006). Further experiments are necessary to investigate the dual role of COP1 and its mechanism of action in response to UV-B.

1.5.3 Cross-talk between UV-B and defence signalling pathways

As described earlier, high fluence rates of UV-B can act as a damaging agent and induce stress responses in higher plants. Gene expression studies have shown that biotic and abiotic stress stimuli can mediate common non-specific stress responses by inducing stress-related genes (Stratmann, 2003). As a result, the phenomenon of cross-tolerance operates in plants that are exposed to distinct and subsequent stress stimuli. An example of cross-tolerance is the increase in resistance of plants to herbivorous insects when pre-exposed to UV-B irradiation (Ballare *et al.*, 1996; Izaguirre *et al.*, 2003).

A number of signalling components involved in defence responses are activated in response to UV-B. In particular, UV-B can induce the biosynthesis of jasmonic acid, a second messenger in wound signalling in *Arabidopsis* (Mackerness *et al.*, 1999). In addition to jasmonic acid, ethylene is another signalling molecule involved in wound responses that is required for UV-B induced gene expression in *Arabidopsis* (Mackerness *et al.*, 1999). The induction of *PR1* and *PDF1.2* genes in response to UV-B is impaired in mutants involved in the ethylene and/or jasmonate signalling pathways (Mackerness *et al.*, 1999).

Furthermore, UV-B can lead to an increase in the levels of ROS, which can induce cellular damage or act as signalling messengers for the regulation of gene expression in response to various stress signals (Mackerness *et al.*, 1999; Stratmann, 2003). ROS, in the form of hydrogen peroxide, have been shown to stimulate MAPK signal transduction, which is involved in systemin induced wound signalling (Kovtun, 2000; Ryan and Pearce, 2003). Systemin is the wound signalling ligand for the leucine-rich-repeat receptor kinase SR160 in tomato (Ryan and Pearce, 2003). Evidence for convergence of the UV-B and wound induced signalling pathways at the level of

MAPK has been recently provided by pharmacological studies involving SR160 receptor activation or inhibition of signal transduction (Yalamanchili and Stratmann, 2002; Holley *et al.*, 2003). Whether SR160 or a similar receptor protein kinase is required for UV-B perception is currently unknown but cannot be excluded.

In general, it is not surprising that stress responses stimulated by UV-B and other abiotic or biotic factors share signalling components and effector secondary metabolite compounds, since plants have evolved mechanisms in order to survive exposure to multiple stresses. In addition to biotic factors, UV-B pre-irradiation enhances the tolerance of plants to either heat, freezing or drought mainly due to the accumulation of phenolic compounds, an acclimation response induced by UV-B (Caldwell *et al.*, 2007). However, further research is essential for the understanding of such complex signalling networks in order to improve agricultural practices and evaluate the implications of UV-B irradiation in a global ecological context.

1.6 UV-B signalling in mammalian systems

Although no UV-B photoreceptor has been identified in animal systems, the mechanisms of UV-B signal transduction in mammals have been more extensively investigated compared to plants. In mammalian systems two distinct sensing mechanisms exist and both have been characterised. The first one involves a nuclear signalling cascade originating from damaged DNA. In this case, DNA acts as the sensor (Devary *et al.*, 1991). Subsequent evidence suggested that a UV response could occur in the absence of a nuclear derived signal. Discovery of the cytoplasmically localised sensing mechanism was achieved by following a “backwards” approach (Devary *et al.*, 1993). First, the UV-induced genes (*c-jun*, *c-fos*) were identified, then their promoters and the phosphorylated transcription factors (AP1, NF- κ B) were analysed. Next, the modifying enzymes (proline-directed protein kinases ERK, MAPK) were traced which finally led to the receptors (receptor tyrosine kinases e.g, EGF). However, RTKs are not the UV-sensors. Upon ligand binding RTKs dimerise and

undergo autophosphorylation. Ras proteins are involved in the phosphorylation cascades triggered after RTK activation. UV radiation rapidly activates Ras and three phosphorylation cascades are involved in UV-induced signalling (Devary *et al.*, 1992). The use of RTKs (EGF inhibitor) inhibitors has been shown to block UV-responses involving ERK and c-jun activation (Sachsenmaer, *et al.*, 1994). It was Knebel and co-workers, who found that the UV-sensor is a tyrosine phosphatase (Knebel *et al.*, 1996). UV-induced oxidation of the –SH group, results in inactivation of its catalytic activity. As a result, higher levels of phosphorylated RTKs trigger the expression of UV-induced genes. The transcription factor NF- κ B is a common component of both nuclear and cytoplasmic pathways. In the absence of a stimulus NF- κ B resides in the cytoplasm due to its interaction with an inhibiting protein (I κ B). Upon UV irradiation, I κ B gets phosphorylated and targeted for proteolysis. Release from I κ B reveals the nuclear localisation signal (NLS) of NF- κ B, which translocates it into the nucleus to induce gene expression. Early UV-induced genes include transcription factors, whereas late genes include collagenase and melanine synthase (Bender *et al.*, 1997). Stabilisation of key regulatory proteins (p53, cdks) is also an important UV-induced regulation at the posttranslational level. Also, an interesting finding indicated that polyphenols from green tea, anthocyanin and hydrolyzable tannin-rich pomegranate fruit extract have a protective role against UV-B by modulating MAPK and NF- κ B pathways and inhibition of skin tumorigenesis in mice (Afaq *et al.*, 2003; 2005).

Other damaging agents such as ROS and γ -rays cause different types of DNA damage, but utilise partly the same signalling components as UV (Bender *et al.*, 1997).

The identity of the putative UV-B photoreceptor in plant systems is still cryptic. Could an equivalent mechanism to the RTK-associated UV-induced signalling exist in plants too? Plants do not have RTKs but have very similar MAPK cascades and transcription factors. So, the equivalent of mammalian growth factor receptors in plants might be a hormone Ser/Thr kinase receptor.

1.7 Mutants altered in UV-B signalling – a genetic approach

As a means to understand the physiological process of plant development and acclimation in response to UV-B a number of mutants have been isolated and characterised in *Arabidopsis thaliana*, the model organism for plants. *Arabidopsis* is a well-characterised plant at the molecular and genetic level with a completely sequenced genome. These mutants, depending on their altered phenotypic response to UV-B can be divided into two classes: UV-B hyposensitive and UV-B hypersensitive mutants.

1.7.1 UV-B tolerant mutants

This classification of mutants is based on gain of function mutations leading to increased resistance to the damaging effects of UV-B. To achieve this, either an overexpression of repair genes or an over-production of UV-absorbing compounds is required. For example, the UV-B insensitive mutant *uvi1* shows an increase in photoreactivation and DNA repair due to higher photolyase transcript levels (PHR1) in response to UV-B compared to wild-type plants. Tanaka et al., (2002) suggested that UVI1 regulates a UV-B induced DNA repair mechanism in a negative manner.

In the case of the *uvi1* mutant, the extreme tolerance to UV-B is conferred by an increased accumulation of phenolic compounds that confer its characteristic darker leaf colouration (Bieza & Lois, 2001). Increased levels of *CHS* expression in the absence of a stimulus followed by a further induction in response to UV-B imply that there is no defect in the UV-B mediated induction of *CHS* expression (Bieza & Lois, 2001). In addition, shorter hypocotyls and a late flowering phenotype suggest that UVT1 plays a role in the photosynthetically active radiation (PAR) regulation of *CHS* expression (Bieza & Lois, 2001).

Another mutant exhibiting an increased expression of *CHS*, *icx1*, was identified by Jackson *et al.*, (1995) based on transgenic lines stably transformed with a

CHS_{pro}::GUS promoter-reporter fusion. Mutagenesis and screening for increased levels of GUS expression identified ICX1, a negative regulator of UV-B induced *CHS* expression. Further experiments have shown that ICX1 regulates negatively multiple *CHS* inducing pathways, involving cry1, phyA, UV-B, cytokinin, sucrose and low temperature (Wade *et al.*, 2003). Further analysis at the protein level could give valuable information in the convergence of many pathways for the induction of a common gene, *CHS*.

1.7.2 UV-B hypersensitive mutants

Hypersensitivity to UV-B usually occurs due to a defect in DNA repair or in the synthesis or accumulation of photoprotective pigments. UV-B induced DNA repair is a damage tolerance mechanism, whereas accumulation of UV-absorbing compounds is a photoprotective mechanism necessary for avoiding damage. The importance of flavonoid accumulation in protection against UV-B is apparent in the *tt4* and *tt5* mutants (transparent testa) (Li *et al.*, 1993). These mutants are deficient in CHS and CHI enzymes of the flavonoid pathway, respectively (Li *et al.*, 1993). Both mutants are impaired in flavonoid synthesis but *tt5* seems to be more sensitive to UV-B than *tt4* due to reduced levels of sinapate esters that also act as UV-B absorbing pigments (Li *et al.*, 1993).

Fahl is a mutant lacking sinapate ester production due to a mutation in the gene encoding ferrulic acid hydroxylase (Chapple *et al.*, 1995). *tt4* and *fahl* mutants showed increased UV-B sensitivity not only at the morphological level (leaf damage), but also at the cellular level (oxidation of proteins and peroxidation of lipids) (Landry *et al.*, 1995).

UV-B irradiation has been used extensively for the identification of genes involved in the DNA repair machinery. Four mutants (*uvr1*, *uvr5*, *uvr7*, *uvh1*) deficient in DNA repair were identified based on their increased levels of photoproduct

accumulation in response to UV-B, compared to wild-type control plants (Britt *et al.*, 1993).

Recent experiments by Sakamoto *et al.*, (2005), identified a novel mechanism in plants that allows tolerance to DNA damage by a putative translesion synthesis machinery. This mechanism exists in animal systems and can use damaged DNA as the template for DNA synthesis by specialised polymerases. As a result, cell cycle arrest is avoided unless the damage is significant (Sakamoto *et al.*, 2005). In the UV-B sensitive mutant *rev3* DNA synthesis is blocked and UV-B irradiated roots show an increased growth arrest compared to a wild-type control (Sakamoto *et al.*, 2005). Further studies are required to characterise this mechanism of repair in plants and its regulation by UV-B.

In order to identify UV-B signalling components that may act independently from the DNA damage response, low levels of UV-B ($< 3 \mu\text{mol m}^{-2} \text{s}^{-1}$) are necessary for mutant screening. Suesslin and Frohnmeyer (2003) used short pulses of UV-B to trigger inhibition of hypocotyl growth without inducing DNA damage. Screening for mutants lacking a UV-B mediated inhibition of hypocotyl elongation led to the isolation of *uli-3* mutant (Suesslin and Frohnmeyer 2003). *Uli-3* showed reduced induction of *CHS* and *PR1* gene expression compared to the response in wild-type plants (Suesslin and Frohnmeyer 2003). In addition, it was found that *ULI-3* gene expression is induced in response to UV-B and the gene itself encodes a cytoplasmic protein. The exact role of *uli-3* in UV-B signal transduction remains to be uncovered.

Most of the mutants described above show defects either in the machinery for DNA repair or in the phenylpropanoid biosynthetic pathway. The only genes that seem to be involved further upstream, near the UV-B sensor, have phenotypes that suggest a possible role in the integration of multiple pathways that regulate the same response (*CHS* induction, inhibition of hypocotyl growth).

1.8 Isolation and characterisation of UVR8

1.8.1 Phenotypic analysis of *uvr8*

UV-resistance locus 8 (uvr8) mutant was isolated in *Arabidopsis* based on its hypersensitivity to low levels of UV-B irradiation (Kliebenstein *et al.*, 2002). *uvr8* is a very interesting mutant for several reasons. Firstly, the total absence of the induction of *CHS* expression in response to UV-B has not been observed before. Western blot analysis has also shown a lack of CHS protein accumulation in response to UV-B (Kliebenstein *et al.*, 2002). These results suggest that UVR8 plays a key role in the UV-B signal transduction pathway that leads to the induction of *CHS* expression, as there is no residual *CHS* increase by a redundant pathway. However, the complete blocking of UV-B induced *CHS* expression was not due to the loss of a general regulator of non-specific stress response. Two stress-induced genes *PR1* and *PR5* as well as ROS scavengers (SOD and vitamin C) were used as positive controls for normal induction of stress responses. *PR1* and *PR5* protein levels were increased even more than the wild-type in response to UV-B in *uvr8* mutant plants, which suggests that the *uvr8* mutant is more stressed than the wild-type plants due to reduced photoprotective pigment accumulation (Kliebenstein *et al.*, 2002). Alternatively, UVR8 may act as a negative regulator of non-specific stress responsive gene expression.

Further examination of the role of UVR8 in UV-B signalling was performed by Jenkins and co-workers (Brown *et al.*, 2005). The UV-B-specificity of UVR8 was established based on gene expression studies of *CHS* induction in response to various stimuli (Brown *et al.*, 2005). These studies showed that *uvr8* mutant plants retain the induction of *CHS* gene expression mediated by cold, sucrose, UV-A and far-red light but are impaired only in the UV-B induction of these genes (Brown *et al.*, 2005).

1.8.2 UVR8 regulates transcription in response to UV-B

In addition to the UV-B-specific induction of *CHS*, microarray analyses have shown that UVR8 regulates the expression of several genes involved in photoprotection and photomorphogenesis in a UV-B-dependent manner (Brown *et al.*, 2005). Among these genes are many coding for enzymes catalysing flavonoid biosynthesis (e.g. *CHS*, *CHI*, flavonol synthase 1), proteins involved in DNA damage repair, protection against oxidative stress and photoprotection (*cry3*, *PHR1*, glutathione peroxidase and *ELIP*) and major transcription factors regulating photomorphogenesis (*HYH*, *HY5*) (Figure 1.4 and Brown *et al.*, 2005). These data provide evidence for the importance of UVR8 in regulating acclimation, photoprotective and developmental responses to UV-B irradiation (Brown *et al.*, 2005).

Further microarray analysis provided evidence that *HY5* acts downstream of UVR8, since half of the genes regulated by UVR8 were also regulated by *HY5* (Brown *et al.*, 2005). *HY5* is a bZIP transcription factor and a signalling component regulating photomorphogenesis induced by phytochromes, cryptochromes and the UV-B receptor(s) (Osterlund *et al.*, 2000; Ulm *et al.* 2004). The importance of *HY5* in UV-protection is reflected on the hypersensitive phenotype of *hy5* mutant plants to higher than ambient levels of UV-B (Brown *et al.*, 2005), which is similar to the phenotype observed in *uvr8* mutant plants (Kliebenstein *et al.*, 2002; Brown *et al.*, 2005). However, UVR8 is the only component that functions upstream of *HY5* in the UV-B-specific signal transduction pathway (Brown *et al.*, 2005), suggesting that UVR8 is the component closest to the site of UV-B photoreception.

1.8.3 UVR8 shows sequence homology to RCC1

Map-based cloning and sequencing of the *UVR8* gene revealed a significant sequence similarity to the human regulator of chromatin condensation (*RCC1*) with 35% sequence identity and 50% similarity at the protein level (Kliebenstein *et al.*,

2002). The RCC1 family of proteins contains homologues in yeast (*PRP20*), *Drosophila* (*BJ1*) and humans (*CHC1*) and many more organisms (Kliebenstein *et al.*, 2002). The *uvr8* mutant contains a 15 base-pair deletion, which includes a highly conserved Gly residue among RCC1 homologues (Kliebenstein *et al.*, 2002).

Human RCC1 is one of the best-studied members of this family of proteins. It is a nuclear protein that binds chromatin and functions as a guanine nucleotide exchange factor (GEF) for the small G protein Ran. GEF activity involves the catalysis of Ran-GDP to Ran-GTP, favouring the latter formation in the nucleus (Renault *et al.*, 1998). RCC1 plays a major role in nucleo-cytoplasmic transport, cell cycle regulation and chromatin decondensation (Seki *et al.*, 1996). Many homologues have been identified in eukaryotic organisms. All homologues contain a seven-fold repeat pattern of 55-70 residues known as the RCC1 repeat. According to its crystal structure, RCC1 forms a seven-bladed β -propeller structure with each blade consisting of 51-68 residues arranged in four antiparallel β - sheets (Renault *et al.*, 1998). A number of highly conserved residues (mostly Gly) have been identified between the repeats and among RCC1 homologues in different species (Renault *et al.*, 1998). These residues are thought to be essential for the structural integrity of the protein (Renault *et al.*, 1998). In *Arabidopsis*, UVR8 contains 90% of these highly conserved Gly residues (Kliebenstein *et al.*, 2002). Most of the mutations in RCC1 affect the invariant Gly residues and as a consequence distort the protein structure.

The region of RCC1 that confers Ran association and GEF catalytic activity is located opposite the chromatin-binding site (Renault *et al.*, 2001). Biochemical and docking experiments have been employed to investigate the Ran-RCC1 interaction. Alanine substitutions based on site-directed mutagenesis of conserved residues and kinetic analyses have identified sites of interaction and catalysis (Renault *et al.*, 2001). Brown *et al.*, (2005) have shown that UVR8 has insignificant (7%) GEF activity when compared to RCC1. In addition no interaction between Ran and UVR8 occurs in the yeast-two-hybrid system (Brown *et al.*, 2005).

Sequence alignment and structure prediction analyses of UVR8 protein based on the crystal structure of RCC1 (Figures 1.5 and 1.6) suggest that UVR8 forms a β -propeller structure similar to RCC1.

1.8.4 UVR8 associates with chromatin at promoter regions of genes that it regulates

Although UVR8 does not seem to have the same function as RCC1, as a GEF factor, Jenkins and co-workers have shown that UVR8 is localised in the nucleus and in the cytosol of plant cells, and it can associated with chromatin via histones, *in vivo* and *in vitro* (Brown et al., 2005; Cloix and Jenkins, 2007). Furthermore, chromatin immunoprecipitation studies have shown that UVR8 associates with the promoter and gene region of *HY5*, *CRYD* and several other genes it regulates (Cloix and Jenkins, 2007). Whether UVR8 could act as a positive regulator of UV-B gene expression by being involved in chromatin remodelling, would be very interesting to examine.

1.9 Conclusions

There have been major breakthroughs in the area of light perception and signal transduction in plants within the last decade. Known photoreceptors have been well characterised, novel families of photoreceptors have been discovered and many light-regulated responses have been attributed to specific signalling components. Although UV-B perception is still elusive, there have been significant advances in the understanding of UV-B mediated responses. It is now established that UV-B does not act only as a damaging agent, but when received at low fluence rates it can act as an informational stimulus, which triggers several acclimation and developmental responses in higher plants. The importance of such UV-B-induced photo-protective responses is reflected on the hypersensitivity demonstrated by mutant plants lacking

major UV-B signalling components such as UVR8, HY5 and COP1. Further investigation of the early UV-B signalling processes is required for the understanding of the regulation of such UV-protective responses in plants and possibly other organisms.

1.10 Aims of this study

The focus of this study is to further investigate the mechanism by which UVR8 acts as a UV-B specific signalling component by a number of approaches such as: spatial, temporal protein analysis, subcellular localisation studies, structure-function analyses, and identification of UVR8-interacting proteins.

1.10.1 Protein analysis & subcellular localisation studies on UVR8

To study the spatial, temporal and wavelength-specific UVR8 protein abundance and localisation, it was necessary to develop UVR8-specific antibodies. Furthermore, in order to examine the subcellular localisation of UVR8, the fluorescent tag GFP was used for tagging UVR8 in order to monitor its fluorescence in plant cells. GFP is a native protein of the jellyfish species *Aequorea victoria*, and is a widely used reporter in a number of heterologous systems (Shaw, 2006). The autocatalytic fluorescence activity and minimal photobleaching are the main advantages for using GFP for direct protein visualisation by microscopy. Modified versions of GFP possess improved characteristics, such as resistance to photobleaching and enhanced expression in higher plants (Shaw, 2006).

Generation of stable transgenic *uvr8* mutant Arabidopsis plants expressing GFP-UVR8 from the native or the constitutive Cauliflower Mosaic Virus 35S promoter were examined to determine the subcellular, temporal and spatial localisation pattern of UVR8 in response to various light stimuli, and UV-B in particular.

1.10.2 Structure-Function Analyses

In order to understand the function of UVR8, comparison with its closest homologue RCC1 and subsequent sequence-specific mutagenesis studies was carried out. Primary and secondary sequence alignments of UVR8 and RCC1 obtained by Clustal X[®] (Figure 1.5) suggest that there are certain differences in the non-conserved regions of the two proteins. First, UVR8 lacks an N-terminal nuclear localisation signal. Second, there is an extra 27 amino acid region near the C-terminal of UVR8, which is absent from RCC1. These discrepancies at the sequence level may suggest that they confer distinct functions to UVR8, possibly UV-B specific. Finally, UVR8 has a putative C-terminal monopartite NLS, identified based on rice NLS motif analyses (Moriguehi *et al.*, 2005). Based on the above observations, constructs of UVR8 with either N-terminal (20 residues), near C-terminal (27 residues) or C-terminal NLS deletions fused to GFP and under the constitutive CaMV35S or the native *UVR8* promoter, were transformed in mutant *uvr8* Arabidopsis. Transgenic plants were screened for UV-B induced *CHS* expression and UV-B hypersensitivity and localisation in order to obtain more information about the function of UVR8 at the molecular and cellular level.

1.10.3 Protein-Protein Interactions

To identify the signalling partners of UVR8, *in vivo* and *in vitro* studies in plants and heterologous systems were carried out. The yeast-two-hybrid system is a widely used molecular-genetic tool for the identification, isolation and characterisation of protein-protein interactions. This assay depends on the expression of a reporter gene (*e.g. gall-lacZ*, the *beta-galactosidase* gene) upon protein interaction giving a colour reaction on selective media. In our case UVR8 was used as the bait for screening two

different cDNA libraries, each containing genes from cDNA isolated from either white light or dark-grown plants.

This technique is prone to limitations and an interaction identified based on the yeast-two-hybrid assay needs to be verified by immunoprecipitation and phenotypic evidence *in planta*. To verify possible UVR8-protein interactions identified by the yeast-two-hybrid system co-immunoprecipitation studies and further protein-protein interaction analyses would be used. A different approach could also be employed in the future involving size exclusion chromatography of protein extracts from plants in order to establish whether UVR8 functions as part of a complex *in vivo*.

In summary, the aim of this study is to try to contribute to the understanding of UVR8 function at the molecular and cellular level. Identification of the regulatory protein regions of UVR8 as well as its interacting partners will provide essential information on the role of UVR8 in UV-B induced signal transduction, which may hopefully illuminate the process of UV-B perception and UVR8 induced signal transduction in Arabidopsis.

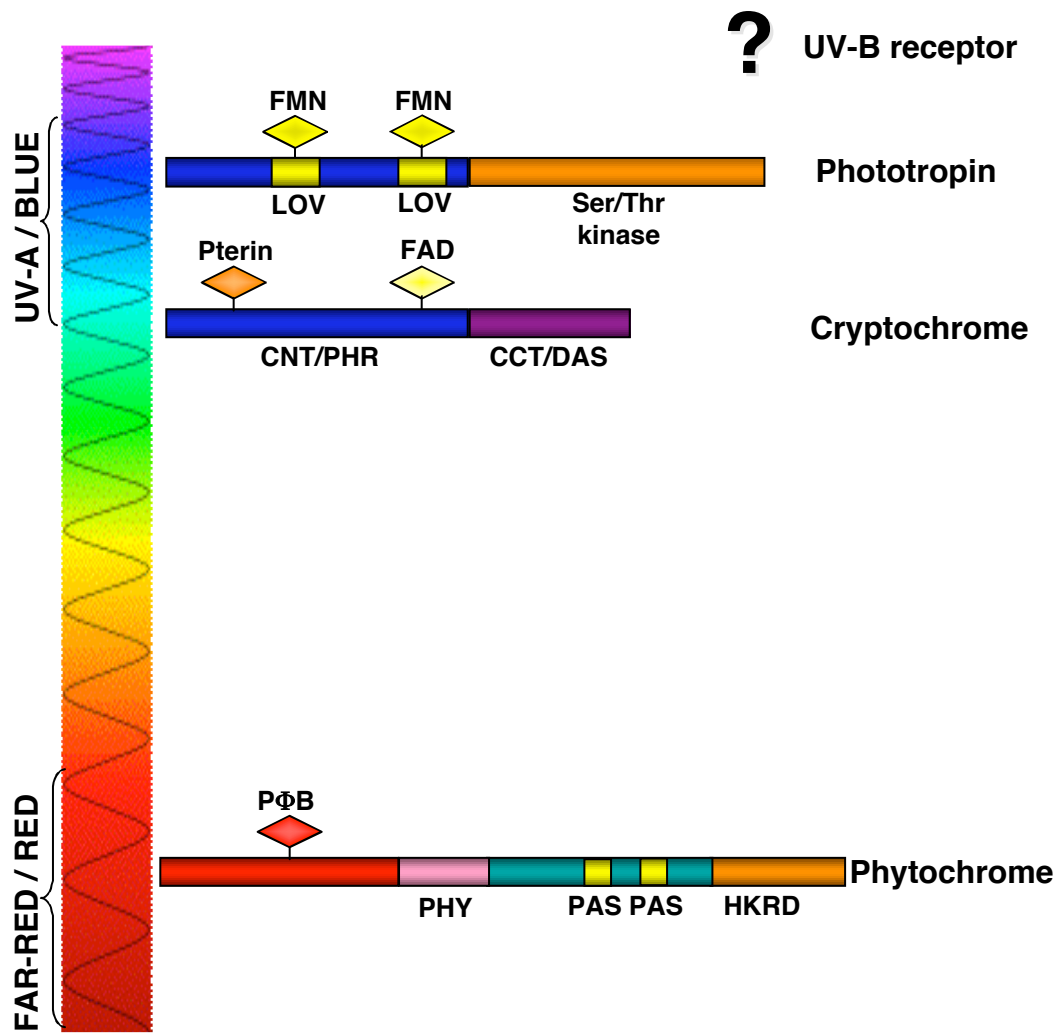


Figure 1.1 Photoreceptor families in Arabidopsis

There are three major families of photoreceptors in Arabidopsis: the phytochromes, the cryptochromes and the phototropins. The phytochrome family absorbs primarily red and far-red light and consists of 5 members: phyA, B, C, D and E. Phytochrome protein structure is characterised by an N-terminal photo-sensory domain, where the chromophore phytochromobilin (PΦB) is bound, and various C-terminal domains necessary for dimerisation, signalling and localisation. Both cryptochromes and phototropins are UV-A/blue light receptors. There are three cryptochromes cry1, cry2 and cry3, all containing a photolyase-related domain at the N-terminus, where the two chromophores pterin and FAD are bound. The phototropin family consists of phot1, phot2, each containing a C-terminal Ser/Thr protein kinase domain and two N-terminal LOV domains as the binding sites for each of the two FMN chromophores. No UV-B photoreceptor has been identified so far.

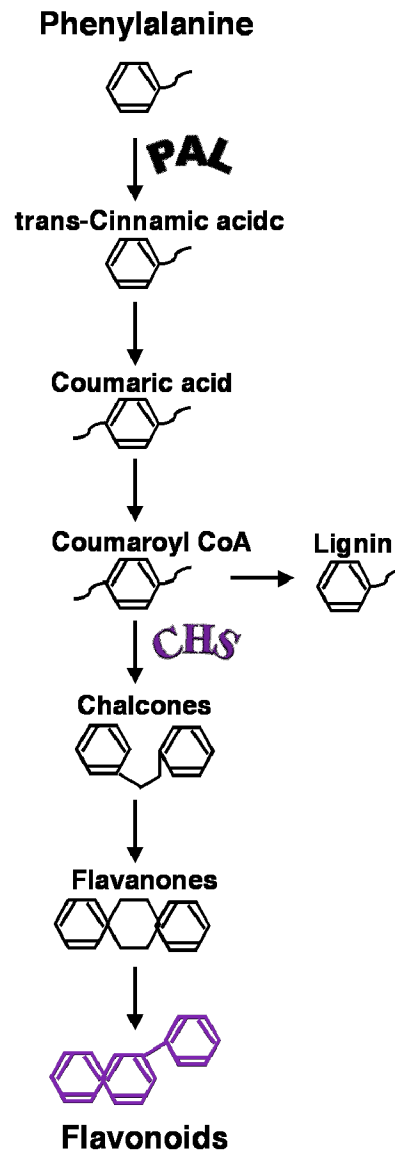


Figure 1.2. A schematic of the phenylpropanoid biosynthetic pathway

CHS catalyses the production of chalcones from coumaroyl, an essential step for flavonoid biosynthesis. PAL : phenylalanine ammonia-lyase, CHS : chalcone synthase (depicted from Taiz and Zeiger, 1998).

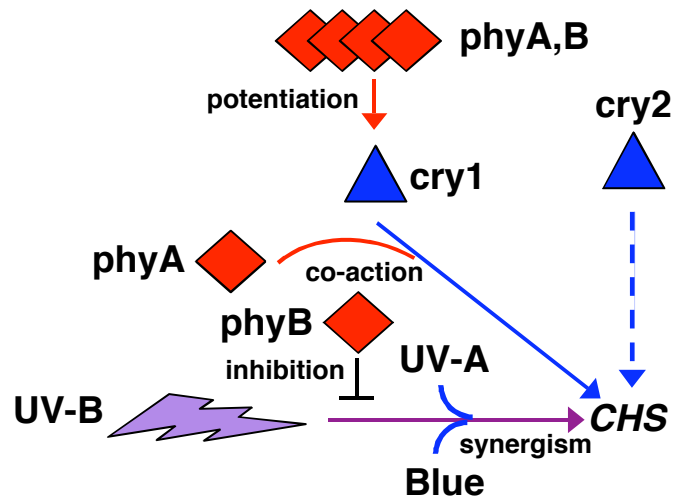


Figure 1.3 Model of the cross-talk between light signalling pathways controlling *CHS* expression in mature Arabidopsis leaf tissue

Cry1, cry2 and UV-B induce the expression of *CHS*. PhyA and phyB can potentiate or co-act with the cry1-mediated response. UV-A and blue light act synergistically with UV-B, whereas phyB is a negative regulator of the UV-B signalling pathway (modified from Wade *et al.*, 2001).

Gene	Name	Function	HY 5
At5g13930	Chalcone synthase	Flavonoid biosynthesis	Yes
At3g55120	Chalcone isomerase	Flavonoid biosynthesis	Yes
At3g51240	Flavanone 3-hydroxylase	Flavonoid biosynthesis	Yes
At5g08640	Flavonol synthase 1	Flavonol biosynthesis	Yes
At5g42800	Dihydroflavonol 4-reductase	Anthocyanin biosynthesis	Yes
At1g65060	4-Coumarate-CoA ligase 3	Phenylpropanoid pathway	Yes
At3g57020	Strictosidine synthase	Alkaloid biosynthesis	No
At1g78510	Solaneyl diphosphate synthase	prenylquinone biosynthesis	No
At4g31870	Glutathione peroxidase	Oxidative stress protection	No
At3g22840	Early light-induced protein (ELIP)	Photoprotection	Yes
At1g12370	PHR 1	type II DNA photolyase	Yes
At5g24850	CryD	blue light photoreceptor	Yes
At5g11260	HY 5	transcription factor	-
At3g17610	HY H	transcription factor	No
At5g24120	RNA polymerase Sigma subunit E	transcription (partially plastid genome)	No

Figure 1.4 A fraction of genes regulated by UVR8 in response to UV-B

Microarray analyses led to the identification of 72 UVR8-regulated genes based on data comparison between wild-type and *uvr8* plants exposed to low fluence rates of UV-B irradiation. The false discovery rate for these data is 0.1%. Three categories of genes are indicated on the panel. The upper category includes genes involved in flavonoid biosynthesis, the middle one indicates genes involved in photoprotection and the lower one contains genes involved in transcriptional control of photomorphogenesis (Brown *et al.*, 2005). The column on the right shows if these genes are also regulated by HY5.

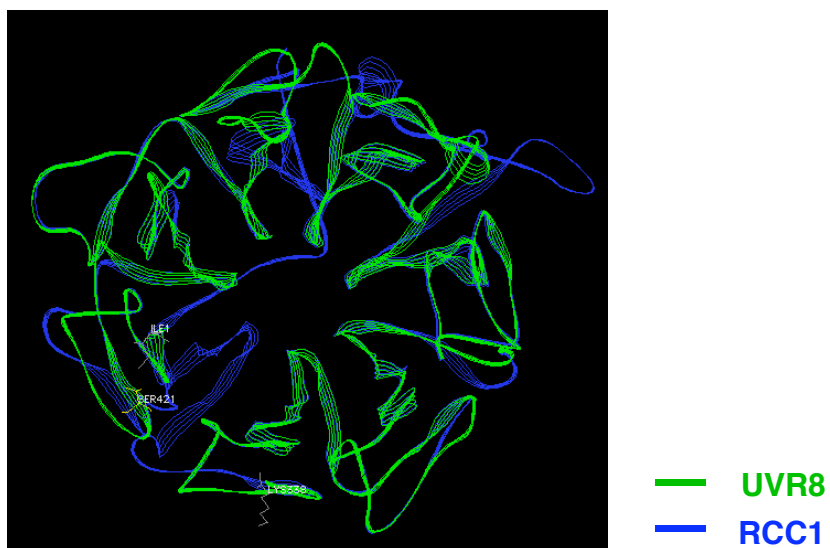


Figure 1.6 Superimposition of RCC1 and UVR8 structure

Protein prediction analysis of UVR8 based on the crystal structure of RCC1 was performed by SwissModel[®] and visualised by PdbViewer[®]. The crystal structure of RCC1 was resolved by Renault *et al.*, (1998).

CHAPTER 2

MATERIALS AND METHODS

2.1 Materials

2.1.1 Chemicals

The chemicals used for all experiments described were obtained from VWR International Ltd. (Poole, U.K.), Fisher Scientific U.K. Ltd. (Loughborough, U.K.) and Sigma-Aldrich Inc. (St. Louis, U.S.A.) unless stated otherwise.

2.1.2 Antibiotics

Antibiotics were purchased from Sigma-Aldrich Inc. and were used as described in the table.

Antibiotic	Solvent	Stock concentration	Working concentration
Ampicillin	H ₂ O	100 mg ml ⁻¹	100 µg ml ⁻¹
Kanamycin	H ₂ O	50 mg ml ⁻¹	50 µg ml ⁻¹
Gentamycin	H ₂ O	30 mg ml ⁻¹	30 µg ml ⁻¹

2.1.3 Inhibitors

All inhibitors for this study were obtained from Sigma-Aldrich Inc. and used as described in the table.

Inhibitor	Solvent	Stock concentration	Working concentration
Cycloheximide	H ₂ O	100 mM	10 µM
Staurosporine	DMSO	1 mM	1 µM
Cantharidin	DMSO	100 mM	100 µM

2.1.4 Enzymes for DNA and RNA Manipulation

DNA restriction, ligation, synthesis and DNA/RNA modification enzymes were purchased from Promega (Wisconsin, U.S.A.), New England Biolabs (Hitchin, U.K.), and Ambion Inc.

2.1.5 Plasmid Vectors

Plasmid DNA vectors used in this study are listed in the table below.

Plasmid Vector	Description	Source
pEZR(K)L-C	GFP tag	Dr. Gert-Jan de Boer
pBluescript II SK	Sub-cloning	Stratagene
pGBKT7	Yeast-two-hybrid	Clontech
pGADT7	Yeast-two-hybrid	Clontech
pCR [®] 4Blunt-TOPO [®]	Blunt-end PCR product cloning	Invitrogen

2.1.6 Bacterial and Yeast Strains

E. coli strains DH5α, TOP10[®] (Invitrogen) and XL-1 Blue (Statagene) were transformed with various plasmid vector constructs for sub-cloning, expression and

amplification purposes. *A. tumefaciens* strain GV3101 was used for Arabidopsis transformation with pEZR(K)L-C vector containing different constructs listed in 2.8.1. *S. cerevisiae* strains AH109 (Clontech) and MaV203 (Invitrogen) were used for protein interaction studies by transformation with bait and prey vectors (pGBKT7 and pGADT7 respectively).

2.1.7 Enzymes for protein manipulation

Protein modifying enzymes were purchased from Promega (Wisconsin, U.S.A.), Roche Diagnostics (Mannheim, Germany), Sigma-Aldrich Inc. (St. Louis, U.S.A.) and were used according to manufacturer's instructions.

2.1.8 Reagents for Protein Quantification, Electrophoresis and Immunoblot Analysis

All reagents necessary for protein work were purchased from Bio-Rad Laboratories (Hercules, California, U.S.A.) unless indicated otherwise.

2.2 General Laboratory Preparation Procedures

2.2.1 pH Measurements

The pH of solutions and media was measured either using a Jenway 3320 pH meter and glass electrode (Jenway, Felsted, Essex) or pH Indicator Strips (BDH, Poole, U.K.).

2.2.2 Autoclaving

Solutions and equipment were sterilised by using a benchtop autoclave (Prestige Medical, Model 220140).

2.2.3 Filter Sterilisation

Solutions of small volume or heat sensitive solutions were sterilised by filtration through a Nalgene filter (pore diameter 0.2 μM).

2.3 Plant Material

2.3.1 Seed Stocks

Wild-type *A. thaliana* cv Landsberg *erecta* and Col-3 seeds were obtained from The European Arabidopsis Stock Centre (NASC, Nottingham, U.K.). Prof. D. Kliebenstein (U.C. Davis, U.S.A.) provided the *uvr8-1* (*Ler*) mutant, Dr. Roman Ulm provided the *cop1-4* (*Ws*) mutant and Dr. R. Sablowski (John Innes Centre, Norwich, U.K.) $35S_{\text{pro}}$ -GFP (*Ler*) seeds.

2.3.2 Growth of Arabidopsis Plants on Soil

Arabidopsis seeds were sown on pots containing compost soaked in 0.15 g l⁻¹ of a solution of the insecticide Intercept® (Scotts U.K., Bramford, Ipswich). The pots were kept under a humidifier during a vernalisation period of 2-5 days and for 1 week after germination in the growth chambers at 22°C. Plants were grown for 3 weeks at a low fluence rate of constant white light (20 $\mu\text{mol m}^{-2} \text{s}^{-1}$) for RT-PCR experiments. For

protein analysis, plants were grown for 12 days at light conditions described in figure legends.

2.3.3 Surface Sterilisation of Arabidopsis Seeds

Arabidopsis seeds were surface sterilised by a 3-minute incubation in a sodium hypochlorite solution (50% (v/v)). Seeds were washed three times in sterile dH₂O and were deposited on sterile filter paper on the surface of agar plates.

2.3.4 Growth of Arabidopsis Plants on Agar Plates

For protein studies and subcellular localisation analyses, sterile seeds were sown on sterile filter paper on 0.8% agar plates containing 2.15 g l⁻¹ Murashige & Skoog salts. For segregation studies of transgenic Arabidopsis plants sterilised seeds were sown on 0.8% agar plates containing 2.15 g l⁻¹ Murashige & Skoog salts and 75 µg ml⁻¹ kanamycin. Plates were cold-treated in the dark at 4°C for 2-4 days and then grown for 12 days in light conditions as described in figure legends.

2.4 Plant Treatments

2.4.1 Light Sources

Light treatments were carried out in growth chambers at 20 °C. The tubes used for white light were warm white fluorescent tubes L36W/30 (Osram, Munich, Germany). The tubes used for UV-A light were F36W/BLB-T8 tubes (GTE Sylvania, Shipley, U.K.). The tubes used for UV-B light were Q-Panel UV-B 313 tubes (Q-Panel Co., U.S.A.) covered by cellulose acetate filter (Catalogue No. FLM400110/2925, West

Design Products, Nathan Way, London), which was changed every 24 hours in order to eliminate any UV-C. This source does not emit below 290 nm and has a maximum emission at 311 nm (Figure 2.1). At the fluence rate used in the experiments, the low levels of emission of wavelengths above 320 nm are insufficient to initiate UV-B-induced *CHS* gene expression (Christie and Jenkins, 1996) or *HY5* gene expression (B.A. Brown and G.I. Jenkins, unpublished data). The spectra of all the light sources are shown in Figure 2.1. Red light tubes were FL20S FR-74 tubes (Toshiba, Japan).

2.4.2 Light Fluence Rate Measurements

Fluence rates of white and red light were measured using a Skye RS232 meter fitted with a quantum sensor which measures wavelengths of light ranging from 400 to 700 nm. (Skye Instruments, Powys, U.K.). Fluence rates of UV-A (315-380 nm) and UV-B (280-315 nm) were measured using a RS232 meter with an SKU 420 or an SKU 430 sensor for UV-A and UV-B respectively. For detailed spectral measurements a Macam Spectroradiometer Model SR9910 (Macam Photometrics Ltd., Livingston, Scotland) recording wavelengths of light between 240 and 800 nm was used.

2.4.3 UV-B Sensitivity Assay

To assess the growth inhibition and leaf tissue necrosis of *Arabidopsis* plants in response to UV-B, a UV-B sensitivity assay was carried out according to Brown *et al.* (2005). Plants were grown in white light ($120 \mu\text{mol m}^{-2} \text{s}^{-1}$) for 12 days and then exposed to UV-B ($5 \mu\text{mol m}^{-2} \text{s}^{-1}$) supplemented with white light ($40 \mu\text{mol m}^{-2} \text{s}^{-1}$) for 24 h. Plants were photographed after return to white light ($120 \mu\text{mol m}^{-2} \text{s}^{-1}$) for 5 days. For this study the UV-B sensitivity assay was used as a means to test functionality of a modified version of UVR8 protein expressed in *uvr8-1* transgenic plants.

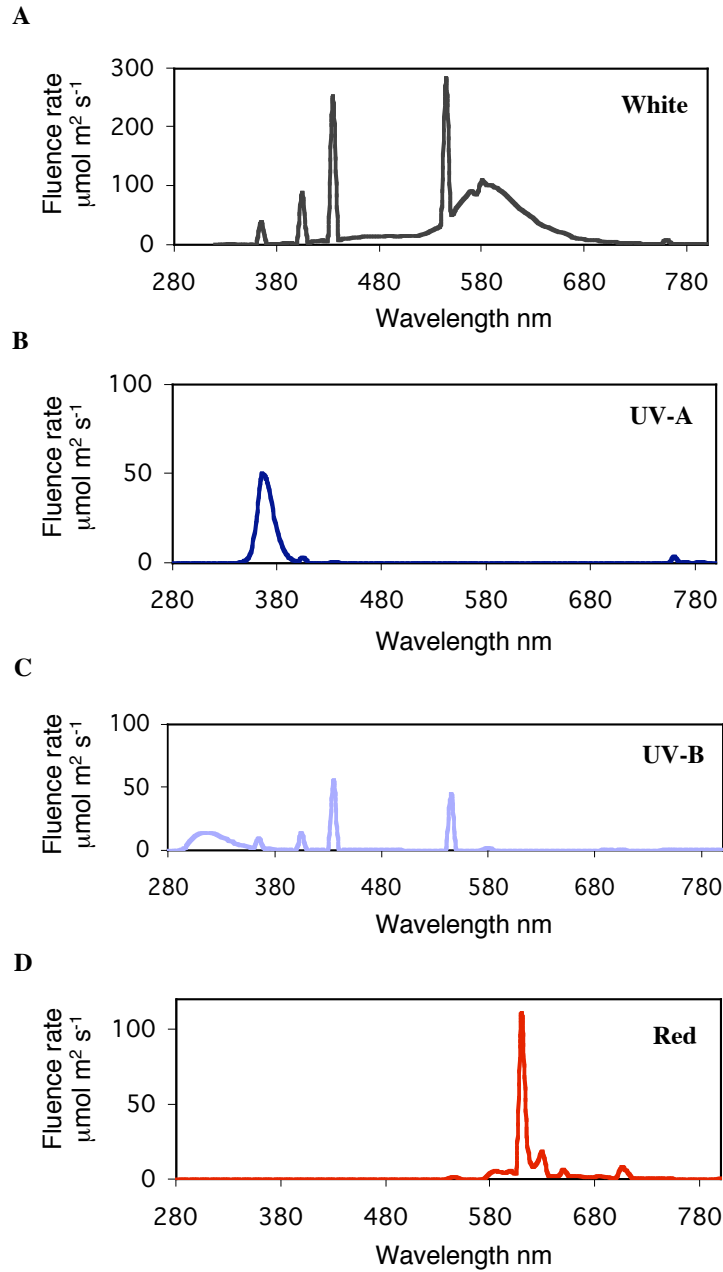


Figure 2.1 Spectra of light qualities used in this study

A) White light, B) UV-A, C) UV-B, D) Red.

2.5 Amplification of Plasmid DNA

2.5.1 Preparation of Competent *E. coli* Cells for Electroporation

A 50 µl aliquot of DH5α competent cells was inoculated in 1 ml of LB medium at 37° C, constantly shaking (220 rpm), overnight. The following day the 1 ml overnight culture was inoculated in 500 ml of LB medium and was grown at 37° C, constantly shaking (220 rpm) until the culture reached an OD at 550 nm of approximately 0.8. The culture was incubated on ice for 15-30 min and subsequently cells were pelleted at 2000 *g* for 5 min at 4° C. The supernatant was discarded and the pellet was gently resuspended in an equal volume (500 ml) of ice-cold sterile dH₂O. Cells were centrifuged as described before, the supernatant was discarded and the pellet was resuspended in 500 ml of ice-cold sterile dH₂O. The cells were centrifuged as before. The pellet was resuspended in 5 ml of ice-cold 10 % (v/v) glycerol. Cells were centrifuged as before, the supernatant was discarded and the pellet was resuspended in 1 ml of ice-cold 10 % (v/v) glycerol. 50 µl aliquots of cells were frozen on dry ice and stored at -80° C.

2.5.2 Transformation of Competent *E. coli* Cells

Competent cells prepared as described in 2.5.1 were placed on ice to thaw. Approximately 1 µl of plasmid DNA (200 ng) or 5 µl of precipitated ligation was added to the competent cells and incubated on ice for 20 min. The cells containing the DNA were transferred into an electroporation cuvette (BioRad) and pulsed using the electroporating device (MicroPulser™ Electroporator, BioRad). 500 µl of LB medium was added immediately to the cells and they were transferred in a clean Eppendorf® tube and incubated at 37° C, constantly shaking (220 rpm) for 1 h (until the antibiotic resistance genes were expressed). Cells were pelleted for 30 s at 10,000 *g*. The pellet

was resuspended in 100 μ l of LB medium and plated with a sterile spreader on agar plates containing LB and the appropriate antibiotic for the selection of the plasmid. The plates were incubated at 37° C overnight until colonies developed.

2.5.3 Isolation of plasmid DNA

Small and large-scale plasmid DNA purification from *E. coli* was performed using the Qiagen® Plasmid Mini or QIAfilter™ Plasmid Maxi Kit respectively. A single bacterial colony containing the plasmid of interest was inoculated in 5 ml (small-scale) or 250 ml (large-scale) of LB medium, containing the appropriate antibiotic selection for the plasmid. The cultures were incubated at 37 °C, constantly shaking (220 rpm), overnight. Cells were pelleted at 6,000 g for 15 min and the supernatant was discarded. Cell lysis and plasmid DNA purification was carried out according to the manufacturer's instructions. The purified plasmid DNA was eluted in a final volume of 50 μ l of the Elution Buffer, provided by Qiagen. The plasmid DNA was stored at -20 °C.

2.6 DNA and RNA methods

2.6.1 Isolation of genomic DNA from Arabidopsis plants

Genomic DNA from Arabidopsis plant tissue was isolated using the DNeasy® Plant Mini Kit (Qiagen) according to the manufacturer's instructions. Approximately 100 mg of tissue was ground into a fine powder in liquid N₂ and then transferred into an Eppendorf tube. Cell lysis and genomic DNA purification was carried out as described in the Qiagen DNeasy® Plant Mini Kit manual. Purified genomic DNA was eluted from the DNeasy membrane by adding 50 μ l of pre-heated buffer AE (provided by Qiagen). Genomic DNA samples were stored at -20 °C.

2.6.2 Isolation of total RNA from Arabidopsis leaf tissue

Total RNA from Arabidopsis leaf tissue was isolated using the RNeasy[®] Plant Mini Kit (Qiagen) according to manufacturer's instructions. Approximately 100 mg of Arabidopsis leaf tissue was ground into a fine powder in liquid N₂ and then transferred into an Eppendorf tube. RLT buffer with added β-mercaptoethanol (10 µl per 1 ml buffer) was the lysis buffer of preference for this study. The procedure described in the Qiagen manual was followed in order to obtain purified RNA, which was eluted from the RNeasy spin column with 30 µl of RNase free water (supplied by Qiagen). RNA samples were stored at -80 °C.

2.6.3 Quantification of DNA and RNA

To quantify purified nucleic acids, 2 µl of DNA or RNA were diluted in 2 ml of dH₂O and the absorbance at 260 and 280 nm was measured (BioRad) against a dH₂O blank sample (no DNA/RNA added). An absorbance of 1 at 260 nm was recorded to measure the following concentrations:

Nucleic Acid	Concentration of OD 260 = 1
Double-stranded DNA	50 µg ml ⁻¹
Single-stranded DNA/RNA	40 µg ml ⁻¹

The ratio of the absorbance 260/280 indicated the purity of the samples (1.8 for DNA, 2.0 for RNA) (Sambrook and Russell, 3rd Edition).

2.6.4 Amplification of DNA by Polymerase Chain Reaction

Approximately 500 ng of DNA (cDNA, genomic or plasmid DNA) was used as a template and added to a master-mix of reaction reagents containing 1 x PCR Buffer (New England Biolabs), 0.1 mM dNTPs, 0.5 μ M of each primer, 0.625 Units of *Taq* DNA Polymerase (New England Biolabs) and sterile water to a final volume of 25 μ l. If the PCR product amplified was for cloning purposes 1.25 units of *Pfu* DNA polymerase (Promega), 0.2 mM dNTPs, 0.6 μ M of each primer and sterile water to a final volume of 50 μ l were used. The PCR conditions varied according to primer length, G/C content, the PCR product size and the type of DNA template. If genomic DNA was used as a template an additional incubation of a total of 5 min at 95 °C (Step 1) was added followed by 45 sec at 95 °C (Step 2) and 1 min at 45 °C (Step 3). The annealing temperature of the primers to the template was calculated by the following formula:

$$T_A = \underbrace{(2 \times (A+T) + 4 \times (G+C))}_{T_M} - 2.$$

For example if $T_M = 60$ °C, the T_A would be at 58 °C for 30 sec (Step 4). The extension period would depend on the size of the DNA to be amplified (1 min per 2000 bases for *Taq* and 2 min per 1000 bases for *Pfu*) at 72 °C (Step 5). Step 2 to step 5 was repeated for 24 times (24 cycles) followed by a final extension period of 7 min at 72 °C (Step 6) (Sambrook and Russell, 3rd Edition).

2.6.5 Restriction Endonuclease Digestion of DNA

Approximately 500 ng of DNA was digested with the appropriate restriction enzyme and the supplied buffers at concentrations and incubation conditions according to the manufacturer's instructions.

2.6.6 Agarose Gel Electrophoresis of DNA

All DNA agarose gels contained 1 % (w/v) agarose melted in TAE buffer (40 mM Tris-acetate, 1mM EDTA) unless otherwise stated. 1 $\mu\text{g ml}^{-1}$ ethidium bromide was added to the agarose solution for DNA labelling. DNA samples were mixed with 5 x loading buffer (0.25 % (w/v) bromophenol blue, 0.25 % (w/v) xylene cyanol FF, 30 % (w/v) glycerol) and separated by agarose gel electrophoresis in TAE buffer at 100 mA.

2.6.7 DNA Extraction and Purification from agarose gel

DNA separated on 1% agarose ethidium bromide-stained gel was separated by electrophoresis. A band of the expected size was excised under a UV-illuminator and the DNA was purified according to the QIAquick[®] Gel Extraction Kit (Qiagen). Purified DNA was eluted in 30 μl of Elution buffer (provided by Qiagen).

2.6.8 DNA Ligation

DNA derived from PCR amplification or plasmid DNA with appropriate restriction sites was restriction digested (2.6.5) and purified (2.6.7). An aliquot of plasmid vector and insert DNA was examined by separation on an agarose gel. Approximately 200 ng of vector and insert DNA in total were used in a ligation reaction containing 1X ligation buffer, 1 unit T4 DNA ligase (Promega) and sterile dH_2O to a final volume of 10 μl . The ligation mix was incubated for 30 min at room temperature, followed by an overnight incubation at 4 °C. Approximately 5 to 8 μl of the ligation was used for transformation of competent *E. coli* cells either made as described in 2.5.1 or purchased from Invitrogen (TOP10 chemically competent cells) according to manufacturer's instructions.

2.6.9 DNA Sequencing

Sequencing of DNA was carried out by Dundee Sequencing Service (University of Dundee) according to the service's instructions. The DNA sequence to be sequenced was either in the form of a purified PCR product (as described in 2.6.7) or as plasmid DNA. Sequencing was always performed before and after a series of sub-cloning reactions to verify the sequence of the DNA insert in every vector used in this study.

2.7 Semi-quantitative Reverse-Transcriptase Polymerase Chain Reaction

2.7.1 DNase Treatment of RNA

In order to abolish possible genomic DNA contamination, purified RNA from *Arabidopsis* leaf tissue (2.6.1) was treated with DNase (Ambion) according to the manufacturer's instructions. Following isolation, the concentration of RNA in each sample was quantified as described in 2.6.3 5 µg of total RNA were incubated with 4 units of DNase, 1x DNase buffer, 48 units of RNase inhibitor and RNase-free water up to 35 µl at 37 °C for 1 h. Efficiency of the DNase treatment was tested by PCR on the DNase-treated samples with primers for *ACTIN2*. If no PCR product was detected from samples that have been DNase-treated, the samples were used for cDNA synthesis as they were devoid of genomic DNA. Otherwise, the DNase treatment was repeated until no PCR product due to genomic DNA contamination was detected.

2.7.2 cDNA synthesis

After successful DNase treatment, cDNA synthesis was performed according to Brown *et al.* (2005). 20 µl of the DNA-free RNA were incubated with 0.24 µM oligo dT (dTTP₁₅) and incubated at 70 °C for 10 min. The mixture was placed on ice and a

master-mix containing 1 x AMV Reverse Transcriptase Reaction Buffer, (Promega), 1 mM of dNTPs (Promega), 48 Units of RNase inhibitor (Promega), 1 mM dithiothreitol, 20 Units of AMV Reverse Transcriptase (Promega) was added. The samples were incubated at 48 °C for 45 min followed by 5 min at 95 °C to inactivate the enzyme. The synthesised cDNA was stored at –20 °C.

2.7.3 Primer Oligonucleotides for RT-PCR

All primer oligonucleotides were synthesised by Invitrogen and were kept at –20 °C as 20 mM stock concentrations.

Primer	Primer Sequence	Fragment	Source
<i>ACTIN2</i>	FOR5'-CTTACAATTTCCCGCTCTGC-3' REV5'-GTTGGGATGAACCAGAAGGA-3'	500 bp	Dr. Helena Wade
<i>CHS</i>	FOR5'-ATCTTTGAGATGGTGTCTGC-3' REV5'-CGTCTAGTATGAAGAGAACG-3'	337 bp	Dr. Bobby Brown Dr. Helena Wade
<i>HY5</i>	FOR5'-GCTGCAAGCTCTTTACCATC-3' REV5'-AGCATCTGGTCTCGTTCTG-3'	404 bp	Dr. Bobby Brown

2.7.4 RT-PCR Conditions

Semi-quantitative RT-PCR was performed at a number of cycles within the linear range of product amplification according to Brown *et al.* (2005) and Dr. Helena Wade. The PCR conditions were the following: (2 min 30 sec at 94 °C, 1 min at 55 °C, 2 min at 72 °C) for one cycle, (45 sec at 94 °C, 1 min at 55 °C, 1 min at 72 °C) for 24 cycles for (*ACTIN2*), 25 cycles for (*CHS*) or 26 cycles (*HY5*); followed by 5 min at 72 °C for one cycle. Reaction ingredients were as described in 2.6.4 for *Taq* DNA Polymerase. 1 µl of cDNA from each sample was used to perform a PCR reaction with *ACTIN2* primers. The reaction samples were separated on a 1 % (w/v) agarose gel and were quantified by the Quantity One[®] Software (BioRad) in order to attain equal cDNA loading. Quantification of RT-PCR products obtained with *CHS* and *HY5* primers was

normalized by dividing with the value obtained from the equivalent RT-PCR products obtained with *ACTIN2* primers. Data are representative of three independent experiments.

2.8 Generation of stable transgenic Arabidopsis lines

2.8.1 Generation of Gene Fusion Constructs for Stable Expression Studies in Arabidopsis

A number of fusion and deletion gene constructs were made in this study in order to examine the localisation and the functionality of modified versions of the UVR8 protein in Arabidopsis plants. All constructs described in this section were sub-cloned in pEZR(K)L-C binary vector which contains a GFP tag. Any modifications made in this vector are mentioned below.

UVR8_{pro} GFP-UVR8

The UVR8 promoter originates from the -1426 to +163 genomic sequence upstream of the coding sequence of the *UVR8* gene and was chosen by inspection. The sequence was PCR amplified and replaced the Cauliflower Mosaic Virus constitutive promoter 35S of pEZRL(K)C vector at restriction sites 5' *SacI* 3' *HindIII*. UVR8 was PCR-amplified from cDNA and cloned at restriction sites 5' *EcoRI* and 3' *SalI* in pEZRL(K)C vector at the C-terminal region of *eGFP*.

UVR8_{pro} GFP-ΔN-UVR8

ΔN-UVR8 (UVR8 lacking the first 23 amino acids) was PCR-amplified from cDNA and cloned at restriction sites 5' *EcoRI* and 3' *SalI* in pEZRL(K)C vector at the C-terminal region of *eGFP* as described for UVR8_{pro}GFP-UVR8.

UVR8_{pro}GFP-ΔC-UVR8

ΔC-UVR8 (UVR8 lacking amino acids 397 to 423) was amplified by reversed PCR from a vector (pBluescript SKII) containing UVR8 cDNA. The product of reverse PCR was cloned at restriction sites 5' *EcoRI* and 3' *SalI* in pEZRL(K)C vector at the C-terminal region of *eGFP* as described for UVR8_{pro}GFP-UVR8.

UVR8_{pro}GFP-ΔNLS-UVR8

ΔNLS-UVR8 (UVR8 lacking the last 5 amino acids) was PCR-amplified from cDNA and cloned at restriction sites 5' *EcoRI* and 3' *SalI* in pEZRL(K)C vector at the C-terminal region of *eGFP* as described for UVR8_{pro}GFP-UVR8.

ΔN, ΔC and ΔNLS-UVR8 were also sub-cloned at restriction sites 5' *EcoRI* and 3' *SalI* in pEZRL(K)C vector which contained the Cauliflower Mosaic Virus 35S promoter instead of the *UVR8* promoter.

UVR8_{pro} NES-GFP-UVR8

The NES sequence used for the generation of NES-GFP-UVR8 constructs is described in Matsushita *et al.* (2003). NES originating from PKI (LQNELALKLAGLDINKTGG) was PCR-synthesised and amplified from pEZRL(K)C vector containing GFP-UVR8. The PCR product of NES-GFP-UVR8 was sub-cloned at restriction sites 5' *HindIII* and 3' *SalI* in pEZRL(K)C vector at the 3' of *UVR8* promoter sequence.

UVR8_{pro} NLS-GFP-UVR8

The NLS sequence used for the generation of NLS-GFP-UVR8 constructs is described in Matsushita *et al.* (2003). NLS originating from SV40 (LQPKKKRKVGG) was PCR-synthesised and amplified from pEZRL(K)C vector containing GFP-UVR8. The PCR product of NLS-GFP-UVR8 was sub-cloned at restriction sites 5' *HindIII* and 3' *SalI* in pEZRL(K)C vector at the 3' of *UVR8* promoter sequence.

The sequences of all constructs were confirmed by sequencing from pEZRL(K)C vector.

Construct	Primer Sequence	PCR conditions
UVR8_{Pro}	FOR5'-CAAGAGCTCGTATATAGTACTTCCAATGGC-3' REV5'-CCAAAGCTTATCACAGTTGCAGTTTTTACA-3'	T _A = 56 °C T _{Ext} = 3 min
ΔNUVR8	FOR5'-GCTAGCCACTCCGTCGCT-3' REV5'-TCAAATTCGTACACGCTTGAC-3'	T _A = 58 °C T _{Ext} = 2 min
ΔCUVR8	FOR5'-AATGGAGGTGATATCAGTGTTTC-3' REV5'-TGAAGATGGATCGATATTAGAAG-3'	T _A = 55 °C T _{Ext} = 8 min
ΔNLSUVR8	FOR5'-TAGAATTCGCGGAGGATATGGCTGCCGAC-3' REV5'-CAAGTCGACTCAGACATCAGTTTTGTGGAACACT-3'	T _A = 58 °C T _{Ext} = 2 min
NES-GFP-UVR8	FOR5'-AAAAGCTTATGCTTCAGAACGAGCTTGC TCTTAAGTTGGCTGGACTTGATATTAACAAG ACTGGAGGAGTGAGCAAGGGCGAGGAGCTG-3' REV5'-TAAGTCGACAATTCGTACACGCTTGAC-3'	T _A = 55 °C T _{Ext} = 7 min
NLS-GFP-UVR8	FOR5'-TAAAGCTTATGCTGCAGCCTAAGAAGAAGAGA AAGGTTGGAGGAGTGAGCAAGGGCGAGGAGCTG-3' REV5'-TAAGTCGACAATTCGTACACGCTTGAC-3'	T _A = 55 °C T _{Ext} = 7 min

2.8.2 Preparation of Competent Agrobacterium Cells for Electroporation

A 50 µl aliquot of Agrobacterium strain GV3101 electro-competent cells was inoculated in 1 ml of LB medium at 30° C, constantly shaking (220 rpm), overnight. The following day the 1 ml overnight culture was inoculated in 500 ml of LB medium and was grown at 30° C, constantly shaking (220 rpm) until the culture reached an O.D. at 550 nm of approximately 0.8. The culture was incubated on ice for 15-30 min and subsequently cells were pelleted at 2000 g for 5 min at 4° C. The procedure described in 2.5.1 for the preparation of electrocompetent *E. coli* cells applies for *A. tumefaciens* cells too (Huala *et al.*, 1997).

2.8.3 Transformation of competent Agrobacterium cells by electroporation

Competent cells of Agrobacterium strain GV3101 prepared as in 2.8.1 were placed on ice to thaw. Approximately 1 µl of plasmid DNA (100-200 ng) was added to the

competent cells and incubated on ice for 20 min. The cells containing the DNA were transferred into an electroporation cuvette (BioRad) and pulsed using the electroporating device (MicroPulser™ Electroporator, BioRad). 1 ml of LB medium was added immediately to the cells, which were then transferred to a clean Falcon® tube and incubated at 30° C, constantly shaking (220 rpm) for 3 h (until the antibiotic resistance genes were expressed). Cells were pelleted for 30 s at 10,000 g. The pellet was resuspended in 100 µl of LB medium and plated with a sterile spreader on agar plates containing LB, gentamycin (30 µg ml⁻¹) and kanamycin (50 µg ml⁻¹). The plates were incubated at 30° C for 2-3 days until colonies developed (modified protocol from Clough and Bent, 1998). The sequence of the plasmid construct of interest was confirmed by colony PCR (2.6.4) with the appropriate primers.

2.8.4 Agrobacterium-mediated transformation of Arabidopsis by floral dip

All the transgenic lines described in this study were generated in the *uvr8-1* mutant background by Agrobacterium-mediated transformation. *uvr8-1* mutant Arabidopsis plants were grown in white light until flowers developed (4-5 weeks). A single colony of *A. tumefaciens* containing the plasmid construct of interest was inoculated in 500 ml LB medium with gentamycin (30 µg ml⁻¹) and kanamycin (50 µg ml⁻¹) at 30° C, constant shaking (220 rpm) overnight until the OD at 550 nm of the culture was 2.0. The cells were pelleted by centrifugation at 2,000 g for 10 min at room temperature. The pellet was resuspended in Infiltration Medium (2.2 g l⁻¹ Murashige and Skoog salts, 50 g l⁻¹ sucrose, 0.5 g l⁻¹ MES, 0.044 µM benzylaminopurine and 200 µl g l⁻¹ Silwet L-77) to an O.D. of 0.8. Plants were immersed in the Agrobacterium solution described above for 1 min. Plants were kept under a humidifier in the growth chamber for 4 days and were immersed once more in the Agrobacterium solution for 1 min (modified protocol from Clough and Bent, 1998). Plants were allowed to develop seeds in the growth chamber and the selection for seeds containing the gene construct of interest was carried out as described in 2.8.5.

2.8.5 Screen for Homozygous Lines

T1 seed from transformed plants was selected on 0.8% agar plates containing 2.15 g l⁻¹ Murashige & Skoog salts and 75 µg ml⁻¹ of kanamycin. T2 generation plants exhibiting 3:1 (75%) segregation were selected. At least 4 independent homozygous T3 lines exhibiting 100 % resistance to kanamycin were used for complementation, protein expression and localisation studies.

2.8.6 Transient expression of gene constructs in *N. benthamiana* by *A. tumefaciens* infiltration

The protocol for Agrobacterium-mediated transformation of *Nicotiana* was provided by Ms Janet Laird and Dr. Lucio Conti (modified protocol from Hajdukiewicz *et al.*, 1994). A single colony from recently transformed Agrobacterium cells with the plasmid DNA of interest was inoculated in 15 ml LB broth and the appropriate antibiotics (gentamycin, 30 µg ml⁻¹ and kanamycin, 50 µg ml⁻¹ at 30 °C, constantly shaking (220 rpm) until it reached an OD at 550 nm of 1.0. Agrobacterium cells were pelleted by centrifugation at 2000 g for 5 min. The cells were washed in 15 ml of sterile 10 mM MgCl₂. The cell suspension was diluted at an OD₅₅₀ of 0.2 with 10 mM MgCl₂ solution containing 200 µM acetosyringone and was incubated at room temperature for 2 hours. The Agrobacterium medium was infiltrated in *N. benthamiana* (provided by Mr. Craig Carr) using a syringe through small incisions made at the lower side of the plant leaves. The infiltrated *Nicotiana* plants were incubated at 30 °C in white light for approximately 60 hours before examining for gene expression by confocal microscopy.

2.9 Protein Methods

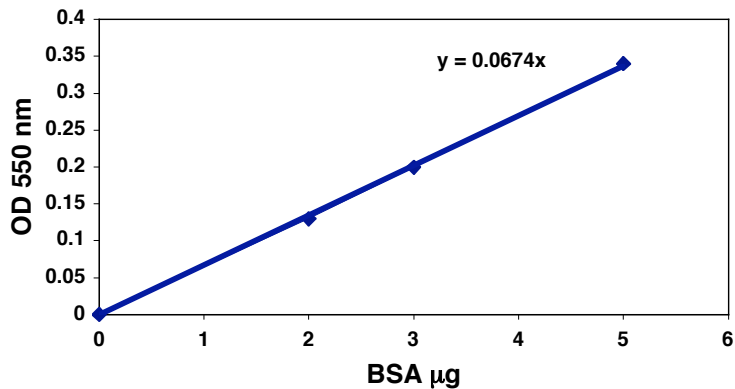
2.9.1 Protein Isolation from Arabidopsis plants

Total protein was extracted from Arabidopsis plants grown in light conditions described in the figure legends by grinding in Micro-Extraction buffer (20 mM HEPES pH 7.8, 450 mM NaCl, 50 mM NaF, 0.2 mM EDTA, 25% (v/v) glycerol, 0.5 mM PMSF, 1 mM DTT and protease inhibitor mix (1 tablet of protease inhibitor mix Complete Mini, Roche per 10 ml of Micro-Extraction buffer) on ice. A freeze-thaw procedure was carried out three times (a 10-s incubation on dry ice followed by a 10-s incubation at 37 °C). The homogenate was centrifuged at 16,000 g for 10 min at 4 °C and the supernatant was transferred to a clean tube (protocol kindly provided by Prof. R.White's lab, University of Glasgow).

Protein extraction for nuclear and cytosolic fractionation was performed as described by Cho *et al.* (2006). Isolation of membrane protein was based on the method described by Christie *et al.* (1997). Plant tissue was ground at 4 °C in 2 ml of homogenisation buffer (25 mM MOPS, 0.25 M sucrose, 0.1 mM MgCl₂, 8 mM L-cysteine, pH 7.8 and 1 tablet of protease inhibitor mix (Complete Mini, Roche) per 10 ml). The homogenate was filtered through nylon mesh cloth and centrifuged at 9,700 g for 10 min at 4 °C. 500 µl of the supernatant was removed and consisted of the total protein extract. The rest of the supernatant (approximately 500 µl) was transferred to an ultracentrifuge tube and was centrifuged at 100,000 g for 1 h at 4 °C. The membrane pellet was resuspended in 500 µl of resuspension buffer (250 mM sucrose, 4 mM KNO₃, 5 mM KNO₄, pH 7.2 and protease inhibitor mix) and the supernatant was transferred to a new tube and comprised of the cytosolic protein fraction. 30 µg of total, membrane and cytosolic protein fraction were separated on a 10 % SDS PAGE gel.

2.9.2 Quantification of protein concentration

The protein concentration of the total, nuclear and cytosolic fractions was determined by a Bradford assay solution (BioRad) diluted 5-fold in dH₂O. 1 µl of protein extract was added in a cuvette containing 900 µl of Bradford solution and 100 µl of dH₂O and mixed to obtain homogeneous colour. The absorbance at 550 nm of the solution was recorded against a blank sample (no protein added) and the concentration of each sample was calculated based on the equation of the standard curve that was plotted for the standards (0, 1, 2, 3, 5 µl of 1 µg µl⁻¹ of BSA). An example is demonstrated below:



Sample	OD 550 nm
0 µg BSA	0
2 µg BSA	0.13
3 µg BSA	0.20
5 µg BSA	0.34
Sample 1 (2µl)	0.23

Sample	Concentration
Sample 1	1.7 µg µl ⁻¹

2.9.3 Sodium Dodecyl Sulfate Polyacrylamide Gel Electrophoresis

Equal amounts of protein containing 4 x protein sample buffer (250 mM Tris-HCl pH 6.8, 2 % (w/v) SDS, 20 % (v/v) β -mercaptoethanol, 40 % (v/v) glycerol, 0.5 % (w/v) bromophenol blue) were boiled for 5 min and loaded on a 10% SDS-PAGE gel ((Separating: 10 % (w/v) acrylamide, 0.38 M Tris-HCl pH 8.8, 0.1 % (w/v) SDS, 0.05% ((w/v)) APS, 0.07 % (v/v) TEMED) (Stacking: 4 % (w/v) acrylamide, 132 mM Tris-HCl pH 6.8, 0.1 % (w/v) SDS, 0.05 % (w/v) APS, 0.15 % (v/v) TEMED)). Proteins were separated according to their size in SDS running buffer (25 mM Tris-HCl pH 8.5, 190 mM glycine and 1% (w/v) SDS) at 200 V for approximately 45 min (Mini-PROTEAN 3 electrophoresis cell, BioRad). A pre-stained protein marker was used for reference (Invitrogen). Silver staining of an SDS-PAGE gel was performed according to the protocol described by Wray *et al.*, (1981).

2.9.4 Western Blot Transfer

Protein extracts separated on SDS-PAGE were transferred to nitrocellulose membrane (BioRad) by western blot (Mini-PROTEAN Trans-Blot transfer cell, BioRad) in transfer buffer (25 mM Tris-HCl pH8.5 and 190 mM glycine) at 100 V for 1 h. The membrane was blocked using 8% (w/v) non-fat dried milk in TBS-T (10 mM Tris-HCl pH 7.5, 150 mM NaCl, 0.1 % (v/v) Triton-X 100) to remove non-specific binding.

2.9.5 Immunolabelling

UVR8-specific peptide antibodies were custom-produced and affinity purified by Sigma-Aldrich by using peptides MAEDMAAEVTAPP, located at the N-terminal region, and VPDETGLTDGSSKGN at the C-terminal region of UVR8. The phot1 antibody was kindly provided by Dr. John M. Christie (University of Glasgow) and

Prof. Winslow R. Briggs (Stanford University). All other antibodies used in this study were commercially purchased. Anti-GFP (Clontech Cat. No. 632375), anti-UGPase (UDP-glucose pyrophosphorylase, Agrisera Cat. No. AS05086), anti-H3K9 (Upstate, Cat. No. 07-441) primary antibodies were used for immunodetection. All primary antibodies were used in 1:3000 dilutions in TBS-T with 8% (w/v) non-fat dried milk and were incubated with the membrane for at least 3 hours. Between primary and secondary antibody incubations, membranes were washed twice with TBS-TT (10mM Tris-HCL pH 7.5, 150 mM NaCl, 0.1 % (v/v) Triton-X 100, 0.05 % (v/v) Tween) and one time with TBS-T for a total of 15 min. Secondary anti-rabbit and anti-mouse HRP or AP conjugated antibodies were obtained from Promega and were used in 1:5000 dilutions in TBS-T with 8% (w/v) non-fat dried milk. The duration of the incubation was at least 1 h followed by five washes with TBS-TT for a total of 25 min.

2.9.6 Immunodetection

Depending on the conjugated label of the secondary antibody, immunodetection was performed either by chemiluminescence or colorimetry for Horse-Radish-Peroxidase and Alkaline Phosphatase conjugates respectively. For chemiluminescent detection the ECL Plus western Blotting Detection system (Amersham) was used according to the manufacturer's instructions. After a 5-min incubation with the ECL reagents, the membrane was covered with clingfilm and placed in an X-ray cassette. General-purpose blue X-ray film (Kodak) was applied on top of the membrane in the cassette under safe red light conditions. The film was developed by the X-OMAT developing system. For colorimetric visualisation of secondary antibodies conjugated to AP, the membrane was incubated in BCIP/NBT pre-mixed reagents (Sigma) for up to 15 min.

2.9.7 Stripping of immunolabelled protein membrane

A stripping procedure is necessary for complete antibody removal from an already immunolabelled protein membrane in order to be re-probed with different antibodies. Membranes developed by chemiluminescence were washed in TBS and then incubated in Stripping Buffer (100 mM β -mercaptoethanol, 2 % (w/v) SDS, 62.5 mM Tris-HCl pH 6.8) at 50 °C for 30 min with gentle agitation (30 rpm). The membrane was washed twice with TBS-T for a total of 10 min at room temperature and then blocked in TBS-T with 8 % (w/v) non-fat dried milk for 45 min to 1 h. Immunolabelling and immunodetection were carried out as described in 2.9.5 and 2.9.6.

2.10 Immunoprecipitation of GFP-tagged proteins from plant extracts

Total protein was extracted from Arabidopsis plants according to 2.9.1 by grinding in Micro-Extraction buffer. The protein samples (500 μ g) were incubated on ice for 30 min with 50 μ l magnetic anti-GFP micro-beads (μ Mac beads 130-091-370, Myltenyi Biotec) according to the manufacturer's instructions. A micro-column was equilibrated with 200 μ l lysis buffer. The protein eluate containing the anti-GFP micro-beads was applied on the column. Non-GFP tagged proteins were allowed to flow through the column and the GFP-tagged proteins were retained on the column via a magnetic interaction through the magnetic anti-GFP micro-beads. The column was washed four times with 200 μ l of lysis buffer and once with Tris-HCl, pH 7.5. To elute the purified GFP-tagged proteins, 20 μ l of elution buffer (0.1 M triethylamine pH 11.8, 0.1% (w/v) Triton X-100) was applied on the column and incubated for 5 min at room temperature. An extra 50 μ l of elution buffer was added and the eluate was collected in a tube containing 3 μ l of 1 M MES, pH 3 in order to neutralise the pH of the sample so as to avoid abnormalities during migration on SDS-PAGE. The identity of the

immunoprecipitated protein was confirmed by western blot and silver staining of the SDS-PAGE gel.

2.11 Chromatin Immunoprecipitation Assay

2.11.1 Chromatin Immunoprecipitation of Arabidopsis plant tissue

For chromatin immunoprecipitation assays Arabidopsis plants were grown in white light ($80 \mu\text{mol m}^{-2} \text{s}^{-1}$) for 12 days and illuminated with UV-B ($3 \mu\text{mol m}^{-2} \text{s}^{-1}$) for 4 hours. The protocol used for ChIP assays in this study is based on Gendrel *et al.* (2002) and was modified by Dr. Cat Cloix (Brown *et al.* 2005). Approximately 2 g of plant tissue was harvested and cross-linked in 1% (w/v) formaldehyde for 15 min under vacuum. The cross-linking was stopped by adding glycine to a final concentration of 0.125 M for 5 min under vacuum. Plants were washed with water to remove formaldehyde and the tissue was ground in liquid nitrogen to obtain a fine powder. The powder was resuspended in buffer containing 0.4 M sucrose, 10 mM Tris-HCl pH 8, 10 mM MgCl_2 , 5 mM β -mercaptoethanol, 0.1 mM PMSF and one protease inhibitor mix tablet (Complete Mini, Roche) per 30 ml of solution. The homogenate was then filtered through two layers of Miracloth and centrifuged for 20 min at 4,000 g. The pellets were resuspended in a buffer containing 0.25 M sucrose, 10 mM Tris-HCl pH 8, 10 mM MgCl_2 , 1% (v/v) Triton X-100, 5 mM β -mercaptoethanol, 0.1 mM PMSF and protease inhibitor, followed by a 10-min centrifugation at 12,000 g. The pellets were resuspended in a buffer containing 1.7 M sucrose, 10 mM Tris-HCl pH 8, 0.15% (v/v) Triton X-100, 2 mM MgCl_2 , 5 mM β -mercaptoethanol, 0.1 mM PMSF and protease inhibitor and were deposited on a layer of the same buffer followed by centrifugation for 1 hour at 16,000 g. The pellets were resuspended in nuclei lysis buffer (50 mM Tris-HCl pH 8, 10 mM EDTA, 1% (w/v) SDS and protease inhibitor). In order to break the chromatin into fragments of approximately 500 basepairs, the resuspended pellets were sonicated six times for 10 s on ice using a sonicator (Soniprep 150, Sanyo) and

centrifuged for 10 min at 16,000 *g*. The supernatant was diluted by 10-fold with ChIP dilution buffer (1.1% (v/v) Triton X-100, 1.2 mM EDTA, 16.7 mM Tris-HCl pH 8, 167 mM NaCl). The chromatin-enriched solution was pre-cleared with 100 μ l of protein A Dynabeads (Invitrogen), at 4°C constantly rotating for 1 hour. Immunoprecipitation of the chromatin associated proteins with specific UVR8 peptide antibodies, anti-GFP antibody (Invitrogen A-11122) at a dilution of 1/500 or no antibody were carried out at 4 °C constantly rotating overnight. The immunoprecipitated chromatin and the associated proteins were collected after incubation with 100 μ l of protein A Dynabeads. The immunoprecipitated chromatin and the associated proteins were washed with salt, LiCl and Tris-EDTA solutions to remove non-specific binding and were subsequently eluted twice with 250 μ l of elution buffer (1% (w/v) SDS, 0.1 M NaHCO₃) at 65 °C for 30 min in total. To reverse the cross-linking the samples were incubated with 0.2 M NaCl at 65 °C for a minimum of 5 hours. Proteins were removed by a Proteinase K (20 μ g ml⁻¹) treatment and DNA was isolated by phenol/chloroform extraction and ethanol precipitation. The purified DNA pellets were resuspended in 30 μ l of Tris-EDTA pH 8.

2.11.2 Conditions of PCR on ChIP

The PCR conditions for the amplification of immunoprecipitated DNA were optimised by Dr. Cat Cloix (Brown *et al.* 2005). The PCR reaction was performed with 1 μ l of immunoprecipitated DNA in a master-mix containing 1 x PCR Buffer (New England Biolabs), 0.2 mM dNTPs, 1 μ M of each primer, 0.625 Units of *Taq* DNA Polymerase (New England Biolabs) and sterile water to a final volume of 25 μ l. The sequence of the primers used for the amplification of the promoter region (-331 to +23) of *HY5* were the following: 5'TTGGTTTATGGCGGCTATAAA3'(forward) and 5'TGGCTACCGCCGTCAGAT3'(reverse). Primers for ACTIN2 (2.7.3) were used as a negative control. The PCR conditions were the following: 5 min 30 sec at 95 °C (Step

1), 30 sec at 95 °C (Step 2) 30 sec at 57 °C (Step 3), 45 sec at 72 °C (Step 4), Step 2 for 39 cycles for *HY5_{pro}* or 34 for *ACTIN2* followed by 45 sec at 72 °C.

2.12 Confocal Microscopy

2.12.1 Co-localisation measurements of GFP and DAPI

Transgenic plants were grown on agar plates containing 2.15 g l⁻¹ Murashige and Skoog salts, 0.8 % agar for 12 days and treated with light conditions as described in the figure legends. To visualise nuclei, plants were incubated with 50 µg ml⁻¹ of 4', 6'-Diamidino-2-phenylindole (DAPI) (Molecular Probes) for 15 min. The subcellular localisation of GFP and DAPI was visualised by a confocal laser scanning microscope (Zeiss LSM 510) under water with a 40 x objective lens. GFP and DAPI fluorescent tags were excited using an argon laser at 488 nm and a UV laser at 395 nm respectively. GFP emission was collected between 505-530 nm to avoid cross-talk with chloroplast autofluorescence. Average nuclear GFP fluorescence intensities were measured using the region of interest function of the Zeiss LSM software. For the ratio of GFP/DAPI colocalisation, approximately 20 separate images containing a mean of 20 cells from 6 different plants were analysed for each time point or fluence rate. Co-localisation analysis was performed on three independent GFP-UVR8 transgenic lines. The data shown are representative of at least three independent experiments.

2.13. Yeast-Two-Hybrid Methods

2.13.1 Yeast Transformation with Plasmid DNA

A protocol for small-scale transformation of yeast cells with plasmid DNA was provided by Dr. Tong-Seung Tseng (Prof. W. Briggs' lab, Carnegie Inst. Washington,

Stanford University). A colony (log-phase dividing cells) of AH109 yeast strain grown on YPD agar plates containing 20 g l⁻¹ peptone, 10 g l⁻¹ yeast extract and 20 g l⁻¹ agar was resuspended in 30 µl of sterile H₂O. Approximately 1 µg of plasmid DNA and 270 µl of transformation solution containing 32 % (w/v) PEG, 0.1 M LiAc and 10 mM TE buffer pH 8.0 was added to the cell suspension followed by vigorous vortexing and an incubation at 42 °C for 15 min. The transformation mix was incubated at room temperature overnight. The next day cells were pelleted by centrifugation at 16,000 g for 30 sec. The pellet was resuspended in 200 µl of sterile H₂O and plated on agar plates containing selective medium for plasmid DNA (46.7 g l⁻¹ Minimal SD Agar Base, 0.64 g l⁻¹ Leu⁻ or/and Trp⁻ DO Supplement, BD Biosciences) or selective medium for plasmid DNA and interacting proteins (46.7 g l⁻¹ Minimal SD Agar Base, 0.64 g l⁻¹ Leu⁻/Trp⁻/Ade⁻/His⁻ DO Supplement, BD Biosciences, 20 mM x-α-gal). The plates were incubated at 30 °C for 2 to 3 days, until colonies developed. If two plasmids were co-transformed and the expressing proteins were interacting the colonies on the selective medium for the interaction plates would turn blue. If there was no interaction or a single plasmid was transformed in yeast cells, colonies would develop only on the plate selecting for the plasmid.

2.13.2 Isolation of Protein from Yeast

A colony of yeast cells containing the plasmid DNA of interest was inoculated in 100 ml of a medium containing 26.7 g l⁻¹ Minimum SD Base and Trp⁻ DO Supplement (for pGBKT7 plasmid vector). The culture was incubated at 30 °C, constantly shaking (200 rpm), overnight. Cells were pelleted by centrifugation at 2000 g for 5 min. The pellet was washed in sterile dH₂O and resuspended in 500 µl of breaking solution (100 mM Tris pH 8.0, 1 mM EDTA, 5 mM MgCl₂, 10 mM β-mercaptoethanol, 1 mM PMSF, 20 % (v/v) glycerol, 0.1 % (v/v) Triton-X100, protein inhibitor mix 1 tablet/10 ml) in presence of 400 µl of acid washed glass beads (Sigma). The cell suspension was

vigorously vortexed at 4 °C for 15 min. To examine if the bait protein is expressed in yeast, protein was extracted and immuno-detected by western blot transfer as described in detail in protein methods.

2.13.3 Large-Scale Yeast Transformation for Library Screening

A large-scale transformation was carried out in order to screen a cDNA library (Theologis λ -ACT from dark-grown 3-day old seedlings) for interacting partners for UVR8. Competent cells (strain MaV203) and reagents for the transformation were purchased from Invitrogen and the procedures followed were according to the manufacturer's instructions. 40 μ g of plasmid DNA of the bait vector (pGBKT7-UVR8) and 40 μ g of the cDNA library were co-transformed in 500 ml of competent yeast cells. Following the heat shock procedure described in the manual supplied with the cells by Invitrogen, cells were pelleted by centrifugation at 640 g for 5 min. The supernatant was decanted and the cells were resuspended in 5 ml YPD medium. The cell suspension was incubated at 30 °C for 90 min, followed by centrifugation at 640 g for 5 min. The supernatant was decanted and the pellets were resuspended in 8 ml of 0.9 % (w/v) NaCl. 400 μ l of cell suspension was plated on each large (140 mm) agar plate containing selective medium for interacting proteins (46.7 g l⁻¹ Minimum SD Agar Base, 0.64 g l⁻¹ Leu⁻/Trp⁻/Ade⁻/His⁻ DO Supplement, BD Biosciences, 50 mM 3-AT).

2.13.4 Isolation of DNA from Yeast

Colonies of yeast strain MaV203 grown on selective medium for interacting proteins (46.7 g l⁻¹ Minimum SD Agar Base, 0.64 g l⁻¹ Leu⁻/Trp⁻/Ade⁻/His⁻ DO Supplement, BD Biosciences, 50 mM 3-AT) were resuspended in 300 μ l lysis buffer (2 % (v/v) TritonX-100, 1 % (v/v) SDS, 100 mM NaCl, 10 mM Tris pH 8, 0.1 mM EDTA), 200 μ l of phenol:chloroform:isoamyl alcohol (1:24:1) and 300 mg of glass beads. The cell

suspension was vigorously vortexed for 6 min and subsequently centrifuged at 16,000 g for 5 min. The supernatant was transferred to a clean tube and the DNA was precipitated at -20 °C overnight by adding 30 µl 3 M NaOAc and 60 µl of 100 % (v/v) ethanol. The pellet was washed with 500 µl of 70 % (v/v) ethanol twice and centrifuged at 16,000 g for 1 min. The supernatant was decanted and the pellet was allowed to dry at room temperature before resuspension in 50 µl of sterile dH₂O. The plasmid DNA expressing the interacting protein partner identified from the screen was transformed in electrocompetent *E. coli*. The DNA was sequenced with the appropriate primers (pACT 5' and pACT 3').

2.13.5 Plasmid DNA constructs for Yeast-Two-Hybrid Analysis

All proteins tested in directed yeast-two-hybrid for interaction with UVR8 were cloned in the plasmid vector pGAD7. The primers and the restriction sites used for cloning are listed in the table below. The sequences of all constructs were confirmed by sequencing from pGADT7 vector.

Primer	Primer Sequence	PCR conditions	Restriction site
HY5	FOR5'-AGCGAATTCATGCAGGAACAAGCGACTAG-3' REV5'-AGCCTCGAGTCAAAGGCTTGCATCAGC-3'	T _A = 55 °C T _{Ext} = 2 min	5' <i>EcoRI</i> 3' <i>XhoI</i>
DET1	FOR5'-GCAAAGCATATGTTTACAAGCGGTAACGTC-3' REV5'-GCATTTATCGATTCATCGCCTAAAAATGGATATTGA-3'	T _A = 55 °C T _{Ext} = 2 min	5' <i>NdeI</i> 3' <i>Clal</i>
COPI	FOR5'-AGCGAATTCATGGAAGAGATTTTCGACGGAT-3' REV5'-GCATTTATCGATTCACGCAGCGAGTACCAGAA-3'	T _A = 55 °C T _{Ext} = 4 min	5' <i>EcoRI</i> 3' <i>Clal</i>
CRY2	FOR5'-GCAAAGATGAACGACCATATCCACCGTGTT-3' REV5'-GCATTTATCGATTCATTTGCAACCATTTTTTCC-3'	T _A = 56 °C T _{Ext} = 5 min	5' <i>NdeI</i> 3' <i>Clal</i>
BRI KIN	FOR5'-AGCGAATTCCTCCATAATGATAGTCTGATT-3' REV5'-ACGGGATCCTCATAATTTTCCTTCAGGAACTTC-3'	T _A = 55 °C T _{Ext} = 4 min	5' <i>EcoRI</i> 3' <i>BamHI</i>

CHAPTER 3

PROTEIN ANALYSIS AND SUBCELLULAR LOCALISATION OF UVR8

3.1 Introduction

In order to investigate the parameters that regulate UVR8 at the protein level two main approaches were developed and are described in this chapter. Initially, UVR8 specific antibodies were produced in order to monitor the levels of the native UVR8 protein. Furthermore, the generation of stable transgenic Arabidopsis lines expressing GFP-UVR8 under the control of the *UVR8* promoter was necessary for examining the intracellular localisation pattern of UVR8. The major findings in this chapter are that UVR8 is abundant in all tissues, under different light qualities and throughout the life cycle of Arabidopsis. At the subcellular level, UVR8 is localised in the nucleus and in the cytoplasm of epidermal cells and UV-B induces a rapid and low fluence rate dependent nuclear translocation of UVR8.

3.2 Characterisation of UVR8-specific antibodies

A great number of signalling components are regulated at the protein level by post-translational modification, protein synthesis, degradation, or protein-protein interactions. For this reason, one of the major priorities for this study was to produce UVR8-specific antibodies in order to examine UVR8 function and abundance. Based on the sequence alignment of UVR8 and its closest homologue, RCC1, (Figure 1.5), UVR8-specific amino acid sequences were selected for the generation of UVR8 peptide antibodies. More specifically, the N-terminal UVR8 antibody was raised against the first 15 amino acids of UVR8 (MAEDMMAADEV TAPP), whereas the C-terminal UVR8 antibody was raised against 15 amino acids near the C-terminus of UVR8 (VPDETGLTDGSSKGN). Both regions chosen for UVR8-specific antibody

production are unique to UVR8 (based on BLAST analyses), so as to avoid cross-reaction with other proteins. According to the immunoblots shown in Figures 3.1 (B) and (C), both N and C-terminal UVR8-specific antibodies recognise UVR8 from total protein extracts from light-grown Arabidopsis plants. UVR8 migrates at the expected molecular weight of 47 kD on a 10 % SDS PAGE gel and there is no obvious non-specific cross-reactivity with non-UVR8 proteins. Furthermore, there is no UVR8 protein detected in *uvr8-1* mutant plants, although there is mRNA transcript produced (B. A. Brown, unpublished data). Therefore, as a null mutant allele, *uvr8-1* is a suitable background to be stably transformed with a modified version of *UVR8* in order to test its functionality *in vivo*.

Both UVR8 antibodies have been successful in recognising not only the denatured but also the native form of UVR8 and are successful in immunoprecipitating UVR8 from total and chromatin enriched protein extracts, as will be described later in Figure 3.6.

3.3 UVR8 is abundant and ubiquitously expressed in Arabidopsis

The importance of UVR8 is to provide the plant with the necessary protection against UV-B irradiation, since *uvr8* mutant plants produce inadequate concentrations of flavonoids and most likely other UV-protective components and consequently are unable to survive under natural sunlight (Kliebenstein *et al.*, 2002 and Brown *et al.*, 2005). However, it is important to establish whether UVR8 is essential in specific tissues of the plant and whether its action is restricted only to the leaf tissue, being the major photosynthetic organ. Since the UVR8-specific antibodies described in 3.2 are available, instead of examining the transcript levels of *UVR8*, the spatial distribution of UVR8 protein was examined. Western blot analysis of total protein extracted from different tissues of Arabidopsis plants and probed with the C-terminal UVR8 antibody is shown in Figure 3.2. From this analysis it is evident that UVR8 is expressed at significant levels in all the major tissues of the plant. As expected, UVR8 protein of the

standard molecular weight is present in all the photosynthetic organs such as the rosette and cauline leaves, the stem and the siliques. Furthermore, UVR8 is highly expressed in the flower and the root tissue. The band-shift observed for UVR8 in these two tissues is probably due to the absence of the large subunit of rubisco, which is very abundant and migrates at the same size as UVR8 in all photosynthetic tissues.

3.4 The abundance of UVR8 is unaffected by light

Since UVR8 is involved in light signalling, it seemed likely that UVR8 expression could be regulated in a light-dependent manner. For this reason wild-type *Arabidopsis* plants were grown or illuminated with various light qualities and quantities and their UVR8 protein levels were examined by western blot analysis. As shown in Figure 3.3 (A), UVR8 is expressed in 5-day old seedlings grown either in complete darkness, low or high fluence rates of white light, suggesting that the abundance of UVR8 protein is not fluence – dependent, whereas the expression of *rbcl* (a light-dependent protein) is insignificant in darkness and increases considerably with increasing fluence rates of white light. Further immunoblot analyses on 12-day old plants grown in low fluence rates of white light ($20 \mu\text{mol m}^{-2} \text{s}^{-1}$) and then illuminated with specific wavelengths of red ($100 \mu\text{mol m}^{-2} \text{s}^{-1}$), UV-A ($100 \mu\text{mol m}^{-2} \text{s}^{-1}$) or UV-B ($3 \mu\text{mol m}^{-2} \text{s}^{-1}$) light for 4 hours (Figure 3.3 (B)) indicate that UVR8 protein expression is also wavelength independent. Furthermore, due to the specificity of UVR8 function in response to UV-B (Brown *et al.*, 2005), wild-type plants were treated with low fluence rates of UV-B ($3 \mu\text{mol m}^{-2} \text{s}^{-1}$) during a time-course ranging from 30 min to 24 hours. Once more, UVR8 abundance exhibited insignificant change. These observations show that UVR8 protein accumulation is fluence rate and wavelength independent.

3.5 GFP-UVR8 stably expressed in Arabidopsis is functional

In addition to protein stability and modification, protein activity can be regulated by compartmentalisation and intracellular trafficking. To monitor a possible re-localisation event for UVR8, a cell biological approach based on tagging UVR8 with a fluorescent marker (Green Fluorescent Protein) was employed. GFP, a native protein derived from the jellyfish species *Aequorea victoria*, is a widely used reporter protein in a number of heterologous systems. The autocatalytic fluorescence activity, minimal photobleaching and improved expression in higher plants are the main advantages for using enhanced versions of GFP for direct protein visualisation by microscopy (Shaw, 2006).

In this study, *uvr8-1* mutant Arabidopsis plants were stably transformed with GFP-UVR8 fusion constructs expressed either from the native *UVR8* promoter or the constitutive *35S Cauliflower Mosaic Virus* promoter. Since both promoters resulted in consistent results, only constructs expressed from the native *UVR8* promoter will be shown in order to avoid repetition and possible artefacts due to overexpression. Data obtained with the *35S* promoter fusion are reported in Brown *et al.* (2005).

Figure 3.4 (B) shows that GFP-UVR8 is expressed and can be detected on a western blot by using the C-terminal UVR8 antibody. Both native UVR8 and GFP-UVR8 migrate on an SDS-PAGE gel at the predictable molecular size of 47 kD and 77 kD respectively. The presence of a double band only for GFP-UVR8 could be due to degradation or post-translational modification of GFP-UVR8. It should be noted that similar occurrence of multiple bands has been observed for the native UVR8 protein too but its presence is inconsistent and non-reproducible. To test if phosphorylation is responsible for the existence of such multiple bands, protein extracts were incubated with phosphatase; however no effect was observed on either forms of the protein (data not shown).

It is also important to assess if GFP-UVR8 is biologically active and stable when expressed in *uvr8-1* mutant plants, as the GFP tag could interfere with the function or the stability of the protein. Immunoblot analysis shown in Figure 3.4 (C)

shows that GFP-UVR8 protein abundance is light quality-independent as observed for UVR8 (Figure 3.3 (B)). The functionality of GFP-UVR8 was determined based on three different assays carried out on three independent homozygous transgenic lines expressing the fusion protein. Kliebenstein *et al.* (2002) and Brown *et al.* (2005) have previously shown that *uvr8* mutant Arabidopsis plants are hypersensitive to UV-B and deficient in the induction of *HY5* and *CHS* gene expression in response to low fluence rates of UV-B. For this reason, RT-PCR analysis of the induction of *HY5* and *CHS* expression in response to UV-B serves as a molecular complementation assay. Figure 3.5 (A) shows that there is an increase in the *HY5* and *CHS* mRNA but not control *ACTIN2* transcript levels when 3-week old wild-type and transgenic lines expressing GFP-UVR8 are exposed to a UV-B fluence rate within the ambient range ($3 \mu\text{mol m}^{-2} \text{s}^{-1}$) for 4 hours. *uvr8-1* mutant plants show no induction of *HY5* or *CHS* gene expression in response to UV-B, although there is still some basal level of expression under white light ($20 \mu\text{mol m}^{-2} \text{s}^{-1}$) conditions.

Furthermore, a UV-B sensitivity assay was performed on wild-type, *uvr8-1* mutant and transgenic plants expressing GFP-UVR8. Figure 3.5 (B) demonstrates that the GFP-UVR8 fusion protein fully complements the *uvr8-1* mutant phenotype, as the transgenic plants expressing GFP-UVR8 survive like the wild-type control after exposure to UV-B irradiation. On the other hand, *uvr8-1* mutant plants are hypersensitive and exhibit severe and irreparable tissue damage after exposure to UV-B.

The third approach for assaying the biological activity of GFP-UVR8 involves chromatin association. In particular, Brown and co-workers (2005) have shown that overexpressed GFP-UVR8 associates with the promoter region of *HY5* in Arabidopsis. In this study, chromatin immunoprecipitation assays are performed on chromatin enriched protein fractions from plant tissue by using anti-GFP and anti-UVR8 specific antibodies. Fragments of DNA associated with proteins, which were immunoprecipitated by the GFP or UVR8 antibodies were recovered by a phenol/chloroform extraction. Specific DNA sequences (*HY5* promoter and *ACTIN2* gene) were amplified by PCR with the appropriate primers as presented in Figure 3.6.

According to Figure 3.6 chromatin immunoprecipitation assay on plants expressing GFP-UVR8 controlled by the *UVR8* promoter shows association of GFP-UVR8 with the promoter region of *HY5*. GFP-UVR8 specifically associates with the *HY5* promoter as no association with the control *ACTIN2* gene region is detected. *uvr8-1* mutant plants are used as a negative control for the immunoprecipitation with anti-GFP and anti-UVR8 antibodies. An additional negative control involves PCR on “mock immunoprecipitation” in the absence of any antibody. A positive control includes an aliquot of the DNA recovered from the chromatin-enriched fraction before the immunoprecipitation and is described as “input”.

As a result, it can be concluded from all the complementation experiments that GFP-UVR8 expressed by the *UVR8* promoter can associate with chromatin and is fully functional in terms of regulating gene expression and surviving in UV-B conditions.

3.6 GFP-UVR8 is localised in the cytoplasm and the nucleus of plant cells

As described in 3.5, GFP-UVR8 fusion protein is biologically active and confers the wild-type phenotype when expressed in *uvr8-1* mutant plants. Therefore, analysis of the subcellular localisation of GFP-UVR8 was made possible. At least three independent transgenic lines expressing GFP-UVR8 from the native promoter were examined by laser-scanning confocal fluorescence microscopy. As presented in Figures 3.7 (A) and (B) respectively, GFP-UVR8 is localised in the cytosol and in the nucleus of epidermal cells, whereas GFP is expressed only in the cytosol and excluded from the nucleus. This suggests that GFP-UVR8 localisation is not due to the addition of the GFP tag but based on the innate properties of UVR8. The nuclear localisation of UVR8 is in accordance with one of UVR8’s site of action, which involves chromatin association and regulation of gene expression (Brown *et al.*, 2005). The detection of GFP-UVR8 fluorescence mainly at the periphery of the cells is due to the expanded vacuoles that push the cytoplasm towards the edges of the cell. However, the presence

of GFP-UVR8 in cytoplasmic strands, observed in Figure 3.7 (B) indicates that GFP-UVR8 is localised in the cytoplasm and not the plasma membrane of epidermal cells.

To examine the cytoplasmic localisation of UVR8 in more detail a biochemical approach was employed. Protein fractionation analysis proved that native UVR8 protein co-purifies with the total and soluble (cytosol and nuclear) protein fraction but is absent from the membrane fraction of the cellular protein extract (Figure 3.8). Therefore, UVR8 mimics the localisation pattern shown for UGPase, which is a cytosolic protein, and not the UV-A/blue light photoreceptor phot1, which is a plasma membrane associated protein (Sakamoto and Briggs, 2002). This result is consistent with the localisation pattern of GFP-UVR8 based on fluorescence microscopy studies.

3.7 GFP-UVR8 subcellular localisation is observed in a range of cell types and throughout development

As shown in Figure 3.2, UVR8 protein abundance is ubiquitous throughout the plant. In order to examine the cellular and subcellular distribution of UVR8 in different tissues and at very early developmental stages, transgenic lines expressing GFP-UVR8 controlled by the UVR8 promoter were used. Consistent with the western blot analysis described in 3.3 for the native UVR8 protein, GFP-UVR8 is also distributed in all tissues examined, including the root, leaf, stem and flower epidermis (Figure 3.9). Furthermore, GFP-UVR8 fluorescence is detected both in the cytoplasm and the nucleus of all cells examined, suggesting that UVR8 is functioning in a uniform manner throughout the plant. The fact that UVR8 is localised in the epidermal cells of all tissues also coincides with the indirect photoprotective function of UVR8 via up-regulating the expression of genes involved in flavonoid photosynthesis and protection against DNA damage. Furthermore, the existence of UVR8 in mesophyll cells is consistent with the role of UVR8 in protecting the plant light-harvesting machinery by inducing the expression of chloroplast proteins (Brown *et al.*, 2005). Figures 3.7 (A) and 3.9 (C) show that GFP-UVR8 is very abundant in the cytosol, the nucleus and

around the stomatal pore of the leaf epidermal guard cells. It would be interesting to investigate whether UVR8 has a specialised function regulating guard cell action or if UVR8 simply protects the stomata of the plant by inducing gene expression in response to UV-B.

The temporal pattern of UVR8 protein distribution was also examined. Figure 3.10 shows there is significant fluorescence of GFP-UVR8 controlled by the *UVR8* promoter in de-etiolated seedlings just one day after germination. GFP-UVR8 is distributed throughout the seedling including the seed coat. Western blot (Figure 3.2) and localisation studies (Figure 3.9) show that UVR8 is present at any point of Arabidopsis life cycle – from germination until flowering and seed production.

From these observations it is evident that UVR8 is expressed constitutively throughout the plant and at all developmental stages, indicating that UVR8 is essential in order to equip plants with the components necessary for protection against UV-B at all times.

3.8 UV-B induces nuclear enrichment of GFP-UVR8 and native UVR8

Many plant photoreceptors and light signalling components have been shown to change intracellular localisation in response to specific wavelengths of light (Sakamoto and Nagatani, 1996, Sakamoto and Briggs, 2002, Oravecz *et al.*, 2006). UVR8 has been characterised as a UV-B specific signalling component that regulates gene expression in Arabidopsis (Kliebenstein *et al.*, 2002 and Brown *et al.*, 2005). For this reason, the subcellular distribution of GFP-UVR8 was analysed in response to UV-B irradiation. GFP-UVR8 expressed in *uvr8-1* transgenic plants from the *UVR8* promoter shows nuclear and cytosolic localisation when grown in constant white light conditions (3.6). However, an identical UV-B treatment to the one necessary for maximal induction of *CHS* expression (Figure 3.4 (A)) is sufficient to trigger an enrichment of the nuclear fraction of GFP-UVR8. Figure 3.11 shows that nuclear fluorescence of GFP-UVR8 increases when plants are illuminated with low fluence rates of UV-B for

4 hours, whereas the GFP control remains excluded from the nucleus at any light condition. Although GFP-UVR8 is present in the nucleus in the absence of UV-B, the fluorescence intensity of nuclear GFP-UVR8 is much brighter after UV-B irradiation (Figures 3.11 (A) and 3.12 (B)), whereas the fluorescence of the cytosolic GFP-UVR8 fraction remains unchanged. In order to quantify this response, two different methods were developed. The first method is based on the co-localisation of GFP-UVR8 and DAPI fluorescence and is the one used for all the quantification measurements of this study unless otherwise stated. According to this method, every single nucleus that is detected by DAPI staining is examined for GFP-UVR8 fluorescence. Even if there is minimal fluorescence of GFP-UVR8 in the nucleus, it is scored as positive. The percentage of the nuclei containing GFP-UVR8 divided by the total number of nuclei labelled with DAPI for approximately 25 images is plotted on the graph (Figure 3.12 (A)). The increase in GFP fluorescence intensity is not taken into consideration in this assay, as every nucleus expressing detectable levels of GFP is regarded as positive. Although this assay is less sensitive, it shows that there is a 50% increase in the total number of nuclei showing detectable levels of GFP-UVR8 fluorescence in response to UV-B based on GFP/DAPI co-localisation (Figures 3.12 (A)).

The second assay for measuring the UV-B induced nuclear enrichment of GFP-UVR8 is based on fluorescence intensity measurements of nuclear GFP-UVR8 of plants illuminated or not with UV-B. Average nuclear GFP fluorescence intensities were measured using the region of interest function of the Zeiss LSM software. Quantification measurements in Figure 3.12 (B) show that there is a ten-fold increase in the number of nuclei exhibiting very high levels of GFP-UVR8 fluorescence intensity (200 to 250) and a decrease in the number of nuclei exhibiting very low levels of fluorescence (0-50) after UV-B irradiation.

In order to confirm the nuclear enrichment of GFP-UVR8 that was observed by fluorescence microscopy, a biochemical approach was employed. In particular, the native UVR8 protein levels derived from wild-type plants were examined by protein fractionation and immunoblot analysis. The western blot in Figure 3.13 shows a significant increase in the abundance of native UVR8 in the nuclear protein fraction

after a 4-hour irradiation with low fluence rate UV-B and a small decrease in the cytosolic fraction. UGPase protein abundance, which serves as a cytosolic marker and a loading control, is unaffected by the UV-B treatment. In addition, there is no detectable UGPase in the nuclear fraction, which confirms that the nuclear fraction is devoid of cytosolic contamination. Equivalent results are obtained for the protein levels of histone H3, a nuclear marker, showing insignificant increase in response to UV-B.

Furthermore, it is worth mentioning that from this western blot analysis it can be deduced that the majority of UVR8 protein within a cell is present in the cytosol and a small fraction resides in the nucleus. These results based on immunoblot analysis (Figure 3.13) are consistent with the fluorescent images (Figures 3.7 (A), 3.11 (A)). Although there is an optical illusion that the nuclear fluorescence of GFP-UVR8 is comparable to the fluorescence of the cytosol, when a Z-stack (vertical slices through the cell) scan is performed and a 3-dimensional image is reconstituted, it is obvious that the volume of the nucleus is minor compared to the substantially larger volume of the cytosol. A more clear representation of the cytosolic abundance of GFP-UVR8 is demonstrated in cells that are not fully vacuolated, such as the epidermal cells of the root tip (Figure 3.9 (A)).

An additional point with regard to the nuclear accumulation of UVR8 is whether UVR8 is translocated into the nucleus or if there is an increase in UVR8 protein synthesis that is triggered by UV-B. From the existing data it is evident that there is a UV-B induced nuclear enrichment of UVR8 observed by fluorescence microscopy (Figure 3.11 (A)) and immunoblot analysis (Figure 3.13), but the total (cytosolic and nuclear) protein levels of UVR8 are not increasing in response to UV-B (Figures 3.3 (B), (C), 3.4 (C)). This suggests that the nuclear accumulation of UVR8 is due to nuclear import and not due to an induction of UVR8 protein expression. However, this subject will be investigated and discussed further in Chapter 4.

3.9 The nuclear accumulation of GFP-UVR8 is specific to UV-B, rapid and sensitive to low fluence rates of UV-B

As demonstrated in Figures 3.11 (A) 3.12 and 3.13, GFP-UVR8 and UVR8 accumulate into the nucleus in response to UV-B. However, it was important to characterise the wavelength specificity, the kinetics and the fluence rate dependency of this nuclear import event. The approach employed was based on fluorescence microscopy and co-localisation studies of DAPI and GFP fluorescence of *uvr8-1* transgenic Arabidopsis expressing GFP-UVR8 from the *UVR8* promoter as described in 3.9 and Figures 3.11 (A) and 3.12 (A).

Although UVR8 has been previously described as a UV-B-specific signalling component (Brown *et al.*, 2005), it was necessary to establish whether the nuclear enrichment of GFP-UVR8 is also UV-B-specific. For this reason, 12-day old transgenic plants expressing GFP-UVR8 from the *UVR8* promoter grown in low fluence rates of white light ($20 \mu\text{mol m}^{-2} \text{s}^{-1}$) were exposed to different light qualities such as UV-A ($100 \mu\text{mol m}^{-2} \text{s}^{-1}$), red ($100 \mu\text{mol m}^{-2} \text{s}^{-1}$) and UV-B ($3 \mu\text{mol m}^{-2} \text{s}^{-1}$) for 4 hours. The fluence rates for red and UV-A light used in these experiments were chosen based on studies that have shown that they are sufficient for induction of *HY5* gene expression in wild-type and *uvr8* mutant plants (Brown *et al.*, 2005). Figure 3.14 (A) demonstrates that there is no significant nuclear enrichment of GFP-UVR8 in response to either white or red or UV-A light based on co-localisation of GFP and DAPI nuclear fluorescence. In contrast, consistent with Figure 3.12 (A), there is 100 % increase on the GFP-UVR8 nuclear fluorescence in response to UV-B only. These results show that white light, red light and even UV-A light are ineffective in terms of mediating the nuclear translocation of GFP-UVR8 and that this response is exclusively controlled by UV-B.

In order to monitor the kinetics of the UV-B induced nuclear accumulation of GFP-UVR8, 12-day old transgenic plants expressing $UVR8_{\text{pro}}:GFP-UVR8$ were irradiated with UV-B ($3 \mu\text{mol m}^{-2} \text{s}^{-1}$) during a time-course ranging from 10 min up to 4 hours. The percentage of the co-localisation of nuclear GFP-UVR8 and DAPI

fluorescence was measured by confocal microscopy for various time-points during the UV-B irradiation and is shown in Figure 3.14 (B). From these data it is evident that 10 min of relatively low fluence rate UV-B ($3 \mu\text{mol m}^{-2} \text{s}^{-1}$) is sufficient to trigger a significant increase in the nuclear fraction of GFP-UVR8, whereas after 30 min of UV-B irradiation the response seems to reach saturation in the total number of nuclei showing GFP-UVR8 fluorescence compared to plants in white light (Figure 3.14 (B)). Longer duration of exposure to UV-B does not seem to produce any further increase in the nuclear enrichment of GFP-UVR8 compared to 30 min of UV-B irradiation. This would suggest that the nuclear import of GFP-UVR8 triggered by UV-B occurs within minutes.

In addition, the kinetics of a possible decrease of GFP-UVR8 nuclear fluorescence was investigated after a 4-hour UV-B inductive period. Transgenic plants expressing GFP-UVR8 by the *UVR8* promoter grown in white light ($20 \mu\text{mol m}^{-2} \text{s}^{-1}$) were treated with UV-B ($3 \mu\text{mol m}^{-2} \text{s}^{-1}$) for 4 hours and subsequently returned to darkness for 24 hours. The percentage of co-localisation of GFP and DAPI nuclear fluorescence shown in Figure 3.14 (B) demonstrates that the kinetics for the recovery of the UV-B induced nuclear accumulation of GFP-UVR8 are much slower, as there is almost a 50% decrease in the total amount of nuclei containing GFP-UVR8 24 hours after the UV-B treatment.

The fluence rate dependence of the nuclear enrichment of GFP-UVR8 in response to UV-B was also examined. Transgenic Arabidopsis expressing GFP-UVR8 from the *UVR8* promoter grown for 12 days in white light ($20 \mu\text{mol m}^{-2} \text{s}^{-1}$) were illuminated with various fluence rates of UV-B, ranging from very low ($0.1 \mu\text{mol m}^{-2} \text{s}^{-1}$) to low ($3 \mu\text{mol m}^{-2} \text{s}^{-1}$) for 4 hours. Figure 3.14 (C) shows the percentage of co-localisation of GFP-UVR8 and DAPI nuclear fluorescence of untreated (white light $20 \mu\text{mol m}^{-2} \text{s}^{-1}$) plants or following illumination with 0.1, 0.3, 0.5, 1 or $3 \mu\text{mol m}^{-2} \text{s}^{-1}$ UV-B for a total of 4 hours. According to these data, there is an apparent increase in the percentage of nuclei showing GFP-UVR8 fluorescence in response to very low fluence rate UV-B ($0.1 \mu\text{mol m}^{-2} \text{s}^{-1}$), whereas $0.5 \mu\text{mol m}^{-2} \text{s}^{-1}$ UV-B is sufficient to trigger

maximal nuclear enrichment of GFP-UVR8. These findings suggest that very low fluence rate UV-B is effective in inducing nuclear import of GFP-UVR8.

The general conclusions from the results described in this section emphasize the UV-B specificity, the rapidity and the sensitivity of the nuclear translocation of GFP-UVR8.

3.10 The induction of UVR8-regulated genes in response to UV-B is consistent with the nuclear enrichment of UVR8

As described in 3.8 and 3.9, the phenomenon of nuclear enrichment of GFP-UVR8 is mediated by a very low fluence rate and short irradiation period of UV-B. In order to correlate the UV-B induced nuclear accumulation of UVR8 with the physiological function of UVR8 in response to UV-B, an approach involving gene expression analysis was undertaken. It has previously been shown that the expression of UV-B-regulated genes, such as *CHS*, is rapidly induced by ambient levels of UV-B (Jenkins *et al.*, 2001; Frohnmeyer *et al.*, 1999). In addition, photomorphogenic responses, such as the inhibition of hypocotyl growth, are induced by a very low fluence rate of UV-B ($0.1 \mu\text{mol m}^{-2} \text{s}^{-1}$; Kim *et al.*, 1998). Furthermore, Brown and coworkers have shown that UVR8 is the most upstream component of UV-B signalling pathway(s) that regulates the expression of a number of genes involved in UV-protection and photomorphogenesis, such as the transcription factor *HY5*. For this reason the mRNA transcript levels of the *HY5* gene were monitored during a time-course and under different fluence rates of UV-B.

To examine the kinetics of the induction of *HY5* gene expression in response to UV-B, RT-PCR analysis of *HY5* and control *ACTIN2* transcripts was performed on tissue from 3-week old *uvr8-1* transgenic plants expressing GFP-UVR8 that were grown in low fluence rate white light ($20 \mu\text{mol m}^{-2} \text{s}^{-1}$) and exposed to ambient UV-B ($3 \mu\text{mol m}^{-2} \text{s}^{-1}$) for 5 min, 30 min, 1h or 4 hours. As shown in Figure 3.15, 5 min of UV-B irradiation is sufficient to stimulate a detectable increase in *HY5* gene expression but not *ACTIN2* in transgenic plants expressing GFP-UVR8. Longer exposure to UV-B

leads to a higher induction of *HY5* gene expression, which reaches saturation approximately after 1 hour. These results are consistent with the observations for the kinetic analysis of the nuclear import of GFP-UVR8 in response to UV-B. The only difference is due to the fact that there was difficulty in detecting very small differences in the fluorescence intensity of nuclear GFP-UVR8 after 5 min of UV-B irradiation (Figure 3.14 (B)). For this reason, a 10-minute time point was chosen where the increase of nuclear GFP-UVR8 fluorescence was more apparent (Figure 3.14 (B)). In Chapter 4 it will be described how this difficulty was overcome. In general, both GFP-UVR8 nuclear import and UVR8-regulated induction of *HY5* expression occur within minutes and follow the same kinetic trend in response to UV-B.

The fluence rate dependence of the induction of *HY5* gene expression in response to UV-B was examined by RT-PCR analysis as described in Figure 3.16. Transgenic plants expressing GFP-UVR8 were grown in low fluence rate white light ($20 \mu\text{mol m}^{-2} \text{s}^{-1}$) and were subsequently illuminated with 0.1, 0.3, 0.5, 1 or $3 \mu\text{mol m}^{-2} \text{s}^{-1}$ UV-B for 4 hours. According to the data presented in Figure 3.16, there is a significant increase in the transcript levels of *HY5* but not *ACTIN2* at fluence rates of UV-B as low as $0.1 \mu\text{mol m}^{-2}$ and the response reaches saturation at $0.3 \mu\text{mol m}^{-2}$. Once more, both the nuclear enrichment of GFP-UVR8 and the UVR8-dependent induction of *HY5* gene expression are stimulated by very low fluence rates of UV-B. It should be mentioned that the kinetic and fluence rate dependence studies of UV-B induced gene expression in wild-type plants are examined in much greater detail by other members of the lab (B. A. Brown, G. I. Jenkins and L. R. Headland unpublished data)

3.11 Discussion

The current chapter is focused on the characterisation of UVR8 at the protein level with respect to its spatial, temporal and light-dependent distribution. According to immunoblot analyses with anti-UVR8 specific antibodies, it is clear that UVR8 is

ubiquitously expressed throughout the plant, at all developmental stages and in response to all light qualities and quantities. Furthermore, the generation of transgenic plants expressing GFP-UVR8 enabled the localisation of UVR8 to be examined at the subcellular level. UVR8 is predominantly localised in the cytosol and the nucleus. However, low fluence rates of UV-B trigger rapid nuclear enrichment of GFP-UVR8.

3.11.1 UVR8 temporal and spatial expression is constitutive

One of the major approaches for understanding the function of newly characterised proteins, such as UVR8, is to thoroughly examine the distribution of the protein in different tissues and at different developmental stages during the plant life cycle. As shown in Figure 3.2, UVR8 is abundant in all plant tissues examined including the root, the stem, the cauline and rosette leaves, the flowers and the siliques of *Arabidopsis* wild-type plants. Independent evidence regarding the spatial protein expression pattern of UVR8 comes from examining the fluorescence of plants expressing GFP-UVR8 controlled by the *UVR8* promoter. Figure 3.9 demonstrates that GFP-UVR8 is present in all plant tissues and epidermal cell types including the guard cells of the stomatal pores.

As mentioned before, UVR8 is involved in signalling and photo-protection against UV-B in *Arabidopsis* (Kliebenstein *et al.*, 2002; Brown *et al.*, 2005), so it would be expected to be present and functional in all major plant organs that are exposed to light (such as leaves and stem). Other tissues such as flowers, siliques and roots also contain significant protein levels of UVR8. However, this is not very surprising as the flowers are the reproductive organs of the plant and the siliques contain the seeds, which are necessary for survival of the species. Both these plant organs are exposed to direct light and protection is essential against the detrimental effects of UV-B irradiation. However, roots are not exposed to light, do not contain light-harvesting photosynthetic apparatus and consequently would not require protection from ultra-violet irradiation. There is evidence that enzymes involved in

flavonoid biosynthesis, such as CHS and CHI, are also localised in Arabidopsis root tissue (Saslowsky and Winkel-Shirley, 2001). Flavonoids are involved not only in protection against UV-B, but also against pathogens. The specificity of UVR8 in UV-B signalling is well established (Brown *et al.*, 2005) and there is no evidence to date suggesting that UVR8 is involved in pathogen-induced signalling. So, the existence of UVR8 in the roots may function in regulating the expression of genes involved in developmental processes other than acclimation and photoprotection induced by UV-B. It is worth mentioning that many photoreceptors such as the phytochromes and the phototropins are localised in all types of tissues examined (Sakamoto and Nagatani, 1996, Sakamoto and Briggs, 2002) demonstrating their importance for plant development and survival.

The temporal distribution of UVR8 was also examined. Figure 3.10 shows that GFP-UVR8 controlled by the *UVR8* promoter is expressed in whole seedlings just hours after germination. This suggests that UVR8 is required to be present as soon as the plant faces the sun. Immunoblot analysis has shown that significant levels of native UVR8 protein can be detected in extracts from 3-day old, 12-day old, 21-day old and 6-week old plants, confirming that UVR8 is present at every developmental stage of the plant (data not shown).

From these observations it could be concluded that the importance of UVR8 is reflected in its constitutive spatial and temporal abundance. It would be very interesting to examine whether there is tissue or temporal specificity in UVR8 signalling, as has been demonstrated for phytochrome signalling by Ma and co-workers (Ma *et al.*, 2005, Lorraine *et al.*, 2006).

3.11.2 UVR8 protein abundance is not regulated by light

Protein synthesis, degradation and stability are key regulatory processes involved in light signalling in Arabidopsis. For instance, the COP1 mediated ubiquitination and subsequent degradation of the transcription factor HY5 in darkness

has been well characterised by Deng and co-workers (Osterlund *et al.*, 2000). In response to light, HY5 accumulates in the nucleus due to the nuclear exclusion of COP1. On the other hand, light can induce protein destabilisation of photoreceptor proteins such as phyA (Jabben *et al.*, 1989), cry2 (Lin and Shalitin 2003), phot1 (Sakamoto and Briggs 2002) and light signalling components such as PIF3 (Park *et al.*, 2004).

For this reason, the protein levels of UVR8 were examined in response to darkness, red, UV-A, UV-B, low and high fluence rate white light. The western blots in Figure 3.3 demonstrate that UVR8 protein is abundant and its abundance remains unaltered in response to any light condition tested. Furthermore, as UVR8 is a UV-B-specific signalling component (Brown *et al.*, 2005), its protein levels were examined during a 24-hour time-course in UV-B. Yet, no significant change was observed in the total protein levels of UVR8 after a short (30 min) or a long (24 hours) exposure to low fluence rate of UV-B. However, these observations do not exclude the possibility that there is balanced degradation and synthesis of UVR8 protein, which would result in constant recycling without any net change in the abundance of the protein.

3.11.3 UV-B induces nuclear import of UVR8

The transition from skotomorphogenesis to photomorphogenesis is a very dramatic event that occurs during plant development. During this transition, various light induced signalling events take place, including gene expression, protein degradation and intracellular trafficking. There is an increasing number of photoreceptors and light signalling components that have been discovered to exhibit subcellular compartmentalisation and nuclear import in response to specific wavelengths of light. One of the first pieces of evidence for light-induced protein translocation of plant photoreceptors was obtained for the phytochromes, which are imported into the nucleus and form speckles (Sakamoto and Nagatani, 1996). Cry1 has been shown to be excluded from the nucleus in a blue light dependent manner (Lin and

Shalitin, 2003). Phot1 and phot2 dissociate from the plasma membrane in response to blue light (Sakamoto and Briggs, 2002; Kong *et al.*, 2006). Furthermore, COP1, a regulator of photomorphogenesis, demonstrates light-induced nuclear exclusion (von Arnim *et al.*, 1994), as well as relatively slow UV-B dependent nuclear import (Oravec *et al.*, 2006).

By taking into consideration the plethora of signalling events involving light-induced protein translocation, the subcellular localisation of UVR8 was investigated in response to different light stimuli. First, it was necessary to generate transgenic Arabidopsis lines expressing UVR8 fused to the GFP fluorescent marker. *uvr8-1* mutant plants were stably transformed with GFP-UVR8, which was under the control of the native *UVR8* promoter. The biological activity of the GFP-UVR8 fusion protein was established based on three independent complementation assays. First, RT-PCR analysis on *uvr8-1* transgenic lines expressing GFP-UVR8 showed an induction of *HY5* and *CHS* gene expression in response to UV-B (Figure 3.5 (A)). Secondly, *uvr8-1* transgenic lines expressing GFP-UVR8 survived when exposed to higher than ambient levels of UV-B (Figure 3.5 (B)). And finally, GFP-UVR8 expressed from the native promoter showed association with the promoter region of *HY5* (Figure 3.6). These results show that the GFP tag does not interfere in any way with UVR8 activity and verify that GFP-UVR8 is fully functional by rescuing the *uvr8-1* mutant phenotypes and by functioning like wild-type UVR8.

After the functionality of the transgenic lines was confirmed, the subcellular localisation of GFP-UVR8 was examined. According to Figure 3.7, GFP-UVR8 is predominantly localised in the cytosol and in the nucleus of epidermal cells. The nuclear localisation of UVR8 was not surprising, as UVR8 has been reported to be involved in the regulation of gene expression via chromatin association in the promoter region of UV-B induced genes. (Brown *et al.*, 2005; Cloix and Jenkins, 2007). Fractionation of soluble and plasma membrane associated proteins confirmed that native UVR8 is located in the cytosol and not in the plasma membrane (Figure 3.8). Furthermore, the subcellular localisation of GFP-UVR8 is nuclear and cytosolic in the epidermal layer of all tissues examined (Figure 3.9), which is also consistent with the

immunoblot analysis showing ubiquitous expression of UVR8 throughout the plant (Figure 3.2), suggesting that UVR8 is present and potentially functional in the epidermis of all plant organs.

The next aspect under investigation was the effect of light on the subcellular localisation of UVR8. As has previously been discussed, the total UVR8 protein concentration is independent of any light quality or quantity. However, this does not exclude the possibility of a light-induced intracellular translocation of GFP-UVR8. Indeed, GFP-UVR8 exhibits a significant nuclear accumulation in response to low fluence rates of UV-B. Although UVR8 resides in the nucleus in the absence of UV-B, there is an apparent increase in the nuclear fluorescence of GFP-UVR8 in response to UV-B, whereas the cytosolic fraction seems relatively unaffected (Figure 3.11 (A)). The quantification of this response was performed based on two different methods. The first method is based on calculating the percentage of the co-localisation ratio of GFP-UVR8 and DAPI fluorescence. According to this method there is an increase of 100 % in the amount of nuclei containing GFP-UVR8 in response to UV-B (Figure 3.12 (A)). The second quantification method is much more sensitive, as it involves measuring the intensity of the nuclear GFP-UVR8 fluorescence under white light or UV-B. Figure 3.12 (B) shows that there is a ten-fold increase in the number of nuclei exhibiting very high fluorescence intensities of GFP-UVR8.

Confirmation of the phenomenon of the UV-B induced nuclear enrichment of GFP-UVR8 was carried out by western blot analysis on nuclear and cytosolic protein fractions from wild-type plants that were illuminated with white light or UV-B. According to Figures 3.11 (A) and 3.13, there is a significant increase in the nuclear fraction of UVR8 in response to UV-B. The consistency of the results indicates that the accumulation of UVR8 into the nucleus is not an artefact of fluorescent microscopy or due to the fusion protein (GFP).

Unlike phytochromes, cryptochromes and COP1, GFP-UVR8 showed no nuclear speckle formation in response to UV-B or any other light quality, suggesting that UVR8 is not a component of the same complex. Subnuclear foci have been associated with active sites of transcription or degradation in response to light (Kircher

et al., 1999, Yamaguchi *et al.*, 1999, Ang *et al.*, 1998). Although UVR8 actively regulates the transcription of many UV-B induced genes, the mechanisms underlying UV-B induced gene expression may involve different complexes than the ones necessary for red and blue light signalling. However, it cannot be excluded that UVR8 could be regulated by COP1 even though they do not share the same patterns of subnuclear localisation.

The phenomenon of nuclear accumulation GFP-UVR8 in response to UV-B and not fluorescent white light (which contains most light qualities) is not surprising. The role of UVR8 exclusively in UV-B signalling is well established (Brown *et al.*, 2005 and Kliebenstein *et al.*, 2002). The UV-B specificity of this response is verified in Figure 3.14 (A), where there is no nuclear enrichment of GFP-UVR8 in response to white, red or even UV-A light. Equivalent results were obtained by Brown and co-workers (2005) with respect to the UVR8 regulated induction of *HY5* gene expression. UVR8 is responsible only for the induction of *HY5* gene expression in response to UV-B, as the *uvr8-1* mutant plants show no increase in the *HY5* transcript levels in response to UV-B but retain the red light and UV-A induced *HY5* gene expression.

Nevertheless, UV-B-specific nuclear translocation has not been previously observed in plants and may act on proteins in addition to UVR8, although none of them is known yet. However, there is evidence for UV-B induces nuclear accumulation of Fyn kinase and the nuclear factor- κ B in mammalian cells (Cho *et al.*, 2005; Jiang and Wek, 2005).

3.11.4 The mode of action of UVR8 is signified by the coordination of the UV-B induced nuclear import and the induction of UVR8-regulated gene expression

The UV-B specificity of UVR8 nuclear enrichment provides a very good system to investigate the kinetic and fluence dependence parameters of this response in more detail. Very elegant studies on phytochromes have shown that the nucleocytoplasmic partitioning of phyB is a relatively slow process that reaches

saturation within 3 hours in continuous red light (Gil *et al.*, 2000). Furthermore, COP1 has recently been discovered to act as a positive regulator of UV-B induced photomorphogenesis and accumulate in the nucleus within 24 hours of supplementary UV-B irradiation (Oravecz *et al.*, 2006).

In our case, kinetic studies on transgenic plants expressing GFP-UVR8 demonstrate that the nuclear accumulation of UVR8 is rapid, as it occurs within 10 min and is saturated after 30 min of continuous UV-B illumination (Figure 3.14 (B)). Such a rapid response is quite surprising as UVR8 is already present at low levels in the nucleus in the absence of UV-B. Whether its nuclear enrichment in response to UV-B is the signal responsible for triggering gene expression is very likely according to gene expression studies. RT-PCR analyses on plants expressing GFP-UVR8 reveal an induction of *HY5* gene expression that follows the same kinetic pattern as the nuclear accumulation of UVR8. As shown in Figure 3.15, there is an apparent increase in the mRNA levels of *HY5* after 5 min and a five-fold increase within 1 hour of UV-B irradiation. There seems to be a difference between the saturation points of the two responses. However, this could possibly be due to the fact that the UV-B induced nuclear import of GFP-UVR8 has to precede in order for the gene expression events to occur, although GFP-UVR8 is present at lower levels in the nucleus in the absence of UV-B. In the absence of UV-B, there are basal levels of *HY5* expression, which cannot be attributed to the basal nuclear levels of UVR8, as they are still present in *uvr8-1* mutant plants. Whether UV-B induced nuclear import of UVR8 precedes and is essential for the induction of UVR8-regulated genes is possible but cannot be concluded based on the data presented above. However, further investigation will be described in Chapters 4 and 5.

To assess the fluence rate dependence of the UVR8 nuclear accumulation, fluorescence microscopy on plants expressing GFP-UVR8 and irradiated with decreasing fluence rates of UV-B was carried out. Figure 3.14 (C) shows that 4 hours of $0.1 \mu\text{mol m}^{-2} \text{s}^{-1}$ UV-B are sufficient to induce a significant increase in UVR8 nuclear accumulation. Yet again, the same trend is observed for the UVR8-regulated induction of *HY5* gene expression in response to UV-B. There is a five-fold increase in

the transcript levels of *HY5* in response to 4 hour of $0.1 \mu\text{mol m}^{-2} \text{s}^{-1}$ UV-B (Figure 3.16). These data show that both the nuclear accumulation of UVR8 and the UVR8-regulated induction of gene expression are very sensitive responses, as they can be triggered by very low fluence rates of UV-B.

The rapidity and the sensitivity of the nuclear enrichment and activity of UVR8 depict the importance of UVR8 function in responding to UV-B stimuli in order to confer protection to the plant.

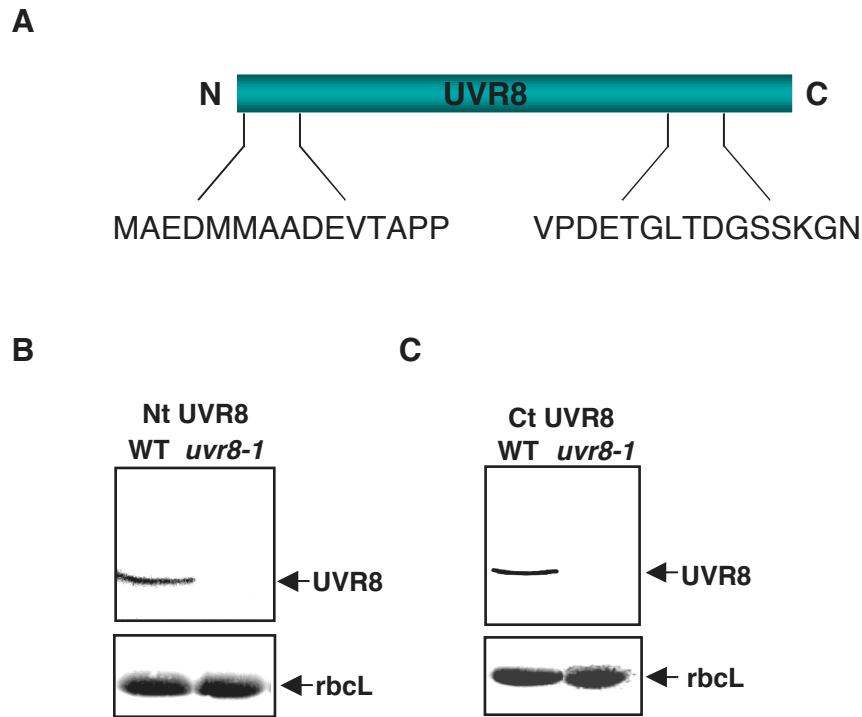


Figure 3.1 Characterisation of UVR8-specific antibodies

(A) Schematic representation of the UVR8 amino acid sequence used for the production of N-terminal and C-terminal specific peptide antibodies. (B) Western blot of total protein extracts (15 μg) from 12-day old wild-type and *uvr8-1* Arabidopsis plants grown under white light (100 $\mu\text{mol m}^{-2} \text{s}^{-1}$) conditions probed with the N-terminal UVR8-specific antibody. (C) Western blot of total protein extracts (10 μg) from wild-type and *uvr8-1* plants grown under white light conditions probed with the C-terminal UVR8-specific antibody. Ponceau stain of rubisco large subunit (*rbcL*) was used as a loading control.

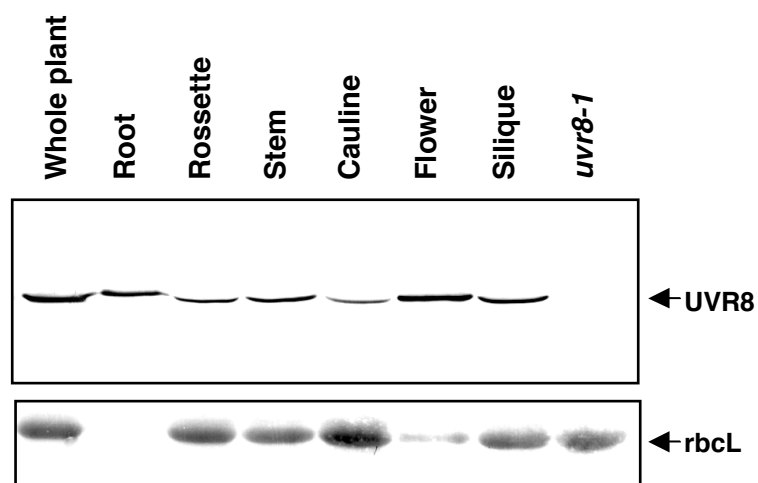
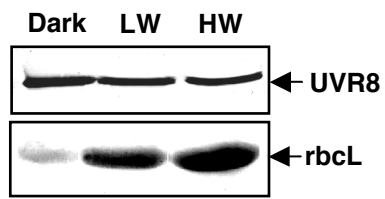


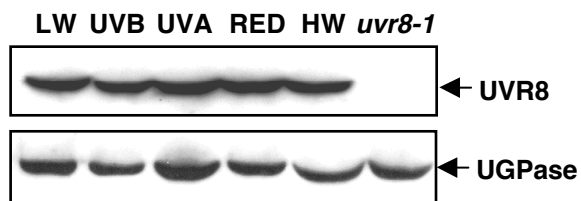
Figure 3.2 UVR8 protein is abundant in most plant tissues

Western blot analysis of total protein extracts (20 μg) from various tissues (whole plant, root, rosette leaf, stem, cauline leaf, flower and silique) of 6-week old wild-type and *uvr8-1* (whole plant) *Arabidopsis* lines grown in white light ($100 \mu\text{mol m}^{-2} \text{s}^{-1}$). The C-terminal UVR8 specific antibody was used to probe the western blot. Ponceau stain of rubisco large unit (rbcL) was used as a loading control.

A



B



C

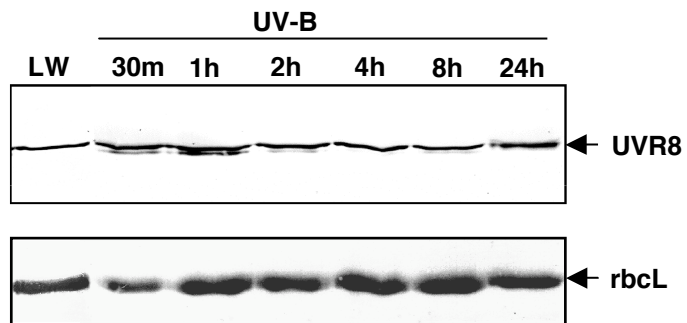


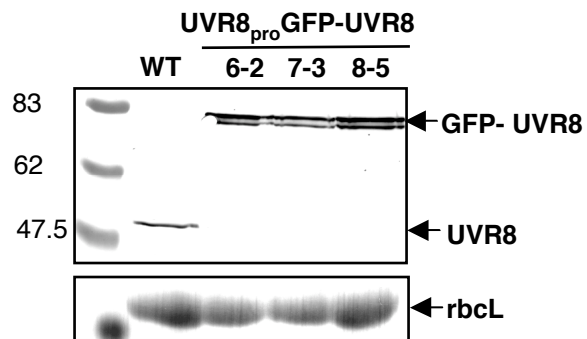
Figure 3.3 UVR8 protein levels are unaffected by different light qualities

(A) Immunoblot analysis of total protein extracts (20 μg) from wild-type plants grown in darkness, or at low ($20 \mu\text{mol m}^{-2} \text{s}^{-1}$; LW) or high ($100 \mu\text{mol m}^{-2} \text{s}^{-1}$; HW) fluence rates of white light for 5 days. The C-terminal UVR8 antibody was used to probe the blot and a ponceau stain of rubisco large subunit (rbcL) was used as a loading control. (B) Immunoblot analysis of total protein extracts (15 μg) from 12-day old wild-type and *uvr8-1* plants grown in a low fluence rate of white light ($20 \mu\text{mol m}^{-2} \text{s}^{-1}$; LW) and illuminated with UV-B ($3 \mu\text{mol m}^{-2} \text{s}^{-1}$), UV-A ($100 \mu\text{mol m}^{-2} \text{s}^{-1}$), red ($100 \mu\text{mol m}^{-2} \text{s}^{-1}$) or a high fluence rate white light ($100 \mu\text{mol m}^{-2} \text{s}^{-1}$; HW) for 4 hours. The western blot was probed with the C-terminal UVR8 antibody and a UGPase antibody as a loading control. (C) Immunoblot analysis of total protein extracts (10 μg) from 12-day old wild-type plants grown in a low fluence rate of white light ($20 \mu\text{mol m}^{-2} \text{s}^{-1}$; LW) and illuminated with UV-B ($3 \mu\text{mol m}^{-2} \text{s}^{-1}$) for 30 min, 1 h, 2 h, 4 h, 8 h and 24 h. The C-terminal UVR8 antibody was used to probe the blot and a ponceau stain of rubisco large subunit (rbcL) was used as a loading control.

A



B



C

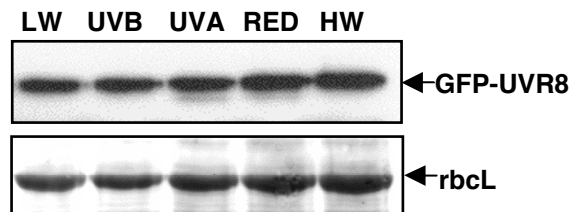


Figure 3.4 Generation of transgenic Arabidopsis plants expressing GFP-UVR8 from the native *UVR8* promoter

(A) Schematic representation of GFP-UVR8 construct driven by the *UVR8* promoter. eGFP is an enhanced GFP variant. (B) Western blot of total protein extracts (15 μg) from 12-day old wild-type or *uvr8-1* transgenic plants expressing UVR8_{pro} -GFP-UVR8 (three independent lines) grown in white light ($100 \mu\text{mol m}^{-2} \text{s}^{-1}$). The N-terminal UVR8 antibody was used to probe the western blot. (C) Immunoblot analysis of total protein extracts (15 μg) from 12-day old *uvr8-1* transgenic plants expressing UVR8_{pro} -GFP-UVR8 grown in a low fluence rate of white light ($20 \mu\text{mol m}^{-2} \text{s}^{-1}$; LW) and illuminated with UV-B ($3 \mu\text{mol m}^{-2} \text{s}^{-1}$), UV-A ($100 \mu\text{mol m}^{-2} \text{s}^{-1}$), red ($100 \mu\text{mol m}^{-2} \text{s}^{-1}$) or high fluence rate white light ($100 \mu\text{mol m}^{-2} \text{s}^{-1}$; HW) for 4 hours. The western blot was probed with a GFP antibody and ponceau stain of rubisco large subunit (rbcL) was used as a loading control.

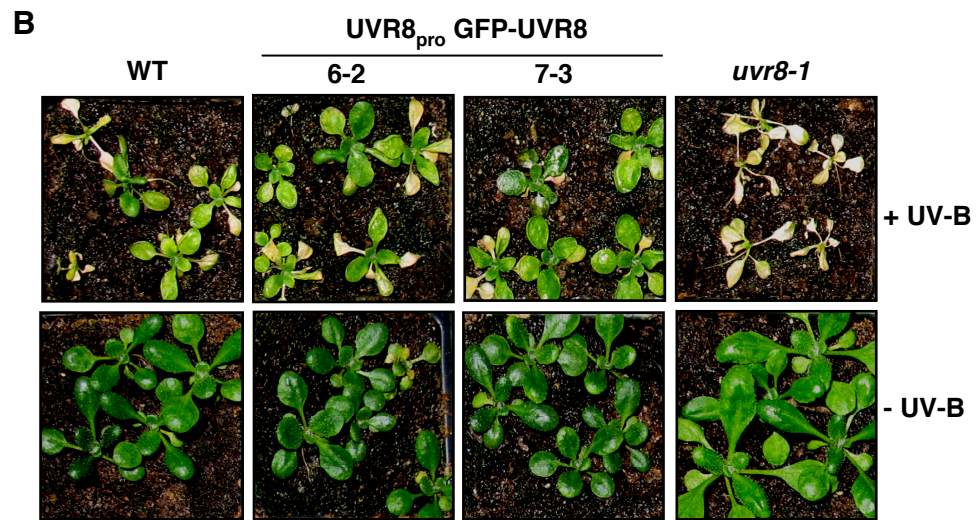
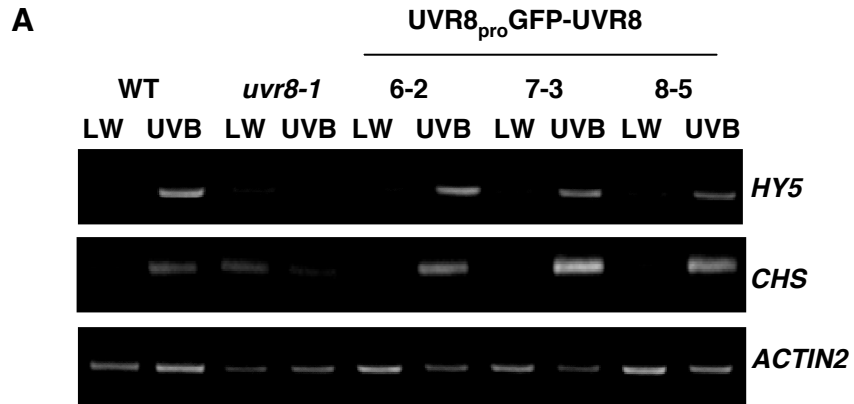


Figure 3.5 GFP-UVR8 is functional in transgenic *uvr8-1* plants

(A) RT-PCR analysis of *HY5*, *CHS* and control *ACTIN2* transcripts in wild-type, *uvr8-1* and UVR8_{pro}GFP-UVR8 lines grown in a low fluence rate of white light ($20 \mu\text{mol m}^{-2} \text{s}^{-1}$; LW) and exposed to UV-B ($3 \mu\text{mol m}^{-2} \text{s}^{-1}$) for 4 hours. (B) UV-B sensitivity assay. Wild-type, *uvr8-1* and UVR8_{pro}GFP-UVR8 lines were grown in white light ($120 \mu\text{mol m}^{-2} \text{s}^{-1}$) for 12 days and then exposed (+) or not (-) to UV-B ($5 \mu\text{mol m}^{-2} \text{s}^{-1}$) supplemented with white light ($40 \mu\text{mol m}^{-2} \text{s}^{-1}$) for 24 h. Plants were photographed after return to white light ($120 \mu\text{mol m}^{-2} \text{s}^{-1}$) for 5 days.

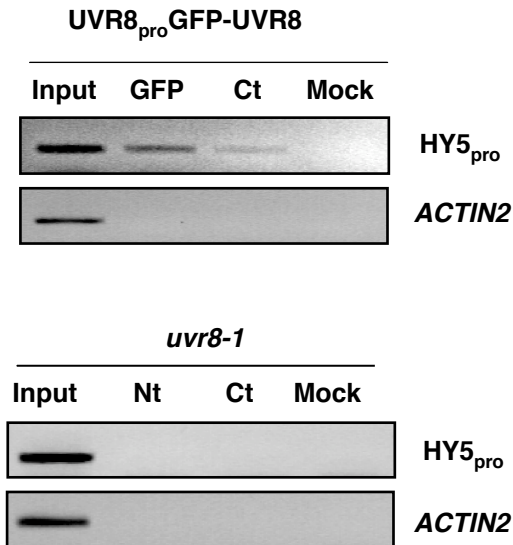


Figure 3.6 GFP-UVR8 is associated with the promoter region of *HY5*

Chromatin immunoprecipitation assay of DNA associated with GFP-UVR8. PCR of *HY5* promoter (-331 to +23) and *ACTIN2* DNA from UVR8_{pro}GFP-UVR8 (upper) and *uvr8-1* (lower) transgenic plants grown in white light (100 $\mu\text{mol m}^{-2} \text{s}^{-1}$) and exposed to UV-B (3 $\mu\text{mol m}^{-2} \text{s}^{-1}$) for 4 hours: lane 1, input DNA before immunoprecipitation; lane 2, DNA immunoprecipitated by using GFP antibody; lane 3, DNA immunoprecipitated by using C-terminal UVR8 antibody; lane 4, no antibody control (mock).

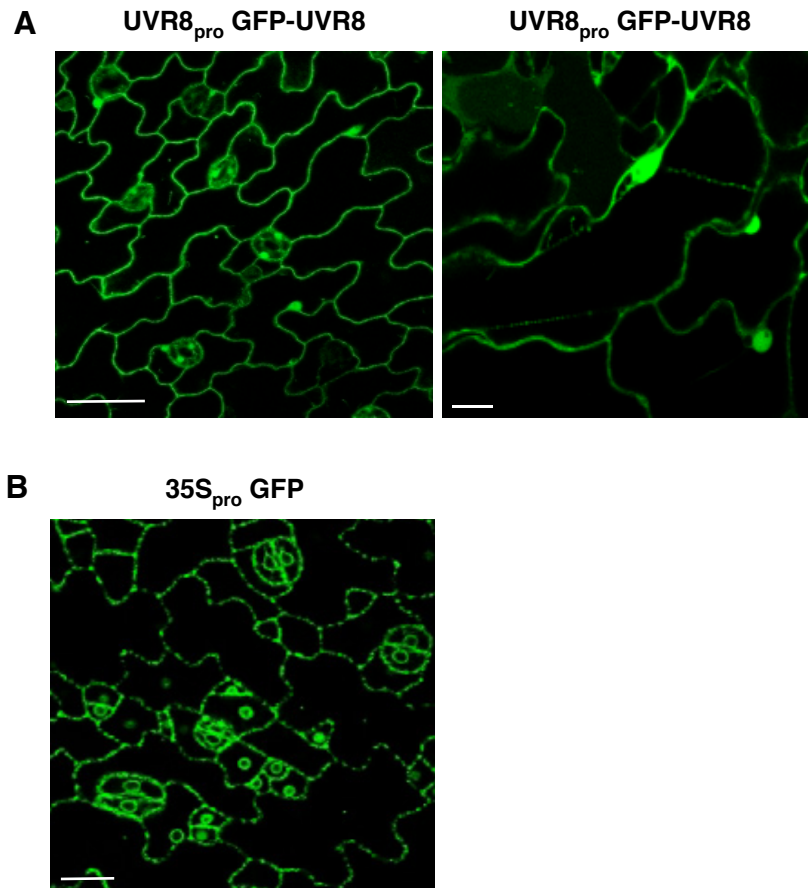


Figure 3.7 GFP-UVR8 is subcellularly localised in the nucleus and cytosol of epidermal cells

(A) Confocal images of GFP fluorescence in leaf epidermal tissue of 12-day old UVR8_{pro}GFP-UVR8 transgenic Arabidopsis (line 6-2) grown in white light ($20 \mu\text{mol m}^{-2} \text{s}^{-1}$) and exposed to UV-B ($3 \mu\text{mol m}^{-2} \text{s}^{-1}$) for 4 hours. (B) Subcellular localisation of wild-type plants expressing GFP under the constitutive Cauliflower Mosaic Virus 35S promoter grown in white light ($20 \mu\text{mol m}^{-2} \text{s}^{-1}$) and exposed to UV-B ($3 \mu\text{mol m}^{-2} \text{s}^{-1}$) for 4 hours. Scale bar = 20 μm .

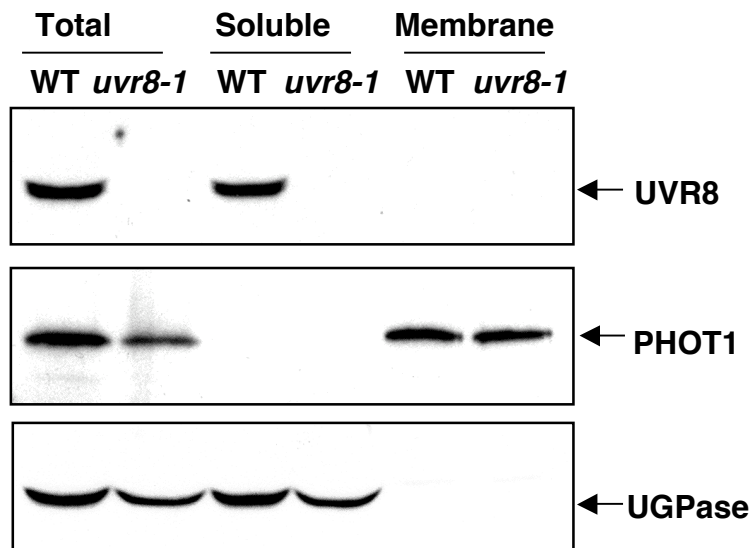


Figure 3.8 UVR8 co-purifies with the total and soluble protein fractions from wild-type plants

Western blot analysis of total, soluble and membrane fractions of protein (30 μg) extracted from 12-day old wild-type plants grown in white light $100 \mu\text{mol m}^{-2} \text{s}^{-1}$. C-terminal UVR8, phot1 (plasma membrane marker) and UGPase (cytosolic marker) antibodies were used to probe the western blot.

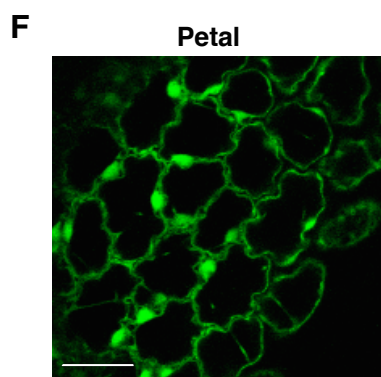
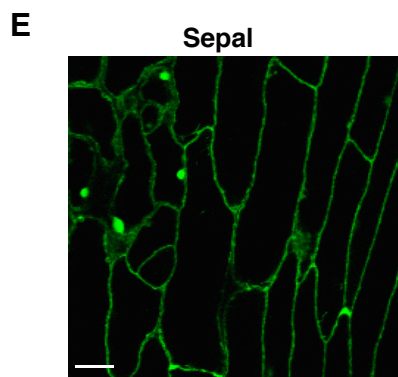
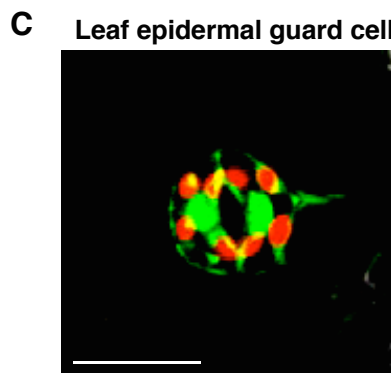
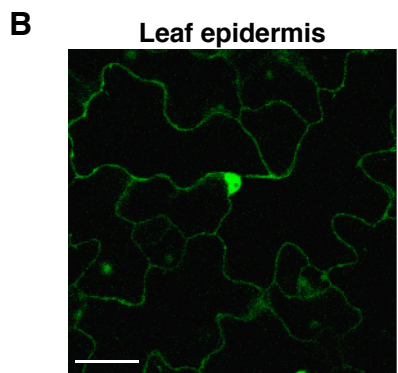
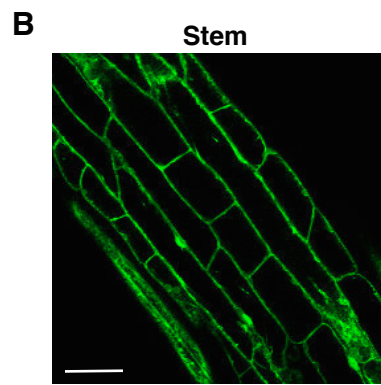
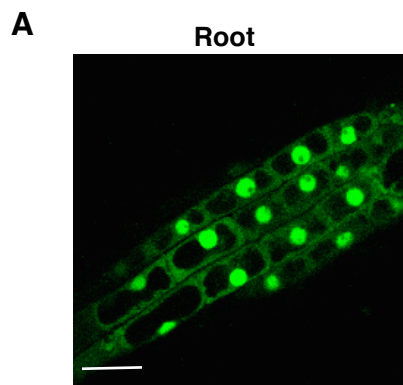


Figure 3.9 GFP-UVR8 is subcellularly localised in the nucleus and cytosol of cells in different plant tissues

Confocal images of GFP fluorescence in root (A), stem (B), leaf (C) (multi-channel image showing the autofluorescence from the chloroplasts in red colour) and (D), sepal (E) and petal (F) tissue of UVR8_{pro}GFP-UVR8 transgenic Arabidopsis (line 6-2) grown in white light ($20 \mu\text{mol m}^{-2} \text{s}^{-1}$) and exposed to UV-B ($3 \mu\text{mol m}^{-2} \text{s}^{-1}$) for 4 hours. Scale bar = 20 μm .

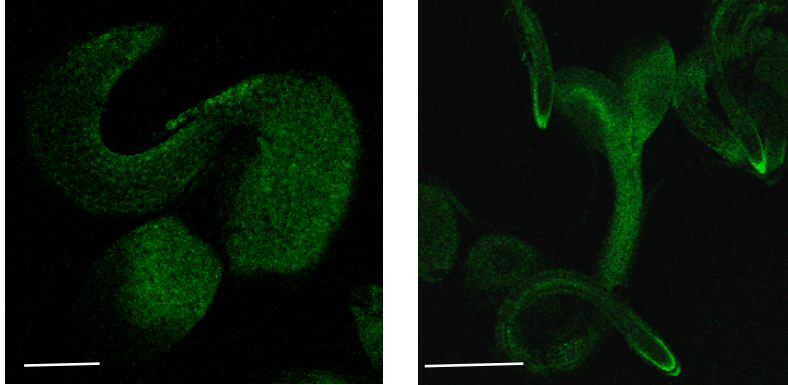


Figure 3.10 $UVR8_{pro}$ GFP-UVR8 is expressed at very early developmental stages

Confocal images of GFP fluorescence in epidermal tissue of $UVR8_{pro}$ GFP-UVR8 Arabidopsis seedlings (line 6-2) grown in white light ($100 \mu\text{mol m}^{-2} \text{s}^{-1}$). Scale bar = 0.5 mm.

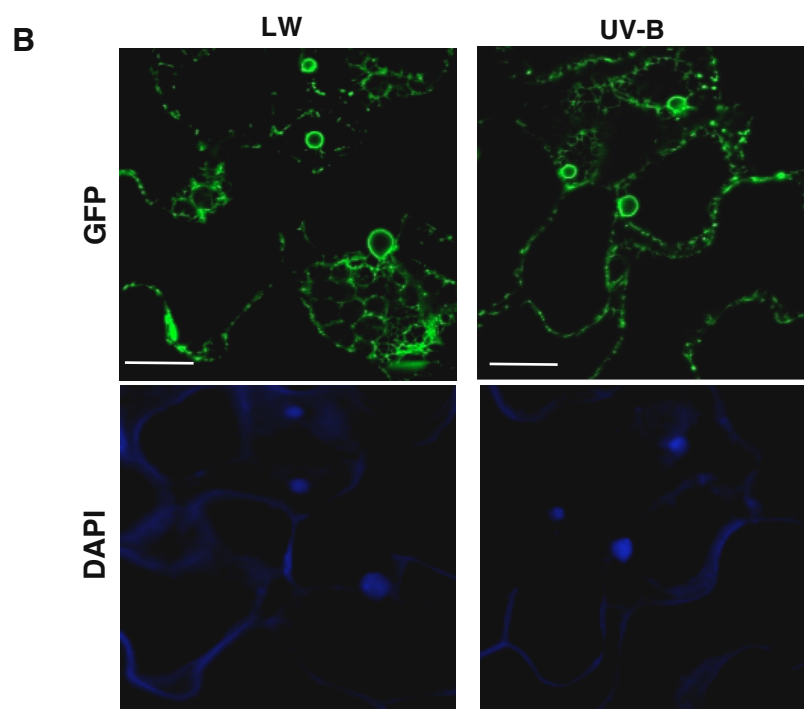
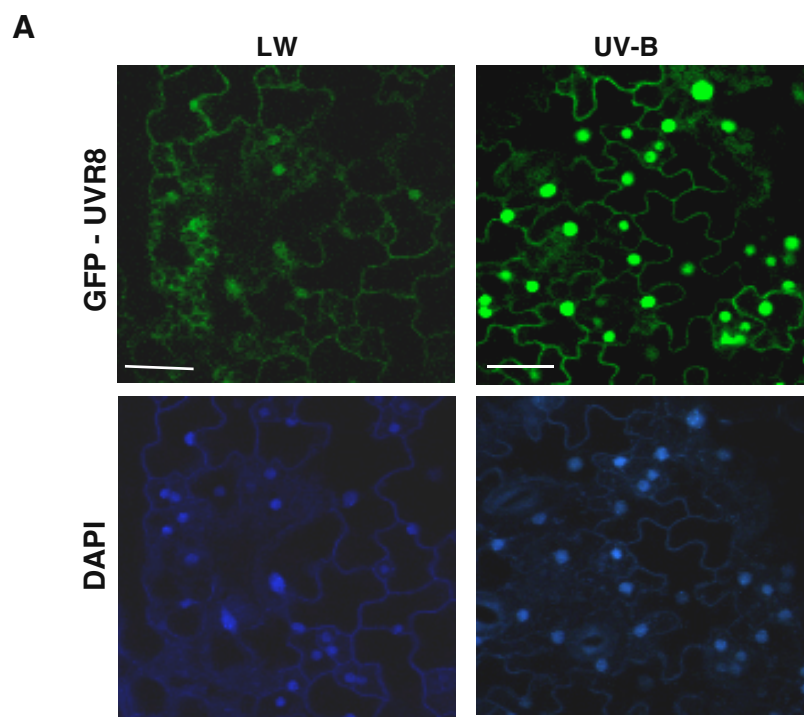


Figure 3.11 UV-B induces nuclear enrichment of GFP-UVR8

(A) Confocal images of GFP and DAPI fluorescence in the leaf epidermal tissue of UVR8_{pro}GFP-UVR8 transgenic plants (line 6-2) grown in white light ($20 \mu\text{mol m}^{-2} \text{s}^{-1}$; LW) and exposed to UV-B ($3 \mu\text{mol m}^{-2} \text{s}^{-1}$) for 4 hours. (B) Confocal images of GFP and DAPI fluorescence in leaf epidermal tissue of wild-type transgenic plants expressing GFP under the 35S promoter grown in white light ($20 \mu\text{mol m}^{-2} \text{s}^{-1}$; LW) and exposed to UV-B ($3 \mu\text{mol m}^{-2} \text{s}^{-1}$) for 4 hours. Scale bar = 20 μm .

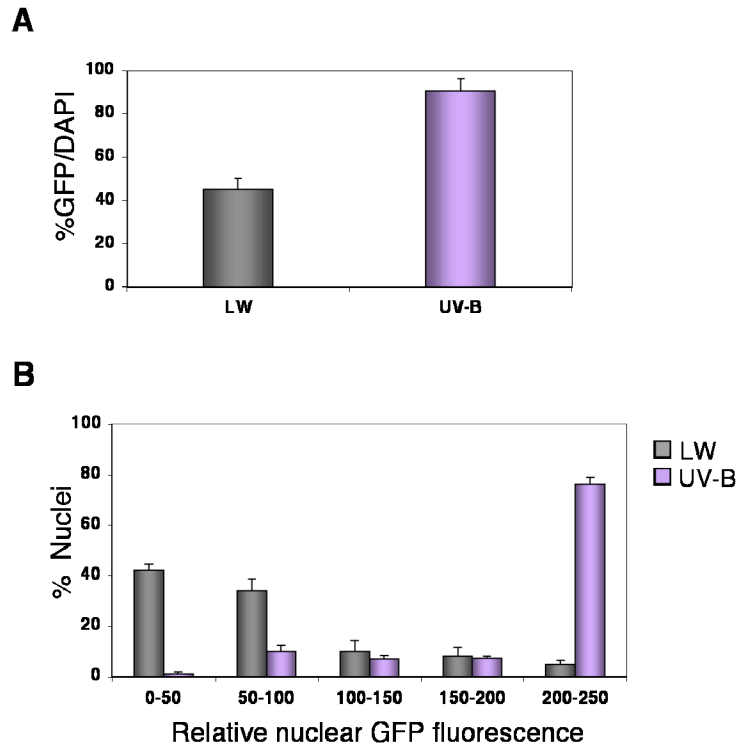


Figure 3.12 Quantification of the UV-B induced nuclear enrichment of GFP-UVR8

(A) The percentage of co-localisation of GFP and DAPI fluorescence from $UVR8_{pro}$ GFP-UVR8 transgenic plants grown in white light ($20 \mu\text{mol m}^{-2} \text{s}^{-1}$; LW) and exposed to UV-B ($3 \mu\text{mol m}^{-2} \text{s}^{-1}$) for 4 hours. (Mean \pm S. E., $n=20$). (B) Relative GFP fluorescence measurements of nuclei from $UVR8_{pro}$ GFP-UVR8 transgenic plants grown in white light ($20 \mu\text{mol m}^{-2} \text{s}^{-1}$; LW) and exposed to UV-B ($3 \mu\text{mol m}^{-2} \text{s}^{-1}$) for 4 hours. ($n = 100$). Average nuclear GFP fluorescence intensities were measured using the region of interest function of the Zeiss LSM software.

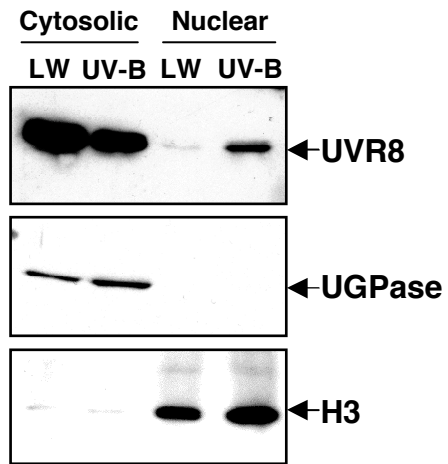
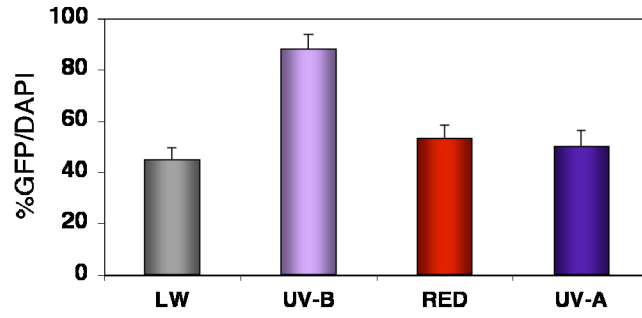


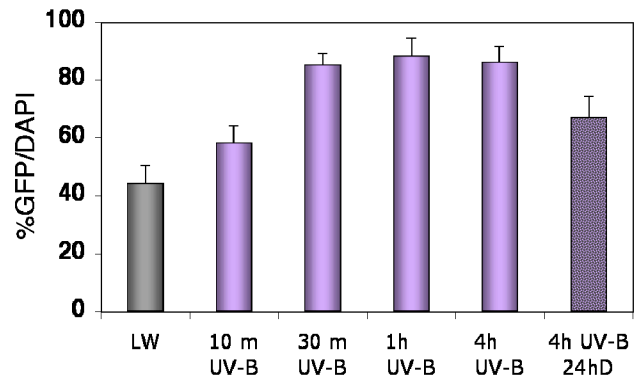
Figure 3.13 UV-B induces nuclear enrichment of UVR8 protein in wild-type plants

Western blot analysis of cytosolic and nuclear fractions of protein (20 and 30 μg respectively) extracted from wild-type plants grown in white light ($20 \mu\text{mol m}^{-2} \text{s}^{-1}$; LW) and exposed to UV-B ($3 \mu\text{mol m}^{-2} \text{s}^{-1}$) for 4 hours. C-terminal UVR8, UGPase (cytosolic marker) and Histone H3 (nuclear marker) antibodies were used to probe the western blot.

A



B



C

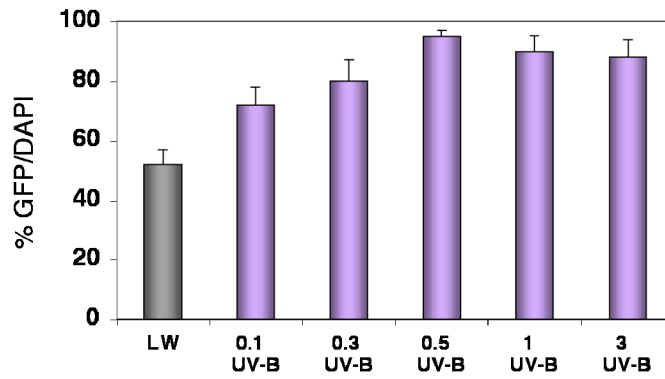


Figure 3.14 Nuclear enrichment of GFP-UVR8 is UV-B specific, rapid and very sensitive to UV-B

(A) The percentage of co-localisation of GFP and DAPI fluorescence from UVR8_{pro}GFP-UVR8 transgenic plants grown in white light ($20 \mu\text{mol m}^{-2} \text{s}^{-1}$; LW) and exposed to UV-B ($3 \mu\text{mol m}^{-2} \text{s}^{-1}$) red ($100 \mu\text{mol m}^{-2} \text{s}^{-1}$) or UV-A ($100 \mu\text{mol m}^{-2} \text{s}^{-1}$) light for 4 hours. (B) The percentage of co-localisation of GFP and DAPI fluorescence from UVR8_{pro}GFP-UVR8 transgenic Arabidopsis grown in white light ($20 \mu\text{mol m}^{-2} \text{s}^{-1}$; LW) and exposed to UV-B ($3 \mu\text{mol m}^{-2} \text{s}^{-1}$) for 10 min, 30 min, 1 h, 4 hours or 4 hours and returned to darkness for 24 hours. (C) The percentage of co-localisation of GFP and DAPI fluorescence from UVR8_{pro}GFP-UVR8 transgenic Arabidopsis grown in white light ($20 \mu\text{mol m}^{-2} \text{s}^{-1}$; LW) and exposed to UV-B (0.1, 0.3, 0.5, 1, 3 $\mu\text{mol m}^{-2} \text{s}^{-1}$) for 4 hours. Data for all graphs are the mean +/- S.E; n = 20.

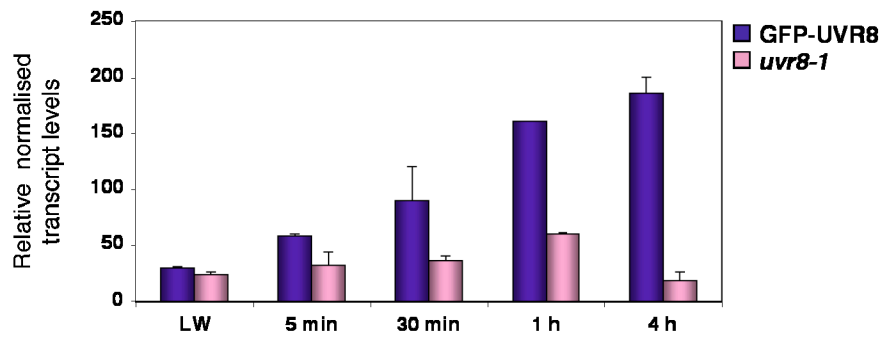
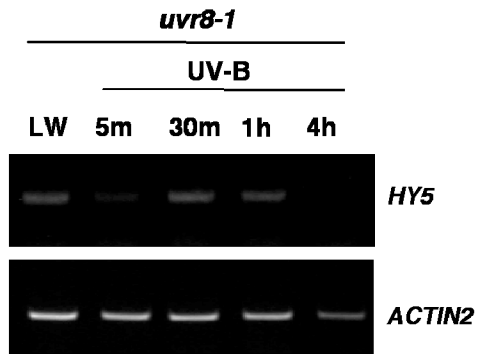
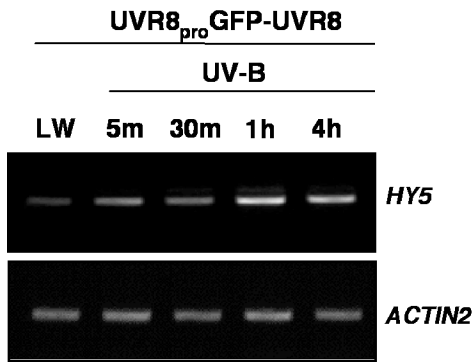


Figure 3.15 UV-B stimulates a rapid increase in UVR8 regulated gene expression

RT-PCR analysis of *HY5* and control *ACTIN2* transcripts in *UVR8_{pro}GFP-UVR8* and *uvr8-1* lines grown in low fluence rate white light ($20 \mu\text{mol m}^{-2} \text{s}^{-1}$; LW) and exposed to UV-B ($3 \mu\text{mol m}^{-2} \text{s}^{-1}$) for 5 min, 30 min, 1 h or 4 hours. The upper panels show representative RT-PCR data and the lower panel the data for three independent experiments. The intensity of the *HY5* band was normalised relative to the *ACTIN* band for each sample and the mean was calculated. Data for all graphs are the mean \pm S.E.; $n = 3$.

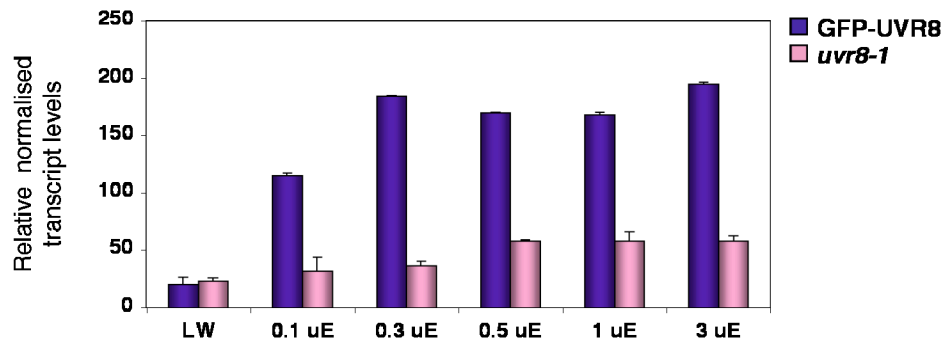
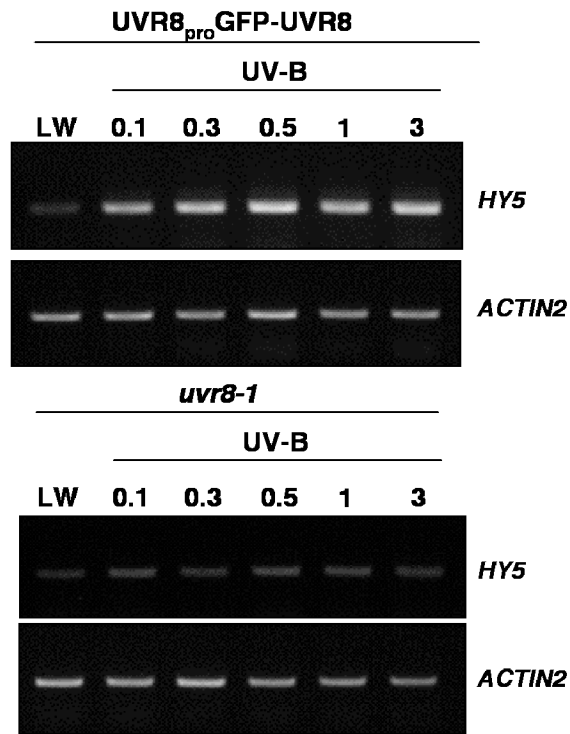


Figure 3.16 UV-B stimulates UVR8 regulated gene expression at very low fluence rates of UV-B

RT-PCR analysis of *HY5* and control *ACTIN2* transcripts in *UVR8_{pro}GFP-UVR8* and *uvr8-1* transgenic lines grown in low fluence rates of white light ($20 \mu\text{mol m}^{-2} \text{s}^{-1}$) and exposed to UV-B (0.1 0.3 0.5, 1, 3 $\mu\text{mol m}^{-2} \text{s}^{-1}$) for 4 hours. The upper panels show representative RT-PCR data and the lower panel the data for three independent experiments. The intensity of the *HY5* band was normalised relative to the *ACTIN* band for each sample and the mean was calculated. Data for all graphs are the mean +/- S.E. Data for all graphs are the mean +/- S.E.; n = 3).

CHAPTER 4

ANALYSIS OF UV-B INDUCED NUCLEAR ACCUMULATION AND ACTIVITY OF CYTOSOLIC AND NUCLEAR UVR8

4.1 Introduction

UVR8 is localised in the nucleus and the cytoplasm of Arabidopsis cells and undergoes rapid nuclear enrichment in response to UV-B, as described in Chapter 3. The major objectives of this chapter are to understand the correlation between UVR8 function and UV-B dependent nuclear accumulation, in an attempt to identify the site of UV-B perception within the cell. The approach employed for these studies is based on constitutive nuclear exclusion or nuclear localisation of UVR8, followed by functional analyses in response to UV-B, combined with pharmacological studies and western blot analyses. The key conclusions of this chapter are that when UVR8 is exclusively localised in the cytosol, it can still be translocated into the nucleus in a UV-B dependent manner. Furthermore, constitutively nuclear localised UVR8 is functional only in response to a UV-B stimulus.

4.2 UVR8 is functional in the presence of a nuclear export signal

As mentioned earlier, native UVR8 and GFP-UVR8 are soluble proteins localised in the cytosol and the nucleus of Arabidopsis, and undergo UV-B induced nuclear accumulation. In order to determine whether the cytosolic fraction of UVR8 is functional and responsible for UV-B signal transduction, it was necessary to prevent UVR8 from entering the nucleus and consequently eliminate the basal levels of nuclear localised UVR8 in white light. To achieve this, it was necessary to construct a GFP-UVR8 fusion protein containing an additional amino acid sequence coding for a nuclear export signal (NES). The method employed for obtaining this construct was

based on the elegant studies on phytochrome carried out by Nagatani and co-workers (Matsushita *et al.*, 2003). The NES amino acid sequence that was used for this study originates from the mammalian PKI protein and was PCR synthesised at the N-terminus of GFP-UVR8. This specific sequence for NES was chosen as it can be recognised by the plant nuclear translocation machinery and has been successful in exporting phyB from the nucleus (Matsushita *et al.*, 2003). To examine the effects of NES on GFP-UVR8 localisation *in vivo*, *uvr8-1* transgenic Arabidopsis plants were generated expressing NES-GFP-UVR8 under the control of the native *UVR8* promoter (Figure 4.1 (A)) and independent homozygous lines were selected as described in Chapter 3. Immunoblot analysis shows that NES-GFP-UVR8 is stable and is expressed at protein levels comparable to GFP-UVR8 (Figure 4.1 (B)).

Furthermore, complementation analysis by RT-PCR and UV-B sensitivity assays demonstrate that NES-GFP-UVR8 is functional. RT-PCR analysis on wild-type and three independent transgenic lines expressing NES-GFP-UVR8 shows a strong induction of *HY5* and *CHS* expression in response to low fluence rates of UV-B ($3 \mu\text{mol m}^{-2} \text{s}^{-1}$), whereas there is no induction in *uvr8-1* mutant plants (Figure 4.2 (A)). Similarly, wild-type and lines expressing NES-GFP-UVR8 are able to survive when exposed to higher than ambient UV-B levels ($5 \mu\text{mol m}^{-2} \text{s}^{-1}$) supplemented with white light ($40 \mu\text{mol m}^{-2} \text{s}^{-1}$) for 24 h, while *uvr8-1* mutant plants are adversely affected and show hypersensitivity to UV-B irradiation (Figure 4.2 (B)). These findings were quite unpredicted, as UVR8 is known to function in the nucleus as a regulator of gene expression via chromatin association (Brown *et al.*, 2005), whereas NES-GFP-UVR8 is excluded from the nucleus under white light illumination.

4.3 Cytosolic NES-GFP-UVR8 is imported into the nucleus in response to UV-B

To understand how a modified version of GFP-UVR8 that is restricted to the cytosol could rescue the *uvr8-1* mutant phenotype, localization studies in response to UV-B irradiation were carried out. Plants expressing NES-GFP-UVR8 were grown in

low fluence rates of white light ($20 \mu\text{mol m}^{-2} \text{s}^{-1}$) for 12 days and then irradiated with UV-B ($3 \mu\text{mol m}^{-2} \text{s}^{-1}$) for 4 h. As shown in Figure 4.3 (A), NES-GFP-UVR8 is excluded from the nucleus and is principally localized in the cytosol and the perinuclear region of epidermal cells in *Arabidopsis* under white light illumination. Detailed microscopic analysis based on progressive cross-sections of the cell (Z-stack) (data not shown) also confirmed that NES-GFP-UVR8 is excluded from the nucleus and sometimes only resides around the nuclear envelope. However, a nuclear translocation event of NES-GFP-UVR8 is observed in response to low fluence rates of UV-B (Figure 4.3 (A)). As described in Chapter 3, in order to identify the nucleus of the cells in each image and examine if NES-GFP-UVR8 is present, plant leaf tissue was infiltrated with DAPI for 15 min before imaging. The percentage of co-localisation between GFP-NES-UVR8 and DAPI was calculated and plotted on the graph of Figure 4.3 (B). There is insignificant (3.3 %) nuclear localisation of NES-GFP-UVR8 in white light ($20 \mu\text{mol m}^{-2} \text{s}^{-1}$), whereas approximately 90 % of the nuclei contain NES-GFP-UVR8 in response to a 4-h UV-B stimulus ($3 \mu\text{mol m}^{-2} \text{s}^{-1}$) (Figure 4.3 (B)). The fact that the UV-B induced nuclear translocation of NES-GFP-UVR8 is so apparent, as there is no basal nuclear concentration of GFP-UVR8, provides a very sensitive system for detailed investigation of this response.

Further analysis on the effects of UV-B on NES-GFP-UVR8 at the protein level was carried out by western blots. Figure 4.4 (A) demonstrates that the total protein concentration of NES-GFP-UVR8 remains unchanged during a time-course of 4 and 24 h of UV-B irradiation ($3 \mu\text{mol m}^{-2} \text{s}^{-1}$) compared to white light ($20 \mu\text{mol m}^{-2} \text{s}^{-1}$). An immunoblot showing a gradient of increasing concentrations of total extracts from plants expressing NES-GFP-UVR8 and probed with an anti-GFP antibody confirms that if there was a considerable increase or decrease in the total protein levels of NES-GFP-UVR8 it would have been detectable by this method (Figure 4.4 (B)). However, immunoblot analysis cannot be quantitative for protein changes of lower magnitude, which are not applicable to the case of NES-GFP-UVR8, as it shows over 90% increase in nuclear accumulation in response to UV-B. These results strengthen the

hypothesis of a UVR8 nuclear translocation event stimulated by UV-B, as there is no increase in UVR8 protein synthesis.

4.4 Kinetics and fluence rate dependence of NES-GFP-UVR8 nuclear import

As shown in Chapter 3, GFP-UVR8 accumulates in the nucleus rapidly and in response to very low intensities of UV-B. To examine if NES-GFP-UVR8 responds in a similar kinetic and fluence rate dependent manner, studies on the nuclear import of NES-GFP-UVR8 were undertaken. The assay used for all experiments in this section was based on NES-GFP-UVR8 and DAPI co-localisation, as described in 4.3. For kinetic analyses, transgenic lines expressing NES-GFP-UVR8 grown in white light ($20 \mu\text{mol m}^{-2} \text{s}^{-1}$) for 12 days were irradiated with UV-B ($3 \mu\text{mol m}^{-2} \text{s}^{-1}$) during a time-course of 5 min, 30 min, 1 h and 4 h. Figures 4.5 (A) and (B) exemplify how the nuclear import of NES-GFP-UVR8 progresses with time in response to UV-B. Fluorescent images of GFP and DAPI demonstrate that there is negligible nuclear fluorescence of NES-GFP-UVR8 in white light (Figure 4.5 (A)). However, within 5 min of UV-B irradiation there is substantial nuclear accumulation of NES-GFP-UVR8, which increases with time. According to the graph of the percentage co-localisation of GFP and DAPI (Figure 4.5 (B)), NES-GFP-UVR8 nuclear import reaches saturation after 30 min of UV-B irradiation, as previously shown for GFP-UVR8. The response is partially reversed when plants that have been irradiated with UV-B for 4 h are returned to complete darkness for a minimum of 24 h before imaging the cells again. This recovery period is very slow, as there is only a 50 % decrease in the nuclear accumulation of NES-GFP-UVR8 after 24 h (Figure 4.5 (B)). Longer incubation in darkness (48 h) has shown that NES-GFP-UVR8 is almost entirely excluded from the nucleus (data not shown). Such observations were made possible thanks to the increased sensitivity of the system, due to the lack of basal nuclear levels of NES-GFP-UVR8. The ideal kinetic analysis of the nuclear import of NES-GFP-UVR8 would require real-time imaging during a time-course ranging from seconds following the

UV-B stimulus. Unfortunately this method was not possible for our studies, as there was no UV-B laser available or incorporated in any of the confocal microscopes in use.

The dependence of the nuclear translocation response to different fluence rates of UV-B was also examined. NES-GFP-UVR8 transgenic plants grown under white light conditions for 12 days were exposed to increasing intensities of UV-B for a period of 4 h. Figure 4.6 (A) contains a series of images showing the fluorescence of NES-GFP-UVR8 or DAPI in response to 0.1, 0.3, 0.5, 1 or 3 $\mu\text{mol m}^{-2} \text{s}^{-1}$ UV-B. Very low fluence rates of UV-B (0.1 $\mu\text{mol m}^{-2} \text{s}^{-1}$) stimulate considerable nuclear accumulation of NES-GFP-UVR8. According to the graph of Figure 4.6 (B), there is a 6-fold increase in the percentage of nuclei that contain NES-GFP-UVR8 in response to 0.1 $\mu\text{mol m}^{-2} \text{s}^{-1}$ compared to white light, where the vast majority of cells show exclusion of NES-GFP-UVR8 from the nucleus. Again, as the sensitivity of this assay is increased compared to GFP-UVR8, it is evident that the response peaks at 0.3 $\mu\text{mol m}^{-2} \text{s}^{-1}$ UV-B with a 10-fold increase in GFP and DAPI co-localisation (Figure 4.6 (B)).

All the above data confirm that the stimulation of GFP-UVR8 nuclear translocation is a very sensitive response, triggered by short (5 min) irradiation or very low fluence rates (0.1 $\mu\text{mol m}^{-2} \text{s}^{-1}$) of UV-B, in spite of the presence of a nuclear export signal.

4.5 Pharmacological studies on the nuclear import of NES-GFP-UVR8

Pharmacological studies on UV-B signalling initiated by Christie and Jenkins (1996) have demonstrated that a number of protein kinase and phosphatase inhibitors result in the prevention of UV-B induction of *CHS* gene expression in Arabidopsis cell culture. Consequently, phosphorylation and de-phosphorylation signalling events are necessary for UV-B signal transduction, resulting in changes in gene expression. Since UVR8 is the major regulator of UV-B stimulated *HY5* and *CHS* gene expression (Brown *et al.*, 2005), the effect of a number of inhibitors on the nuclear translocation of NES-GFP-UVR8 was tested. Fluorescent images of Figure 4.7(A) show that 1 h

incubation with the general Ser/Thr protein kinase inhibitor staurosporine (1 mM) does not disturb the nuclear import of NES-GFP-UVR8 in response to 4 h of UV-B irradiation ($3 \mu\text{mol m}^{-2} \text{s}^{-1}$). Similar results are obtained after infiltrating plant leaf tissue with cantharidin (100 μM), an inhibitor for protein phosphatases 1 and 2A. Transgenic plants treated with cantharidin for 1 h before the UV-B stimulus retained the UV-B induced nuclear accumulation of NES-GFP-UVR8 (Figure 4.7 (A)).

Analogous studies have shown that cytosolic protein synthesis is required for the UV-B stimulated *CHS* expression in Arabidopsis (Christie and Jenkins, 1996). Therefore, the effect of cycloheximide, a protein synthesis inhibitor, on the nuclear translocation of UVR8 was examined in plants expressing NES-GFP-UVR8. Once more, 20 μM cycloheximide infiltrated in plant leaf tissue for 1 h prior to UV-B illumination, had no inhibitory effects on the nuclear import of NES-GFP-UVR8 (Figure 4.7(A)).

The concentrations used for all inhibitors were those giving the maximum effect on the UV-B induced gene expression in Arabidopsis cell suspension cultures based on (Christie and Jenkins, 1996). Neither higher concentrations nor longer incubation periods with each inhibitor had any effects on the UV-B induced nuclear import of NES-GFP-UVR8 (data not shown).

Infiltration with the control chemical DMSO (1 mM), which serves as the solvent for the inhibitors, was used to confirm that the experimental procedure does not interfere with the nuclear import of NES-GFP-UVR8 in response to UV-B (Figure 4.7 (A)) and that if there was any effect observed it would be solely due to the action of the inhibitors.

In addition, in order to confirm that the inhibitors were taken up by the plant cells and were functional, gene expression studies were carried out by RT-PCR on a fraction of the tissue used for microscopy studies. RT-PCR analysis in Figure 4.7 (B) demonstrates that all three inhibitors, staurosporine, cantharidin and cycloheximide, substantially reduce the induction of *CHS* gene expression in response to UV-B. However, phosphorylation, de-phosphorylation or protein synthesis are not involved

either directly or indirectly in the NES-GFP-UVR8 nuclear translocation event occurring in response to UV-B as shown in Figure 4.7 (A).

4.6 A transient expression system for rapid analysis of UVR8 nuclear import

In the present study, all localisation and functional analyses have been conducted in stably transgenic *Arabidopsis* plants expressing a tagged version of UVR8 protein. However, the generation of stable, homozygous transgenic plants carrying the gene construct of interest is a time-consuming and laborious procedure. Unless functional information is required, transient expression of a modified version of UVR8 could provide very important information in terms of subcellular localisation within a very short period of time. For this reason, the transient expression of NES-GFP-UVR8 in leaf tissue of *Nicotiana benthamiana* plants was developed. The original vector expressing NES-GFP-UVR8 driven by the *UVR8* promoter that was used for generating stable *Arabidopsis* plants by *Agrobacterium*-mediated transformation, was also used to transiently transform leaves of tobacco plants by *Agro*-infiltration. The plants were kept for 60 h in white light conditions at temperature ideal for *Agrobacterium* growth (28° C) in order to achieve optimum transient expression of NES-GFP-UVR8. Leaf tissue infiltrated with a medium of *Agrobacteria* that contained NES-GFP-UVR8 was examined by fluorescent confocal microscopy prior and subsequent to UV-B irradiation. Figure 4.8 demonstrates that transiently expressed NES-GFP-UVR8 in tobacco is responsive to UV-B by being successfully translocated into the nucleus in a similar manner to stably transformed plants. This finding indicates that the cellular machinery for UV-B-stimulated nuclear translocation is conserved in *N. benthamiana*.

The limitations of this approach do not allow assessment of the functionality of the modified version of UVR8, as there is no *uvr8-1* mutant Tobacco line available. Transient expression in temporarily silenced *UVR8* lines could be a possible solution for complementation analysis of the transgene. In this case, it has previously been

shown that NES-GFP-UVR8 is functional in Arabidopsis (4.2), so there was no need to proceed with complementation analysis in Tobacco.

4.7 Constitutively nuclear localised NLS-GFP-UVR8 is functional

To further investigate whether the site of initiation of UV-B signal transduction that triggers gene expression via UVR8 is in the nucleus or in the cytosol, UVR8 was restrained in the nuclei of the plant cells. This was made possible by generating *uvr8-1* transgenic plants expressing the GFP-UVR8 fusion protein joined to a nuclear localisation signal peptide (NLS). The NLS peptide used in this study derived from SV40 and was PCR generated at the N-terminus of GFP-UVR8 in a similar way to NES-GFP-UVR8 according to Matsushita *et al.* (2003).

Western blot analysis shows that NLS-GFP-UVR8 controlled by the native *UVR8* promoter is expressed at comparable protein levels to GFP-UVR8, whereas there is no protein produced in non-transformed plants (Figure 4.9 (B)). To test if NLS-GFP-UVR8 is functional, complementation analysis by gene expression and UV-B sensitivity studies was carried out. As shown in Figure 4.10 (A), three independent homozygous lines expressing NLS-GFP-UVR8 exhibit induction of *HY5* and *CHS* gene expression in response to 4 h of low fluence rates of UV-B ($3 \mu\text{mol m}^{-2} \text{s}^{-1}$), similar to the response of wild-type plants (Figure 4.10 (A)). Rescue of the mutant *uvr8-1* phenotype is also observed when transgenic lines expressing NLS-GFP-UVR8 are subjected to higher than ambient levels of UV-B for 24 h. The images in Figure 4.10 (B) show that wild-type and NLS-GFP-UVR8 transgenic lines survive under stress conditions caused by UV-B, whereas *uvr8-1* mutant plants fail to recover. This suggests that although NLS-GFP-UVR8 is restricted to the nucleus, it is still functional. Furthermore, the constitutive nuclear localisation of NLS-GFP-UVR8 does not trigger constitutive activation of UVR8, as there is no induction of *HY5* or *CHS* expression in the absence of UV-B (Figure 4.10 (A)).

4.8 Nuclear accumulation of NLS-GFP-UVR8 is unaffected by UV-B

To establish whether NLS-GFP-UVR8 is constitutively localised in the nucleus, images from transgenic *Arabidopsis* expressing NLS-GFP-UVR8 were analysed by confocal microscopy. Figure 4.11 demonstrates that NLS-GFP-UVR8 is localised only in the nuclei of epidermal plant cells and is entirely excluded from any cytosolic structures, contrary to NES-GFP-UVR8 when irradiated with white light. In addition, the effect of UV-B light on the subcellular localisation of NLS-GFP-UVR8 was examined. Transgenic lines expressing NLS-GFP-UVR8 were grown for 12 days in white light and subsequently illuminated with UV-B ($3 \mu\text{mol m}^{-2} \text{s}^{-1}$) for 4 h. However, no change in the localization or fluorescence intensity of NLS-GFP-UVR8 in response to UV-B was observed (Figure 4.11).

As mentioned earlier, GFP-UVR8 and NES-GFP-UVR8 undergo UV-B dependent nuclear enrichment. However, the mechanism by which this enrichment occurs is not fully understood. To investigate the possibility if the UV-B induced UVR8 protein accumulation is due to inhibition of protein degradation, it was necessary to examine transgenic lines expressing NLS-GFP-UVR8, where UVR8 is solely localized in the nucleus. Western blot analysis on total protein extracts from plants expressing NLS-GFP-UVR8 indicates that NLS-GFP-UVR8 protein concentration remains unaltered in plants grown in white light ($20 \mu\text{mol m}^{-2} \text{s}^{-1}$) or irradiated with UV-B ($3 \mu\text{mol m}^{-2} \text{s}^{-1}$) for 4 or 24 h (Figure 4.12 (A)). A control immunoblot of increasing concentrations of protein shows that if there was a significant increase or decrease in the total levels of NLS-GFP-UVR8 it would have been detected (Figure 4.12 (B)). If the nuclear enrichment of UVR8 was due to protein accumulation and not nuclear import, then an increase in the protein levels of NLS-GFP-UVR8 would have been expected and it would have been possible to detect as the total amount of UVR8 protein within the cell resides in the nucleus. Such evidence confirms that the nuclear enrichment of UVR8 in response to UV-B is most likely triggered by nuclear import.

4.9 Discussion

The current chapter mainly focuses on the activity of UVR8 based on its restricted localisation to specific subcellular compartments. In particular, *in planta* studies on NES-GFP-UVR8 transgenic lines show that even if UVR8 is excluded from the nucleus in white light, it is still responsive to UV-B, undergoes nuclear import and consequently is functional. In contrast, NLS-GFP-UVR8 is restricted to the nucleus of Arabidopsis cells and shows no changes in localisation or protein concentration in response to UV-B. However, NLS-GFP-UVR8 is active, in terms of regulating gene expression, only in response to UV-B.

Due to their cellular fractionation properties, NES-GFP-UVR8 or NLS-GFP-UVR8 became ideal candidates for more sensitive characterisation of the mechanism involved in the UV-B dependent nuclear enrichment of UVR8 based on kinetic, fluence rate dependence, pharmacological and immunoblot analyses.

4.9.1 NES-GFP-UVR8 is functional and overcomes the nuclear export signal in response to UV-B

Chapter 3 describes the temporal and spatial expression of UVR8 and its subcellular localisation in Arabidopsis plants. Furthermore, it is shown that UVR8 undergoes nuclear enrichment induced by UV-B irradiation. In order to test if the nuclear localisation of UVR8 is essential for its function, it was necessary to restrict UVR8 in the cytosol of the cells, thus inhibiting its basal nuclear accumulation. This was achieved by generating transgenic plants expressing GFP-UVR8 fused to an N-terminal nuclear export signal peptide (NES). The localisation of NES-GFP-UVR8, monitored by confocal microscopy, was successfully restricted to the cytosol of Arabidopsis epidermal cells in white light conditions. Since, UVR8 has been shown to regulate gene expression via chromatin association (Brown *et al.*, 2005), it is not expected to be functional, if it is excluded from the nucleus. However,

complementation analyses by RT-PCR and UV-B sensitivity assays demonstrate that even if NES-GFP-UVR8 is not localised in the nucleus in white light, it is still functional and responsive to UV-B light (Figures 4.2 (A) and (B)). The only possibility for cytosolic NES-GFP-UVR8 to be functional in response to UV-B would require its nuclear translocation. To test this hypothesis, the subcellular localisation of NES-GFP-UVR8 was examined before and after UV-B illumination. And, as predicted, NES-GFP-UVR8 somehow manages to prevail over the NES signal peptide and enter the nucleus in response to UV-B exclusively (Figures 4.3 (A) and (B)). This is quite surprising, especially since this particular NES signal peptide seems to be recognised by the Arabidopsis cellular machinery in white light conditions in this study and in all light conditions in studies performed on phytochrome (Matsushita *et al.*, 2003).

The mode of NES action involves the recognition of its Leu-rich motif by Exportin 1. Association of the NES-target protein/Exportin 1 complex with RanGTP results in the facilitated nuclear export of the complex through the nuclear pores (Merkle, 2004). In order to inhibit the recognition of NES by Exportin 1, either the accessibility of the NES peptide needs to be blocked or the recognition site of Exportin 1 needs to be occupied (e.g. by an inhibitor such as Leptomycin B). Masking of the NES can occur either due to an intramolecular interaction (e.g. the NES of the *Drosophila* homeobox protein Prospero is masked by the homeo-domain itself), or due to an intermolecular association with other macromolecules, such as DNA (e.g. the masking of the NES of the STAT1 transcription factor by DNA binding in mammalian cells) or proteins (Bi *et al.*, 2005; McBride *et al.*, 2000). Whether a UV-B stimulus causes masking of the NES of NES-GFP-UVR8 or triggers an interaction with a protein that facilitates the UV-B induced nuclear import of UVR8, similar to the FHY1-mediated nuclear import of phyA, needs to be examined and will be discussed further in Chapters 6 and 7 (Hiltbrunner *et al.*, 2005).

4.9.2 NES-GFP-UVR8 provides a more sensitive system for kinetics and fluence rate dependence studies

The UV-B induced nuclear enrichment of UVR8 was characterised as rapid and very sensitive to low fluence rates of UV-B, according to kinetic and fluence rate dependence studies on transgenic *Arabidopsis* expressing GFP-UVR8 (Chapter 3). The method used for monitoring the nuclear accumulation of GFP-UVR8, based on the co-localisation of GFP-UVR8 and DAPI fluorescence, proved to be successful for detecting significant changes in the nuclear accumulation of GFP-UVR8. Changes smaller than 20 % of the initial nuclear levels of GFP-UVR8 are very difficult to detect and can only be determined based on the GFP fluorescence intensity measurements. This was due to the fact that GFP-UVR8 is still present in the nucleus under low fluence rates of white light, although at considerably lower amounts than in response to UV-B.

The fact that NES-GFP-UVR8 is responsive to UV-B and undergoes UV-B specific nuclear import provides a considerably more sensitive approach for a more precise characterisation of the parameters involved in the UV-B stimulated nuclear import of UVR8. The advantage of using NES-GFP-UVR8 lies in its virtual absence from the nucleus under white light conditions. Therefore, any minor nuclear translocation event could be very easily detected in response to a brief or very low intensity UV-B stimulus. Kinetic studies show that only 5 minutes of UV-B are sufficient to induce a ten-fold increase in the percentage of nuclei containing NES-GFP-UVR8 (Figure 4.5 (B)). Furthermore, a decrease of approximately 50 % in the nuclear accumulation of NES-GFP-UVR8 is observed when plants that have reached saturation for UVR8 nuclear import ($3 \mu\text{mol m}^{-2} \text{s}^{-1}$ UV-B for 4 h) are moved to complete darkness for 24 h (Figure 4.5 (B)). Complete recovery is attained after a period of 48 h in darkness (data not shown). As explained in 4.4, it was not possible to carry out live imaging of NES-GFP-UVR8 or irradiate with UV-B for shorter periods of time, as there was no UV-B laser incorporated in the microscope and an incubation

for a minimum of 15 min with DAPI was required after each light treatment, in order to stain the plant cell nuclei.

Fluence rate dependence measurements on NES-GFP-UVR8 show that $0.1 \mu\text{mol m}^{-2} \text{s}^{-1}$ UV-B induces a six-fold increase in the number of nuclei exhibiting GFP fluorescence, whereas the nuclear import response reaches saturation at $0.3 \mu\text{mol m}^{-2} \text{s}^{-1}$ of UV-B (Figure 4.6 (B)). The fact that the nuclear import of UVR8 occurs at fluence rates of UV-B that are less than 3 % of the UV-B content in natural sunlight indicates that this is not a stress-related but a UV-B specific physiological response.

In conclusion, the kinetic and fluence rate dependence analyses on NES-GFP-UVR8 confirm and follow a very similar pattern to the results obtained with GFP-UVR8. The nuclear enrichment of UVR8 occurs within 5 min of UV-B irradiation and is induced by very low fluence rates of UV-B. The characteristics of the UV-B induced nuclear import of GFP-UVR8 and NES-GFP-UVR8 are consistent with the parameters governing the induction of gene expression in response to UV-B. Jenkins and co-workers demonstrated that 5 min of UV-B is sufficient to trigger an induction in *CHS* expression and Frohnmeyer and co-workers have shown that even milliseconds of UV-B light pulses can induce *CHS* expression (Jenkins *et al.*, 2001; Frohnmeyer *et al.*, 1999). Furthermore, *HY5* expression has been shown to be induced by very low fluence rates of UV-B in wild-type and GFP-UVR8 plants (B. A. Brown and G. I. Jenkins, unpublished and Figure 3.16). These data suggest that there is a parallel correlation between UVR8 nuclear import and UVR8-regulated gene expression. The only discrepancy between GFP-UVR8 and NES-GFP-UVR8 is mainly the sensitivity of the system using NES-GFP-UVR8, where the nuclear import response is more pronounced than the response observed in GFP-UVR8.

The sensitivity of the system also offers the opportunity to investigate further the requirements for the UV-B induced nuclear import by developing a transient expression assay in *Nicotiana*. Figure 4.8 shows that NES-GFP-UVR8 is active in terms of nuclear translocation in response to UV-B, thus allowing rapid analysis of this response without the need of generating and obtaining homozygous stable transgenic *Arabidopsis* lines. However, the functional activity of UVR8 modified protein can only

be tested in a background lacking native UVR8, which could only be achieved by transient silencing in *Nicotiana*, as there are no *uvr8-1* mutant alleles available in plant species other than *Arabidopsis*.

4.9.3 The UV-B induced nuclear enrichment of UVR8 is independent of phosphorylation or protein synthesis

Regulation of protein synthesis and post-translational modification are universal mechanisms involved in signal propagation in eukaryotic and prokaryotic cells. In particular, UV-B irradiation has been shown to trigger phosphorylation and protein turnover of signalling components (eukaryotic initiation factor-2 and inhibitor of κ B α respectively) that are involved in damage repair and cell cycle progression (Jiang and Wek, 2005). Furthermore, UV-B dependent phosphorylation has been associated with the regulation of nuclear translocation of transcription factors involved in antioxidant production in skin fibroblast cells (Sankaranayanan and Jaiswal, 2006). In *Arabidopsis*, phosphorylation, de-phosphorylation and protein synthesis are biochemical events necessary for the UV-B dependent induction of *CHS* expression (Jenkins and Christie, 1996). Although the protein kinase(s) and phosphatase(s) responsible for this response remain unidentified in *Arabidopsis*, it was logical to examine whether the same type of post-translational modifications are directly or indirectly regulating the nuclear accumulation of UVR8. As discussed earlier, the lines expressing NES-GFP-UVR8 provide a more sensitive system for the analysis of the UV-B induced nuclear import of UVR8. Therefore, a pharmacological approach was used to test the effects of specific inhibitors on the nuclear enrichment of NES-GFP-UVR8 in response to UV-B. More specifically, the Ser/Thr protein kinase inhibitor staurosporine and the protein phosphatase (PP1 and PP2A) inhibitor cantharidin were infiltrated in whole plants for 1 h prior to a UV-B illumination. No inhibition was observed in the UV-B induced nuclear accumulation of NES-GFP-UVR8 in the presence of the above chemicals, in spite of the fact that it has previously been

demonstrated that staurosporine and cantharidin block the UV-B induced expression of *CHS* in Arabidopsis (Christie and Jenkins, 1996). The effect of the protein synthesis inhibitor cycloheximide was also investigated in a similar manner. However, the nuclear translocation of NES-GFP-UVR8 was once more unaffected. Inhibition of the UV-B induction of *CHS* gene expression shown in Figure 4.7 (B) confirmed that the compounds successfully entered the Arabidopsis cells. These data imply that neither phosphorylation/dephosphorylation nor protein synthesis is essential for the regulation of the UV-B induced nuclear import of UVR8. However, UV-B specific signalling components downstream to UVR8 could be controlled by protein kinase/phosphatases and by protein synthesis without playing any role in UVR8 stimulation in response to UV-B. It would be very interesting to identify a method to retain UVR8 in the cytosol in the presence of UV-B and try to understand the mechanism underlying UV-B dependent nuclear translocation.

4.9.4. Constitutively nuclear localised UVR8 is responsive to UV-B

As mentioned earlier, UVR8 is present in the nucleus and the cytosol of Arabidopsis cells. However its function, so far, has been associated with chromatin binding and control of gene expression (Brown *et al.*, 2005). In an attempt to discriminate what is the function of the cytosolic and nuclear pools of UVR8, constitutive localisation of GFP-UVR8 in the nucleus was achieved by adding a nuclear localisation signal peptide (NLS) at the N-terminus. Studies on constitutively cytosolic NES-GFP-UVR8 have shown that UVR8 can only be restrained in the cytosol in the absence of UV-B. Therefore, UV-B triggers its nuclear import followed by the regulation of gene expression. The fact that NES-GFP-UVR8 is fully functional in response to UV-B, suggests that the basal nuclear localisation of UVR8 in white light is not essential for function, as there is no evidence so far for any UVR8 specific function in light conditions other than UV-B. To investigate if the cytosolic fraction of UVR8 is essential for function in response to UV-B, the transgenic lines expressing

constitutively nuclear localised NLS-GFP-UVR8 were examined. According to the data obtained from complementation assays, it is evident that NLS-GFP-UVR8 is fully functional in response to UV-B. In spite of its constant nuclear localisation, NLS-GFP-UVR8 is not constitutively active in the absence of UV-B, as there is no increase in the induction of *CHS* or *HY5* expression in low fluence rates of white light (Figure 4.10 (A)). These findings demonstrate that UV-B is required to activate UVR8 function, either directly or indirectly in the nucleus. Furthermore, the data suggest that the cytosolic fraction of UVR8 is not required for function. Nevertheless, it could act as a reservoir for newly synthesised protein, which is imported into the nucleus when required, thus in response to UV-B.

However, there is still no strong evidence showing whether UV-B perception occurs in the cytosol or in the nucleus. If the signal is perceived in the nucleus, the signal must somehow be transmitted to the cytosol and trigger the nuclear import of NLS-GFP-UVR8. If the UV-B photoreceptor resides in the cytosol, the signal is transmitted by a component other than UVR8 into the nucleus, where nuclear NLS-GFP-UVR8 is activated. Whether the component transmitting the cytosolic UV-B signal is the same component that facilitates UVR8 import in response to UV-B is unknown but quite possible. Otherwise, UVR8 could act as the UV-B photoreceptor and independent to its localisation it could carry and transmit the signal appropriately and induce gene expression. However, there is currently no experimental evidence that supports the hypothesis of UVR8 being a photoreceptor.

4.9.5 The UV-B induced nuclear enrichment of UVR8 is due to nuclear import

Fluorescence microscopy and biochemical analyses have demonstrated that the nuclear fraction of UVR8 increases in response to UV-B irradiation. As UVR8 is localised in the nucleus and in the cytosol at all light conditions, it is very difficult to distinguish if the UV-B dependent nuclear enrichment is due to translocation of the cytosolic fraction, due to an increase in the total protein levels or due to suppression of

protein degradation in the nucleus in response to UV-B. To address these questions, a series of immunoblot analyses on all three differently localised UVR8 transgenic lines (GFP-UVR8, NES-GFP-UVR8 and NLS-GFP-UVR8) were carried out. Data from Chapter 3 have shown that there is no change in the total protein levels of UVR8 and GFP-UVR8 during a time-course of UV-B irradiation. Similar results were obtained for NES-GFP-UVR8, where there is no difference in its protein levels between low fluence rates of white light and short or long exposure to UV-B (Figure 4.4). These data imply that there is no increase or decrease in the rate of UVR8 protein synthesis in response to UV-B irradiation. So, the increase in the nuclear UVR8 fraction could be due to trafficking within the cell without any changes in the total amount of protein produced. To test if UV-B triggers the nuclear enrichment of UVR8 by inhibiting protein degradation in the nucleus, immunoblot analysis was carried out on total protein extracts from plants expressing only nuclear localised NLS-GFP-UVR8. Therefore, any change occurring at the nuclear fraction of UVR8 in response to UV-B will be reflected in the total protein fraction, as the total NLS-GFP-UVR8 protein is targeted into the nucleus. So, if UVR8 nuclear enrichment was not due to translocation but due to suppression of protein turnover in response to UV-B, there should have been an increase in the total protein amount of NLS-GFP-UVR8. Figure 4.12 (A) shows that there is no difference observed in the protein levels of NLS-GFP-UVR8 in response to 4 or 24 h of UV-B, thus contradicting the latter hypothesis. Furthermore, microscopic analysis confirms that there is no increase in the nuclear fluorescence of NLS-GFP-UVR8 in response to UV-B, confirming the observations based on western blot analyses. Further experimentation is essential in order to elucidate the exact mechanism that regulates nuclear translocation of UVR8 in a UV-B dependent manner.

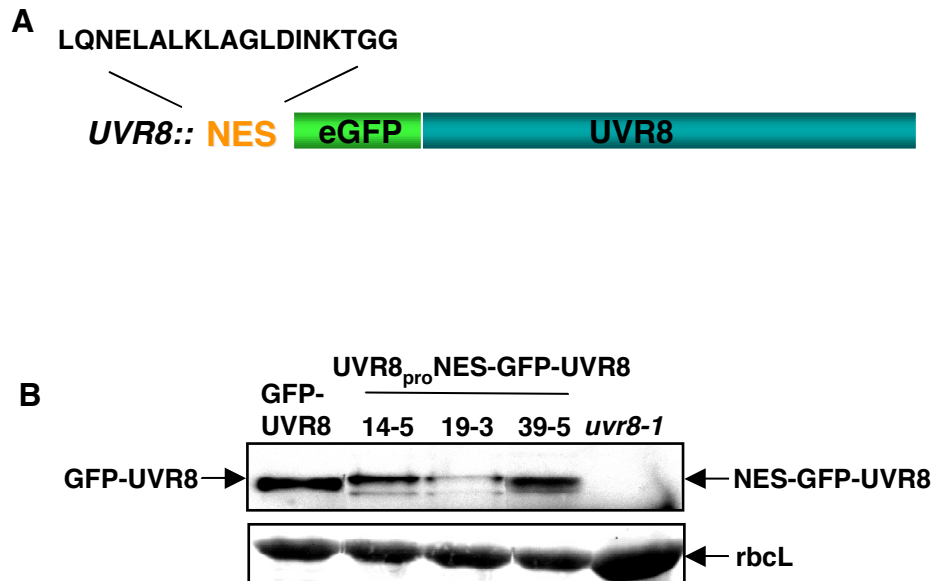


Figure 4.1 Generation of transgenic Arabidopsis plants expressing NES-GFP-UVR8

(A) Schematic representation of the NES-GFP-UVR8 construct driven by the *UVR8* promoter (B) Western blot of total protein extracts (15 μ g) from UVR8_{pro}GFP-UVR8, UVR8_{pro}NES-GFP-UVR8 (three independent lines) or *uvr8-1* Arabidopsis lines grown in white light (100 μ mol m⁻² s⁻¹) for 12 days. An anti-GFP antibody was used to probe the western blot and ponceau stain of rubisco large subunit (rbcL) was used as a loading control.

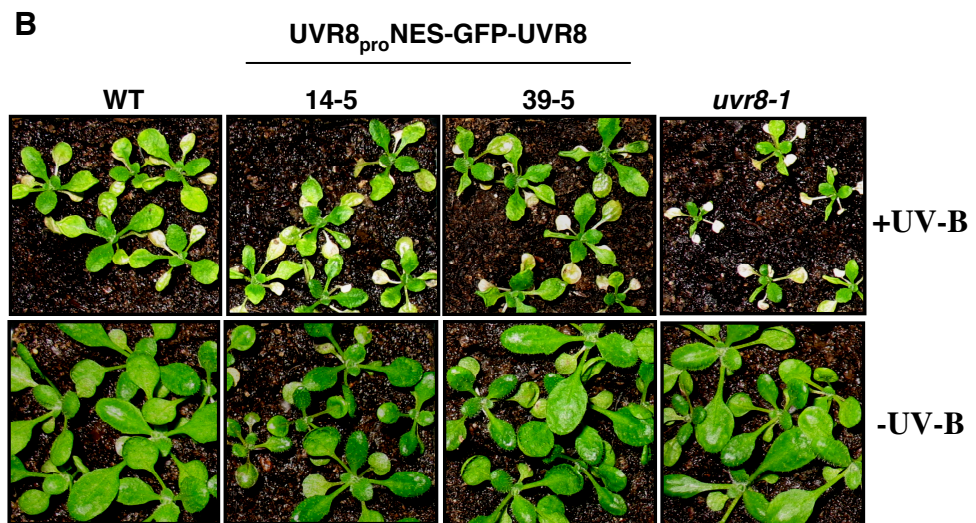
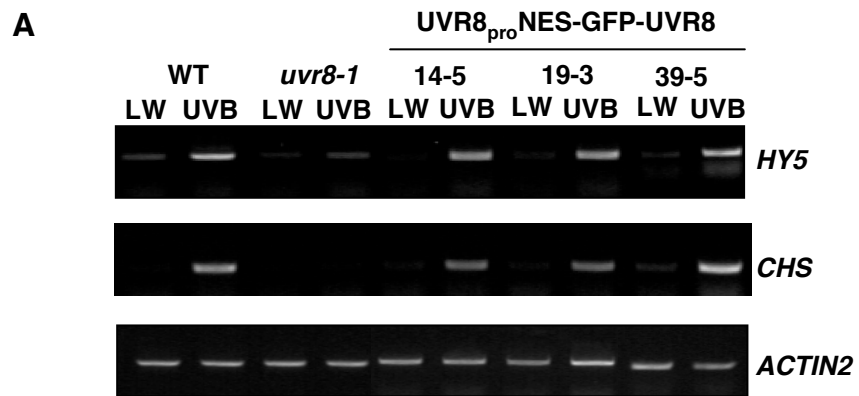


Figure 4.2 NES-GFP-UVR8 is functional in *uvr8-1* transgenic plants

(A) RT-PCR analysis of *HY5*, *CHS* and control *ACTIN2* transcripts in wild-type, *uvr8-1* and UVR8_{pro}-NES-GFP-UVR8 plants grown in low fluence rate white light ($20 \mu\text{mol m}^{-2} \text{s}^{-1}$; LW) and exposed to UV-B ($3 \mu\text{mol m}^{-2} \text{s}^{-1}$) for 4 h. (B) UV-B sensitivity assay. Wild-type, *uvr8-1* and UVR8_{pro}-NES-GFP-UVR8 plants were grown in white light ($120 \mu\text{mol m}^{-2} \text{s}^{-1}$) for 12 days and then exposed (+) or not (-) to UV-B ($5 \mu\text{mol m}^{-2} \text{s}^{-1}$) supplemented with white light ($40 \mu\text{mol m}^{-2} \text{s}^{-1}$) for 24 h. Plants were photographed after return to white light ($120 \mu\text{mol m}^{-2} \text{s}^{-1}$) for 5 days.

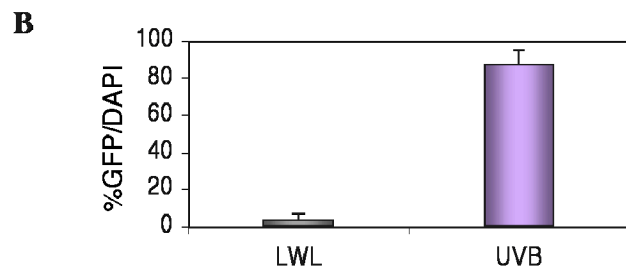
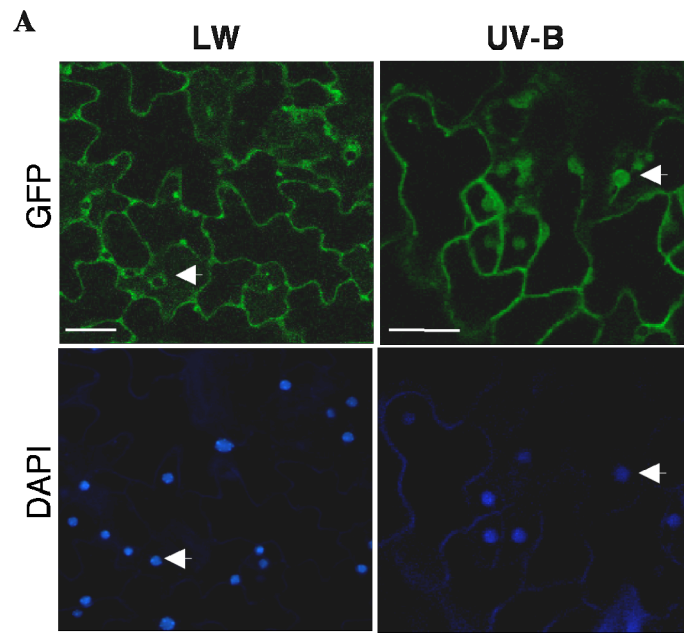


Figure 4.3 UV-B overcomes the nuclear export signal (NES) and induces nuclear import of NES-GFP-UVR8

(A) Confocal images of GFP and DAPI fluorescence in leaf epidermal tissue of UVR8_{pro}NES-GFP-UVR8 transgenic plants (line 14-5) grown in white light (20 $\mu\text{mol m}^{-2} \text{s}^{-1}$; LW) and exposed to UV-B (3 $\mu\text{mol m}^{-2} \text{s}^{-1}$) for 4 h. The arrows indicate specific nuclei in the cells. Scale bar = 20 μm . **(B)** The percentage of co-localisation of GFP and DAPI fluorescence from UVR8_{pro}NES-GFP-UVR8 transgenic lines grown in white light (20 $\mu\text{mol m}^{-2} \text{s}^{-1}$; LW) and exposed to UV-B (3 $\mu\text{mol m}^{-2} \text{s}^{-1}$) for 4 h. (Data are the mean \pm S.E.; n = 20).

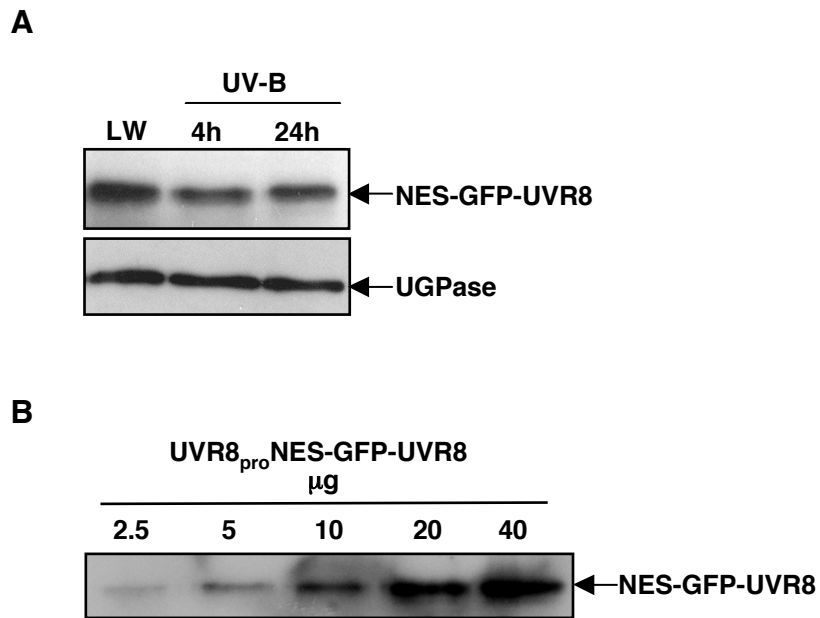
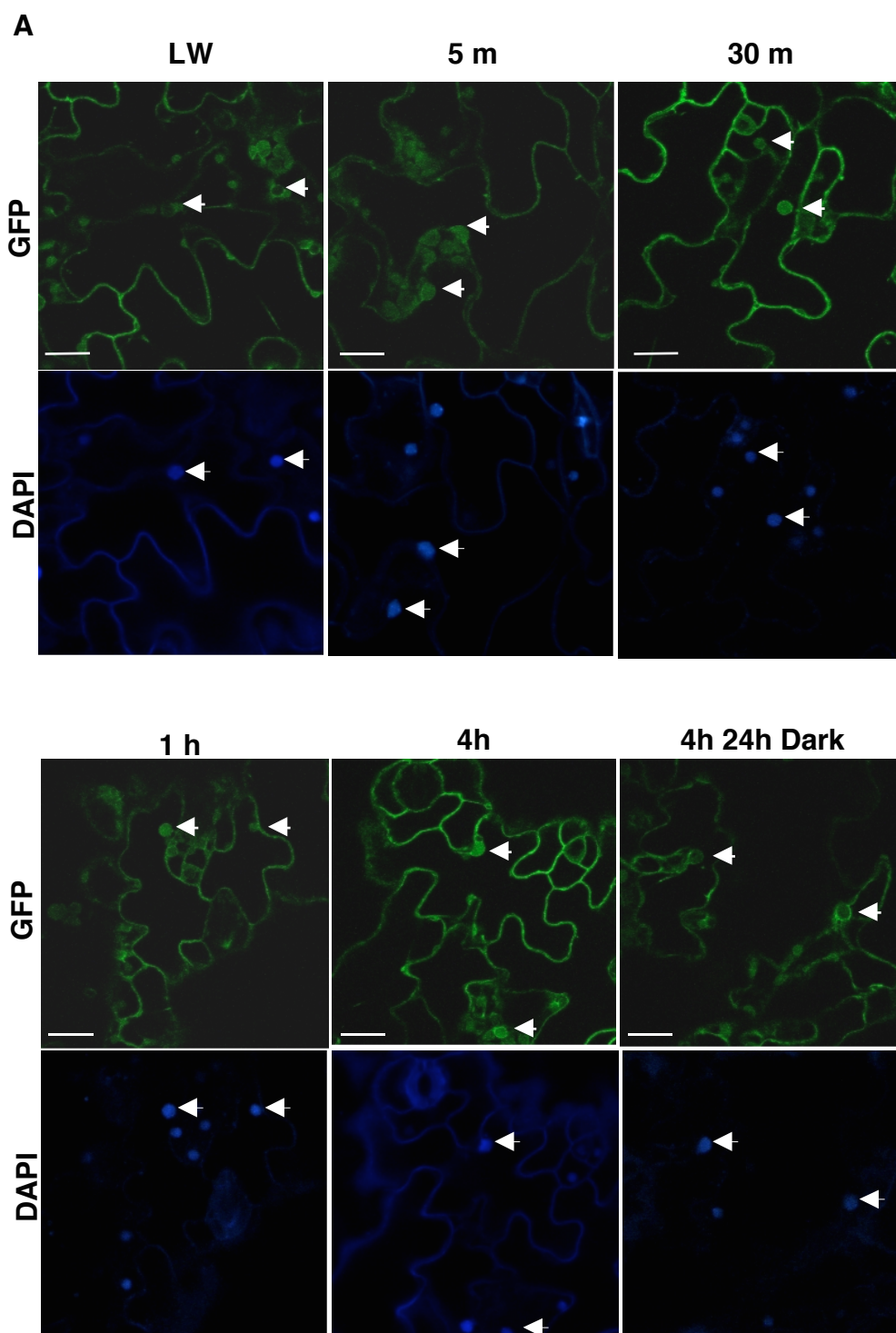


Figure 4.4 NES-GFP-UVR8 protein levels are unaffected by UV-B exposure

(A) Immunoblot analysis of total protein extracts (5 μg) from UVR8_{pro} NES-GFP-UVR8 transgenic plants (line 14-5) grown in low fluence rates of white light (20 $\mu\text{mol m}^{-2} \text{s}^{-1}$; LW) and illuminated with UV-B (3 $\mu\text{mol m}^{-2} \text{s}^{-1}$) for 4 or 24 h. The western blot was probed with anti-GFP and anti-UGPase antibodies. (B) Immunoblot demonstrating relative quantitative measurements of protein abundance of total protein extracts (2.5, 5, 10, 20 or 40 μg) from UVR8_{pro} NES-GFP-UVR8 Arabidopsis grown in low fluence rates of white light (20 $\mu\text{mol m}^{-2} \text{s}^{-1}$). The western blot was probed with a GFP antibody.



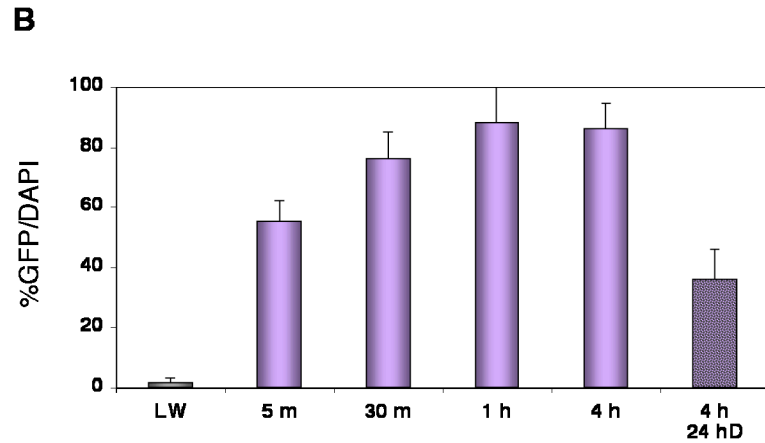
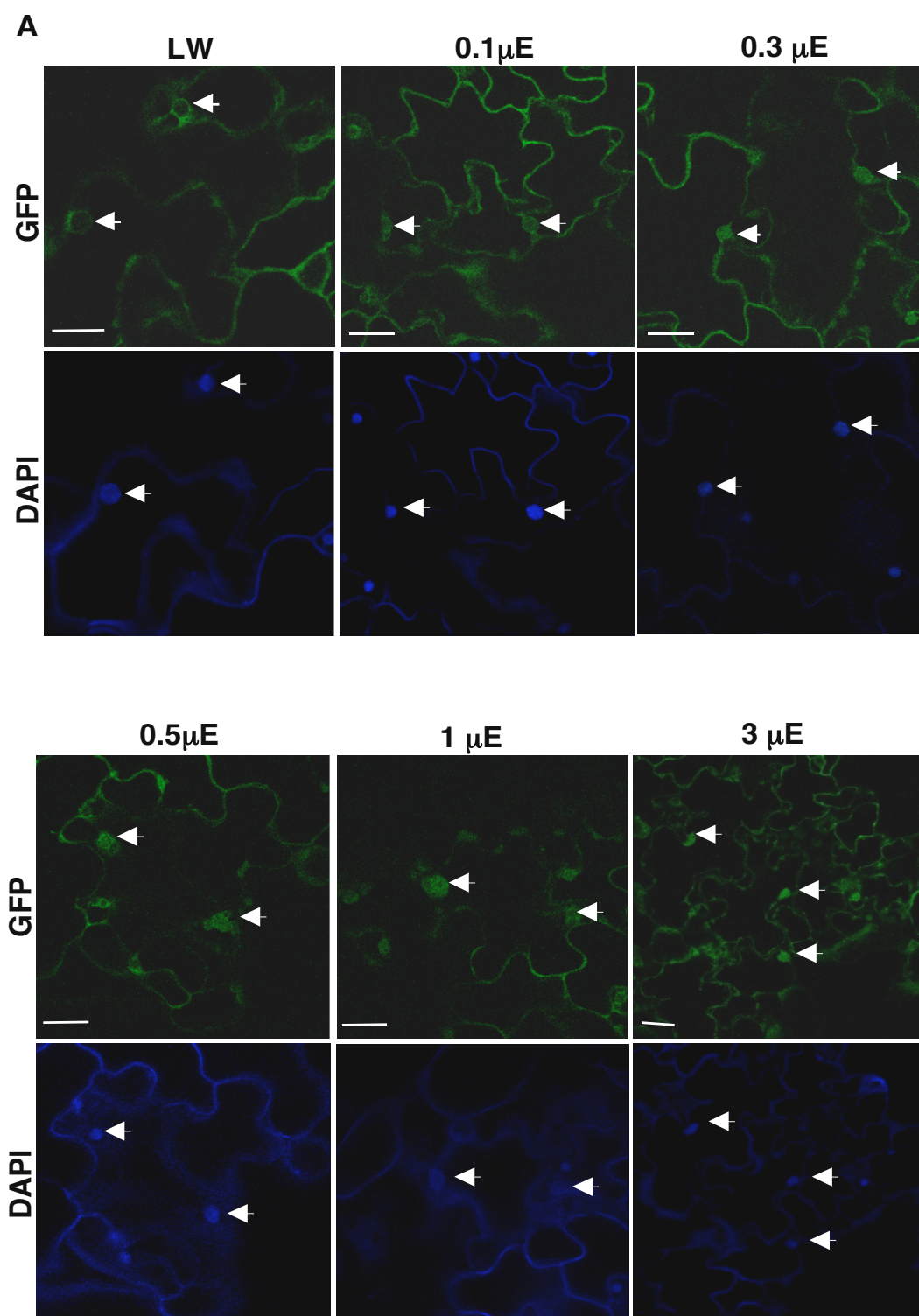


Figure 4.5 UV-B stimulates a rapid nuclear enrichment of NES-GFP-UVR8

(A) Confocal images of GFP and DAPI fluorescence in leaf epidermal tissue of UVR8_{pro}-NES-GFP-UVR8 transgenic plants (line 14-5) representing the time points and light treatments described in graph (B). The arrows indicate specific nuclei in the cells. Scale bar = 20 μm . (B) The percentage co-localisation of GFP and DAPI fluorescence from UVR8_{pro}-NES-GFP-UVR8 transgenic plants grown in white light ($20 \mu\text{mol m}^{-2} \text{s}^{-1}$; LW) and exposed to UV-B ($3 \mu\text{mol m}^{-2} \text{s}^{-1}$) for 5 min, 30 min, 1 h, 4 h or 4 h and returned to darkness for 24 h. Data are the mean \pm S.E.; $n = 20$.



B

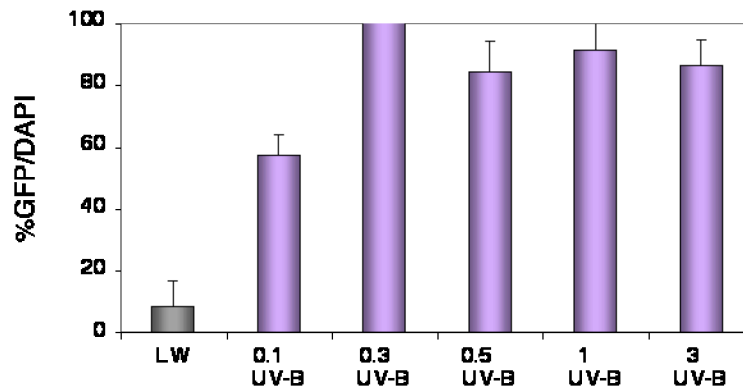
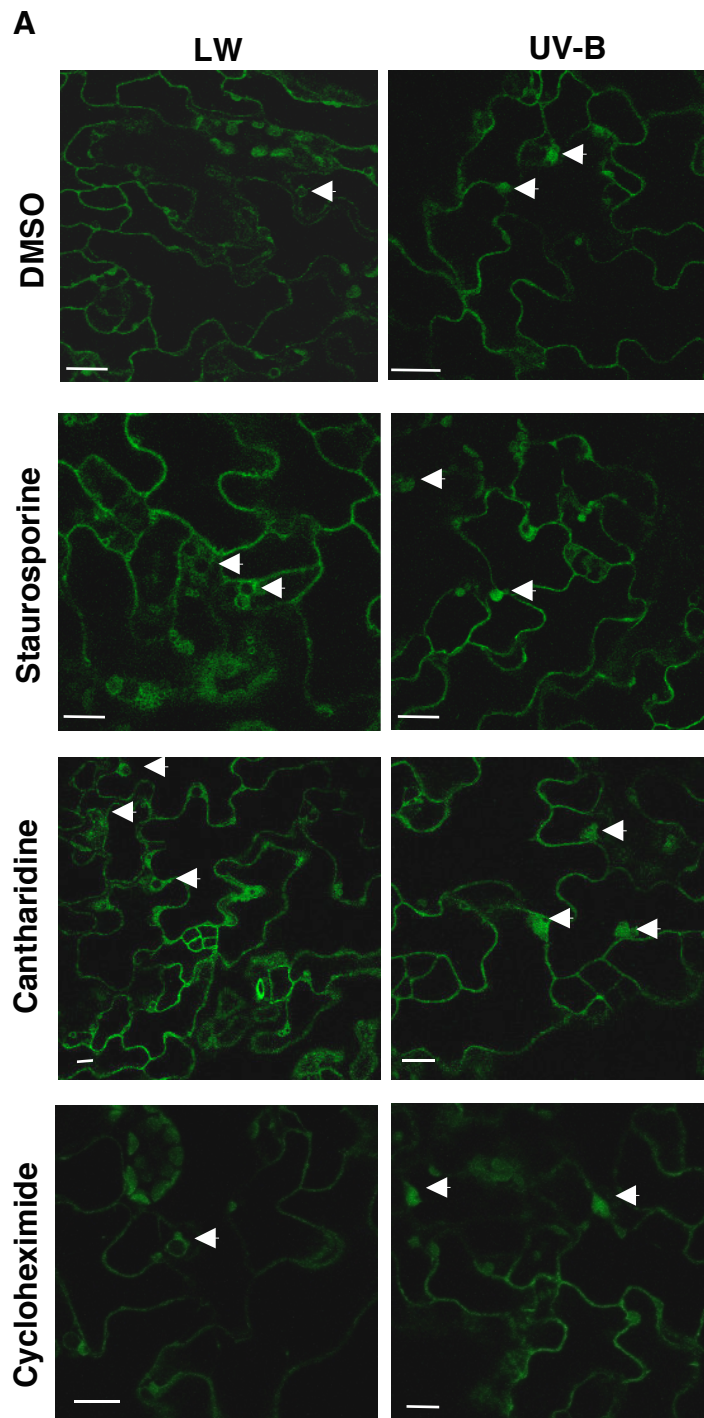


Figure 4.6 UV-B stimulates nuclear enrichment of NES-GFP-UVR8 at very low fluence rates

(A) Confocal images of GFP and DAPI fluorescence in leaf epidermal tissue of UVR8_{pro}-NES-GFP-UVR8 transgenic plants (line 14-5) representing the light treatments described in graph (A). The arrows indicate specific nuclei in the cells. Scale bar = 20 μm . (B) The percentage co-localisation of GFP and DAPI fluorescence from UVR8_{pro}-NES-GFP-UVR8 transgenic plants grown in white light ($20 \mu\text{mol m}^{-2} \text{s}^{-1}$; LW) and exposed to UV-B (0.1, 0.3, 0.5, 1 or $3 \mu\text{mol m}^{-2} \text{s}^{-1}$) for 4 h. Data are the mean \pm S.E.; n = 20.



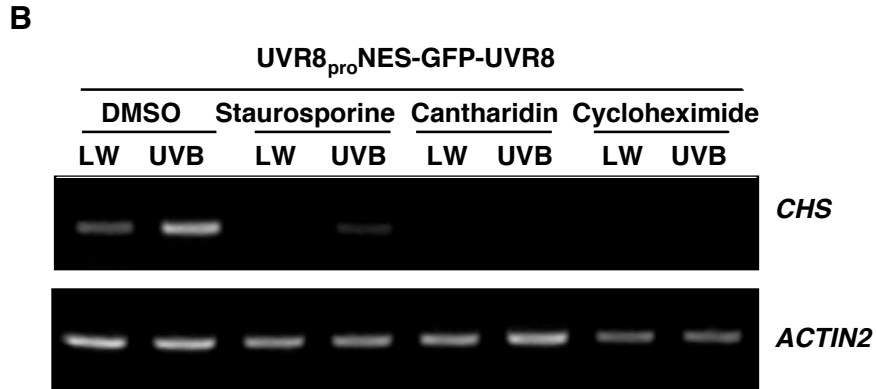


Figure 4.7 UV-B induced nuclear enrichment of NES-GFP-UVR8 is unaffected by inhibitors of phosphorylation, de-phosphorylation or protein synthesis

(A) Confocal images of GFP fluorescence in leaf epidermal tissue from UVR8_{pro}NES-GFP-UVR8 transgenic Arabidopsis (line 14-5) grown in a low fluence rates of white light ($20 \mu\text{mol m}^{-2} \text{s}^{-1}$; LW) infiltrated with DMSO (control, 1 mM), staurosporine (1 mM), cantharidin (100 μM) or cycloheximide (20 μM) for 1 h and subsequently exposed to UV-B ($3 \mu\text{mol m}^{-2} \text{s}^{-1}$) for 4 h. The arrows indicate specific nuclei in the cells. Scale bar = 20 μm . (B) RT-PCR analysis of *CHS* and control *ACTIN2* transcripts in UVR8_{pro}NES-GFP-UVR8 plants grown in a low fluence rate white light ($20 \mu\text{mol m}^{-2} \text{s}^{-1}$; LW) infiltrated with DMSO (control, 1 mM), staurosporine (1 mM), cantharidin (100 μM) or cycloheximide (20 μM) for 1 h and subsequently exposed to UV-B ($3 \mu\text{mol m}^{-2} \text{s}^{-1}$) for 4 h.

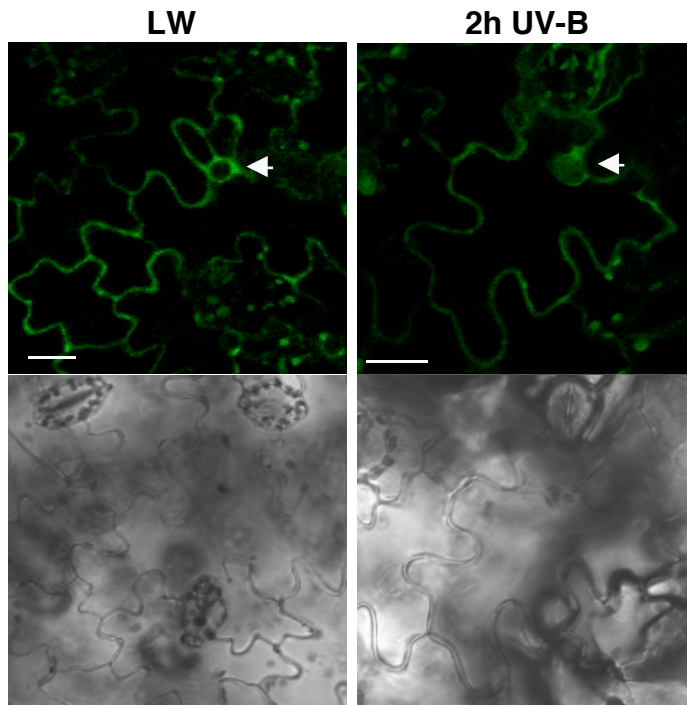


Figure 4.8 UV-B induces nuclear enrichment of transiently expressed NES-GFP-UVR8 in *Nicotiana benthamiana*

Confocal images of GFP fluorescence in leaf epidermal tissue of *Nicotiana* plants expressing transiently UVR8_{pro}GFP-UVR8 by *Agrobacterium* infiltration. Infiltrated plants were incubated for 60 h in white light ($20 \mu\text{mol m}^{-2} \text{s}^{-1}$; LW) and exposed to UV-B ($3 \mu\text{mol m}^{-2} \text{s}^{-1}$) for 4 h. The arrows indicate specific nuclei in the cells. Scale bar = 20 μm .

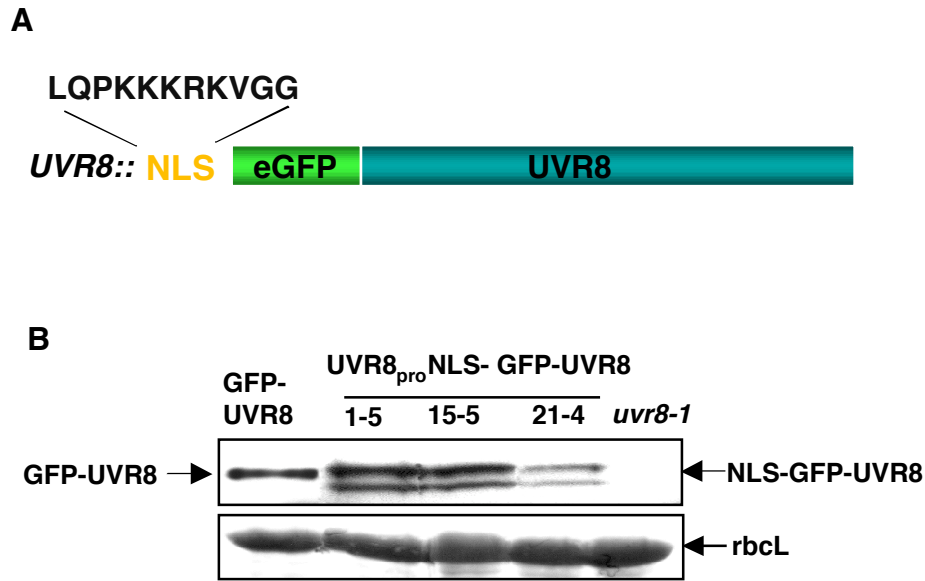
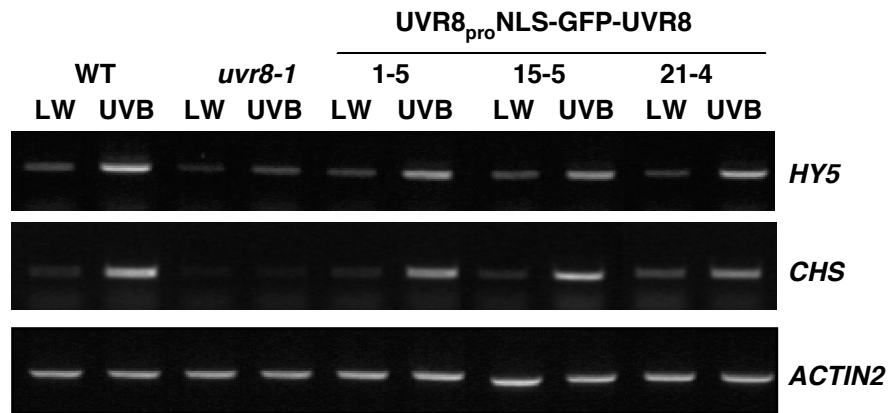


Figure 4.9 Generation of transgenic Arabidopsis plants expressing NLS-GFP-UVR8

(A) Schematic representation of the NLS-GFP-UVR8 construct driven by the *UVR8* promoter (B) Western blot of total protein extracts (15 μ g) from *uvr8-1* Arabidopsis plants expressing GFP-UVR8 or NLS-GFP-UVR8 (three independent lines) from the *UVR8* promoter, grown in white light ($100 \mu\text{mol m}^{-2} \text{s}^{-1}$) for 12 days. An anti-GFP antibody was used to probe the western blot and ponceau stain of rubisco large subunit (rbcL) was used as a loading control.

A



B

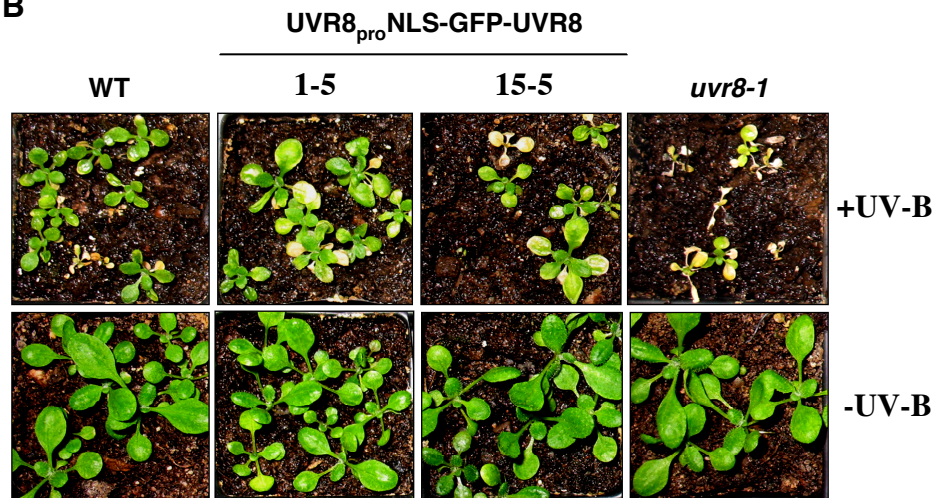


Figure 4.10 NLS-GFP-UVR8 is functional in *uvr8-1* transgenic plants

(A) RT-PCR analysis of *HY5*, *CHS* and control *ACTIN2* transcripts in wild-type, *uvr8-1* and UVR8_{pro}-NLS-GFP-UVR8 lines grown in low fluence rates of white light (20 $\mu\text{mol m}^{-2} \text{s}^{-1}$; LW) and exposed to UV-B (3 $\mu\text{mol m}^{-2} \text{s}^{-1}$) for 4 h. (B) UV-B sensitivity assay. Wild-type, *uvr8-1* and UVR8_{pro}-NLS-GFP-UVR8 plants were grown in white light (120 $\mu\text{mol m}^{-2} \text{s}^{-1}$) for 12 days and then exposed (+) or not (-) to UV-B (5 $\mu\text{mol m}^{-2} \text{s}^{-1}$) supplemented with white light (40 $\mu\text{mol m}^{-2} \text{s}^{-1}$) for 24 h. Plants were photographed after return to white light (120 $\mu\text{mol m}^{-2} \text{s}^{-1}$) for 5 days.

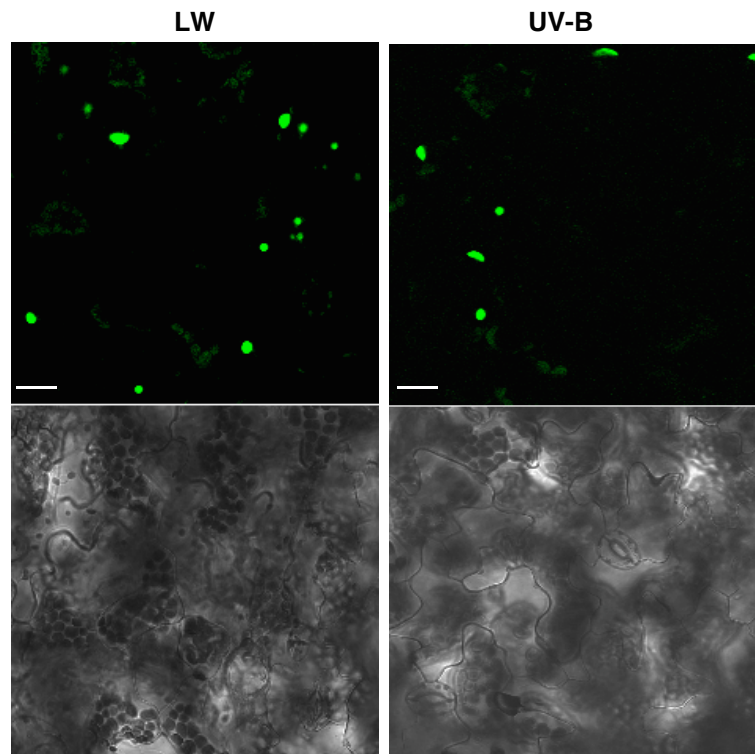


Figure 4.11 NLS-GFP-UVR8 is constitutively localised in the nucleus in all light conditions

Confocal images of GFP fluorescence in leaf epidermal tissue of $UVR8_{pro}$ -NLS-GFP-UVR8 transgenic Arabidopsis (line 15-5) grown in white light ($20 \mu\text{mol m}^{-2} \text{s}^{-1}$; LW) and exposed to UV-B ($3 \mu\text{mol m}^{-2} \text{s}^{-1}$) for 4 h. Scale bar = 20 μm .

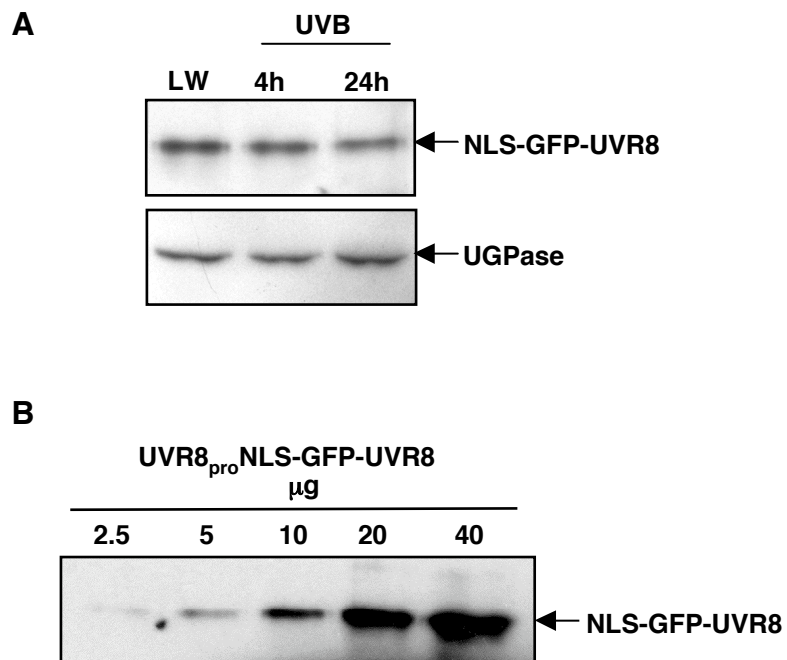


Figure 4.12 NLS-GFP-UVR8 protein levels are unaffected by UV-B exposure

(A) Immunoblot analysis of total protein extracts (5 µg) from 12-day old UVR8_{pro}NLS-GFP-UVR8 plants (line 15-5) grown in a low fluence rate of white light (20 µmol m⁻² s⁻¹; LW) and illuminated with UV-B (3 µmol m⁻² s⁻¹) for 4 or 24 h. The western blot

was probed with a GFP antibody and a UGPase antibody as a loading control. **(B)** Immunoblot demonstrating relative quantitative measurements of protein abundance of total protein extracts (2.5, 5, 10, 20 or 40 μg) from UVR8_{pro}-NLS-GFP-UVR8 plants grown in low fluence rates of white light (20 $\mu\text{mol m}^{-2} \text{s}^{-1}$). The western blot was probed with a GFP antibody.

CHAPTER 5

STRUCTURE – FUNCTION ANALYSES OF UVR8

5.1 Introduction

Sequence comparison has shown that UVR8 has 35 % identity and 50 % similarity, at the protein level, to the human regulator of chromatin condensation 1 (RCC1) (Kliebenstein *et al.*, 2002). In order to relate protein structure with function, UVR8 specific amino acid sequences were identified by primary sequence alignment of RCC1 and UVR8, and were examined based on deletion mutagenesis. Complementation studies and functional analyses demonstrate that both the N and the C-terminal UVR8 specific peptide regions of UVR8 are essential for the activity of the protein. Furthermore, the importance of the N-terminal region of UVR8 is associated with its UV-B specific nuclear enrichment. A highly basic region at the extreme C-terminus of UVR8, considered as a putative nuclear localisation signal peptide, is neither essential for UVR8 function nor required for nuclear localisation.

5.2 Deletion analysis of UVR8 based on sequence alignment with RCC1

UVR8 is very similar to the highly conserved family of RCC1 proteins (Kliebenstein *et al.*, 2002). RCC1 proteins form a 7-blade β -propeller structure, are principally localised in the nucleus and regulate nucleo-cytoplasmic transport by acting as guanine nucleotide exchange factors (GEF) for the small G protein, Ran (Renault *et al.*, 1998). It has previously been shown that UVR8 has insignificant GEF activity and is localised in the nucleus but also exists in great abundance in the cytosol of Arabidopsis cells (Brown *et al.*, 2005 and Chapter 3). These observations suggest that UVR8 is unlikely to be the homologue of RCC1 in Arabidopsis and may have evolved to perform a specialised function in response to UV-B. The primary sequence

alignment shown in Figure 5.1 was used in order to identify amino acid sequences that are unique to UVR8 and not conserved in RCC1, and establish whether these regions confer the UV-B specificity of UVR8 in Arabidopsis. In particular, the first 23 amino acids at the N-terminus of RCC1 contain a classical bipartite nuclear localisation signal (NLS), which is not conserved in UVR8. Furthermore, there is a region of sequence (27 amino acids) near the C-terminus of UVR8 that cannot be aligned with RCC1 due to the lack of identity or even similarity. And finally, there is a short region comprised of highly basic amino acids at the extreme C-terminus of UVR8, which could act as a putative monopartite NLS. The deletion of the amino acid sequences at the N-terminus, near the C-terminus or at the extreme C-terminus of UVR8 are designated and will be mentioned from now on as ΔN , ΔC and ΔNLS respectively. The generation of each deletion and its effect on UVR8 localisation and activity are described in detail below.

5.3 The N-terminus of UVR8 is important for function

To establish the importance of the UVR8-specific sequence at the N-terminus of the protein, it was necessary to introduce a mutated version of UVR8 lacking the first 23 amino acids in the *uvr8-1* mutant background. As shown in Chapter 3 (Figures 3.1 (B) and (C)) *uvr8-1* is a null mutant, as there is no UVR8 or UVR8-like protein detected with either of the anti-UVR8 antibodies. Therefore, the activity of the mutated protein can be fully assessed. The deletion mutation was generated by PCR with specific primers annealing downstream of the 23rd amino acid of UVR8. The PCR product, $\Delta NUVR8$, was subcloned in a vector containing a GFP tag at the N-terminus and the fusion construct, GFP- $\Delta NUVR8$, was controlled by the native *UVR8* promoter. At least three independent homozygous lines containing GFP- $\Delta NUVR8$ were selected and examined for protein expression. Figure 5.2 (B) shows that deletion of the N-terminus of UVR8 does not decrease the stability of the protein. The lower expression levels of two of the GFP- $\Delta NUVR8$ lines could be due to positional effects in the Arabidopsis chromosomal region into which the transgene has been inserted.

Complementation analysis was also investigated by RT-PCR and UV-B sensitivity assays. RT-PCR analysis suggests that *uvr8-1* transgenic plants expressing GFP- Δ NUVR8 do not complement the mutant phenotype in terms of the induction of *HY5* and *CHS* expression in response to UV-B (Figure 5.3 (A)). Lack of complementation was also observed when plants expressing GFP- Δ NUVR8 were irradiated with higher than ambient fluence rates of UV-B ($5 \mu\text{mol m}^{-2} \text{s}^{-1}$) supplemented with white light ($40 \mu\text{mol m}^{-2} \text{s}^{-1}$). Figure 5.3 (B) demonstrates how GFP- Δ NUVR8 and *uvr8-1* lines show significant growth impairment and leaf necrosis in response to UV-B, whereas wild-type plants recover fully after the UV-B treatment. The possibility that GFP- Δ NUVR8 is non-functional due to the addition of the GFP tag is ruled out, as GFP-UVR8 (Chapter 3) was found to complement fully when expressed in *uvr8-1* lines. So, the extreme N-terminus of UVR8 is essential for function. Detailed investigation of how the N-terminus could affect the activity of UVR8 is described below.

5.4 GFP- Δ NUVR8 is defective in the UV-B dependent nuclear enrichment response but retains its chromatin association

It is very important to understand in what way the first 23 amino acids of UVR8 are essential for its function and consequently for inducing gene expression in response to UV-B. To examine whether deletion of the N-terminus of UVR8 impairs its UV-B responsiveness or its general protein integrity, localisation and chromatin association assays were performed. Confocal microscopy images demonstrate that GFP- Δ NUVR8 is localised both in the nucleus and in the cytosol, like GFP-UVR8. However, when plants expressing GFP- Δ NUVR8 are irradiated with UV-B for 4 hours, there is no nuclear accumulation observed in contrast to the wild-type protein (Figure 5.4 (A)). More detailed analysis based on co-localisation of GFP and DAPI fluorescence shows that the nuclear accumulation of GFP- Δ NUVR8 is increased by

only 18 % (Figure 5.4 (B)), compared to 100 % observed for GFP-UVR8 (3.12 (A)). These data imply that the N-terminus of UVR8 is necessary for its UV-B dependent nuclear import.

To test whether the loss of function in GFP- Δ NUVR8 is solely due to its insufficient nuclear import in response to UV-B or because of a change in the general conformation of the mutated protein, the association of GFP- Δ NUVR8 with chromatin was examined. Chromatin immunoprecipitation assays on tissue from plants expressing GFP- Δ NUVR8 and immunoprecipitated with anti-GFP or anti-C terminus UVR8 antibodies show an interaction of GFP- Δ NUVR8 with the promoter region of *HY5* (Figure 5.5), as has been shown for GFP-UVR8 but not for *uvr8-1* (Brown *et al.*, 2005 and Figure 3.6). Therefore, if GFP- Δ NUVR8 is still able to associate with chromatin, it is very likely that there are no major conformational changes caused by the deletion, which could lead to loss of the protein activity. So, it can be concluded that the N-terminus region of UVR8 confers the necessary information for the UV-B induced nuclear enrichment of UVR8.

5.5 GFP- Δ CUVR8 is not functional in Arabidopsis

The C-terminus of UVR8 seems to be very critical for protein function, as the *uvr8-2* mutant allele lacks 41 amino acids from the C-terminus of the protein (Brown *et al.*, 2005) and although it still produces protein, it is non-functional (data not shown). Furthermore, sequence alignment analysis between UVR8 and RCC1, reveals that there is a region of 27 amino acids at the C-terminus of UVR8 that is absent from RCC1 (Figure 5.1). Deletion of this specific region was necessary to assess its importance for UVR8 activity. Mutagenesis was performed by inverted PCR, where each primer annealed at the two opposite ends of the region to be deleted. The PCR product obtained, lacking the 27 amino acids was fused to a GFP tag at the N-terminus of the protein and was stably transformed in *uvr8-1* mutant plants for functional analysis. To test if the GFP- Δ CUVR8 mutated protein is expressed and if it is stable,

western blot analysis was carried out. Immunoblot studies of equal amounts of protein extracted from plants expressing GFP- Δ CUVR8, GFP-UVR8 or *uvr8-1* and probed with the anti-N-terminal UVR8 antibody show that GFP- Δ CUVR8 is expressed at comparable levels to GFP-UVR8, whereas there is no protein detected in *uvr8-1* (Figure 5.6 (B)).

Complementation studies carried out by RT-PCR demonstrate that there is no induction of *HY5* or *CHS* expression in response to UV-B in any of the three independent homozygous lines expressing GFP- Δ CUVR8 (Figure 5.7 (A)). Moreover, plants expressing GFP- Δ CUVR8 fail to recover when exposed to higher than ambient levels of UV-B irradiation (Figure 5.7 (B)). Complementation data indicate that the 27-amino acid region near the C-terminus of UVR8 is essential for protein activity, since GFP- Δ CUVR8 cannot rescue the *uvr8-1* mutant phenotype.

5.6 The C-terminus of UVR8 is not required for UV-B specific nuclear enrichment

In order to assess if GFP- Δ CUVR8 is impaired in the UV-B induced nuclear translocation observed in GFP-UVR8, GFP and DAPI fluorescent images of plants grown in white light or irradiated with UV-B ($3 \mu\text{mol m}^{-2} \text{s}^{-1}$) were analysed. Figure 5.8 (A) shows that there is a significant increase in the nuclear GFP fluorescence of GFP- Δ CUVR8 in response to UV-B. Quantitative analysis based on co-localisation of GFP and DAPI fluorescence shows a substantial increase in the number of nuclei containing GFP- Δ CUVR8 in response to UV-B compared to white light (Figure 5.8 (B)). The magnitude of GFP- Δ CUVR8 nuclear enrichment is not as high as that demonstrated by GFP-UVR8 in response to UV-B, due to the increased basal nuclear accumulation of GFP- Δ CUVR8. Based on the graph of Figure 5.8 (B), there is over 60 % of nuclei containing GFP- Δ CUVR8 under white light conditions, whereas for GFP-UVR8 there is only 45 % thus, the difference in response to UV-B is greater than the one observed

for GFP- Δ CUVR8. So, the UV-B induced nuclear import of GFP- Δ CUVR8 is considered similar to GFP-UVR8, unlike GFP- Δ NUVR8, which exhibits significantly reduced nuclear translocation.

To test if the 27-amino acid region near the C-terminus of UVR8 is necessary for chromatin association, chromatin immunoprecipitation assays were performed. Chromatin enriched fractions extracted from GFP- Δ CUVR8 and GFP-UVR8 transgenic lines were immunoprecipitated with anti-GFP and anti-N or C-terminus UVR8 antibodies respectively. Figure 5.9 shows that GFP- Δ CUVR8 can still associate with the promoter region of *HY5*. The N-terminus UVR8 antibody was used for the immunoprecipitation of GFP- Δ CUVR8, as the C-terminus antibody was raised against the 27-amino acid region (Figure 3.1 (C)), which is deleted in GFP- Δ CUVR8. Western blot and immunoprecipitation studies have shown that the N-terminus UVR8 antibody is less sensitive than the C-terminus one (data not shown). For this reason a fainter signal is detected in the PCR on the DNA immunoprecipitated with the N-terminus UVR8 antibody compared to that obtained with the anti-GFP antibody (Figure 5.9). By taking the complementation and functional analyses into consideration, it is evident that GFP- Δ CUVR8 is responsive to the UV-B dependent nuclear import and can associate with chromatin, but is not functional in terms of regulating *HY5* and *CHS* gene expression, nor survival when exposed to UV-B irradiation.

5.7 GFP- Δ NLSUVR8 is active in Arabidopsis

UVR8 has been shown to reside in the nucleus and cytosol of epidermal plant cells (Brown *et al.*, 2005 and Chapter 3). However, no canonical nuclear localisation signal (NLS) has been identified within the sequence of UVR8, unlike RCC1, which contains a bipartite NLS at the N-terminus (Seino *et al.*, 1992). A very short and highly basic amino acid sequence (KRVRI) at the extreme C-terminus of UVR8 is the only putative monopartite NLS contained in the whole UVR8 sequence. In order to establish if this peptide provides UVR8 with the necessary signal for nuclear targeting, deletion

of this region was performed. The deletion of Δ NLSUVR8 was introduced by PCR, using primers annealing at the N-terminus and upstream of the first amino acid desired to be deleted. A GFP fusion tag was added to the N-terminus of Δ NLSUVR8 and the fusion protein was introduced into plants by *Agrobacterium*-mediated transformation. At least three independent homozygous *uvr8-1* transgenic lines expressing GFP- Δ NLSUVR8 from the *UVR8* promoter were examined for protein expression and stability. The immunoblot in Figure 5.10 (B) shows that the protein levels of GFP- Δ NLSUVR8 are comparable to the intact GFP-UVR8 protein, thus complementation analysis could be investigated.

RT-PCR studies in Figure 5.11 (A) demonstrate that GFP- Δ NLSUVR8 fully complements the induction of *HY5* and *CHS* gene expression in response to low fluence rates of UV-B when expressed in *uvr8-1* mutant plants. More evidence for the activity of GFP- Δ NLSUVR8 is obtained from the UV-B sensitivity assay. Similar to wild-type but unlike *uvr8-1*, GFP- Δ NLSUVR8 transgenic lines survive after exposure to higher than ambient UV-B irradiation (Figure 5.11 (B)).

According to the data from gene expression and UV-B tolerance functional assays, it is apparent that the putative NLS is not required for UVR8 activity, as GFP- Δ NLSUVR8 fully rescues the *uvr8-1* mutant phenotype.

5.8 Deletion of the putative NLS does not impair UVR8 nuclear localisation or UV-B induced nuclear import

As mentioned above, the main reason for generating GFP- Δ NLSUVR8 transgenic plants was to assess if the basic cluster of amino acids at the extreme C-terminus of UVR8 could operate as an NLS peptide. For this reason, the subcellular localisation of GFP- Δ NLSUVR8 was examined by fluorescence confocal microscopy. Initially, the general distribution of GFP- Δ NLSUVR8 was examined in plants grown in white light conditions. Figure 5.12 (A) shows that GFP- Δ NLSUVR8 is localised in the

nucleus and the cytoplasm of epidermal cells, thus excluding the possibility that this region functions as a general NLS peptide. In addition, the UV-B induced nuclear enrichment of GFP- Δ NLSUVR8 was tested, in case the absence of the basic-rich peptide has an effect on nuclear translocation. Once more, GFP- Δ NLSUVR8 exhibited normal nuclear import in response to UV-B (Figure 5.12 (A)). Quantification of this response indicates that there is an 80 % increase in the amount of nuclei containing GFP- Δ NLSUVR8 in response to UV-B, which is comparable to the nuclear enrichment observed for the unmodified GFP-UVR8 (Figure 5.12 (B)). In conclusion, data from fluorescence microscopy suggest that the basic amino acid sequence at the C-terminus of UVR8 plays no role in the subcellular localisation or the UV-B induced translocation of the protein.

Finally, the ability of GFP- Δ NLSUVR8 to associate with chromatin, and in particular with the promoter region of *HY5*, was investigated. ChIP assays performed on chromatin-enriched extracts from plants expressing GFP- Δ NLSUVR8 show association with the promoter of *HY5* when the anti-GFP antibody was used for the immunoprecipitation (Figure 5.13). This result was unsurprising, since GFP- Δ NLSUVR8 fully rescues the *uvr8-1* mutant phenotype. However it was interesting to investigate whether this cluster of basic amino acids was required for chromatin binding. No signal was detected when the anti C-terminus UVR8 antibody was used, possibly due to a minor conformational change caused by the deletion in GFP- Δ NLSUVR8 leading to decreased recognition by the C-terminal antibody.

5.9 UVR8 antibodies are highly specific

As described in Chapter 3, two UVR8 specific peptide antibodies were generated, both recognising a protein of the predicted molecular weight from total protein extracted from wild-type or GFP-UVR8 plants. No cross-reaction with other, non-UVR8, proteins was observed in extracts from *Arabidopsis*, *E.coli* or yeast. Both antibodies recognise UVR8 in its native or denatured form, although the C-terminus

UVR8 antibody is more sensitive than the one raised against the N-terminus of UVR8. Each antibody was designed based on the two highly specific UVR8 peptide regions, which were also chosen for deletion analysis, the extreme N-terminus and near the C-terminus. For this reason plants expressing the mutagenised versions of UVR8, GFP- Δ NUVR8, GFP- Δ CUVR8 and GFP- Δ NLSUVR8 provided the ideal candidates for testing the specificity of the antibodies and at the same time demonstrate by immunoblot analysis the identity of each modified UVR8 construct. The western blot in Figure 5.14 shows that UVR8, GFP- Δ NUVR8 and GFP- Δ NLSUVR8 proteins are recognised by the C-terminus UVR8 antibody, whereas GFP- Δ CUVR8 protein that does not contain the region against which the antibody was raised is not detected. Stripping and re-probing of the same western with the anti-N-terminal UVR8 antibody, reveals protein bands corresponding to UVR8, GFP- Δ CUVR8 and GFP- Δ NLSUVR8 but not GFP- Δ NUVR8 as it lacks the peptide that the N-terminal antibody recognises. Although these experiments do not provide much information on UVR8 protein *per se*, they confirm that the antibodies recognise only the specific regions of UVR8 used as antigens that they can be used for characterisation of other *uvr8* mutant alleles or even for co-immunoprecipitation studies to test the possibility of UVR8 protein dimerisation.

5.10 Discussion

The study described in this chapter is principally focused on the structure-function relationship of UVR8. The approach used was based on deletion mutagenesis of UVR8 specific peptide regions, followed by functional analysis. Although deletion of either the first 23 amino acids at the N-terminus or 27 amino acids near the C-terminus of UVR8 impaired its activity, neither of them affected its association with chromatin. Furthermore, the N-terminus of UVR8 plays a fundamental role in the UV-B induced nuclear import. Deletion of a putative NLS at the C-terminus of the protein had no effect on UVR8 nuclear localisation or function.

5.10.1 Structure-function studies based on deletion mutagenesis

Correlation between the structure and the function of a protein can be investigated by different approaches. The first one is based on random mutagenesis and genetic analysis of different mutant alleles of the same protein, as shown for phytochrome B localisation by Chen *et al.*, (2003). Another approach involves directed mutagenesis of amino acids predicted to be critical either due to their structural context or their conservation among related proteins in the same or different species. An excellent example for this approach is demonstrated by the analysis of the phototropin LOV domains, where signal perception and transduction are affected by a single amino acid change (Christie *et al.*, 2000 and 2002). And finally, the approach adopted in this study is based on deletion mutagenesis of larger peptide regions, which are defined by motif recognition or sequence alignments. There is extensive literature with regard to structure-function analyses on phytochromes (Oka *et al.*, 2004 and Chen *et al.*, 2005) cryptochromes (Lin and Shalitin, 2003) and downstream light signalling components (Stacey *et al.*, 1999) using deletion mutagenesis of structural domains or conserved sequences. This approach was also employed for understanding the relationship between the structure and function of UVR8. Detailed structural information on the protein is a requirement for directed mutagenesis. However, thanks to the sequence similarity of UVR8 to RCC1, identification of conserved or non-conserved UVR8 specific peptide regions and deletion analyses were made possible. As described in the alignment of Figure 5.1, there are some amino acid regions of UVR8 that are not equivalent to RCC1 and *vice versa*. Deletion of UVR8 specific regions (ΔN , ΔC and ΔNLS) and generation of GFP-tagged modified versions of UVR8 were tested for activity in terms of gene expression, chromatin association, subcellular localisation, nuclear accumulation and UV-B sensitivity.

5.10.2 The N-terminus of UVR8 is essential for function and UV-B induced nuclear translocation

Sequence alignment of UVR8 and RCC1 exhibits a significant difference in the first 23 amino acids at the N-terminus of the proteins. For RCC1 this N-terminal region is occupied by its bipartite NLS peptide (Seino *et al.*, 1992). UVR8 contains no basic amino acid signature motif at the N-terminus, which would define a putative NLS. However, the possibility of this UVR8 specific region to be involved in localisation or protein activity was investigated. As mentioned above, deletion mutagenesis is the approach employed for this study. The modified version of Δ NUVR8, lacking the first 23 amino acids was expressed stably in *uvr8-1* mutant Arabidopsis plants in order to assess its activity. A fusion with an N-terminal GFP tag also allowed monitoring the subcellular localisation of the protein. Gene expression studies by RT-PCR showed that the N-terminal region of UVR8 is necessary for the UV-B induction of UVR8-regulated genes, such as *HY5* and *CHS* (Figure 5.3 (A)). More evidence for the lack of functionality of GFP- Δ NUVR8 was provided from a UV-B sensitivity assay, which demonstrated an increased sensitivity of GFP- Δ NUVR8, similar to that observed in *uvr8-1* mutant plants (Figure 5.3 (B)). To further investigate the basis for the loss of the molecular and physiological activity of GFP- Δ NUVR8, the ability of GFP- Δ NUVR8 to associate with chromatin was examined. Chromatin immunoprecipitation assays on plants expressing GFP- Δ NUVR8 proved that the N-terminal region of UVR8 is not essential for association with the promoter region of *HY5* (Figure 5.5). This would mean that the first 23 amino acids do not form the binding site for chromatin or histones or any other protein complex that facilitates UVR8 chromatin association. In order to examine if the N-terminal deletion has any effects on UVR8 subcellular localisation and/or the UV-B mediated nuclear translocation, the fluorescence of GFP- Δ NUVR8 was monitored by confocal microscopy. According to the images of Figure 5.4 (A), the localisation of GFP- Δ NUVR8 under white light conditions is nuclear and cytosolic, consistent with GFP-UVR8. However, a UV-B stimulus ($3 \mu\text{mol m}^{-2} \text{s}^{-1}$ for 4

h) fails to trigger nuclear translocation of GFP- Δ UVR8. Quantitative analysis indicates that there is less than 20 % increase in the number of nuclei containing GFP- Δ UVR8 in response to a saturating 4-hour UV-B irradiation, compared to the increase observed for GFP-UVR8. The fact that GFP- Δ UVR8 protein is stable (Figure 5.2 (B)) and still able to associate with chromatin *in planta* (Figure 5.5), suggests that the deletion of the first 23 amino acids did not interfere with the protein conformation. Therefore its inactivity is attributed to an impairment of the UV-B induced nuclear import.

The ideal assay for verifying that the N-terminus of UVR8 promotes the UV-B induced nuclear enrichment of the protein would require generation of GFP-N23 constructs. If this region is sufficient for nuclear import, then a UV-B stimulus should mediate translocation of this construct into the nucleus. Furthermore, for additional functional analyses, the generation of transgenic plants expressing NLS-GFP- Δ UVR8, constitutively localised in the nucleus, would reveal if the loss of function of GFP- Δ UVR8 is due to the lack of the UV-B induced nuclear import, or to loss of activity following translocation.

5.10.3 The C-terminus of UVR8 is essential for activity

A 27-amino acid region near the C-terminus of UVR8 was identified as specific to UVR8, as there is no equivalent sequence in RCC1 or any known plant protein. Protein structure prediction analysis (data not shown) suggests that the 27 amino acids near the C-terminus of UVR8 would form an additional loop and consequently would not disturb the 7-blade β -propeller structure of UVR8, based on the resolved crystal structure of RCC1 (Renault *et al.*, 1998). To establish the importance of this region for the activity of UVR8, transgenic plants lacking the 27-amino acid sequence (GFP- Δ CUVR8) were generated. Functional analyses based on molecular and physiological complementation assays demonstrate that the deletion of the 27-amino acid region impedes the UV-B induced regulation of gene expression controlled by UVR8 and

leads to increased susceptibility to UV-B damage (Figures 5.7 (A) and (B)). Moreover, fluorescence microscopy studies show that the subcellular localisation GFP- Δ CUVR8 is largely unaffected by the deletion of this region. GFP- Δ CUVR8 is still localised in the nucleus and the cytosol of epidermal cells in white light and retains the nuclear translocation in response to UV-B (Figures 5.8 (A) and (B)). Once more, chromatin immunoprecipitation assays and immunoblot analysis indicate that the lack of GFP- Δ CUVR8 activity is not due to the lack of chromatin association or protein instability (Figures 5.6 (B) and 5.9)). However, it is not surprising that the deletion of this particular sequence leads to loss of UVR8 function, as the *uvr8-2* mutant allele contains a premature stop codon at Trp⁴⁰⁰ (Brown *et al.*, 2005), which is part of the UVR8 specific 27-amino acid region. Although *uvr8-2* is not functional, immunoblot analysis has shown that there is protein of the predicted molecular weight produced (data not shown). It is possible that this region confers the function of UVR8 or signifies the site of interaction with a protein partner for UVR8.

5.10.4 UVR8 enters the nucleus in the absence of a canonical nuclear localisation signal

As mentioned earlier, UVR8 exhibits the highest sequence similarity to the human RCC1 (Kliebenstein *et al.*, 2002). RCC1 is localised primarily in the nucleus and contains a bipartite NLS at the N-terminus of the protein (Seino *et al.*, 1992). Sequence analysis of UVR8 revealed a short sequence rich in highly basic amino acids (KRVRI) at the extreme C-terminus of the protein. Although this peptide is not an RCC1-like bipartite NLS, it is considered as a putative NLS. To test its nuclear import activity, transgenic plants lacking the amino acids KRVRI were generated linked to a GFP tag. Initially, the functionality of the modified protein GFP- Δ NLSUVR8 was confirmed by complementation analysis involving RT-PCR and UV-B tolerance (Figures 5.11 (A) and (B)). Next, fluorescence microscopy studies demonstrated that nuclear localisation of GFP- Δ NLSUVR8 was unaffected by the deletion of the putative

NLS in the absence and presence of UV-B (Figures 5.12 (A) and (B)), implying that this region is not necessary for basal or UV-B induced nuclear import of UVR8. In order to entirely exclude the possibility that this peptide could function as an NLS, transgenic plants expressing a GFP-tagged KRVRI peptide would have to be made and examined. If this sequence alone was sufficient for transport of the tag into the nucleus, then KRVRI would be considered as a functional NLS. Nevertheless, the experiments reported here show that the peptide is not required for UVR8 nuclear localisation. Such experiments involving more detailed analysis of KRVRI were not carried out since GFP- Δ NLSUVR8 proved to be fully functional. Detailed analysis of the mechanism involved in the nuclear import of RCC1 has shown that deletion of the NLS does not inhibit its nuclear translocation, suggesting that there is an additional mechanism mediating nuclear import (Nemergut and Macara, 2000). Whether an analogous dual mechanism exists for UVR8 nuclear localisation is still unclear.

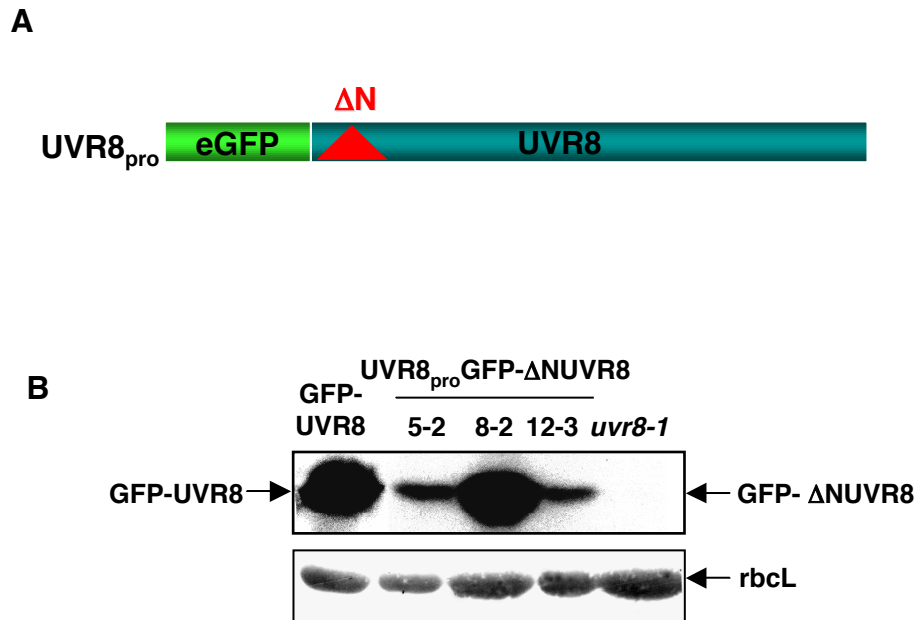
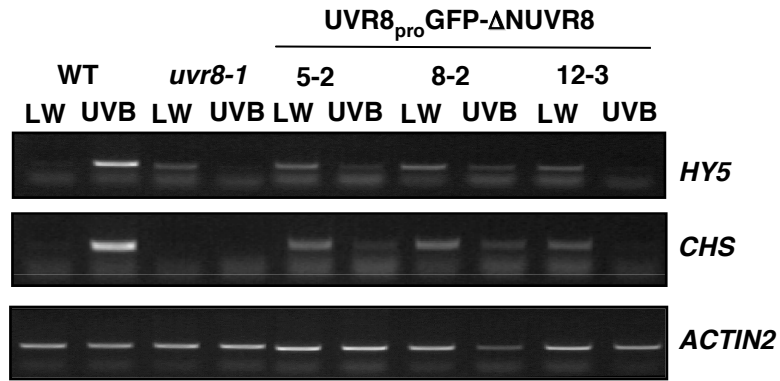


Figure 5.2 Generation of transgenic Arabidopsis plants expressing GFP- Δ NUVR8

(A) Schematic representation of the GFP- Δ NUVR8 construct driven by the *UVR8* promoter (B) Western blot of total protein extracts (15 μ g) from *uvr8-1* transgenic Arabidopsis plants expressing UVR8_{pro}GFP-UVR8 or UVR8_{pro}GFP- Δ NUVR8 (three independent lines) grown in white light (100 μ mol m⁻² s⁻¹) for 12 days. An anti-GFP antibody was used to probe the western blot and a Ponceau stain of Rubisco large subunit (rbcL) was used as a loading control.

A



B

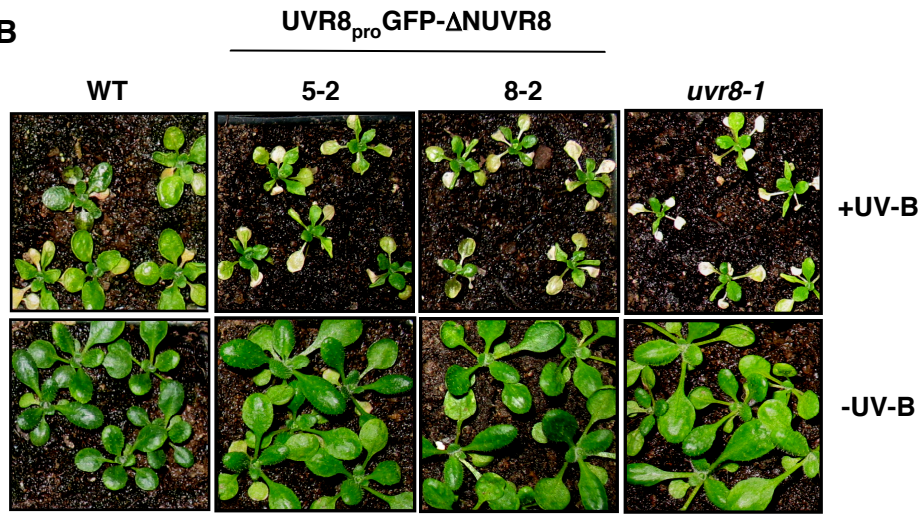


Figure 5.3 GFP- Δ NUVR8 is not functional in transgenic *uvr8-1* plants

(A) RT-PCR analysis of *HY5*, *CHS* and control *ACTIN2* transcripts in wild-type, *uvr8-1* and UVR8_{pro} GFP- Δ NUVR8 lines grown for 3 weeks in a low fluence rate of white light ($20 \mu\text{mol m}^{-2} \text{s}^{-1}$; LW) and exposed to UV-B ($3 \mu\text{mol m}^{-2} \text{s}^{-1}$) for 4 h. (B) UV-B sensitivity assay. UVR8_{pro} GFP-UVR8, UVR8_{pro} GFP- Δ NUVR8 and *uvr8-1* plants were grown in white light ($120 \mu\text{mol m}^{-2} \text{s}^{-1}$) for 12 days and then exposed (+) or not (-) to UV-B ($5 \mu\text{mol m}^{-2} \text{s}^{-1}$) supplemented with white light ($40 \mu\text{mol m}^{-2} \text{s}^{-1}$) for 24 h. Plants were photographed after return to white light ($120 \mu\text{mol m}^{-2} \text{s}^{-1}$) for 5 days.

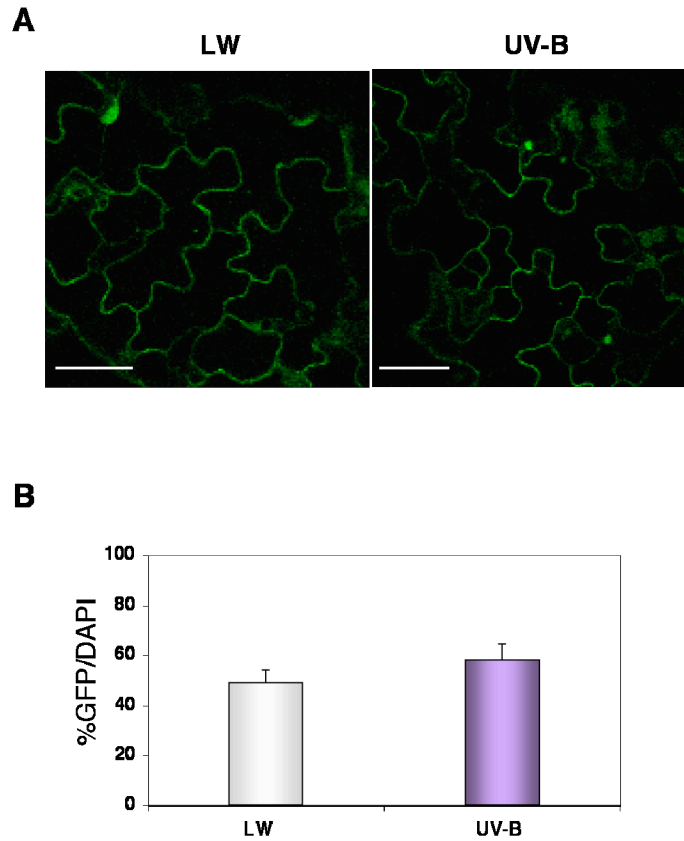


Figure 5.4 GFP- Δ NUVR8 shows impaired nuclear accumulation in response to UV-B

(**A**) Confocal images of GFP in leaf epidermal tissue of Arabidopsis UVR8_{pro}GFP- Δ NUVR8 transgenic plants (line 8-2) grown in white light ($20 \mu\text{mol m}^{-2} \text{s}^{-1}$; LW) for 12 days and exposed to UV-B ($3 \mu\text{mol m}^{-2} \text{s}^{-1}$) for 4 h. Scale bar = $20 \mu\text{m}$. (**B**) The percentage co-localisation of GFP and DAPI fluorescence from UVR8_{pro}GFP- Δ NUVR8 transgenic plants grown in white light ($20 \mu\text{mol m}^{-2} \text{s}^{-1}$; LW) and exposed to UV-B ($3 \mu\text{mol m}^{-2} \text{s}^{-1}$) for 4 h. Data are the mean \pm S.E.; $n = 20$.

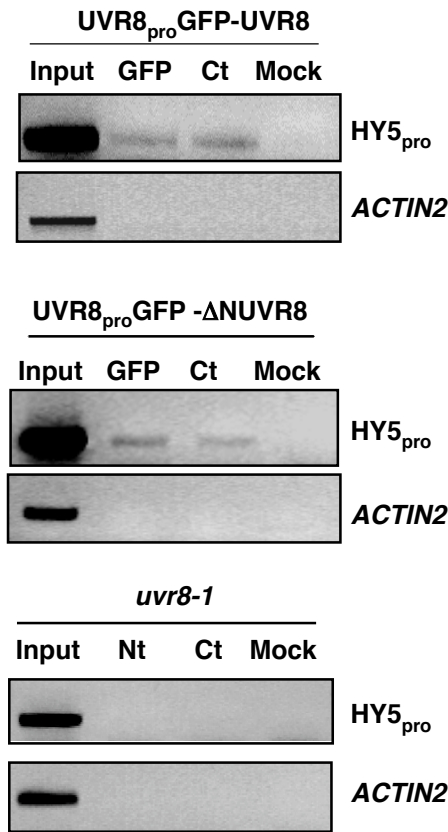


Figure 5.5 GFP-ΔNUVR8 is associated with the promoter region of *HY5*

Chromatin immunoprecipitation assay of DNA associated with GFP-UVR8 or GFP-ΔNUVR8. PCR of *HY5* promoter (-331 to +23) and *ACTIN2* DNA from UVR8_{pro}GFP-UVR8 (upper) UVR8_{pro}GFP-ΔNUVR8 and *uvr8-1* (lower) plants grown in white light (100 μmol m⁻² s⁻¹) for 12 days and exposed to UV-B (3 μmol m⁻² s⁻¹) for 4 h: lane 1, input DNA before immunoprecipitation; lane 2, DNA immunoprecipitated by using GFP antibody (or N-terminal UVR8 for *uvr8-1*); lane 3, DNA immunoprecipitated by using C-terminal UVR8 antibody, lane 4, mock (no antibody) control.

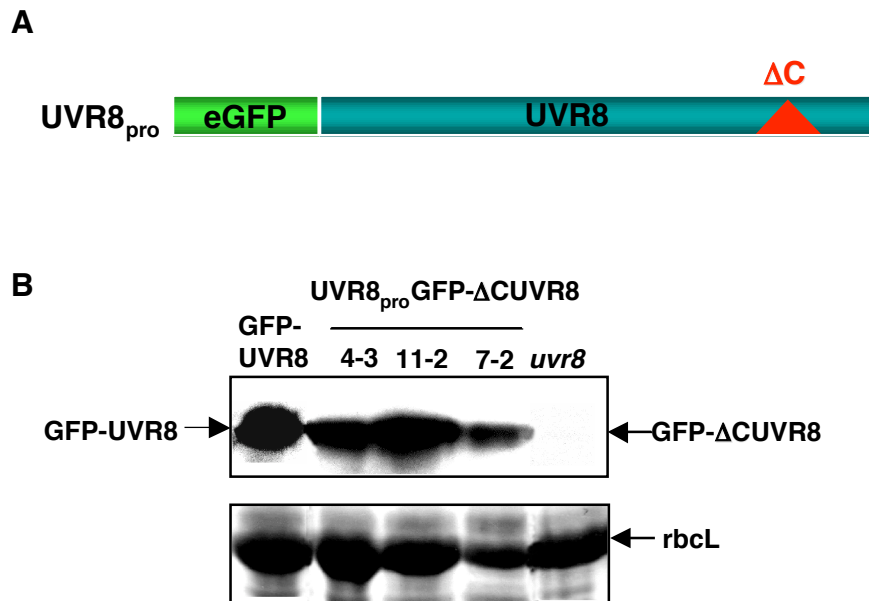
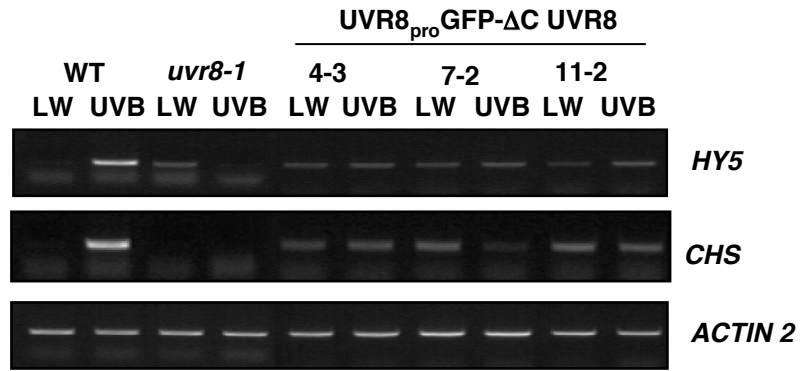


Figure 5.6 Generation of transgenic Arabidopsis plants expressing GFP-ΔCUVR8

(A) Schematic representation of the GFP-ΔC-UVR8 construct driven by the *UVR8* promoter (B) Western blot of total protein extracts (15 μg) from *uvr8-1* transgenic Arabidopsis plants expressing UVR8_{pro}GFP-UVR8 or UVR8_{pro}GFP-ΔCUVR8 (three independent lines) grown in white light (100 μmol m⁻² s⁻¹) for 12 days. An anti-GFP antibody was used to probe the western blot and a ponceau stain of rubisco large subunit (*rbcL*) was used as a loading control.

A



B

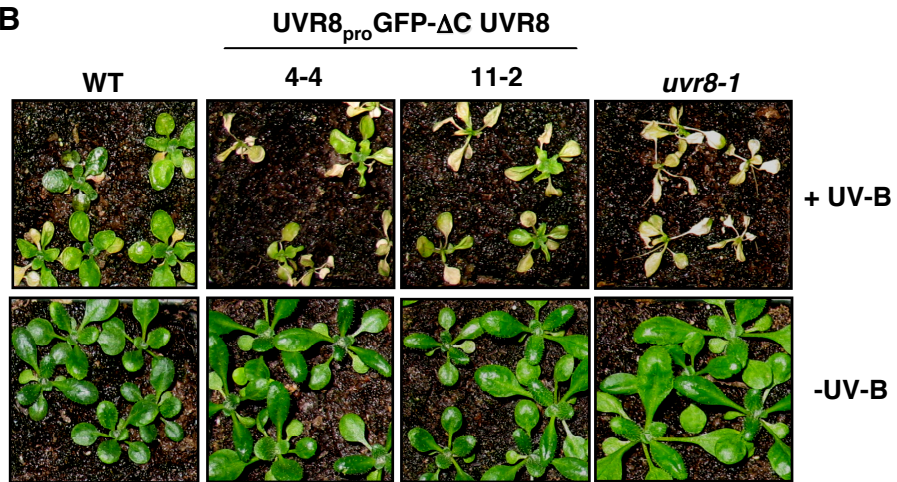


Figure 5.7 GFP- Δ CUVR8 is not functional in *uvr8-1* transgenic plants

(A) RT-PCR analysis of *HY5*, *CHS* and control *ACTIN2* transcripts in wild-type, *uvr8-1* and $UVR8_{pro}$ -GFP- Δ CUVR8 lines grown in a low fluence rate of white light ($20 \mu\text{mol m}^{-2} \text{s}^{-1}$; LW) for 3 weeks and exposed to UV-B ($3 \mu\text{mol m}^{-2} \text{s}^{-1}$) for 4 h. (B) UV-B sensitivity assay. $UVR8_{pro}$ -GFP-UVR8, $UVR8_{pro}$ -GFP- Δ CUVR8 and *uvr8-1* plants were grown in white light ($120 \mu\text{mol m}^{-2} \text{s}^{-1}$) for 12 days and then exposed (+) or not (-) to UV-B ($5 \mu\text{mol m}^{-2} \text{s}^{-1}$) supplemented with white light ($40 \mu\text{mol m}^{-2} \text{s}^{-1}$) for 24 h. Plants were photographed after return to white light ($120 \mu\text{mol m}^{-2} \text{s}^{-1}$) for 5 days.

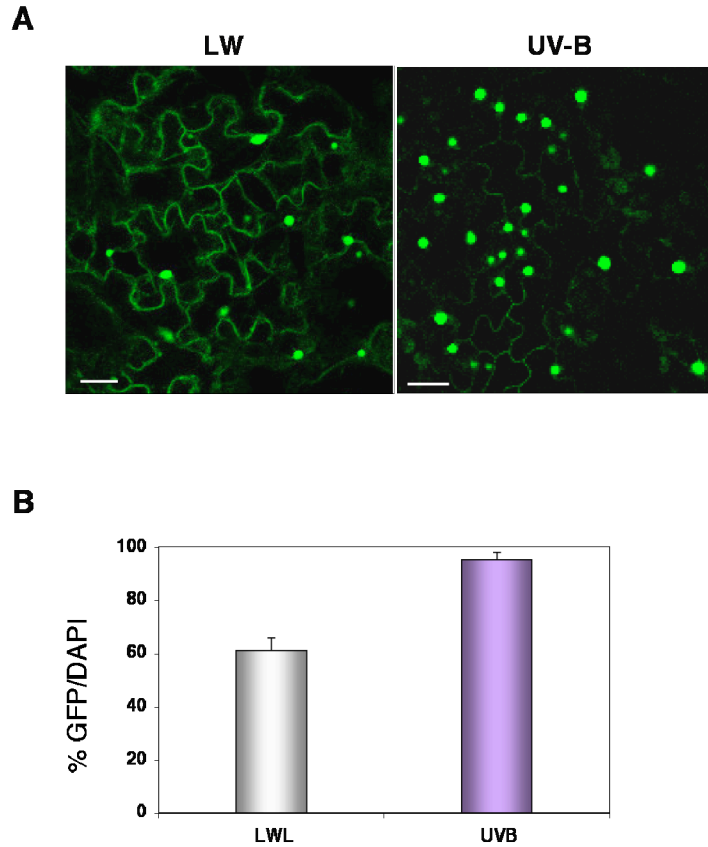


Figure 5.8 UV-B induces nuclear accumulation of GFP- Δ CUVR8

(**A**) Confocal images of GFP in leaf epidermal tissue of $UVR8_{pro}GFP-\Delta CUVR8$ transgenic plants (line 11-2) grown in white light ($20 \mu\text{mol m}^{-2} \text{s}^{-1}$; LW) for 12 days and exposed to UV-B ($3 \mu\text{mol m}^{-2} \text{s}^{-1}$) for 4 h. Scale bar = $20 \mu\text{m}$. (**B**) The percentage co-localisation of GFP and DAPI fluorescence from $UVR8_{pro}GFP-\Delta CUVR8$ transgenic plants grown in white light ($20 \mu\text{mol m}^{-2} \text{s}^{-1}$; LW) and exposed to UV-B ($3 \mu\text{mol m}^{-2} \text{s}^{-1}$) for 4 h. Data are the mean \pm S.E.; $n = 20$.

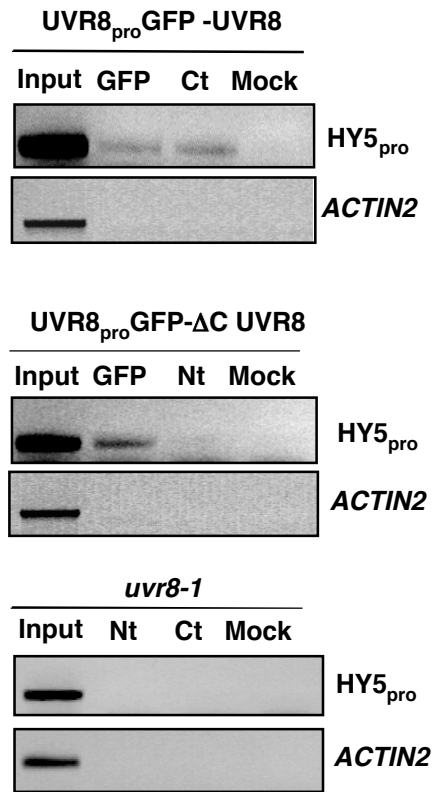


Figure 5.9 GFP-ΔCUVR8 is associated with the promoter region of *HY5*

Chromatin immunoprecipitation assay of DNA associated with GFP-UVR8 or GFP-ΔCUVR8. PCR of *HY5* promoter (-331 to +23) and *ACTIN2* DNA from UVR8_{pro} GFP-UVR8 (upper) UVR8_{pro} GFP-ΔCUVR8 and *uvr8-1* (lower) plants grown in white light (100 μmol m⁻² s⁻¹) and exposed to UV-B (3 μmol m⁻² s⁻¹) for 4 h: lane 1, input DNA before immunoprecipitation; lane 2, DNA immunoprecipitated by using GFP antibody; lane 3, DNA immunoprecipitated by using C-terminal or N-terminal (for GFP-ΔCUVR8) UVR8 antibody, lane 4, Mock (no antibody) control.

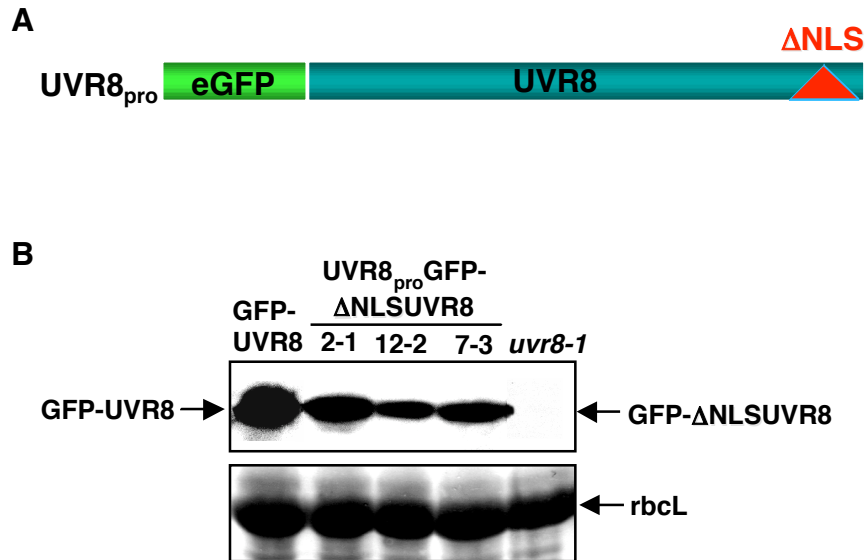


Figure 5.10 Generation of transgenic Arabidopsis plants expressing GFP-ΔNLSUVR8

(A) Schematic of the GFP-ΔNLSUVR8 construct driven by the UVR8 promoter (B) Western blot of total protein extracts (15 μg) from *uvr8-1* Arabidopsis plants expressing UVR8_{pro}GFP-UVR8 or UVR8_{pro}GFP-ΔNLSUVR8 (three independent lines) grown in white light (100 μmol m⁻² s⁻¹). A GFP antibody was used to probe the western blot and ponceau stain of rubisco large subunit (rbcL) was used as a loading control.

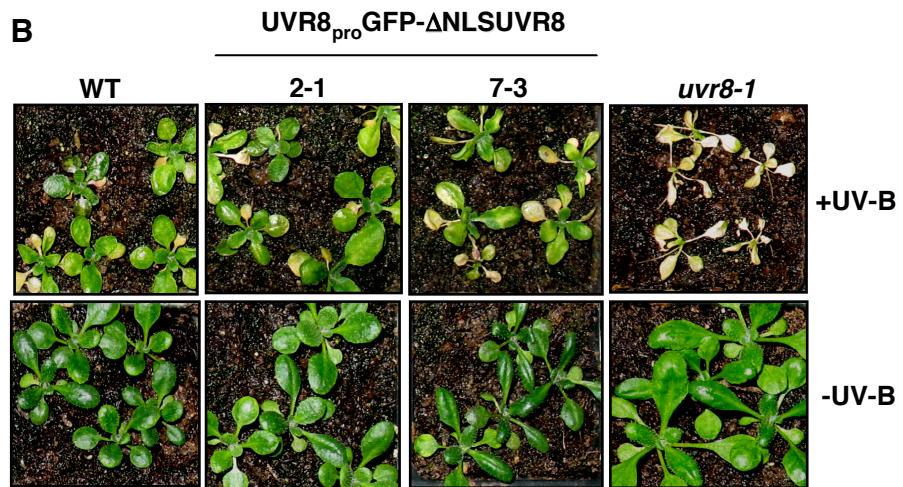
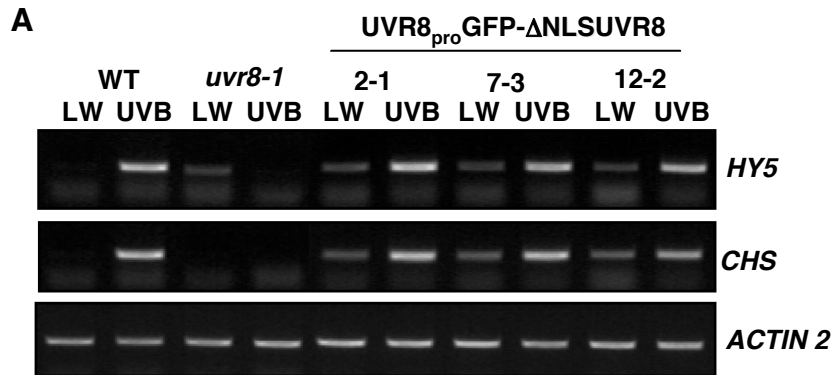


Figure 5.11 GFP- Δ NLSUVR8 is functional in *uvr8-1* transgenic plants

(A) RT-PCR analysis of *HY5*, *CHS* and control *ACTIN2* transcripts in wild-type, *uvr8-1* and UVR8_{pro}GFP- Δ NLSUVR8 lines grown in a low fluence rate of white light (20 $\mu\text{mol m}^{-2} \text{s}^{-1}$; LW) for 3 weeks and exposed to UV-B (3 $\mu\text{mol m}^{-2} \text{s}^{-1}$) for 4 h. (B) UV-B sensitivity assay. UVR8_{pro}GFP-UVR8, UVR8_{pro}GFP- Δ NLSUVR8 and *uvr8-1* plants were grown in white light (120 $\mu\text{mol m}^{-2} \text{s}^{-1}$) for 12 days and then exposed (+) or not (-) to UV-B (5 $\mu\text{mol m}^{-2} \text{s}^{-1}$) supplemented with white light (40 $\mu\text{mol m}^{-2} \text{s}^{-1}$) for 24 h. Plants were photographed after return to white light (120 $\mu\text{mol m}^{-2} \text{s}^{-1}$) for 5 days.

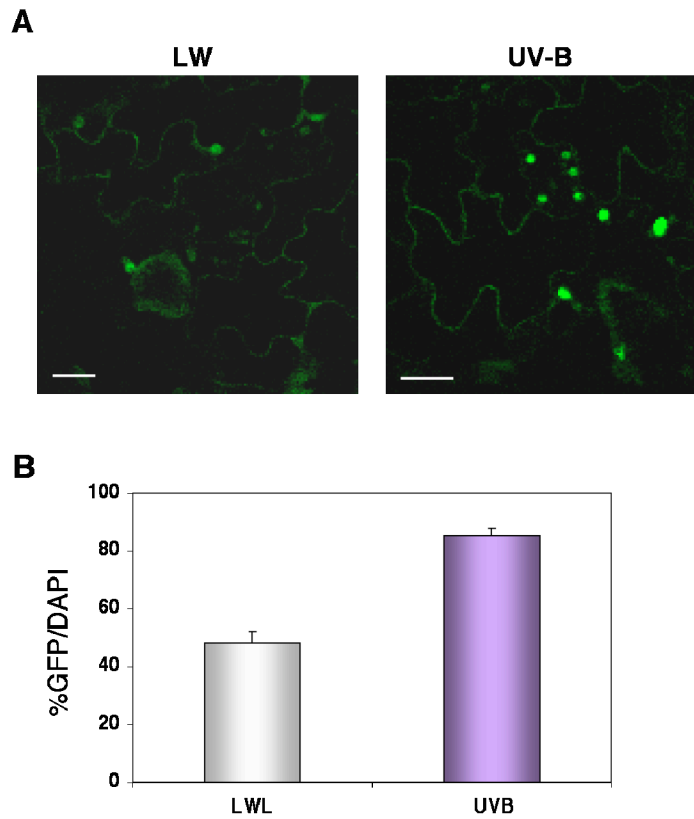


Figure 5.12 UV-B induces nuclear accumulation of GFP- Δ NLSUVR8

(A) Confocal images of GFP in leaf epidermal tissue from UVR8_{pro}GFP- Δ NLSUVR8 transgenic plants (line 2-1) grown in white light ($20 \mu\text{mol m}^{-2} \text{s}^{-1}$; LW) for 12 days and exposed to UV-B ($3 \mu\text{mol m}^{-2} \text{s}^{-1}$) for 4 h. (Scale bar = $20 \mu\text{m}$) (B) The percentage co-localisation of GFP and DAPI fluorescence from UVR8_{pro}GFP- Δ NLSUVR8 transgenic plants grown in white light ($20 \mu\text{mol m}^{-2} \text{s}^{-1}$; LW) and exposed to UV-B ($3 \mu\text{mol m}^{-2} \text{s}^{-1}$) for 4 h. Data are the mean \pm S.E.; n = 20.

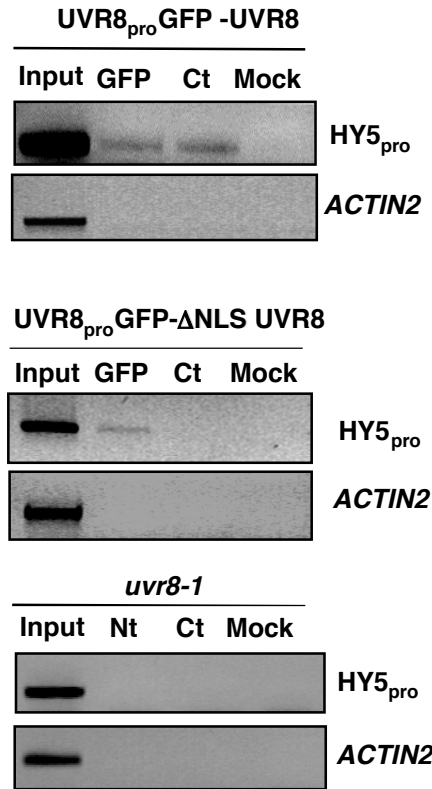


Figure 5.13 GFP-ΔNLSUVR8 is associated with the promoter region of *HY5*

Chromatin immunoprecipitation assay of DNA associated with GFP-UVR8 or GFP-ΔNLSUVR8. PCR of *HY5* promoter (-331 to +23) and *ACTIN2* DNA from UVR8_{pro}GFP-UVR8 (upper) UVR8_{pro}GFP-ΔCUVR8 and *uvr8-1* (lower) transgenic plants grown in white light ($100 \mu\text{mol m}^{-2} \text{s}^{-1}$) and exposed to UV-B ($3 \mu\text{mol m}^{-2} \text{s}^{-1}$) for 4 h: lane 1, input DNA before immunoprecipitation; lane 2, DNA immunoprecipitated by using GFP antibody or N-terminal UVR8 antibody (for *uvr8-1*), lane 3, DNA immunoprecipitated by using C-terminalUVR8 antibody, lane 4, Mock (no antibody) control.

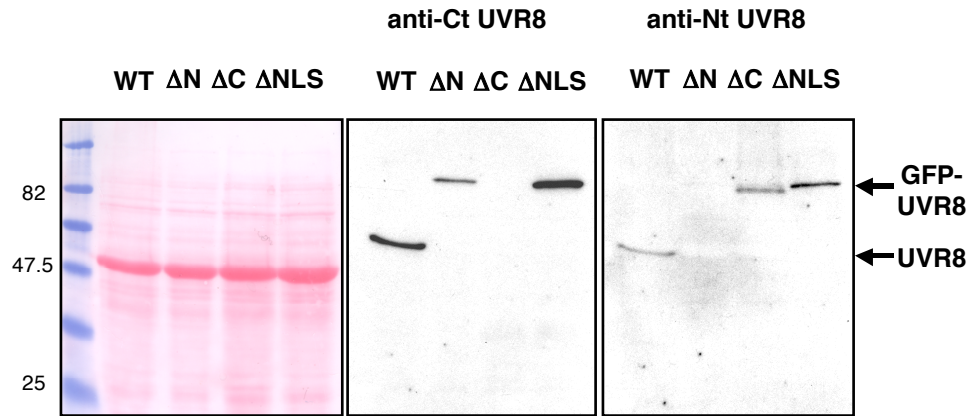


Figure 5.14 Specificity of UVR8 antibodies

Western blot of total protein extracts (20 μg) from *uvr8-1* transgenic Arabidopsis plants expressing UVR8_{pro} GFP-UVR8 (WT), UVR8_{pro} GFP- ΔNUVR8 , UVR8_{pro} GFP- ΔCUVR8 or UVR8_{pro} GFP- $\Delta\text{NLSUVR8}$ grown in white light ($100 \mu\text{mol m}^{-2} \text{s}^{-1}$) for 12 days. Anti-C-terminal (middle) and anti-N-terminal (right) UVR8-specific antibodies were used to probe the western blot and ponceau stain of rubisco large subunit (rbcL) was used as a loading control (left).

CHAPTER 6

YEAST-TWO-HYBRID STUDIES FOR THE IDENTIFICATION OF PROTEINS INTERACTING WITH UVR8

6.1 Introduction

The aim of the current chapter is to characterise the signal transduction pathway upstream or downstream of UVR8 in response to UV-B. The approach employed is based on the identification of direct UVR8-protein interactions using the yeast-two-hybrid system. UVR8 is used as the bait in order to isolate interacting partners from an Arabidopsis cDNA library. Furthermore, a directed method is used to examine whether specific light signalling components directly interact with UVR8, when co-expressed in yeast. Finally, a proteomic approach is developed involving GFP-UVR8 protein purification from Arabidopsis tissue, valuable for future isolation of protein complexes associated with UVR8.

6.2 UVR8 used as a bait protein in the yeast-two-hybrid system

The yeast-two-hybrid system, originally developed by Fields and Song (1989), is a widely used molecular genetic approach for identifying and characterising protein-protein interactions *in vivo* (Causier and Davies, 2002). The system used in this study is based on the fusion of the DNA binding domain (BD) of the yeast GAL4 transcription factor to UVR8 (bait protein) and the GAL4 activation domain (AD) to the putative prey protein(s) expressed in the form of a cDNA library or a clone (prey). Reconstitution of the full-length GAL4 transcription factor is only possible if GAL4BD-UVR8 associates with GAL4AD-X protein. Evidence for an interaction is demonstrated by the expression of a number of reporter genes, which are induced only

when the GAL4 transcription factor is active, thus the binding domain and the activation domain are united via the interacting proteins. The ProQuest™ Two Hybrid System (Clontech) used for this study involves the expression of three reporter genes, *HIS3*, *URA3* and *lacZ*, all integrated stably in the yeast genome. All three reporter genes are controlled by independent promoters containing the GAL4 binding region, thus reducing the possibility of false positives. In case of a positive interaction, the expression of *HIS3* and *URA3* allows yeast cell growth on medium lacking the respective amino acids. Furthermore, the existence and the strength of a protein-protein interaction can be monitored by the third reporter gene, *lacZ*, which produces a blue colour when assayed with X- α -gal. The vectors containing the GAL4BD-bait and GAL4AD-prey constructs are selected based on *Trp*⁻ and *Leu*⁻ auxotrophic selection, respectively in the appropriate yeast strains.

In order to establish if UVR8 is suitable to be used as the bait protein in the yeast-two-hybrid system, the vector pGBKT7 containing the BD-UVR8 fusion, was transformed and expressed in yeast (strains MaV203 and AH109). To test if BD-UVR8 protein can be expressed and is stable in yeast immunoblot analysis was carried out on total yeast protein extracts. A protein of the expected molecular mass using an anti-UVR8 antibody was detected (Figure 6.1). A different protein p53 expressed from the same vector shows no cross-reaction with the UVR8 antibody, thus confirming the authenticity of BD-UVR8 protein expression (Thukral *et al*, 1994).

Subsequently, an auto-activation test was performed to assess if BD-UVR8 can induce the expression of the reporter genes in the absence of an interaction with a protein fused to the GAL4 activation domain. Figure 6.2 shows the cell growth of yeast on non-selective medium (selective only for the vectors) or selective medium for the reporter genes, when BD-UVR8 and AD are co-expressed. It is evident that there is yeast cell growth on the medium lacking *Trp*⁻ and *Leu*⁻, thus the transformation has been successful. However, there is neither yeast cell growth nor blue colour produced on selective medium for the expression of the reporter genes, suggesting that UVR8 cannot auto-activate the system in the absence of an interacting partner. Positive

(vectors expressing known interacting proteins) and negative (empty vectors) controls are also included to confirm the viability of the system and the selection.

Specific yeast strains, such as MaV203, express basal levels of the *HIS3* reporter gene, which increases the sensitivity of the assay, so as to detect very weak protein interactions. However, for eliminating false positive interactions further stringency can be achieved by suppressing *HIS3* activity. The chemical 3-Amino-1, 2, 4-Triazole (3AT) can act as a specific inhibitor of *HIS3* in a dose-dependent manner. For this reason, titrations of 3AT in the selective medium lacking His is necessary in order to determine the threshold at which weak interactions can be detected but neither the bait protein (UVR8) co-transformed with the empty vector nor the empty vectors (negative control) exhibit cell growth, which would lead to growth in the absence of an interaction. Figure 6.3 describes this test and shows that 25 mM is the minimum concentration of 3AT needed for the detection of positive interactions and the elimination of the false positive ones.

6.3 Screening of an Arabidopsis cDNA library for identification of UVR8 interacting partner(s)

A large-scale approach to screen a significant population of proteins for interacting partners is possible by subsequent or simultaneous yeast transformation of the vector expressing the bait protein and the cDNA library from the tissue of interest. Since UVR8 can be expressed in yeast at sufficient protein levels and does not auto-activate transcription of the reporter genes, it is suitable to act as a bait protein for preying on peptide sequences encoded by the cDNA library screened.

In this study, two cDNA libraries were used, both supplied by the Arabidopsis Stock Centre. The mRNA required for the generation of the cDNA libraries derived from three-day old etiolated Arabidopsis seedlings or from light grown mature tissue. Each cDNA fragment of 600 to 2500 bp was fused to the GAL4 activation domain. Initially the cDNA library derived from light-grown tissue was screened, as UVR8 is a

light signalling component. However, isolation and sequencing of a cDNA clone that resulted in yeast growth and thus to a putative interaction with UVR8, showed that all fragments were less than 200 bp, contained large parts of the vector (pACT) instead of the Arabidopsis genome and most were out of frame. Independent screens with this library were performed in other labs using different bait proteins obtained similar results.

Since, UVR8 is abundant in darkness, under all light conditions and throughout the life cycle of Arabidopsis (Chapter 3), the second library originating from dark-grown tissue was also screened for interacting partners. Co-transformation of the pGBKT7 vector containing UVR8 and the cDNA library was performed in competent yeast cells of the strain MaV203 according to supplier's instructions (Invitrogen). Two independent screens with the latter cDNA library were carried out. Although the transformation efficiency of both screens was adequate (approximately 8×10^6), and the stringency of the assay sufficient, there were 15 clones isolated, of which none proved to be a real positive interacting partner for UVR8; either the induction of the transcription of the reporter genes was not reproducible when re-transformed with BD-UVR8, or the isolated clone was auto-activating the system in the absence of UVR8. Data from these screens is not shown, as there was no positive interacting protein isolated or verified for UVR8. The limitations of this approach and the problems encountered will be discussed. In the meantime, a variation of the yeast-two-hybrid approach employed will be described in the next section.

6.4 UVR8 used as the bait in a directed yeast-two-hybrid approach

Since the screening of Arabidopsis cDNA libraries for UVR8 protein partners was unsuccessful, a directed yeast-two-hybrid approach was developed. According to this approach, selected light signalling components were tested for a putative interaction with UVR8. The proteins to be examined were selected based on their

localisation, mode of action and their involvement in regulation of light or, in particular, UV-B signalling.

The possibility of a direct interaction between UVR8 and Arabidopsis DE-ETIOLATED 1 (DET1) was examined. DET1 is a nuclear protein, which acts as a repressor of photomorphogenesis (Pepper *et al.*, 1994). Although its exact function remains a mystery, DET1 is thought to regulate gene expression via chromatin remodelling, based on its association with the amino-terminal tails of histone H2B (Benvenuto *et al.*, 2002). Furthermore, biochemical and genetic evidence demonstrates an interaction between DET1 and DDB1 (DAMAGED DNA BINDING PROTEIN 1), which is associated with histone acetyltransferase complexes regulating gene expression (Schroeder *et al.*, 2002). Since UVR8 is a nuclear localised protein that regulates UV-B induced gene expression via chromatin (Brown *et al.*, 2005) and histone association (Cloix and Jenkins, 2007), it was interesting to test if it is part of the same complex as DET1 via a direct interaction. Figure 6.4 shows that when BD-UVR8 and AD-DET1 are co-transformed in yeast (strain AH109), there is cell growth on the non-selective medium (Leu⁻, Trp⁻) but there is no growth on the medium selective for a positive interaction. The positive and the negative controls confirm the activity of the assay.

Another signalling component selected as a candidate for the directed yeast-two-hybrid approach is ELONGATED HYPOCOTYL 5 (HY5). HY5 is a bZIP transcription factor that activates the expression of a number of genes in response to light (Osterlund *et al.*, 2000). Recent evidence has shown that HY5 also controls the induction of gene expression in response to UV-B (Ulm *et al.*, 2004). Brown and co-workers have demonstrated that UVR8 regulates *HY5* gene expression in a UV-B dependent manner by associating with the *HY5* promoter region (2005), suggesting that both UVR8 and HY5 act in the same signal transduction pathway, with the latter acting downstream of the former. To test if UVR8 transmits the UV-B signal to HY5 via a direct interaction, both proteins fused to the binding or the activation domain of GAL4 transcription factor were co-expressed in yeast. However, no interaction was observed,

as there was no growth when the transformed yeast cells were plated on selective medium (Figure 6.4).

Another light signalling component tested for UVR8 association is the negative regulator of photomorphogenesis CONSTITUTIVE PHOTOMORPHOGENIC 1 (COP1). COP1 is an E3 ubiquitin ligase that acts as a repressor of light signal transduction by mediating the degradation of HY5 in the nucleus in the absence of light (Osterlund *et al.*, 2000). The ubiquitin ligase activity of COP1 is enhanced via a direct interaction with the DDB1/DET1/COP10 complex and the COP9 signalosome (Yanagawa *et al.*, 2004). Recent evidence, provided by Oravec *et al.* (2006), has shown that COP1 is required for UV-B induced gene expression and photomorphogenesis in Arabidopsis and it exhibits relatively slow nuclear accumulation in response to UV-B only. As UVR8 regulates UV-B induced gene expression and also undergoes UV-B dependent nuclear translocation, it seems highly likely that it could associate with COP1. However, there is no interaction observed between UVR8 and COP1 during co-expression in yeast (Figure 6.5 (A)). To test if COP1 has any effects on the protein levels of UVR8, immunoblot analyses were carried out on protein extracts from wild-type (*Ler* and *Col*), *cop1-4* and *uvr8* mutant Arabidopsis and probed with an anti-UVR8 antibody. Figure 6.5 (B) demonstrates that there are equal levels of UVR8 protein in the presence and in the absence of functional COP1. Thus UVR8 neither interacts directly with COP1, nor is targeted for degradation by COP1.

The brassinosteroid receptor BRI1 was another candidate for UVR8 binding assay in yeast. Brassinosteroids are plant hormones regulating growth development and stress tolerance in Arabidopsis. In particular, BRI1 has been shown to be involved in UV-B regulated gene expression necessary for plant survival (Savenstrand *et al.*, 2004). For this reason the kinase domain of BRI1, which resides in the cytosol, was co-expressed with UVR8 in yeast in order to assess a possible interaction. Once more, no cell growth was observed on the medium selective for a positive interaction (Figure 6.6), therefore UVR8 does not interact with the kinase domain of BRI1 in yeast.

The UV-A/Blue light photoreceptor cryptochrome 2 (*cry2*) was also examined for association with UVR8 in yeast. *Cry2* was selected over *cry1* due to the former's constitutive nuclear localisation (Guo *et al.*, 1999) and ability to associate with chromatin (Lin and Shalitin, 2003). Furthermore, *cry2* has been shown to associate directly with phyB (Mas *et al.*, 2000), which acts as a negative regulator of the UV-B induction of *CHS* expression (Wade *et al.*, 2001). Again, expression of UVR8 and *cry2* in yeast did not result in a positive interaction between the two proteins (Figure 6.6). PhyB and DDB1 were also candidates for the directed yeast-two-hybrid approach for identifying partners for UVR8. However, due to time limitation neither of the proteins was tested for interaction. Although all the results obtained from this approach are negative, it is possible that the proteins tested may interact indirectly with UVR8 *in planta*. Therefore, a different system based on immunoprecipitation of UVR8 and the associated proteins from plant tissue is required.

6.5 Purification of GFP-UVR8 *in planta*

An alternative experimental approach for identifying interacting partners for UVR8 involves the purification of UVR8 along with any other protein complexes associated with it. The first step was to develop a purification system that obtains sufficient UVR8 protein levels for visualisation on a stained SDS protein gel, in the absence of antibodies. To achieve this, total protein extracted from *uvr8* transgenic plants expressing GFP-UVR8 from the UVR8 promoter was purified by passing through a magnetic resin. The purified fraction was eluted from the beads and loaded on a denaturing protein gel. In order to visualise the purified protein, the protein gel was silver-stained. Figure 6.7 (A) shows that GFP-UVR8 can be detected on the stained gel at the expected size. A protein extract from plants over-expressing GFP was used as a control, showing that the purified protein is the appropriate size for GFP and there is no band of the size of GFP-UVR8 (Figure 6.7 (A)). Furthermore, a western blot was performed on a small aliquot from the extracted protein before the purification

and was probed with an anti-GFP antibody, so as to confirm the identity of the bands observed on the silver-stained gel (Figure 6.7 (B)).

The advantage of this method over the yeast-two-hybrid approach is mainly the fact that the experiments are performed *in planta*, where UVR8 is in its physiological context. However, significant UVR8 protein concentration is required in order to visualise it on a silver or coomassie-stained gel and to further proceed with proteomic analysis. Scaling up of this purification procedure is necessary for identification of possible UVR8-associated proteins by mass spectrometry.

6.6 Discussion

UVR8 is a key component of the UV-B signal transduction pathway and regulates the expression of genes essential for UV-protection and photomorphogenesis (Brown *et al.*, 2005). Although the function of UVR8 is involved with chromatin association and histone binding in the promoter regions of genes induced by UV-B (Cloix and Jenkins, 2007), there is no evidence for the exact mechanism of UVR8 action. As a means of understanding further how UVR8 responds to UV-B and stimulates gene expression, a number of approaches were used or developed aiming to identify interacting partners. Yeast-two-hybrid library screening and directed yeast-two-hybrid were both unsuccessful in the isolation of UVR8 protein partners. However, the purification of GFP-UVR8 from Arabidopsis tissue provides a very powerful tool for identifying UVR8 associated protein complexes *in planta*.

6.6.1 The yeast-two-hybrid system was employed for identifying protein partners for UVR8

In order to understand better the role of UVR8 in UV-B signalling, the identification of UVR8-interacting proteins was pursued, which would contribute

valuable information on the mechanism of UV-B dependent nuclear translocation and regulation of gene expression by UVR8. The yeast-two-hybrid is a sensitive, molecular genetic approach and has been extensively used in plant molecular research and in particular light signalling. An elegant example of the potential of the yeast-two-hybrid system was demonstrated by Professor Quail's lab, where both phyA and phyB associate with PIF3 (PHYTOCHROME-INTERACTING FACTOR 3), which is an important component in phytochrome signal transduction in *Arabidopsis* (Ni *et al.*, 1998). Another example determined by the yeast-two-hybrid system is the interaction of both cry1 and phyB with components of the circadian clock (Jarrillo *et al.*, 2001).

UVR8 was used as the bait protein for screening *Arabidopsis* cDNA libraries by the yeast-two-hybrid approach. Although UVR8 fulfils the criteria for being used in the yeast-two-hybrid system, as it can be expressed in yeast and does not auto-activate any of the reporter genes in the absence of a positive interaction, unfortunately no clones were identified coding for UVR8 interacting proteins. The reasons why the system did not provide any results for UVR8 vary. Since none of the initial positive interactions was reproducible, there did not seem to be excessive stringency that would not allow the identification of possible interactions. Furthermore, the transformation efficiency of the yeast cells with the library and the bait was sufficient to isolate interacting proteins, based on studies done by members of other labs (data not shown). A possibility explaining why no UVR8-interacting proteins were identified is that UVR8 could act as a transcriptional repressor. Therefore, even if an interaction occurred, it would not be possible to monitor, as the expression of the reporter genes would be repressed. If this is the case it would be very interesting to investigate in what way UVR8 functions as a positive regulator of gene expression and if this would mean that it suppresses the action or the expression of a negative regulator in response to UV-B.

6.6.2 UVR8 fails to interact with specific light signalling components

Since “fishing” an Arabidopsis cDNA library for isolating UVR8-protein partners was unfruitful, a directed yeast-two-hybrid approach was employed. The main questions for UVR8 function and activity are focused on the mechanism involved in its UV-B induced nuclear import and regulation of gene expression. An example where similar questions were addressed by directed yeast-two-hybrid studies includes the direct interaction between phyA and FHY1, which confers the nuclear accumulation of the former (Hiltbrunner *et al.*, 2005).

In the case of UVR8, specific proteins that act as components of light signal transduction and whose function could be associated with UVR8, were chosen and were tested for putative interaction with UVR8. In Arabidopsis, there are two major classes of photomorphogenesis mutants: the ones demonstrating de-etiolated phenotypes in the absence of light (*cop/det/fus*) and the ones that exhibit a skotomorphogenic phenotype in the presence of a light stimulus, such as *hy5* (Jiao *et al.*, 2007). DET1 has been characterised as a negative regulator of photomorphogenesis and although its exact mechanism of action is not clear yet, it has been shown to involve chromatin remodelling via direct interaction with histone H2B (Pepper *et al.*, 1994; Benvenuto *et al.*, 2002). Furthermore, DET1 is part of a complex containing COP10, COP1 and DDB1, which physically interacts with the COP9 signalosome and components of the proteasome (Yanagawa *et al.*, 2004). COP1 is an E3 ubiquitin ligase, also acting as a repressor of photomorphogenesis by targeting for degradation transcription factors such as HY5 (Osterlund *et al.*, 2000). However, COP1 functions as a positive regulator of UV-B specific responses (Oravecz *et al.*, 2006). In addition, COP1 exhibits nuclear accumulation in response to a 24-hour UV-B treatment and the *cop1* mutant shows increased sensitivity to UV-B irradiation (Oravecz *et al.*, 2006). On the contrary, HY5 is a bZIP transcription factor, which induces the expression of white light and UV-B regulated genes (Osterlund *et al.*, 2000; Ulm *et al.*, 2004; Brown *et al.*, 2005). HY5 is positively regulated by UVR8 at the mRNA level in a UV-B dependent manner via a chromatin association of UVR8 on the *HY5* promoter and within the *HY5*

gene region (Brown *et al.*, 2005; Cloix and Jenkins 2007). Since UVR8 is a nuclear protein that regulates UV-B induced gene expression via chromatin association, its direct interaction with the HY5 transcription factor and the chromatin and proteasomal complex associated proteins DET1 and COP1 was examined. Unfortunately, no interaction was observed with UVR8 (Figures 6.4 and 6.5 (A)), even though there was evidence that UVR8, HY5 and COP1 share mutant phenotypes in terms of their hypersensitivity to higher than ambient levels of UV-B (Brown *et al.*, 2005; Oravec *et al.*, 2006).

The UVA/blue light photoreceptor cry2 was also examined for UVR8 binding, although there is no direct correlation between cry2 and UVR8 function or mutant phenotypes. However, cry2 is a constitutively nuclear photoreceptor that associates with chromatin and regulates gene expression by integrating red and UV-A/blue light induced signalling via an interaction with phyB (Lin and Shalitin, 2003). Also, phyB has been shown to have an inhibitory role in the UV-B induction of *CHS* gene expression (Wade *et al.*, 2001), so whether cry2 is the intermediate for the phyB-regulated inhibition of UVR8 regulated gene expression was tested. Figure 6.6 shows that this hypothesis is unlikely based on co-expression of the two proteins in yeast.

Finally, the brassinosteroid receptor BRI1 was examined for directly associating with UVR8. The integration of brassinosteroid and light signalling pathways is based on the association of BRASSINAZOLE RESISTANT 1 (BZR1) with the promoter region of the *CONSTITUTIVE PHOTOMORPHOGENESIS AND DWARFISM (CPD)* gene (Li, 2005). More relevant to this study, however, is the involvement of BRI1 in UV-B induced gene expression, as the brassinosteroid mutants (*bri1*, *det2*, *dim1* and *cpd*) were reported to show a decrease in the UV-B dependent induction of *CHS* expression (Savenstrand *et al.*, 2004). BRI1 is a leucine-rich-repeat (LRR) receptor-like kinase (RLK) that undergoes heterodimerisation and activation via trans-phosphorylation and signal propagation in response to brassinosteroids (Li, 2005). The possibility that BRI1 could act as the UV-B photoreceptor is likely, since in mammalian cells, receptor tyrosine kinases (RTK) dimerise and undergo autophosphorylation upon ligand binding and trigger phosphorylation cascades, which

are involved in UV-induced signalling (Devary *et al.*, 1992). If this is the case for plants, then activated BRI1 could transmit the signal to UVR8 through its cytosolic kinase domain. This possibility was assayed by the yeast-two-hybrid system, and once again, there was no interaction observed between UVR8 and BRI1 kinase (Figure 6.6).

In summary, the yeast-two-hybrid was unsuccessful in identifying an interaction between UVR8 and specific light signalling components. Whether the possibility that UVR8 acts as a suppressor of reporter gene expression is the reason that masks any putative interaction, or simply UVR8 does not interact with any of the proteins tested in yeast cannot be concluded. However, it cannot be excluded that any of these proteins may be associated with UVR8 in an indirect manner and they co-exist in the same protein complex. As this would not be possible to examine in yeast, a different approach is required.

6.6.3 Purification of UVR8_{pro}GFP-UVR8 from Arabidopsis provides a tool for identifying UVR8-containing protein complexes

An alternative way to identify interacting proteins is to biochemically purify UVR8 along with any protein complex associated with it. In order to develop this system, it is required to optimise the conditions for the purification of the protein of interest. In our case, the best possible way to achieve this is to use total protein extract from the characterised transgenic plants expressing GFP-UVR8 under the control of the native promoter. Purification of GFP-UVR8 was made possible by applying specific GFP-binding magnetic beads (μ MACS) to the plant protein extract. As a result, only the proteins associated with GFP-UVR8 would bind the beads and be isolated enabling their subsequent visualisation on a stained denaturing protein gel. Although the experiment was performed in relatively small scale, a band of the predicted size for UVR8 can be distinguished on the silver-stained protein gel (Figure 6.7 (A)) and its identity is confirmed by immunoblot analysis (Figure 6.7 (B)). Scaling-up of the experimental procedure and better separation of the proteins obtained from

the purification is essential for identifying specific proteins that co-immunoprecipitate with UVR8 by mass spectrometry and proteomic analyses. An indication that the system is effective is given by Cloix and Jenkins (2007), where they have shown that GFP-UVR8 co-immunoprecipitates with specific histone variants (2007). Furthermore, preliminary data obtained from size exclusion chromatography (SEC) demonstrates that native UVR8 is found in fractions corresponding to 500 kDa and 47.5 kDa, suggesting that UVR8 is a component of a large protein complex (personal communication with Dr. Catherine Cloix).

Co-immunoprecipitation studies have proved very successful for the identification of interacting proteins within a complex. For example the COP10-containing complex was purified by immunoprecipitation and its components were identified by SEC (Yanagawa *et al.*, 2004). An alternative approach was employed for the characterisation of the nuclear hexokinase1 complex, which is involved in glucose signalling. In this case the hexokinase receptor 1 (HXK1) was purified by immunoprecipitation based on its fusion tag. The co-immunoprecipitated proteins were identified by MALDI-TOF MS after their separation on a denaturing protein gel (Cho *et al.*, 2006). Equivalent approaches can be employed for the identification a UVR8 associated protein complex in the absence or presence of a UV-B stimulus, so as to understand in more detail how UVR8 functions and, if possible, identify the UV-B receptor.

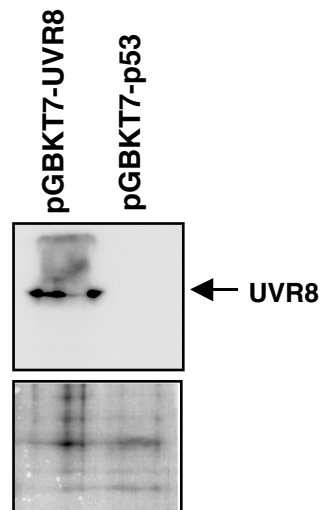


Figure 6.1 Expression of UVR8 in yeast

Western blot of total protein extracts (50 μ g) from yeast strain AH109 expressing UVR8 or p53. The western blot was probed with the C-terminal UVR8 antibody and a Ponceau stain of total protein (lower panel) was used as a loading control.

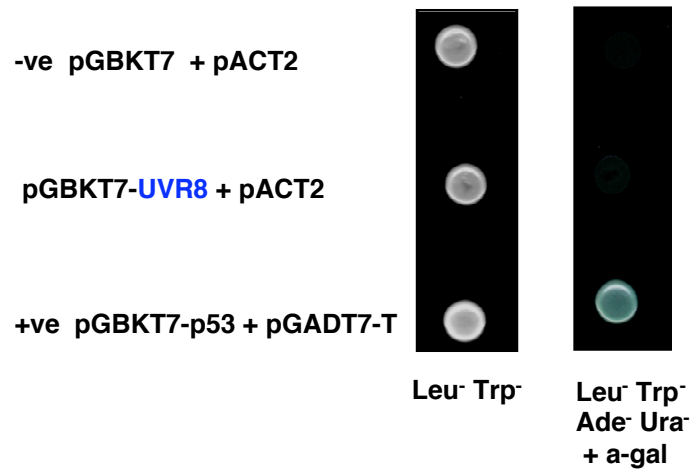


Figure 6.2 Autoactivation test of UVR8 in yeast

Cell growth of yeast strain AH109 transformed with pGBKT7 and pACT (empty vectors as negative control), pGBKT7-UVR8 and pACT (test bait protein and empty vector) or pGBKT7-p53 and pGADT7-T (interacting proteins as positive control) on selective media for the vectors only (Leu⁻, Trp⁻) or for interactive proteins (Leu⁻, Trp⁻, Ade⁻, Ura⁻ and a-gal).

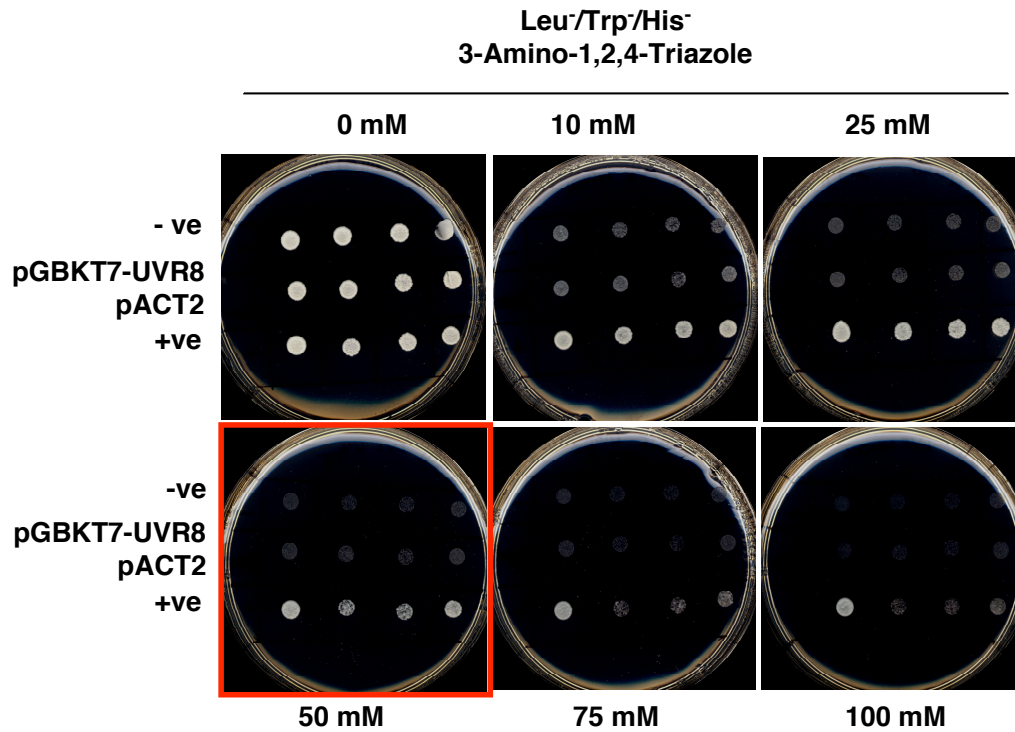


Figure 6.3 Titration test of 3-Amino-1, 2, 4-Triazole concentration as a His⁻ reporter marker

Cell growth of yeast strain MaV203 transformed with pGBKT7 and pACT (empty vectors as negative control), pGBKT7-UVR8 and pACT (test bait protein and empty vector) or pGBKT7-p53 and pGADT7-T (interacting proteins as positive control) on selective medium for interacting proteins (Leu⁻, Trp⁻, His⁻) with added various concentrations of 3AT (0, 10, 25, 50, 75, 100 mM). The lowest 3AT (25 mM) concentration for which there is no growth for neither the test protein nor the negative control, after 3–4 days at 30 °C was chosen for screening cDNA libraries for interacting partners for UVR8.

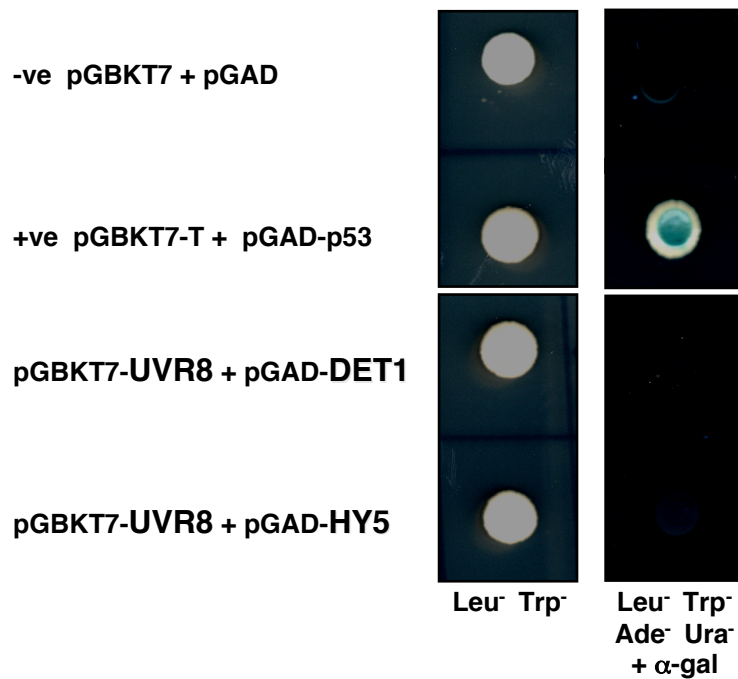


Figure 6.4 UVR8 does not interact with either DET1 or HY5 in yeast

Cell growth of yeast strain AH109 transformed with pGBKT7 and pACT (empty vectors as negative control), pGBKT7-UVR8 and pGAD-DET1 (test bait and prey proteins) pGBKT7-UVR8 and pGAD-HY5 (test bait and prey proteins) or pGBKT7-p53 and pGADT7-T (interacting proteins as positive control) on selective media for the vectors only (Leu⁻, Trp⁻) or for interacting proteins (Leu⁻, Trp⁻, Ade⁻, Ura⁻ and α -gal).

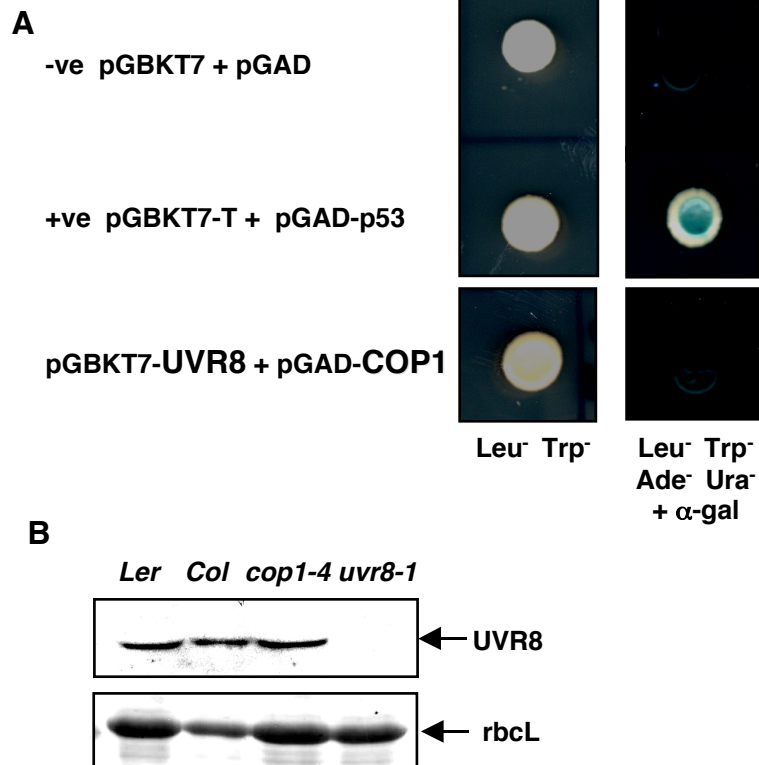


Figure 6.5 UVR8 does not interact with COP1 in yeast and is not degraded via COP1 in Arabidopsis

(A) Cell growth of yeast strain AH109 transformed with pGBKT7 and pACT (empty vectors as negative control), pGBKT7-UVR8 and pGAD-COP1 (test bait and prey proteins) pGBKT7-UVR8 or pGBKT7-p53 and pGADT7-T (interacting proteins as positive control) on selective media for the vectors only (Leu⁻, Trp⁻) or for interacting proteins (Leu⁻, Trp⁻, Ade⁻, Ura⁻ and α-gal). (B) Western blot of total protein extracts (15 μg) from Arabidopsis *Ler*, *Col*, *cop1-4* or *uvr8-1* transgenic plants grown in white light. The C-terminal UVR8 antibody was used to probe the western blot and ponceau stain of rubisco large subunit (rbcL) was used as a loading control.

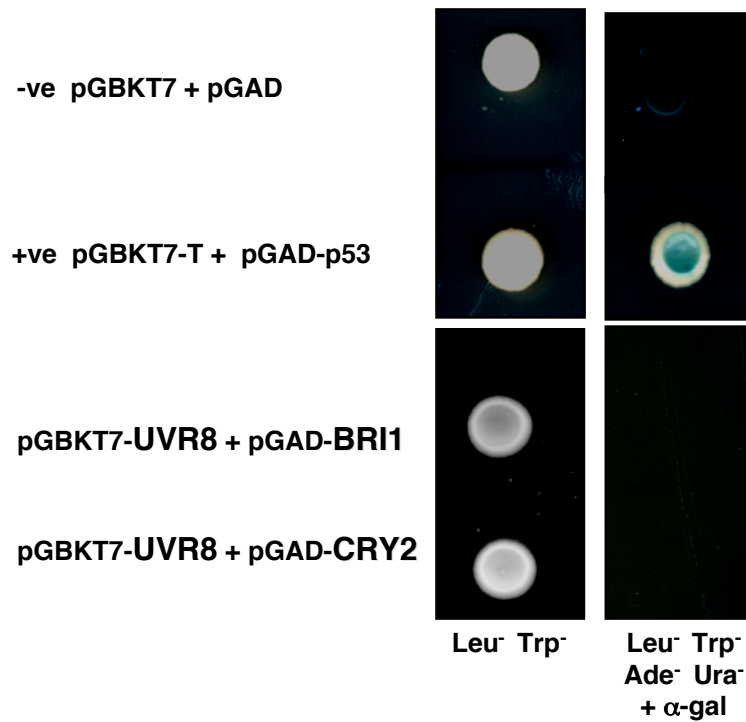


Figure 6.6 UVR8 does not interact with either BRI1 kinase or CRY2 in yeast

Cell growth of yeast strain AH109 transformed with pGBKT7 and pACT (empty vectors as negative control), pGBKT7-UVR8 and pGAD-BRI1 (test bait and prey proteins) pGBKT7-UVR8 and pGAD-CRY2 (test bait and prey proteins) or pGBKT7-p53 and pGADT7-T (interacting proteins as positive control) on selective media for the vectors only (Leu⁻, Trp⁻) or for interacting proteins (Leu⁻, Trp⁻, Ade⁻, Ura⁻ and α -gal).

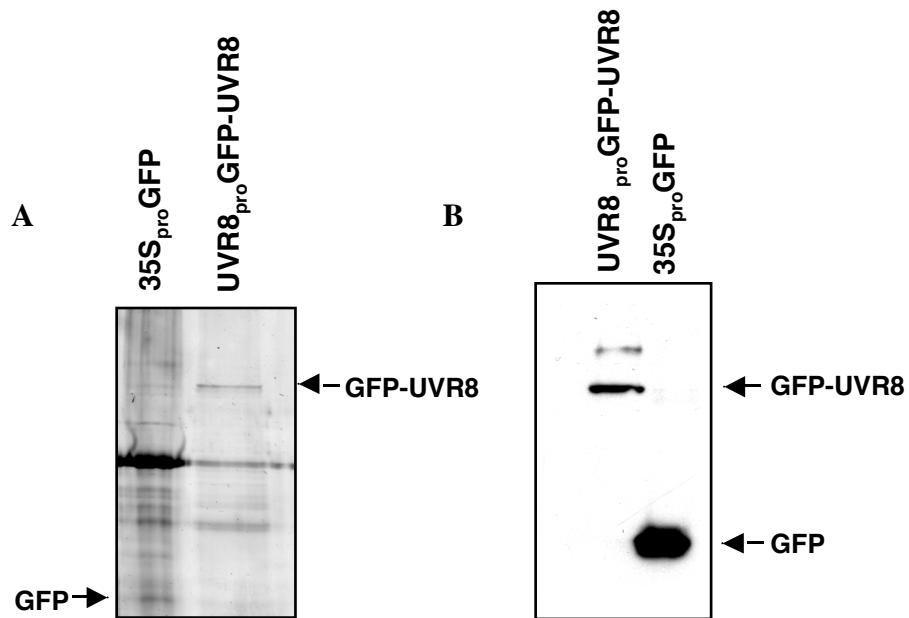


Figure 6.7 GFP-UVR8 can be immunoprecipitated and detected on a silver-stained protein gel

(A) Silver-stained SDS-PAGE gel of immunoprecipitated proteins based on a magnetic GFP-binding system of total soluble protein extract (500 mg) from UVR8_{pro}GFP-UVR8 or 35S_{pro}GFP transgenic Arabidopsis grown in white light (B) Western blot of total protein extracts (10 μg) before the immunoprecipitation of UVR8_{pro}GFP-UVR8 or 35S_{pro}GFP transgenic plants. An anti-GFP antibody was used to probe the western blot.

CHAPTER 7

FINAL DISCUSSION

7.1 Introduction

UV-B is an integral component of natural sunlight, therefore UV-B induced development and photo-protection is essential for plant survival (Brown *et al.*, 2005). UVR8 is a fundamental UV-B specific signalling component, which regulates acclimation responses stimulated by non-damaging levels of UV-B in Arabidopsis (Kliebenstein *et al.*, 2002; Brown *et al.*, 2005). The function of UVR8 is primarily focused on the regulation of gene expression most likely at the transcriptional level. Evidence is provided by microarray analyses showing that UVR8 regulates a number of genes, the majority of which are implicated in flavonoid biosynthesis, DNA-damage repair, photo-protection and photomorphogenesis (Brown *et al.*, 2005). Furthermore, chromatin immunoprecipitation studies have shown that UVR8 controls gene expression by associating with chromatin via histones in the promoter and the gene region of *HY5* and other genes (Brown *et al.*, 2005; Cloix and Jenkins, 2007).

Although the importance of UVR8 and the transcriptional events necessary for plant survival are well characterised (Kliebenstein *et al.*, 2002; Ulm *et al.*, 2004; Brown *et al.*, 2005), there seems to be limited information on the mechanism underlying signal perception, transmission and UVR8 activation in response to UV-B. For this reason, the effects of light, and in particular UV-B, on UVR8 protein and its localisation were examined, as a means of providing information for the understanding of the early events involved in UV-B signalling and UVR8 activation in Arabidopsis. Furthermore, the yeast-two-hybrid approach was employed for identifying protein partners for UVR8, in order to obtain information on the signalling components acting upstream, downstream or in concert with UVR8 to mediate UV-B signal transduction.

7.2 UV-B stimulates rapid nuclear accumulation of UVR8

In this study, the production of UVR8 specific antibodies raised against the N or the C-terminus of the protein enabled detailed characterisation of UVR8 protein at different developmental stages, in various plant organs and in response to different qualities and quantities of light stimuli. Immunoblot analyses show that UVR8 protein is ubiquitously distributed within the plant and throughout its development. Furthermore, the abundance of UVR8 protein is independent of light intensity and light quality, including long exposure to UV-B irradiation. It has also been shown that UVR8 gene expression is unaffected by UV-B, although UVR8 induces the transcription of a number of genes in a UV-B dependent manner (Kliebenstein *et al.*, 2002; Brown *et al.*, 2005). The widespread and constitutive distribution of UVR8 demonstrates the importance of this protein for protecting the whole plant against the adverse effects of UV-B irradiation on plant growth during various developmental stages.

Although light in general has no effect on total UVR8 protein abundance, sub-cellular localisation studies performed in this study show that the nucleo-cytoplasmic distribution of the protein is altered specifically in response to UV-B irradiation. Stable transgenic *Arabidopsis* lines expressing GFP-UVR8 from the *UVR8* promoter in the *uvr8-1* mutant background, show that GFP-UVR8 resides both in the nucleus and in the cytosol in all light conditions and in all tissues examined. The functionality of the construct was determined based on complementation analyses of the induction *HY5* and *CHS* in response to UV-B in the *uvr8-1* mutant background. However, when plants were exposed to low fluence rates of UV-B, GFP-UVR8 exhibited increased nuclear accumulation compared to plants that had not been exposed to UV-B. This phenomenon has also been confirmed for native UVR8 in wild-type plants by a biochemical approach involving nuclear and cytosolic protein fractionation analysis. The UV-B induced nuclear accumulation of UVR8 does not seem to follow a circadian pattern of regulation (data not shown), however, kinetic and fluence rate dependence

studies have shown that this response occurs rapidly, within 5 min of UV-B irradiation ($3 \mu\text{mol m}^{-2} \text{s}^{-1}$), and at fluence rates as low as $0.1 \mu\text{mol m}^{-2} \text{s}^{-1}$.

The significance of this finding is that it provides novel information on the mechanism inducing UV-B signal transduction via UVR8 in *Arabidopsis*. Although an analogous light-induced nuclear enrichment event has been observed for major light signalling components, like the photoreceptors phyA, phyB and cry1, it is the first time that a UV-B signalling component demonstrates UV-B specific nuclear accumulation in *Arabidopsis* (Sakamoto and Nagatani, 1996; Kircher *et al.*, 1999; Yang *et al.*, 2000). However, UV-B induced nuclear accumulation has been previously observed in mammalian cell culture systems. Ultra-violet irradiation elicits early and late signalling events involving post-translational modifications and nucleo-cytoplasmic partitioning leading to the induction of gene expression in mammalian cells (Bender, *et al.*, 1997). In particular, UV-B induces the phosphorylation and nuclear accumulation of the Fyn kinase, which is a member of the non-receptor protein tyrosine kinase Src family (He *et al.*, 2005). Fyn kinase is responsible for the phosphorylation of H3 at Ser 10, which induces chromatin relaxation and consequently induction of gene expression during interphase (He *et al.*, 2005). Another mammalian UV-B signalling component, NF- κ B, has also been shown to undergo activation and nuclear translocation in response to UV-B. Unlike other UV-B activated proteins that reside in the nucleus, studies on enucleated cells have shown that the UV-B dependent activation of NF- κ B is triggered by cytoplasmic signals, suggesting that it is not a response induced by DNA-damage (Brenneisen *et al.*, 2002). Furthermore, the mammalian transcription factor Nrf2, which induces the expression of antioxidant proteins in response to chemical stress, shows a fluence dependent nuclear import in response to UV-B (Sankaranarayanan and Jaiswal, 2006). In particular, low levels of UV-B induce nuclear accumulation of Nrf2, whereas high levels of UV-B lead to its nuclear exclusion (Sankaranarayanan and Jaiswal, 2006).

These data indicate that UV-B may trigger fluence-dependent responses divided in photo-protective responses to low fluence rate UV-B and non-specific stress responses to high fluence rate UV-B in mammalian systems similar to plant systems.

Whether, high levels of UV-B irradiation are perceived in the nucleus and trigger stress responses, such as cell cycle arrest, and whether low fluence rate UV-B signalling that induces photoprotective responses, such as biosynthesis of vitamin D and defensin, is initiated in the cytoplasm is not clear yet (Krutmann, 2006). In any case, UV-B signal transduction in mammalian systems could provide evidence for the understanding of UV-B induced signalling in *Arabidopsis* and other higher plants and *vice versa*.

7.3 What is the mechanism underlying the UV-B induced nuclear accumulation of UVR8?

Nucleo-cytoplasmic partitioning and nuclear translocation of proteins involve mechanisms that are highly conserved between animal and plant systems and provide a very elegant way of rapidly regulating gene expression in response to a plethora of environmental stimuli (Yamamoto and Deng, 1999; Merkle, 2004). The general principle of nuclear transport requires either passive diffusion of proteins of small molecular mass, or facilitated transport of larger molecules by nuclear importin or exportin proteins depending on the signal peptide of the cargo proteins (Merkle, 2004). Receptor-substrate (cargo) recognition is achieved either by the existence of a nuclear localisation or nuclear export signal (NLS or NES) on the surface of the cargo protein. Furthermore, post-translational modifications (phosphorylation, de-phosphorylation), protein-protein interactions, conformational changes or protein anchoring can regulate nuclear translocation by facilitating or preventing the cargo-receptor protein association (Merkle, 2004).

In plants, the light-induced nuclear translocation mechanism of the red/far-red photoreceptors phytochrome A and B has been extensively investigated and has revealed that intramolecular masking of the NLS peptide of phyB and intermolecular association of phyA with the FHY1 and FHL adaptor proteins are the main mechanisms regulating nuclear import in response to light (Chen *et al.*, 2005; Hiltbrunner *et al.*, 2006).

In the case of UVR8, there is no classic NLS peptide contained within its sequence, apart from a very short basic peptide at the extreme C-terminus of the protein. Generation of transgenic plants expressing a GFP-tagged version of UVR8 lacking the putative NLS peptide (GFP- Δ NLSUVR8) showed that this sequence is not necessary for nuclear localisation, suggesting that a different mechanism must operate in order to target UVR8 in the nucleus.

Further investigations on the mechanism involved in UV-B dependent nuclear accumulation of UVR8 were carried out using various experimental approaches. The first approach involved the restriction of UVR8 in either the cytosol or the nucleus of the cells at all times. This was achieved by generating stable transgenic Arabidopsis lines expressing GFP-UVR8 fused to either a NLS or a NES signal peptide at the N-terminus of the construct. Sub-cellular localisation studies based on fluorescence microscopy revealed that the NES-GFP-UVR8 and NLS-GFP-UVR8 constructs were successfully retained in the cytosol or in the nucleus respectively. Nevertheless and surprisingly enough, NES-GFP-UVR8 was functional and was able to accumulate into the nucleus in response to very short exposure and very low fluence rates of UV-B. The response was reversed at a much slower rate when plants that had been exposed to UV-B were subsequently transferred to complete darkness for 48 hours.

In order to understand how UV-B could overcome the NES signal peptide, a pharmacological approach was employed. Christie and Jenkins (1996) have demonstrated that protein kinases, protein phosphatases and protein synthesis are required for the UV-B induction of *CHS* in an Arabidopsis cell culture system. Since UVR8 is the key regulator of the induction of *CHS* gene expression in response to UV-B in Arabidopsis, the same inhibitors used by Christie and Jenkins (1996) were also tested for inhibition of the UV-B induced nuclear accumulation of NES-GFP-UVR8. However, incubation of plants expressing NES-GFP-UVR8 with staurosporine, cantharidine or cycloheximide failed to stop the protein from entering the nucleus in a UV-B dependent manner. These data suggest that neither phosphorylation nor dephosphorylation or protein synthesis is required for the UV-B induced nuclear accumulation of UVR8. However, it cannot be excluded that any of these events may

be involved in the UV-B dependent activation of UVR8 in order to induce the expression of *CHS* and other genes.

A biochemical approach was used to establish if the UV-B triggered nuclear accumulation of UVR8 is due to a nuclear translocation event or due to inhibition of protein degradation within the nucleus. Immunoblot analyses on native UVR8, GFP-UVR8, NES-GFP-UVR8 and NLS-GFP-UVR8 show that there is no change in the total UVR8 protein concentration in response to UV-B. If UV-B induced an inhibition of protein degradation in the nucleus, then NLS-GFP-UVR8 that is constitutively localised in the nucleus would have shown an apparent increase in response to UV-B. However this is not the case, and microscopy studies also demonstrate that there is no increase in the fluorescence of NLS-GFP-UVR8 in response to a UV-B stimulus. From these data, it is highly likely that UV-B induces nuclear translocation of UVR8. Alternatively, simultaneous protein synthesis and degradation of UVR8 could account for the lack of net change in UVR8 protein abundance in response to UV-B. Direct evidence for a UV-B induced nuclear translocation of UVR8 could only be obtained by micro-injection studies showing that a tagged UVR8 molecule injected in the cytosol could move into the nucleus in response to UV-B.

Preliminary data, however, suggest that UV-B could also be inhibiting the nuclear export of UVR8, which would also account for the accumulation of NES-GFP-UVR8 in the nucleus, in response to UV-B. Experiments using Leptomycin B (LMB), a specific nuclear export inhibitor that interferes with the association of the export receptor exportin 1 with the leucine-rich NES peptide of the cargo protein (Fukuda *et al.*, 1997), demonstrate a clear accumulation of NES-GFP-UVR8 in the nucleus in the absence of a UV-B stimulus (data not shown). This suggests that Leptomycin B can mimic the effects of UV-B on the sub-cellular localisation pattern of UVR8. Furthermore, plants pre-treated with LMB and subsequently irradiated with UV-B showed an apparent increase in the magnitude of the UV-B induced nuclear accumulation response of NES-GFP-UVR8, indicating that inhibition of nuclear export can enhance this response. LMB has been extensively used in mammalian systems in order to understand the mechanism of nuclear translocation of major signalling

components such as Mdm2 and MAPKAP kinase 2 (Menendez *et al.*, 2003; Engel *et al.*, 1998). However, in most cases, LMB either inhibits or interferes with a response, rather than mimicking a stimulus. Further experiments are essential in order to understand the significance of the effect of LMB on UVR8 nuclear translocation. Most importantly, it would be very interesting to examine if LMB can induce nuclear accumulation of native UVR8 and if it can induce the expression of *HY5* or *CHS* in the absence of a UV-B signal.

A genetic approach was also employed in order to examine the mechanism involved in the nuclear accumulation of UVR8. As mentioned earlier, the red light induced nuclear import of phyA requires direct association with both FHY1 and FHL proteins (Hiltbrunner *et al.* 2006). For this reason, the *Arabidopsis* mutant lines *fhy1* and *fhy1/fhl*, kindly donated by Dr. Franklin and Dr. Zeidler, respectively, were examined for the UV-B induction of *HY5* and *CHS* gene expression in case they were altered in the activity or the localisation of UVR8. Unfortunately, no effect was observed on the functionality of UVR8 in the absence of either of these proteins, suggesting that they are not essential for the nuclear localisation of UVR8 (data not shown).

In conclusion, the experiments performed in this study show that UVR8 can accumulate into the nucleus in response to UV-B either by nuclear import or/and inhibition of nuclear export. Phosphorylation or protein synthesis is not required for this response, but could be involved in UVR8 function. Furthermore, the nuclear localisation of UVR8 is NLS-independent, since no classical NLS is contained within the sequence of the protein. However, it is possible that an unidentified NLS-containing adaptor protein, other than FHY1 or FHL, mediates import of UVR8 into the nucleus.

7.4 The N-terminus of UVR8 is required for nuclear accumulation in response to UV-B

In order to characterise the relationship between the structure and the function of UVR8 at the protein level, deletion-mutagenesis analysis was employed. As mentioned previously, UVR8 shows 30 % identity at the primary sequence level with the human regulator of chromatin condensation RCC1 (Kliebenstein *et al.*, 2002). The amino acid conservation between the two proteins mainly involves the sequence required for the formation of each of the seven blades of the β -propeller structure, which is predicted for UVR8 based on the resolved crystal structure of RCC1 (Renault *et al.*, 1998). Although RCC1 contains a bipartite NLS peptide at the extreme N-terminus, UVR8 shows no sequence similarity to RCC1 in this part of the protein.

Deletion analysis of the N-terminal region of UVR8 and generation of stable transgenic Arabidopsis lines expressing GFP- Δ NUVR8 in the *uvr8-1* mutant background demonstrates that this part of the protein is required for function. GFP- Δ NUVR8 fails to induce expression of *HY5* and *CHS* in response to UV-B, and consequently fails to confer the necessary protection for plant survival under higher than ambient UV-B irradiation conditions. Examination of how the deletion of the N-terminus of UVR8 may interfere with the function of the protein was carried out. Chromatin immunoprecipitation assays confirmed that GFP- Δ NUVR8 could still associate with the promoter region of *HY5*, indicating that the loss of GFP- Δ NUVR8 functionality is not due to its inefficient association with chromatin.

Fluorescence microscopy studies have shown that although the sub-cellular localisation pattern of GFP- Δ NUVR8 is normal under white light conditions, there is a significant decrease in its nuclear accumulation in response to UV-B. These data suggest that the N-terminus of UVR8 is required for the regulation of the UV-B induced nuclear accumulation of the protein, either by being the site of post-translational modification or interaction with another protein. It is very likely that the lack of nuclear accumulation in response to UV-B may account for the impairment of activity of GFP- Δ NUVR8, especially since there is evidence of a direct correlation

between UV-B induced UVR8 nuclear accumulation and function. For example, studies have shown that UVR8 regulated gene expression follows a similar time-scale and fluence rate dependent pattern to the UV-B induced nuclear accumulation of UVR8. However, the possibility that the N-terminal region may contain the necessary information not only for UV-B-dependent nuclear translocation but also for UV-B induced activation, cannot be excluded. Although GFP- Δ NUVR8 can associate with chromatin, the N-terminal region may still undergo post-translational modification, conformational change or may serve as the interaction site with other nuclear proteins in a UV-B-dependent manner.

7.5 UVR8 is responsive to UV-B in the cytosol and in the nucleus

Sub-cellular localisation and immunoblot analyses carried out in this study have shown that UVR8 resides both in the cytosol and the nucleus of Arabidopsis cells. However, Brown and co-workers (2005) and Cloix and Jenkins (2007) have recently shown that UVR8 primarily functions as a UV-B-dependent regulator of gene expression by associating with chromatin via histones. As a means of understanding the significance of the cytosolic fraction of UVR8, the constitutive nuclear NLS-GFP-UVR8 and the constitutive cytosolic NES-GFP-UVR8 stable transgenic Arabidopsis lines described in the previous section were examined for functionality.

Despite the fact that NES-GFP-UVR8 is excluded from the nucleus in the absence of a UV-B stimulus, it has the ability to induce gene expression, since UV-B induces its rapid translocation into the nucleus. Furthermore, it is obvious that UVR8 is not required for the basal expression levels of *HY5* and *CHS* genes, as NES-GFP-UVR8 still shows basal levels and more importantly, *uvr8* mutant plants also retain this response, although they lack the UV-B-dependent induction of these genes (Brown *et al.*, 2005). Although the data obtained from the transgenic plants expressing NES-GFP-UVR8 do not really provide information on the importance on the cytosolic or the

nuclear pool of UVR8, they indicate that the cytosolic pool of UVR8 is responsive to UV-B by accumulating in the nucleus.

In contrast, NLS-GFP-UVR8 is restricted to the nucleus in all light conditions tested and UV-B has no effect on its sub-cellular localisation or total protein abundance. Although NLS-GFP-UVR8 is constitutively targeted to the nucleus, it does not mediate constitutive induction of *HY5* and *CHS* transcription in the absence of a UV-B stimulus. Furthermore, NLS-GFP-UVR8 is still functional and mediates a UV-B dependent induction of *HY5* and *CHS* gene expression, suggesting that UV-B can activate it in the nucleus. Although the association of UVR8 with chromatin is UV-B independent, thus constitutive, there may be other factors, such as post-translational modifications of the histones, which may activate UVR8 and induce gene expression in response to UV-B (Cloix and Jenkins, 2007). This could also explain why NLS-GFP-UVR8 is functional when expressed constitutively in the nucleus. Either a signal is coming into the nucleus or the signal is perceived in the nucleus and transmitted to UVR8.

In summary, although the site of UV-B perception cannot be determined based on the data obtained from these experiments, it is evident that UVR8 can be activated both in the nucleus and in the cytosol in response to UV-B. Also, the fact that NLS-GFP-UVR8 is functional indicates that the cytosolic pool of UVR8 is not essential for function. However, unidentified cytosolic component(s), which could facilitate the nuclear accumulation of UVR8, may be required to enter the nucleus and activate UVR8 in response to UV-B.

A very elegant study published by Zeidler and co-workers demonstrates that although phyA is mostly associated with nuclear translocation and regulation of gene expression, it also has cytoplasmic-specific functions, such as the blue-light induced gravitropism and the red light enhancement of blue light-induced phototropism (Rosler *et al.*, 2007). Whether an equivalent scenario applies for UVR8 or whether the cytosolic pool of UVR8 serves simply for “storage” purposes is not clear yet.

Alternatively, UVR8 could serve as a dual UV-B signal transducer, which would be able to mediate UV-B-induced responses perceived in two distinct cellular

compartments – the nucleus and the cytosol. As mentioned earlier, mammalian cells demonstrate two different UV-B induced signal transduction pathways, one perceived in the nucleus and the other in the cytosol or the plasma membrane (Brenneisen *et al.*, 2002; Krutmann, 2006). Whether two independent and possibly fluence-dependent pathways operate in plants in response to UV-B is likely, and whether UVR8 is a key signalling component for both of them is currently unknown. Further experiments are essential for understanding fully the significance of the sub-cellular partitioning and nuclear translocation of UVR8 and its role in UV-B signal transduction

7.6 The C-terminus of UVR8 is essential for function

A great part of this work is focused on the relationship between the sub-cellular localisation of UVR8 and its function. However, it is equally important to understand how the structure of UVR8 protein regulates its function. As described earlier, there is high sequence similarity between UVR8 and RCC1 (Kliebenstein *et al.*, 2002). However, there are UVR8 specific amino acid sequences which do not align with the equivalent of RCC1. For example the extreme N-terminus of UVR8, that was discussed previously, seems to confer the UV-B-specific nuclear accumulation of UVR8, although it does not contain a canonical NLS peptide.

Furthermore, there is a sequence near the C-terminus of UVR8 that not only is very different to RCC1, but also to any other Arabidopsis protein, indicating that this region may be important by conferring the UV-B specific function of UVR8. Indeed, deletion analysis of this region and generation of transgenic lines expressing GFP- Δ CUVR8 proved that this part of the protein is essential for UVR8 function, although it has no effect on UVR8 sub-cellular localisation, nuclear accumulation, protein stability or chromatin association. The importance of this C-terminal region of UVR8 is also demonstrated by genetic studies leading to the isolation of the *uvr8-2* mutant allele, which expresses a shorter polypeptide due to a mutation resulting in a premature STOP codon within the UVR8-specific C-terminal region of the protein. This

polypeptide is not functional but can still associate with chromatin (data not shown). Whether the importance of the C-terminal region is based on its interaction with another protein or on being a site of modification has yet to be determined.

7.7 Attempts to identify UVR8-interacting proteins

As discussed previously, UVR8 is regulated by UV-B at the sub-cellular level by undergoing a rapid nuclear translocation. Furthermore, specific UVR8 protein regions have been assigned specific functions, such as the requirement of the N-terminal region for the UV-B-dependent nuclear accumulation and the importance of the region near the C-terminus of the protein for the general activity of the protein. The next step is to identify how certain responses are performed or mediated by UVR8. For this reason the yeast-two-hybrid system was employed in order to identify interacting partners for UVR8. Unfortunately, no UVR8-interacting proteins were isolated from a yeast-two-hybrid screen or a directed yeast-two-hybrid approach due to various possible reasons discussed in Chapter 6. However, in order to understand further the mechanism of UVR8 function and UV-B signal perception, it is essential to discover the molecular components that may interact with UVR8.

The evidence for the direct involvement of UVR8 in regulating gene expression by associating with chromatin via specific histones is of major significance. However, more information is vital so as to assign a specific function to UVR8 in terms of directly controlling transcription by modifying chromatin conformation or by activating transcription factors (Brown *et al.*, 2005; Cloix and Jenkins, 2007). Also, at the cytoplasmic level, the identification of an interacting partner for UVR8 may supply further information on the mechanism of nuclear import or even UV-B perception.

7.8 Conclusions

The major conclusions based on the data obtained from this study are the following:

- a) UVR8 protein is ubiquitously expressed in all plant organs and throughout the life-cycle of Arabidopsis plants
- b) The abundance of UVR8 at the protein level is unaffected by darkness, white, red, blue and UV-B light
- c) The sub-cellular localisation of UVR8 is cytosolic and nuclear in all tissues examined and at various developmental stages in the absence of a classic NLS
- d) UV-B induces a rapid nuclear accumulation of UVR8
- e) The UV-B induced nuclear accumulation of UVR8 correlates with its function, in terms of regulating gene expression
- f) The mechanism of the UV-B dependent nuclear accumulation of UVR8 does not appear to involve phosphorylation, de-phosphorylation or protein synthesis. However, UV-B may induce nuclear import or inhibition of nuclear export of UVR8
- g) The N-terminus of UVR8 is required for its nuclear translocation and consequently function in response to UV-B
- h) The C-terminus of UVR8 is required for function without affecting its sub-cellular localisation or chromatin association
- i) UVR8 can be activated in the nucleus and in the cytosol in response to UV-B, though the cytosolic pool of UVR8 is not essential for function
- j) No interacting partners have been identified for UVR8 by using the yeast-two-hybrid system, however, purified GFP-tagged UVR8 could help in identifying protein complexes associated with UVR8 *in planta*.

Based on these conclusions, a simple and preliminary model of UVR8 action can be formulated (Figure 7.1). However, future experiments are essential for elucidating

the fundamental question of the site(s) of UV-B perception and most importantly the molecular identity of the UV-B photoreceptor.

7.9 Future Work

Although the work described in this study has provided information on the characterisation of UVR8 and the understanding of some of the basic aspects involved in the regulation of UVR8 in response to UV-B, there are still fundamental aspects of UVR8 action and UV-B perception and signal transduction that remain elusive. For this reason further work is required.

One of the major priorities for this research area, as mentioned earlier, is the identification of upstream and downstream UV-B signalling components that are directly associated with UVR8. Recognition of such components not only will provide information on UVR8 function, but will also enlighten the mechanism involved in UV-B perception. Further yeast-two-hybrid experiments using UVR8 as the bait protein for screening cDNA libraries from plants treated either with UV-B or white light may provide important information. Furthermore, transgenic plants expressing GFP-UVR8 from the native promoter can be used for either immuno-precipitation or purification studies in order to identify complexes that associate with UVR8 and directly or indirectly regulate its function and mediate UV-B signal transduction. Since UVR8 is the most upstream UV-B specific signalling component identified in plants (Brown *et al.*, 2005), the use of it as the bait either in the yeast-two-hybrid system or for purifying complexes from plant extracts may result in the identification of the UV-B photoreceptor.

The use of the cytosolically-restrained NES-GFP-UVR8 or the constitutive nuclear localised NLS-GFP-UVR8 lines may be very useful for identifying sub-cellular-specific interacting partners for UVR8, which regulate it at different signalling levels (upstream or downstream).

Also, the fact that the 27 amino acid region near the C-terminus of UVR8 is essential for protein function, but is not involved in any of the responses tested (localisation, nuclear accumulation or chromatin association) may indicate that this is the site of interaction with another protein. This region could be employed as a bait for a yeast-two-hybrid screen or for purification of UVR8 Ct-interacting complexes from plant extracts.

Although the identification of protein complexes based on protein purification is one of the main approaches proposed for future work, there are major difficulties involved. The identity of the components of a putative UVR8-interacting complex can be determined either by direct immuno-detection, if there are antibodies available for the “suspected” interacting candidates, or by mass spectrometry. Although the latter technique requires large amounts of protein that could be visible on a silver-stained gel, the sensitivity of this method is constantly improved and there are major developments in the field of proteomic research, which is very promising.

Another aspect of this research that requires further investigation involves the UV-B induced protein translocation of UVR8, which seems to be important for UVR8 function. Although the data obtained from this study have led to the identification of the region of UVR8 that is required for this response (the N-terminus of the protein), it is still unknown how this response is mediated and if other proteins are involved. Evidence for a direct involvement of the N-terminus of UVR8 in the UV-B-dependent nuclear import can only be provided by generating GFP fusion constructs with the N-terminal region of UVR8 and testing if this region is sufficient for this response. Furthermore, functional analysis of a constitutive nuclear-localised NLS-GFP- Δ NUVR8 construct will prove whether the lack of GFP- Δ NUVR8 functionality is due to the lack of its UV-B induced nuclear accumulation or due to impairment of its function in the nucleus.

Furthermore, the exact mechanism of the nuclear import and the UV-B-dependent nuclear accumulation of UVR8 needs to be established. Whether an interacting protein or post-translational modification other than phosphorylation is required could be investigated. Additional experiments using the nuclear export

inhibitor Leptomycin B may provide information on this specific response or the nuclear accumulation of other light signalling components.

Finally, the nuclear activation of UVR8 demonstrated by NLS-GFP-UVR8 requires further examination. Is the activation of UVR8 originating from the DNA via the UV-B-dependent modification of histones or do other non-chromatin associated nuclear components transmit the signal and activate UVR8 by modifying or simply associating with it in response to UV-B so as to initiate gene expression? All these are fundamental questions that may be difficult to answer by using only one specific approach. For these reason, it is essential to utilise the wealth of different systems and techniques that are available in our era, in order to understand basic mechanisms involved in UV-B signalling and the mechanisms underlying UV-protection.

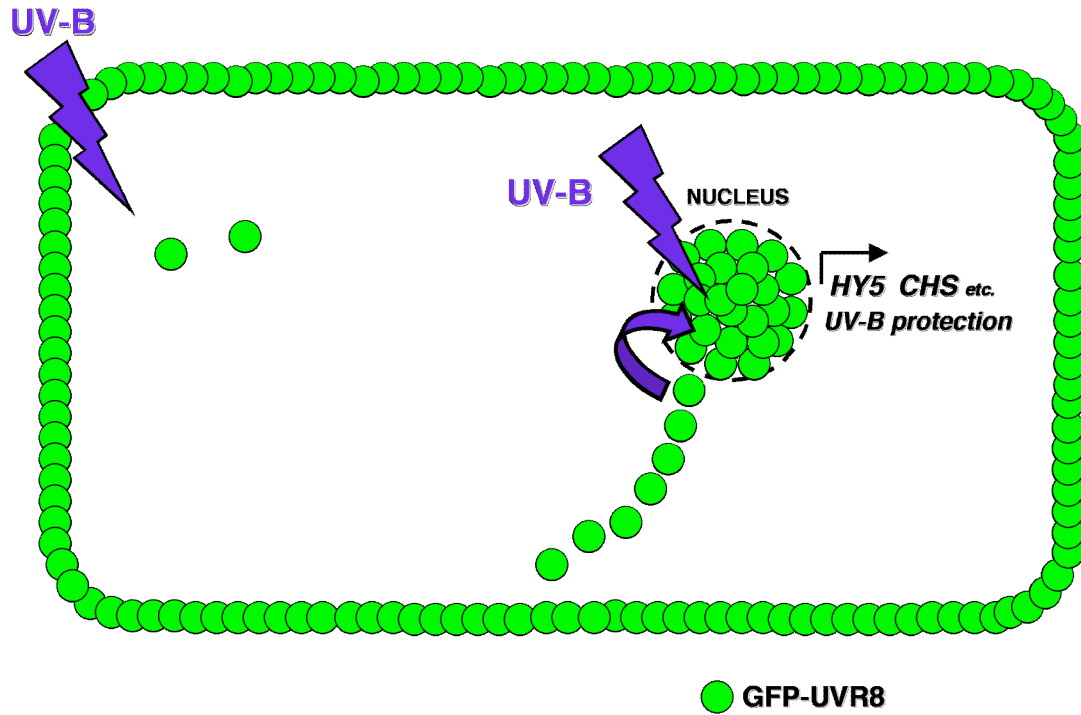


Figure 7.1 Schematic of UVR8 activation in response to UV-B

UVR8 is responsive to UV-B both in the cytosol and in the nucleus. UV-B induces a rapid nuclear accumulation of the cytosolic UVR8 and activates nuclear UVR8 in order to induce the transcription of genes essential for photo-protection.

REFERENCES

- Afaq, F., Ahmad, N. and Mukhtar, H. (2003) *Oncogene*, **22**, 9254-9264.
- Afaq, F., Malik, A., Syed, D., Maes, D., Matsui, M.S. and Mukhtar, H (2005)
Photochemistry and Photobiology, **81**, 38-45.
- Ahmad, M., Jarillo, J.A., Smirnova, O. and Cashmore, A.R. (1998) *Molecular Cell*,
1, 939-948.
- Ang, L.H., Chattopadhyay, S., Wie, N., Oyama, T., Okada, K., Batschauer, A. and
Deng, X.W. (1998) *Molecular Cell*, **2**, 213-222.
- von Arnim, A.G. and Deng, X. W. (1994) *Cell*, **79**, 1035-1045.
- Ballare, C.L., Scopel, A.L., Stapleton, A.E. and Yanovsky, M.J. (1996) *Plant
Physiology*, **112**, 161-170.
- Batschauer, A., Banerjee, R. and Pokorny, R. (2007) *Annual Plant Reviews*, **30**, 17-
48.
- Bender, K., Blattner, C., Knebel, A., Jordanov, M., Herrlich, P. and Ramsdorff, H.J.
(1997) *Journal of Photochemistry and Photobiology*, **37**, 1-17.
- Benvenuto, G., Formiggini, F., Laflamme, P., Malakhov, M. and Bowler, C. (2002)
Current Biology, **12**, 1529-1534.
- Bi, X., Jones, T., Abbas, F., Lee, H., Stultz, B., Hursh, D.A. and Mortin, M.A. (2005)
Oncogene, **24**, 8229-8239.

- Bieza, K. and Lois, R. (2001) *Plant Physiology*, **126**, 1105-1115.
- Brenneisen, P., Sies, H. and Scharffetter-Kochanek, K. (2002) *Annals of the New York Academy of Sciences*, **973**, 31-43.
- Briggs, W.R. and Christie, J.M. (2002) *Trends in Plant Science*, **7**, 204-210.
- Briggs, W.R. and Spudich, J.L. (2006) *Handbook of Photosensory Receptors*
- Brosche, M., Schuler, M., Kalbina, I., Connor, L. and Strid, A. (2002) *Photochemical and Photobiological Sciences*, **1**, 656-664.
- Britt, A.B., Chen, J.J., Wykoff, D. and Mitchell, D. (1993) *Science*, **261**, 1571-1574.
- Brosche, M. and Strid, A. (2003) *Physiologia Plantarum*, **117**, 1-10.
- Brown, B.A., Cloix, C., Jiang, G.H., Kaiserli, E., Herzyk, P., Kliebenstein, D. and Jenkins, G.I. (2005) *Proceedings of the National Academy of Sciences of the United States of America*, **102**, 18225-30
- Caldwell, M.M., Ballare, C.L., Flint, S.D., Bjorn, L.O., Teramure, A.H., Kulandaivelu, G. and Tevini, M. (2003) *Photochemical and Photobiological Sciences*, **2**, 29-38
- Caldwell, M.M., Bornmann, J.F., Ballare, C.L., Flint, S.D. and Kulandaivelu, G. (2007) *Photochemical and Photobiological Sciences*, **6**, 252-266.
- Casati, P. and Walbot, V. (2004) *Plant Physiology*, **136**, 3319-3332.
- Casati, P., Stapleton, A. E., Blum, J. E., and Walbot, V. (2006) *Plant Journal*, **46**,

613-627.

Causier, B. and Davies, B. (2002) *Plant Molecular Biology*, **50**, 855-870.

Chapple, C.C.S., Vogt, T., Ellis, B.E. and Somerville, C.R. (1992) *Plant Cell*, **4**, 1413-1424.

Chattopadhyay, S., Ang, L.-H., Puente, P., Deng, X.-W. and Wei, N. (1998) *Plant Cell*, **10**, 673-683.

Christie, J.M., (2007) *Plant cell and Environment*, **20**, 773-778.

Christie, J.M. and Jenkins, G.I. (1996) *Plant Cell*, **8**, 1555-1567.

Christie, J.M., Reymond, P., Powell, G.K., Bernasconi, P., Raibekas, A.A., Liscum, E. and Briggs, W.R. (1998) *Science*, **282**, 1698-1701.

Christie, J.M., Swartz, T.E., Bogomolni, R.A. and Briggs, W.R. (2002), *Plant Journal*, **32**, 205-219.

Cloix, C. and Jenkins, G.I. (2007), *Molecular Plant*, in press.

Clough, S. J., and Bent, A. F. (1998), *Plant Journal*, **16**, 735-743.

Day, T.A. and Vogelmann, T.C. (1995) *Physiologia Plantarum*, **94**, 433-440.

Devary, Y., Gottlieb, R.A., Lau, L.F. and Karin, M. (1991) *Molecular Cell Biology*, **11**, 2804-2811.

Devary, Y., Gottlieb, R.A., Smeal, T. and Karin, M. (1992) *Cell*, **71**, 1081-91.

- Devary, Y., Rosette, C., DiDonato, J. and Karin, M. (1993) *Science*, **261**, 1442-1445.
- Docquier, S., Tillemans, V., Deltour, R. and Motte, P. (2004) *Chromosoma*, **112**, 255-266.
- Eisinger, W., Swartz, T.E., Bogomolni, R.A. and Taiz, L. (2003) *Plant Physiology*, **122**, 99-106.
- Engel, K., Kotlyarov, A. and Gaestel, M. (1998) *EMBO Journal*, **17**, 3363-3371.
- Fankhauser, C., Yeh, K.C., Lagarias, J.C., Zhang, H., Elich, T.D. and Chory, J. (1999) *Science*, **284**, 1539-1541.
- Franklin, K. A., Larner, V. S. and Whitelam, G. C. (2005) *International Journal of Developmental Biology*, **49**, 653-664.
- Frohnmeier, H., Ehmann, B., Kretsch, T., Rocholl, M., Harter, K., Nagatani, A., Furuya, M. and Batschauer, A. (1992) *Plant Journal*, **2**, 899-906.
- Frohnmeier, H., Bowler, C. and Schafer, E. (1997) *Journal of Experimental Botany*, **48**, 739-750.
- Frohnmeier, H., Bowler, C., Zhu, J.K., Yamagata, H., Schafer, E. and Chua, N.H. (1998) *Plant Journal*, **13**, 763-772.
- Frohnmeier, H., Loyall, L., Blatt, M.R. and Grabov, A. (1999) *Plant Journal*, **20**, 109-118.
- Frohnmeier, H. and Staiger, D. (2003) *Plant Physiology*, **133**, 1420-1428.

- Fuglevand, G., Jackson, J.A. and Jenkins, G.I. (1996) *Plant Cell*, **8**, 2347-2357.
- Fukuda, M., Asano, S., Nakamura, T., Adachi, M., Yoshida, M., Yanagida, M. and Nishida, E. (1997) *Nature*, **390**, 308-311.
- Gil, P., Kircher, S., Adam, E., Bury, E., Kozma-Bognar, L., Schafer, E. and Nagy, F. (2000) *Plant Journal*, **22**, 135-145.
- Green, R. and Fluhr, R. (1995) *Plant Cell*, **7**, 203-212.
- Guo, H.W., Duong, H., Ma, N. and Lin, C.T. (1999) *Plant Journal*, **19**, 279-87.
- Hajdukiewicz, P., Zora, S., and Maliga, P. (1994) *Plant Molecular Biology*, **25**, 989-994.
- Harper, S.M., Neil, L.C. and Gardner, K.H. (2003) *Science*, **301**, 1541-1544.
- Harter, K., Frohnmeyer, H., Kircher, S., Kunkel, T., Herrlich, P., Blattner, C., Knebel, A., Bender, K. and Rahmsdorf, H.J. (1997) *Biological Chemistry*, **378**, 1217-1229.
- Hartmann, U., Valentine, W.J., Christie, J.M., Hays, J., Jenkins, G.I. and Weisshaar, B. (1998) *Plant Molecular Biology*, **36**, 741-754.
- Hiltbrunner, A., Viczian, A., Bury, E., Tscheuschler, A., Kircher, S., Toth, R., Honsberger, A., Nagy, F., Fankhauser, C. and Schafer, E. (2005) *Current Biology*, **15**, 2125-2130.
- Hiltbrunner, A., Tscheuschler, A., Viczian, A., Kunkel, T., Kircher, S. and Schafer, E. (2006) *Plant Cell Physiology*, **47**, 1023-1034.

- Hisada, A., Kanzawa, H., Weller, J.L., Nagatani, A., Reid, J.B. and Furuya, M. (2000) *Plant Cell*, **12**, 1063-1078.
- Huala, E., Oeller, P.W., Liscum, E., Han, I.S., Larsen, E. and Briggs, W.R. (1997) *Science*, **278**, 2120-2123.
- Huang, S., Dai, Q., Peng, S., Chavez, A.W., Miranda, L.L., Visperas, R.M. and Vergara, B.S. (1997) *Plant Growth Regulation*, **21**, 59-64.
- Izaguirre, M.M., Scopel, A.L., Baldwin, I.T. and Ballare, C.T. (2003) *Plant Physiology*, **132**, 1755-1767.
- Jabben, M., Shanklin, J. and Vierstra, R.D. (1989) *Journal of Biological Chemistry*, **264**, 4998-5005.
- Jackson, J.A., Fuglevand, G., Brown, B.A., Shaw, M.J. and Jenkins, G.I. (1995) *Plant Journal*, **8**, 369-380.
- Jackson, J.A. and Jenkins, G.I. (1995) *Planta*, **197**, 233-239.
- Jansen, M.A.K., Gaba, V. and Greenberg, B.M. (1998) *Trends in Plant Science*, **3**, 131-135.
- Jarillo, J.A., Cape, J., Tang, R.H., Yang, H.Q. and Alonso, J.M. (2001) *Nature*, **410**, 487-490.
- Jenkins, G.I. (1997) *Plant Cell and Environment*, **20**, 773-778.

- Jenkins, G.I., Long, J.C., Wade, H.K., Shenton, M.R. and Bibikova, T.N. (2001) *New Phytologist*, **151**, 121-131.
- Jenkins, G.I. and Brown, B.A. (2007) *Annual Plant Reviews*, **30**, 155-182.
- Jiang, H.Y. and Wek, R.C. (2005) *Biochemical Journal*, **385**, 371-380.
- Jiao, Y., Lau, O.S. and Deng, X.W. (2007) *Nature Reviews in Genetics*, **8**, 217-230.
- Jordan, B.R. (1996) *Advances in Botanical Research*, **22**, 98-138.
- Kagawa, T., Sakai, T., Suetsugu, N., Oikawa, K., Ishiguro, S., Kato, T., Tabata, S., Okada, K. and Wada M. (2001) *Science*, **291**, 2138-2141.
- Kalbin, G., Hidema, J., Brosche, M., Kumagai, T., Bornmann, J.F. and Strid, A. (2001) *Plant Cell and Environment*, **24**, 983-990.
- Kim, B.C., Tenessen, D. and Last, R. (1998) *Plant Journal*, **15**, 667-674.
- Kircher, S., Kozma-Bognar, L., Kim, L., Adam, E., Harter, K., Schafer, E. and Nagy, F. (1999) *Plant Cell*, **11**, 1145-1456.
- Kleine, T., Lockhart ,P. and Batschauer, A. (2003) *Plant Journal*, **35**, 93-103.
- Kliebenstein, D.J., Lim, J.E., Landry, L.G., Last, R.L. (2002) *Plant Physiology*, **130**, 234-243.
- Knebel, A., Rahmsdorf, H.J., Ullrich, A. and Herrlich, P. (1996) *EMBO Journal*, **15**, 5314-5321.

- Kong, S.G., Suzuki, T., Tamura, K., Mochizuki, N., Hara-Nishimura, I. and Nagatani, A. (2006) *Plant Journal*, **45**, 994-1005.
- Koorneef, M., Rolff, E. and Spruit, C. (1980) *Zeitschrift fur Pflanzenphysiologie*, **100**, 147-160.
- Kovtun, Y, Chiu, Y.L., Tena, T. and Sheen, J. (2000) *Proceedings of the National Academy of Sciences of the United States of America*, **97**, 2940-2945.
- Krutmann, J. (2006) *Progress in Biophysics and Molecular Biology* **92**, 105-107.
- Kucera, B., Leubner-Metzger, G. and Wellman, E. (2003) *Plant Physiology*, **133**, 1445-1452.
- Landry, L., Chapple, C. and Last, R. (1995) *Plant Physiology*, **109**, 1159-1166.
- Lee J, He, K., Stolc, V., Lee, H., Figueroa, P., Gao, Y., Tongprasit, W., Zhao, H., Lee, I. and Deng, X.W. (2007) *Plant Cell*, **19**, 731-745.
- Li, J., Ou-Lee, T.M., Raba, R., Amundson, R.G. and Last, R.L. (1993) *Plant Cell*, **5**, 171-179.
- Li, J. (2005) *Current Opinions in Plant Biology*, **8**, 526-531.
- Lin, C. and Shalitin, D. (2003) *Annual Reviews in Plant Biology*, **54**, 469-496.
- Liscum, E. and Stowe-Evans, E.L. (2000) *Photochemistry and Photobiology*, **72**, 273-282.

- Lorraine, S., Genoud, T. and Fankhauser, C. (2006) *Current Opinions in Plant Biology*, **9**, 509-514.
- Ma, L., Sun, L., Liu, X., Jiao, Y., Zhao, H. and Deng, X.W. (2005) *Plant Physiology*, **138**, 80-91.
- Mackerness, S., John, C.F., Jordan, B.R. and Thomas, B. (2001) *FEBS Letters*, **489**, 237-242.
- Mackerness, S., Surplus, S.L. and Blake, P. (1999) *Plant, Cell and Environment*, **22**, 1413-1423.
- Martinez-Garcia, J.F., Huq, E. and Quail, P.H. (2000) *Science*, **288**, 859-863.
- Mas, P., Devlin, P.F., Panda, S. and Kay, S.A. (2000) *Nature*, **408**, 207-211.
- McBride, K.M., McDonald, C. and Reich, N.C. (2000) *EMBO Journal*, **19**, 6196-6206.
- Menendez, S., Higgins, M., Berkson, R.G., Edling, C., Lane, D.P. and Lain, S. (2003) *British Journal of Cancer*, **88**, 636-643.
- Merkle, T. (2004) *Current Opinions in Genetics*, **44**, 231-260.
- Moller, S., Kim, Y.S., Kunkel, T., Chua, N.H. (2003) *Plant Cell*, **15**, 1111-1119.

- Monte, E., Al-Sady, B., Leivar, P. and Quail, P.H. (2007) *Journal of Experimental Botany*, In press
- Moriguchi, K., Suzuki, T., Ito, Y., Yamazaki, Y., Niwa, Y. and Kurata, N. (2005) *Plant Cell*, **17**, 389-403.
- Muhlbauer, S. and Schafer, E. (1994) *Proceedings of the National Academy of Sciences of the United States of America*, **91**, 5038-5048.
- Nemergut, M.E. and Macara, I.G. (2000) *Journal of Cell Biology*, **149**, 835-849.
- Ni, M., Tepperman, J.M. and Quail, P.H. (1998) *Cell*, **95**, 657-667.
- Osterlund, M.T., Hardke, C.S., Wei, N. and Deng, X.W. (2000) *Nature*, **405**, 462-466.
- Osterlund, M.T., Wei, N. and Deng X.W. (2000) *Plant Physiology*, **124**, 1520-1524.
- Oravecz, A., Baumann, A., Mate, Z., Brzezinska, A., Molinier, J., Oakeley, E.J., Adam, E., Schafer, E., Nagy, F., and Ulm, R. (2006) *Plant Cell*, **18**, 1975-1990.
- Park, E., Kim, J., Lee, Y., Shin, J., Oh, E., Chung, W.I., Liu, J.R. and Choi, G. (2004) *Plant Cell and Physiology*, **45**, 968-975.
- Pepper, A., Delaney, T., Washburn, T., Poole, D. and Chory, J. (1994) *Cell*, **78**, 109-116.
- Rao, M.V., Paliyath, G., Ormrod, D.P. (1996) *Plant Physiology*, **110**, 125-136.

- Renault, L., Nassar, N., Vetter, I., Becker, J., Klebe, C., Roth, M. and Wittinghofer, A. (1998) *Nature*, **392**, 97-100.
- Renault, L., Kuhlmann, J., Henkel, A. and Wittinghofer, A. (2001) *Cell*, **105**, 245-255.
- Rigaut, G., Shevchenko, A., Rutz, B., Bouveret, B., Bragado-Nilsson, E., Wilm, M. and Seraphin, B. (1999) *Nature Biotechnology*, **17**, 1030-1032.
- Ries, G., Heller, W., Puchta, H., Sandermann, H., Seidlitz, H.K. and Hohn, B. (2000) *Nature*, **406**, 98-101.
- Rosler, J., Klein, I. and Zeidler, M. (2007), *Proceedings of the National Academy of Sciences of the United States of America*, **104**, 10737-10742.
- Rubio, V., Shen, Y., Saijo, Y., Liu, Y., Gusmaroli, G., Dinesh-Kumar, S.P. and Deng, X.W. (2005) *Plant Journal*, **41**, 767-778.
- Ryan, C.A. and Pearce, G. (2003) *Proceedings of the National Academy of Sciences of the United States of America*, **100**, 14577-14580.
- Ryu, H., Kim, K., Cho, H., Park, J., Choe, S. and Hwang, I. (2007) *Plant Cell Preview*
- Sachsenmaier, C., Radier-Pohl, A., Zinck, R., Nordheim, A., Herrlich, P. and Ramsdorf, H.J. (1994) *Cell*, **78**, 963-972.
- Sakamoto, K. and Briggs, W.R. (2002) *Plant Cell*, **14**, 1723-1735.
- Sakamoto, K. and Nagatani, A. (1996) *Plant Journal*, **10**, 859-868.

Sakamoto, A., Lan, V.T.T., Hase, Y., Shikazono, N., Matsunaga, T. and Tanaka, A. (2005) *Plant Cell*, **15**, 2042-2057.

Sambrook and Russell, *Molecular Cloning*, 3rd Edition, CSHL press.

Sankaranarayanan, K. and Jaiswal, A.K. (2006) *Cancer Research*, **66**, 8421-8429.

Saslowski, D. and Winkel-Shirley B. (2001) *Plant Journal*, **27**, 37-48.

Savenstrand, H., Brosche, M. and Strid, A. (2004) *Plant Physiology and Biochemistry*, **42**, 687-694.

Schultze-Lefert, P., Becker-Andre, M., Schulz, W., Hahlbrock, K. and Dangl, J.L. (1989) *Plant Cell*, **1**, 707-714

Schroeder, D., Gahrtz, M., Maxwell, B., Cook, K., Kan, J., Alonso, J.M., Ecker, J.R. and Chory, J. (2002) *Current Biology*, **12**, 1462-1472.

Seino, H., Hisamoto, N., Uzawa, S., Sekiguchi, T. and Nishimoto, T. (1992) *Journal of Cell Science*, **102**, 393-400.

Seki, T., Hayashi, N. and Nishimoto, T. (1996) *Journal of Biochemistry*, **120**, 207-214.

Selp, C.P. and Sancar, A. (2006) *Proceedings of the National Academy of Sciences of the United States of America*, **47**, 17696-17700.

- Shalitin, D., Yang, H., Mockler, T.C., Maymon, M., Guo, H., Whitelam, G.C. and Lin, C. (2002) *Nature*, **417**, 763-767.
- Shaw, S. (2006), *Plant Journal*, **45**, 573-598.
- Shinkle, J.R., Atkins, A.K., Humphrey, E.E., Rodgers, C.W., Wheeler, S.L. and Barnes, P.W. (2004) *Physiologia Plantarum*, **120**, 240-248.
- Spalding, E.P. (2000) *Plant, Cell and Environment*, **23**, 665-674.
- Spalding, E.P. and Folta, K. (2005) *Plant, Cell and Environment*, **28**, 39-53.
- Stratmann, J. (2003) *Trends in Plant Science*, **8**, 525-532.
- Suesslin, C. and Frohnmeyer, H. (2003) *Plant Journal*, **33**, 591-601
- Taiz, L. and Zieger, E. (1998) *Plant Physiology*, 2nd Edition
- Tanaka, A., Sakamoto, A., Ishigaki, Y., Nikaido, O., Sun, G., Hase, Y., Shikazono, N., Tano, S. and Watanabe, H. (2002) *Plant Physiology*, **129**, 64-71.
- Thukral, S. K., Blain, G. C., Chang, K. and Field, S. (1994) *Molecular Cell Biology*, **14**, 8315-8321.
- Ulm, R., Baumann, A., Oravecz, A., Mate, Z., Adam, E., Oakeley, E.J., Schafer, E. and Nagy, F. (2004) *Proceedings of the National Academy of Sciences of the United States of America*, **101**, 1397-1402.
- Ulm, R. and Nagy, F. (2005) *Current Opinions in Plant Biology*, **8**, 477-482.

- Vass, I. (1996) *Biochemistry*, **35**, 8964-8973.
- Wade, H.K., Bibikova, T.N., Valentine, W.J. and Jenkins, G.I. (2001) *Plant Journal*, **25**, 675-685.
- Wade, H.K., Awinder, K.S. and Jenkins, G.I. (2003) *Plant Physiology*, **131**, 707-715.
- Wang, H., Ma, L.G., Li, J.M., Zhao, H.Y. and Deng, X.W. (2001), *Science*, **294**, 154-158.
- Waterworth, W.M., Jiang, Q., West, C.E., Nikaido, M. and Bray, C.M. (2002) *Journal of Experimental Botany*, **53**, 1005-1015.
- Weisshaar, B., Armstrong, G.A., Block, A., Da Costa, E., Silva, O. and Hahlbrock, K. (1991) *EMBO Journal*, **10**, 1777-1786.
- Wray *et al.*, (1981) *Analytical Biochemistry*, **118**, 197-203.
- Yamaguchi, R., Nakamura, M., Mochizuki, N., Kay, S. and Nagatani, A. (1999) *Journal of Cell Biology*, **145**, 437-445.
- Yamamoto, N. and Deng, X.W. (1999) *Genes to Cells*, **4**, 489-500.
- Yanagawa, Y., Sullivan, J.A., Komatsu, S., Gusmaroli, G., Suzuki, G., Yin, J., Ishibasi, T., Saijo, Y., Rubio, V., Kimura, S., Wang, J. and Deng, X.W. (2004) *Genes and Development*, **18**, 2172-2181.
- Yang, H.Q., Tang, R.H. and Cashmore, A.R. (2001) *Plant Cell*, **13**, 2573-2587.